OPERATING PARAMETERS FOR CAPILLARY ELECTROCHROMATOGRAPHY (CEC)

Robert J Boughtflower

A thesis submitted in partial fulfillment of the requirements of Edinburgh University for the degree of Doctor of Philosophy

Analytical Technologies Group, GlaxoWellcome
in collaboration with Chemistry Department, Edinburgh University
Submitted November 2000.

Abstract

Chromatography is one of the most widely used techniques in modern industry. The most common form of chromatography currently used is HPLC which utilises pumped mechanical flow. Electrochromatography (CEC) offers performance improvements over HPLC. Due to the inherently lower dispersion produced by the electrically induced flow profile, it gives typically 2-3 times better efficiency than the same system used with pressure flow. It is also by design a miniaturised process. This offers further benefits of reduced eluent consumption, smaller sample requirements and better compatibility with mass spectrometric detectors. These advantages are particularly useful when we consider the extra difficulty of miniaturising HPLC. Miniaturisation of chromatographic systems is becoming increasingly desirable. Future developments will demand the analysis of smaller samples, at faster rates, with increasingly complex separations required. These demands are already starting to exceed the capabilities of conventional HPLC systems. Systems will require more column efficiency, operation at higher flow rates and detection of the undiluted eluent in the most sensitive detectors available. CEC offers the opportunity to achieve these goals.

The main obstacles to using CEC reliably are the relatively unstable nature of purely electrically driven flows in packed beds, the lack of good quality CEC columns and the lack of dedicated instruments to perform CEC analysis. Also, CEC shares some of the same problems with HPLC of miniaturising the separation system without incurring dispersion related losses.

The work detailed in this thesis contributes considerable advancements in most of these areas. Novel methods to produce high quality columns are described. The work demonstrates effective methods for coupling CEC to MS that make allowance for control of dispersion. The thermal limits of operation are discussed and demonstrated. Pressure-assisted CEC, demonstrating the practicality of performing CEC based analysis that is as reliable as current HPLC systems is shown. Proper optimisation of these type of uses will ultimately deliver CEC in a reliable format which will encourage a whole new audience of users to reap the benefits available.

Declaration

This declaration is to certify that I have solely composed this thesis. Also, all work detailed in this thesis has been carried out by me, except in a few cases, dutifully referenced, where the work was a result of collaboration with colleagues in my Research Group.

Signed
Dated .

Thesis – Contents list and pages. Page no.

Chapter 1 – Introduction to Chromatography. 1
1.1 Objectives 5
Chapter 2. The Story so far... 6
2.1 The development of HPLC 6
2.1.1 Partition Coefficients 8
2.1.2 Retention Time and capacity factors. 9
2.1.3 Theoretical Plates and Column Efficiency 12
2.1.4 Reduced Parameters 15
2.1.5 Dispersion 16
2.1.5.1 Optimisation of performance 23
2.1.6 Practical Equipment 26
2.1.7 The need for miniaturisation 30
2.1.8 The problems with miniaturisation 31
2.2 Capillary electrophoresis 32
2.2.1 The Origin of Electrically-Driven Flow 34
2.2.2 More about the double-layer and the Zeta Potential 38
2.2.3 Flow Rates and the effects of Self-Heating 43
2.3 Capillary Electrochromatography (CEC), the future of miniaturised systems? 47
2.3.1 The Use of Packed Capillaries for CEC 47
2.3.2 Improvements of CEC over Pressure Driven Systems 49
2.3.3 Dispersion in Flow versus Electrodrive systems 50
2.4 Review of developments to date. 52
2.4.1 Instrumentation 52
2.4.2 Stationary Phases 54
2.4.3 Practice 58
2.4.4 Applications 61
Figures for chapter 2. 65-79
References for chapter 2. 80-83

Chapter 3. Introduction to Mass Spectrometry 84

3.1 Introduction 84
3.2 Development of Mass Spectrometry. 84
3.3 Basic Instrumentation. 86
3.4 Electrospray mechanism. 87
3.5 Electrospray Instrumentation 93
3.5.1 Electrospray Sources 94
3.5.2 Mass Analysers 95
3.5.3 The Quadrupole Mass Analyser 97
3.5.4 Quadrupole Ion Optics 98
Figures for chapter 3. 101-104
References for chapter 3. 105-106

Chapter 4 Experimental 107

4.1 Instrumentation 107
4.1.1 CEC Instrumentation 107
4.1.2 Mass Spectrometry Instrumentation 107
4.2 Chemicals 107
4.3 Preparation of Test Mixes 108
4.4 Preparation of Mobile Phases 108
4.5 Injection procedure 109
4.6 CEC Columns 109

Chapter 5 Capillary Column Production Methods 110

5.1. Discussion of packing strategy 110
5.2 Existing packing methods 112
5.3 The Development of a Novel Method for Producing Packed Capillaries 116
5.4 Frit requirements and production 120
5.5 Packing procedure 122
5.6 Troubleshooting 126
Figures for chapter 5. 133-142
References for chapter 5. 143

Chapter 6 Control of dispersion in coupling CEC columns to various detectors. 144

6.1 Capillary Electrochromatography – Mass Spectrometry (CEC/MS) 144
6.1.1 Preparation of capillary column 146
6.1.2 Chromatography 146
6.1.3 Mass Spectrometry 147
6.2 Results and discussion of initial MS work 148
6.2.1 Dedicated probe design 150
6.3 Conclusions of initial MS work 150
6.4 Minimising dispersion in CEC-UV-MS coupled systems 151
6.5 Band spreading in the open tube following CEC 151
6.6 Experimental 157
6.6.1 Instrumentation 157
6.6.2 Chemicals and materials 159
6.7 Experimental Design 160
6.8 Observations of joining columns 161
6.9 Results and discussion 162
6.9.1 Dispersion factors for different CEC column/ open tube configurations 162
6.9.2 Discussion of Additional Variance 166
6.9.3 Dispersion associated with CEC-MS coupling 168

Figures for chapter 6. 170-178
References for chapter 6. 179

Chapter 7. Thermal Effects in CEC 180
7.1 Introduction 180
7.2 Experimental design to test thermal contributions in CEC 189
7.3 Results and Discussion 191
7.3.1 Experiments E1 191
7.3.2 Measurement of Current (I) versus Buffer concentration (c) for open tubes of 50μm diameter at various solvent/buffer compositions 193
7.3.3 Thermal Data for 50μm diameter columns in experiment E2 195
7.3.4 Thermal Data for 100 μm diameter columns in experiment E2 196
7.3.5 Thermal data for 150 μm diameter columns in experiment E2 197
7.3.6 Summary of Thermal Effects data for all column diameters 199
7.4 Calculation of the Capillary Temperature from Data Obtained in E2 202
7.5 Conclusions of Thermal limits for CEC operation 204
Figures for chapter 7. 206-220
Tables for chapter 7 221-224
References for chapter 7. 225

Chapter 8 The use of pressure assisted flow systems for CEC operation (pCEC) 226
8.1 Introduction 226
8.2 Pressure-assisted or pure EOF? 227
8.3 Experiments in pure and combined flow modes 229
8.3.1 Experimental 229
8.4 Results 230
8.4.1 Pressure drive only 232
8.4.2 Electrodrive only (CEC mode) 233
8.4.3 Constant Pressure with Electrodrive assistance 234
8.4.4 Constant voltage with pressure assistance 234
8.4.5 Electrokinetic vs. Pressure injection 235
8.4.6 Gradient elution mode 236
8.4.6.1 Pressure driven gradients 237
8.4.6.2 CEC-driven gradients 239
Figures for chapter 8. 241-248

Chapter 9. Conclusions and future directions. 249
9.1 Dispersion 250
9.2 Thermal limits of operation 251
9.3 Practical robustness 252
9.4 Future for miniaturised separations. 253

Appendix 1. Molecular structures of Cefuroxime axetil and fluticasone Propionate. 255

Chapter 1 – Introduction to Chromatography.

Chromatography is a technique used to separate mixtures by passing them, while dissolved in a fluid, through a column or bed in which they can be partitioned between the fluid phase(the mobile phase) and a phase fixed within the column or bed (the stationary phase). The fluid may be either a gas or a liquid. We are concerned in this thesis with the technique in which the fluid is a liquid. The technique is then called liquid chromatography. Its use in modern analytical techniques is of paramount importance.

All forms of chromatography work on the same, basic principle. The components of a mixture are propelled, in a carrier or mobile phase, through a column or bed that contains the adsorbent or stationary phase. The process of the natural distribution of the different substances between the stationary and mobile phases as they pass through, leads to them moving at different overall speeds. If this process can be adjusted so that the natural separative process occurs within a reasonable and therefore useable time frame, it forms the basis of a powerful separation technique. Different forms of chromatography merely exploit different propellants and adsorbents. In liquid chromatography or LC, the mobile phase is a liquid and the stationary phase is very often a chemically coated, rigid, porous particle fabricated from silica. The adsorbent is contained in a tube or column, and the liquid or "eluent" is pumped through the column by a pump. The sample to be analysed is dissolved in eluent and a small volume of this is "injected" into the column by means of a valve. The different

components of the analyte mixture are thereby separated (or partially separated) and as they emerge from the column they pass through a "detector" which gives a quantitative measure of the concentration of the different components.

Although liquid chromatography was the earliest form of chromatography originating with Tswett in the early years of the century, the development of modern chromatography started around 50 years ago with the more or less independent invention of gas chromatography by Phillips (1949) and by Martin and James (1952). During the early years, the theory of gas chromatography was rapidly developed and soon provided a good understanding of band spreading and of the mechanism of retention. Application of this theory to liquid chromatography took place in the late 1960's and led to the development of what is now termed "High Performance Liquid Chromatography" or HPLC. HPLC is now arguably the most widely used form of chromatography.

If you walked today into any modern laboratory performing routine HPLC analysis, you would be likely to find the chromatography column to be a 10-25cm long steel tube containing porous, chemically bonded silica particles of about 3-5μm in diameter. Liquid leaving the column (eluent), carrying the separated bands, would then flow through a detector (normally UV), which would detect the presence of these individual bands. Each successive sample would be introduced into the separation system (as a solution) by an automated device (autosampler) and the whole process would likely to be managed by software running on a personal computer. To enable a suitable mobile phase flow through rate to be achieved and provide an analysis in no

longer than 20 minutes, we would need to 'pump' mobile phase through the column at about 1ml/ min. This would create a flow resistance (or back pressure) sufficiently high (100 bar+), that high quality pumps would be necessary to maintain consistent, reliable performance.

Currently these methods of analysis form the basis of an extremely powerful and enormously versatile range of techniques used in many chemical based industries to give previously unobtainable speed of analysis, selectivity and sensitivity. The use of chromatography in conjunction with mass spectrometric (MS) detection particularly, has vastly expanded the qualitative aspects of the individual techniques. The availability of increasingly effective bench-top type MS detectors with electrospray ionisation and improved user interfacing, requiring far less expertise to use effectively, indicates that the use of these systems will increase substantially in the future.

Surprisingly perhaps, the practice of HPLC has changed very little in the last 15 years or so, apart from significant improvements to the stationary phase chemistry and modest improvements in controlling the particle size distribution range, both of which have improved the reproducibility of the columns. Although there have been several predictions of the inevitable miniaturisation of techniques such as HPLC and many publications supporting these arguments, the majority of HPLC analyses are still performed on 4.6mm diameter columns (an odd diameter in itself!) of varying lengths at flow rates in the region of 1-2ml/min. Indeed, the whole of the highly lucrative support business in liquid chromatography is dedicated to supporting this format and is indeed, optimised for this format.

The relatively few excursions into miniaturised chromatography have not actually created a significant impact in the uptake and use of these techniques for a number of reasons. Liquid chromatography becomes substantially more difficult to use well on a miniaturised (<1mm column diameter) scale. There is little support from within for commercial vendors to design dedicated equipment to make these issues easier. On the other hand with the recent development of Capillary Electrophoresis, where the use of miniaturised columns are mandatory for heat reduction reasons, there is now a strong belief, in the scientific community, that electrically induced flows should be used to extract maximum performance from purely chromatographic systems using similar levels of miniaturisation.

These are powerful arguments and it is clear that knowing what 'direction' to follow is more important at this stage than following each one and seeing whether it leads anywhere. Electrically driven systems offer certain advantages. The purpose of this study is primarily to investigate the opportunities offered by capillary electrochromatography (CEC), which is the term used to describe chromatography under conditions of electrically driven flows in small diameter packed HPLC-type columns. More formally, the objectives which follow identify key pieces of knowledge, that are needed to understand the best way to configure and operate CEC systems to enable us to evaluate their real, routinely obtainable performance.

1.1 Objectives

To investigate and reduce to common practice the methods to produce reproducible packed capillaries of high quality, capable of performing reliable analysis with the expected performance benefits associated with electrically induced flow profiles.

To develop routine analysis methods that utilise the best practices for performing CEC within the confines of its operational limits.

To study the factors affecting solute band broadening, particularly at the interface of the packed and open tube sections of the column. To develop a strategy to minimise this broadening to acceptable levels and demonstrate this is achievable. To discuss the opportunities to perform these tasks routinely and where possible advise on further work to enhance these capabilities even more.

To study the thermal effects on the efficiency of CEC separations, determine where the operational limits lie, and compare the practically obtained data with what has been predicted theoretically

To use the knowledge obtained in understanding the operational limits of the system and the mechanisms of controlling dispersion to improve current practice for combining CEC separations with mass spectrometry. To demonstrate the feasibility of this technique and comment on future improvements necessary to reduce this to routine.

Chapter 2. The Story so far...

In this thesis we shall be dealing primarily with the technique called Capillary Electrochromatography (CEC). This may be regarded as a hybrid between HPLC and capillary electrophoresis (CE). Before proceeding further, it will be helpful to deal with the background theory to these two techniques.

2.1 The development of HPLC

The current practice of HPLC, described in outline in the previous chapter, originated in the pioneering work of Martin and Synge in 1941 [1]. Their initial process was a tedious, step-wise counter current separation but this was soon improved using a column filled with silica gel particles and eluting with an organic solvent (chloroform) as mobile phase. In their seminal paper of 1941 describing this work, they also proposed their well known plate theory of chromatography, the terminology of which has survived to this day. Most importantly, they recognised the importance of reducing the stationary phase particle diameter in order to improve the speed of their method. They also recognised that high pressure would be required in order to generate the necessary flow rates and they predicted that sophisticated separations could be achieved by using a gas instead of a liquid as the mobile phase. This suggestion was not taken up until the 1950's when Phillips (1949) and Martin and James (1952) gave the first successful demonstrations of gas chromatography. Very quickly the method became popular, especially with petroleum companies. The elucidation of the theory of band spreading

by van Deemter, Klinkenberg and Zuiderweg in 1956 was a major breakthrough which led to optimisation of the operating conditions for GC.

It was the application of GC theory to liquid chromatography in the 1960's following the ideas of J. C. Giddings which really drove the development of HPLC. But it was not the early 1970's that the methods to fabricate high quality uniform stationary phase particles were developed. So it transpired that the 1970's saw an explosion in the use and understanding of HPLC [2]. Thereafter, sufficient separation power became available to tackle almost any separation problem, with good performance, in a reasonable time. In the pharmaceutical business in particular, HPLC became an instantaneous success. During the 1980's most work in the area of HPLC was aimed at consolidation of existing knowledge and an expansion of the applications into new areas. Most developments from 1972 onwards, seemed superficially small, but actually were focussed mainly on improvements to the reproducibility of bonded stationary phases. In reality, significant advances were made. Also the HPLC equipment was increasingly connected to more information-rich detectors, such as mass spectrometers (MS) and even NMR, that vastly improved the qualitative aspects of the technique. These detectors also promised desirable benefits from a miniaturisation of the separation system so that during this time the compromises surrounding smaller diameter columns were explored, through the work of Novotny [3,4], and Ishii [5].

As in the early 1970's when rapid column development drove the requirement for new instrumentation, the same issues are arising today with miniaturisation of the HPLC column.

2.1.1 Partition Coefficients

The ability of a chromatographic column to separate two analytes depends on two main factors, firstly the relative rates at which the two species are eluted, and secondly on the rate of band broadening as the bands move along the column. The elution rate of any analyte is determined by the magnitude of its partition or distribution coefficient between the mobile and stationary phases. This distribution may be represented as a "chemical equilibrium" between the analyte in the stationary and mobile phases respectively.

$$A_M \leftrightarrow A_S \qquad (2.1)$$

The equilibrium constant K for this reaction is termed the partition, or distribution coefficient and is given by equation 2.2

$$K = \frac{c_S}{c_M} \qquad (2.2)$$

Where c_S is the concentration of analyte in the stationary phase and c_M is the concentration of the analyte in the mobile phase. Each component separated will, in principle, have a different value for K, each reflecting its affinity for the stationary phase. Phase preference can also be expressed in terms of capacity factor k'

$$k' = \frac{q_S}{q_M} \qquad (2.3)$$

Where q_s and q_m are the total quantities of analyte (rather than their concentrations) in the stationary and mobile phase respectively. The components present in a mixture must have different K and k′ for a separation to be achieved. Equation 2.2 and 2.3 are related by Equation 2.4

$$k' = K\phi_p \qquad (2.4)$$

Where ϕ_p is the phase ratio in the mobile and stationary phase and equal to V_S/V_M. Where V_S is the volume of stationary phase and V_M the volume of mobile phase in the column. It may be noted that with an adsorbent, the stationary phase is more usefully characterised by its area rather than its volume. The concentration of analyte in the stationary phase then has to be given in terms of amount per unit area rather than amount per unit volume.

2.1.2 Retention Time and capacity factors.

Retention time, t_R is the time it takes, after the sample is injected, for the analyte peak to reach the detector. When the peak has eluted , its width (w) can be measured by physically measuring the width from the recording medium, eg chart paper and

expressing this in appropriate units. $w_{1/2}$, the width of the peak at half height can be measured instead. It is usually more accurate to use $w_{1/2}$ since this value is not affected by baseline disturbances or peak tailing. The void time (t_0), is the time taken for any one molecule of mobile phase solvent to pass through the column. This is measured by injecting an unretained species (ie. one that does not interact with the stationary phase). Therefore anything eluting at this time has passed through a single interstitial column volume. The void time t_0 is difficult to measure with high confidence, but is usually taken as the retention time of a solute such as a solvent (acetone or uracil are often chosen), or as the retention time of the perturbation often seen on the baseline associtated with the 'shockwave' or refractive effect propagated following sample injection.

Another useful retention parameter is the net retention time defined in equation 2.5.

$$t'_R = t_R - t_0 \qquad (2.5)$$

The average velocity (u), at which an analyte moves through the column of length L, is given by the equation 2.6

$$u_{band} = \frac{L}{t_R} \qquad (2.6)$$

The linear flow rate of mobile phase is defined by;

$$u_0 = \frac{L}{t_0} \qquad (2.7)$$

Where t_0 is the time required for a molecule of the mobile phase to pass through the column.

So far we have relied on attempting to characterise a peak by its retention time. The parameter in which we are really interested is k', as this is related to fundamental thermodynamic properties which are unique, at a given temperature, for each solute. The retention times represent the experimentally measurable parameters that allow access to k'. The relationship between these parameters is given in equation 2.8.

$$k' = \frac{t_R - t_0}{t_0} \qquad (2.8)$$

The more a component interacts with the stationary phase, the more it is delayed relative to t_0 and the greater the capacity factor (k') value. For HPLC separations it is a general rule of thumb to keep the capacity factors of solutes between 1 and 10. If k' values are too low it is possible that the solutes may not be adequately resolved since little stationary phase interaction occurs, while for high k' values the analysis time becomes unnecessarily long.

2.1.3 Theoretical Plates and Column Efficiency

Martin and Synge [1] defined theoretical plates as a series of discrete contiguous narrow transverse segments of the column. They postulated that, within each theoretical plate, an equilibrium was established between the analyte in the mobile and stationary phases. They further postulated that the chromatographic process could be mimicked by sequentially moving the mobile phase in each plate into the next plate and then allowing re-equilibration to occur. This process was then repeated a very large number of times so that a band of analyte would slowly migrate along the column. They showed that a band eluted through a large number of plates assumed a Gaussian profile whose width (standard deviation in fact) equalled the square root of the number of plates through which the band had migrated. A given column could thus be characterised by the height equivalent to a theoretical plate, denoted by HETP or more simply H, and by the number of theoretical plates to which it was equivalent, denoted by N.

While the terminology of the theoretical plate is both misleading and archaic it still remains, and the way in which the HETP is interpreted has been explored extensively since it was originally proposed. In reality, when a small quantity of analyte is injected onto the column it should form a narrow band at the column top. As it gradually migrates through the column, the band becomes broader. In a uniform packed bed the band will broaden at a rate proportional to the square root of the total length it has travelled. Fortunately for chromatography, because bands get wider more slowly than they separate from one another (the distance between adjacent band centres

increases proportionately with total distance travelled), a separation actually improves the further a band migrates along any column.

A chromatographic band can be considered to be a statistical distribution of molecules. A characteristic parameter of **any** distribution is its second moment, or variance σ^2. The width of a band is always proportional to the square root of the variance of the distribution, with the proportionality factor depending on the type of distribution. For a well behaved chromatographic peak the profile should be a symmetrical Gaussian, the standard deviation of the distribution, i.e. the square root of its variance, is the half-width of the distribution at 0.606 of its full height. As has been explained, if the width of a peak increases with the square root of the distance travelled, then the variance increases linearly with the distance travelled. Therefore a plot of variance against length is a straight line with the slope giving us the HETP, more often called H. That is:

$$H = \sigma^2/L \qquad \textbf{(2.9a)}$$

Column efficiency and plate count are synonyms. The plate count is a measure of the quality of the separation, by giving an indication of the amount of dispersion taking place. The plate count (N) is given by the length of the column (L) divided by the HETP

$$N = \frac{L}{H} \text{ or } = \frac{L^2}{\sigma^2} \qquad (2.9)$$

The plate count is a measurement based on a single peak. Since H is a function of many different parameters, the plate count is not a specific property of a column and therefore not strictly a measure of column quality. It can sometimes be used inappropriately by column manufacturers in this way. N can be obtained very conveniently from a chromatogram by comparing the peak width and corresponding retention time, **providing** that the peak has had a constant migration velocity through the column during the recording of the chromatogram. This condition only applies with isocratic elution, that is elution with a solvent of constant composition. The plate height cannot be measured when using so-called "gradient elution", where the composition of the eluent is progressively changed throughout the chromatographic run.

There are a number of different ways to measure the plate count. All approximate the variance of the peak, by comparing the ratio of the peaks retention time to the peaks width at alternative positions in its height. In general this takes the form;-

$$N = \frac{L^2}{\sigma^2} = f\frac{t_r}{w_p^2} \qquad (2.10)$$

Where f denotes the particular height position at which the peak width is measured. Retention times and widths are measured in the same units, f has the following values.

Method	Percentage of peak height at which peak width is measured.	Factor f.
Inflection point	60.7%	4.000
Half-height	50%	5.545
4σ method	13.4%	16.00
5σ method	4.4%	25.00
Tangent method	Intersection of tangents with baseline	16.00

Table 1. Different parameter values used for calculating plate count at different positions of a peak's height (substituted in equation 2.10).

2.1.4 Reduced Parameters

The concepts of reduced velocity (ν) and reduced plate height (h) are useful when comparing columns with one another under a wide range of mobile phase conditions and over a range of particle sizes. We can use the principle of corresponding states to form dimensionless parameters from H and the linear velocity. The HETP (H) has a dimension of length, to make it dimensionless we simply divide by the particle diameter;-

$$h = \frac{H}{d_p} \qquad (2.11)$$

Similarly, we can do the same for the linear velocity by multiplying it by the particle diameter and dividing by the diffusion coefficient in the mobile phase. Such that;-

$$v = \frac{ud_p}{D_m} \qquad (2.12)$$

2.1.5 Dispersion

Chromatographic peaks have a finite width. The wider a peak becomes, the more it impairs the chance of chromatographic resolution. Therefore it is in the chromatographers' interest to minimise the amount by which a band 'widens' during chromatography. This is best achieved by understanding the factors that contribute to band broadening, this is often termed the 'hydrodynamics' of chromatography.

There are three primary mechanisms that produce dispersion of a solute band as it travels through a packed bed. In order to achieve an efficient separation i.e. one that produces a high number of theoretical plates, all these mechanisms need to be optimised to reduce H to its minimum value. Since each of the dispersion mechanisms has its own independent variance, and since variance for independent random processes are

additive, we can assume that the contributions to plate height are also additive [6] The three dispersion mechanisms can be discussed separately and the final plate height equation (Equation 2.14) obtained by adding their contributions as shown in Equation 2.13

$$h_{Total} = h_A + h_B + h_C \qquad (2.13)$$

It was Van Deemter, Klinkenberg and Zuiderweg in 1956 who first identified the three independent processes which contributed to band dispersion in chromatography.

Their first contribution to H, now generally called A-term, arises from the existence of alternative flow paths by which the solutes can travel through the column. These different paths arise due to the random irregularities in the size and shape of the stationary phase particles. This creates an opportunity for molecules in initially the same place, to end up travelling the same distance in the same time, but to end up in different places. This effectively creates a 'spread' of the same solute molecules along the length of the column. This is a significant contribution to the overall dispersion. The flow contribution arises from purely geometric effects and is independent of flow rate. The contributions to H and h from Eddy diffusion are represented by Equation 2.14.

$$H = Ad_p \text{ or } h = A \qquad (2.14)$$

Where A is a constant. The value of A can be as low as 1 for a uniformly packed column, but values in the range of 2-4 suggest a poorly packed chromatographic bed

The 'A' term contribution to H, as conceived by Van Deemter et al, is independent of the mobile phase velocity but does depend on the size of the stationary phase particles and how well the column is packed. A low van Deemter A-term will be achieved by using small, regular shaped particles, which are uniformly packed into short columns. This will reduce the difference in the flow paths travelled by identical particles.

The second contribution identified by Van Deemter et al, the B-term contribution, arises from molecular diffusion (B), that is from random molecular motion of solute molecules in the mobile phase. As the mobile phase moves through the column solute molecules diffuse in all directions. The longitudinal component of this diffusion, which is along the axis of the column, results in axial spreading of the zone, a similar outcome to that obtained by A-term contributions. Its value is proportional to the time the sample spends in the column, and is reduced by any tactic which reduces the chromatographic analysis time, as long as it is at the same temperature.

The dispersion of a band of solute σ_z, within the column is the same whether stationary or moving and is given by the Einstein Equation, 2.15

$$\sigma_z^2 = 2D_{eff}t \qquad (2.15)$$

Where, t is the time spent in the bed and D_{eff} is the effective diffusion coefficient.

The time for diffusion is the total time that the solute resides in the column $(1+k')t_0$ and therefore

$$\sigma_L^2 = 2\gamma D_M (1+k')t_0 \qquad (2.16)$$

Where D_M is the solute diffusion coefficient, σ_L is the dispersion of a solute band measured at the outlet, k' is the capacity factor and γ is the tortuosity constant. Since t_0 = L/u then σ_L is equal to

$$\sigma_L^2 = 2\gamma D_M (1+k') \ L/u \qquad (2.17)$$

u is the linear velocity of the mobile phase. D_M is the solute diffusion coefficient where D_{eff} is equal to γD_M. Equation 2.17 can be rewritten in terms of particle size and h, since

$$h = \frac{\sigma_Z^2}{L d_p} \qquad (2.18)$$

then

$$h = 2\gamma(1+k') \ (D_M/ud_p) \qquad (2.19)$$

For ease of comparison column efficiency is best stated using reduced parameters, since ν is defined as

$$\nu = \frac{u d_p}{D_M} \tag{2.20}$$

hence

$$h = 2\gamma(1 + k') \ (1/\nu) \tag{2.21}$$

$2\gamma(1+k')$ is often quoted as B. Thus the plate height contribution is obtained by substituting Equation 2.21 into Equation 2.20 to give

$$h = \frac{B}{\nu} \tag{2.22}$$

The experimentally determined value of B is generally around 2 but exact measurement is difficult [6].

The third contribution identified by Van Deemter et al, the C-term contribution arises because the rate of the partitioning process of the solute species between mobile and stationary phases is not instantaneous when compared to the rate at which the solute is moving in the mobile phase. When the solute species come in contact with the stationary phase, they may spend some time in or on the stationary phase before they rejoin the mobile phase, and during this time they are left behind by the solute molecules that do not interact. Commonly, the stationary phase has an open porous structure and the internal pores will contain immobile, or stagnant mobile phase, which

the solutes will have to pass through before they can interact with the stationary phase. Solutes that diffuse a long way into the porous phase will be left behind by the solute molecules that by-pass the particles or only travel a short distance into it.

The diffusion time for this process is given by Equation 2.23

$$t = q' d_p^{\,2} / D_S \qquad (2.23)$$

D_S is the diffusion coefficient in the stationary phase and q' is a constant that for a regular spherical particle $q = 1/30$ [7].

The distance that the eluent flows in this time (ut) is defined as

$$r = \left(q' d_p^2 / D_S\right) u \qquad (2.24)$$

which can be expressed in terms of d_p to give

$$r/d_p = q' u d_p / D_S \qquad (2.25)$$

Substituting for u using Equation 2.20 gives

$$r/d_p = \left(q' D_M / D_S\right) v \qquad (2.26)$$

The plate height contribution h is proportional to (r/d_p). Since the band as a whole is moving, the proportionality involves k'', where k'' is the zone capacity ratio, and represents the quantities of solute in the moving and static zones. The final equation for the plate height contribution is

$$h = \left[q'k''/(1+k'')^2\right] \ (D_M/D_S)v \qquad (2.27)$$

The term preceding v for ease of clarity is usually termed C and therefore

$$h = Cv \qquad (2.28)$$

Theoretically C should be in the region of 0.01 to 0.02, but experimentally determined value of C are more normally around 0.1 [6].

The van Deemter analysis results in an overall equation for h, or H of the form

$$H = A + B/v + Cv \qquad (2.29)$$

The van Deemter equation, which shows the contributions from the various band spreading mechanisms is displayed graphically in Figure 1. The important thing to note from this plot is that each component contribution to dispersion (A, B or C) plays a

more dominant part depending on the flow through the column. At low flow rates (or reduced velocities) the B term contribution (diffusion) dominates dispersion effects. At higher flow rates the non-instantaneous nature of the solutes' interaction with the stationary phase (C term) is the major contributor. At this time, the A-term dependence was considered to be largely independent of flow rate. The outcome of the individual contributions to dispersion is that there is an optimum flow rate to obtain minimum H. If we assume that the A term contributes about the same amount of dispersion, whatever the flow rate, and that the B term is minimised at higher flow rates, yet the C term is minimised at lower flow rates, there is going to be an optimum. Accordingly chromatographic parameters should be adjusted so that one works at the minimum h. There is a complication here that if you work in reduced terms it is not immediately clear that minimum h gives the optimum, whereas with a straight plot of H versus u it is clear that one should work at the lowest u for the highest N with any given column.

2.1.5.1 Optimisation of performance.

The work of van Deemter et al indicated clearly that there is an optimum 'set' of conditions to perform any given chromatographic separation. However, they considered that that the dispersion caused by the flow was a purely geometrical effect that was unaffected by flow rate. Subsequent work by Golay [8] illustrated well that, in an open tube, without transverse diffusion there would be near infinite dispersion due to the wide range of velocities of the stream lines within the tube (ie slow at the walls, fastest down the centre). This led to recognition that there were two mobile phase processes

contributing to dispersion in a packed column. The effect of obstructed flow around and through the particles, and the effect of the flow profile across the column bore, which was partly compensated for by transverse diffusion (across the bore). Giddings [9] recognised that these two processes actually combined to reduce overall dispersion and over time developed the 'coupling' principles [7]. Subsequent work by Knox and co-workers practically refined these principles to simple equations for the A term contribution, which closely fitted data obtained over a wide range of operating conditions. This led to the Knox form of the equation (2.30), which fitted practical data well over the most likely range of operation [10]. This equation is probably the most widely used form of the original van Deemter equation and has been used extensively to deduce optimised conditions for various chromatographic systems.

$$h = Av^{1/3} + \frac{B}{v} + Cv \qquad \textbf{(2.30)}$$

In a system with pumped flow, the flow rate is governed by the following relationship;-

$$u = (d_p^2 / \phi\, \eta)\, (\Delta p / L) \qquad \textbf{(2.30a)}$$

Where ϕ is the column resistance factor.

The message, from the dependence of both the flow and pressure drop on the square of the particle size is quite clear. If small particles are used, and we know from the analysis of the Van Deemter or Knox equations that they are beneficial to minimise dispersion, then it will cost in terms of equipment specifications. A detailed study of optimisation parameters was carried out by Knox and Saleem in 1969 [11] and the conclusions drawn in this paper were very much the same as they are today. The ultimate limit to chromatographic performance in any pressure driven system is the maximum pressure drop the equipment can develop. As we want to use the smallest possible stationary phase particles to give the lowest h or greatest N, but we don't want to suffer long analysis times, we will develop a high pressure as a consequence of driving the flow as fast as possible.

To consider some 'ball park' figures for a typical system, we have a linear flow rate of 1.5-2 mm/ sec, through a suitable column diameter of 10cm length, packed with 5μm diameter particles, pumping water as a mobile phase. This will produce about 1000 psi (70 bar) on a system that is configured with suitable connection tubing. This could easily be managed by a typical HPLC system. If we were to repeat this operation with 3μm particles the pressure drop for the same arrangement would be more like 2,500 psi (180 bar). Or, for the same pressure drop we could only run at a flow rate of 0.6-0.8 mm/ sec. This would mean that our analysis would take over twice as long on the smaller particle size material. The current practical limit lies with the maximum pressure setting that the instruments will tolerate without difficulty. This is about 6,000psi (400 bar) and this limitation is generally caused by the sealing face of the

sample valve, which will start to leak much above this. The practical maximum flow rates achievable on our model system would be about 3-3.5 mm/sec for 3μm particles. This would enable overall analysis times, for a k′ value of the most retained peak of 10, of about 5-6 minutes. If we were to consider using 1μm particles in a similar way it would require a pump capable of delivering liquid at pressures above 50,000psi (3600 bar) to achieve these flow rates. This type of equipment is not commercially available at this time and we would be likely to encounter other difficulties within the column, as frictional resistance to flow would cause heating and this may well cancel any potential gains in separation performance. So, current 'state of the art' performance for HPLC is the use of 5-15cm long columns of 2-5mm in diameter packed with 3μm particles, at linear flow rates of 1.5-2.5 mm s^{-1}.

2.1.6 Practical Equipment

The design of HPLC equipment has changed very little in the last 25 years or so. Most of the instrument design is effectively limited by the physical requirements necessary to optimise the chromatography separation. The most important part of the chromatography system is undoubtedly the column itself. The column has been tweaked over time to become a very efficient, reproducible device with predictable behaviour, although it has taken rather a long time considering current 'best practice' was predicted in the late 1960's [11].

The basic HPLC equipment shown diagramatically in Figure 1a consists of a solvent reservoir, a solvent filter, a high pressure pump, a sample injection valve, the

separation column, a detector all coupled to an electronic data handling and control system which amongst other functions records the detector response as a function of time.

On a journey through a HPLC system, a solvent molecule would first of all start in the mobile phase reservoir. It would pass through a pick-up filter on the end of the solvent line connected to the inlet of the pump. At this point it is being filtered to remove any contaminant solids such as hairs, fibres etc. The mobile phase is being 'sucked' towards the pump by the vacuum action of the pistons causing a drag as they refill. This suction opens the inlet check-valve at the bottom of the pump head, allowing a free movement of fresh mobile phase to be drawn into the pump head. The mobile phase may well pass through a vacuum degasser unit on its way down the inlet line, if it has not already been degassed 'off-line'. Degassing effectively removes dissolved gas, which could otherwise come out of solution during the pumping cycle and cause flow fluctuations. On entering the pump the mobile phase first passes through an inlet check valve which allows only forward flow of liquid. Once in the pump head the mobile phase is compressed by the action of the piston on the compression stroke. Pumps generally employ dual reciprocating pistons, which operate180 degrees out of phase, so cancelling out any pulsation effects through the fluid path by the principle of annihilation. This compression raises the pressure in the pump head to just above the current system pressure. This has the effect of shutting the inlet check valve to make sure no mobile phase flows backwards, and opening the outlet check valve so the pumped flow is pushed through and towards the column. Just prior to the column the

mobile phase flows through the internal fluid path of the sample valve. This valve contains a sample loop, filled with sample, which at this point is isolated from the pumped flow. The valve is designed so that the sample can be put in the correct place in the valve without stopping the flow. At a convenient point the valve is switched such that the sample loop is now connected to the flow and therefore the sample is swept onto the column. From this point on, until detection, it is very important that all volumes introduced by the necessary connection of column to valve and so on, are minimised. Otherwise unnecessary extra-column dispersion will occur which will broaden eluted bands and reduce separation efficiency. The separation takes place in the column and as the molecule travels down the columns length, the pressure it is experiencing is dropping lower and lower. The separated components are then carried, in the mobile phase, through the detector cell which is only slightly above atmospheric pressure. It is again important that this cell has a very small volume, compared to the volume of the peak it is detecting, otherwise chromatographic efficiency will suffer. After being detected the mobile phase travels to waste or possibly a programmed fraction collector to isolate separated bands. The whole process from reservoir to waste would take about 5-10 minutes with only 1-5 minutes of this being from sample valve to detector.

The requirements of the instrumentation to manage this process as described would typically be;-

Pump – High pressure, dual reciprocating pistons with out of phase eccentric cam drives. Electric motor powered. Piston shafts constructed of industrial sapphire.

Check valves with ruby-ball and seat valves. The maximum operating pressure of modern HPLC pumps is around 400 bar or 6000 psi.

Sample valve – High quality stainless steel and inert polymer construction. All fluid paths inert (sometimes even biocompatible such as titanium or PEEK construction).Very low volume internal fluid paths (< 2μl) to minimise extra-column dispersion.

Detector – Variable wavelength or diode-array (allows on-line real-time spectra acquisition) via very low volume cell (<10 μl) which to maintain sensitivity would have >5mm path length.

Plumbing – All high pressure connections prior to sample introduction from the pump outwards would be in 0.030" diameter steel or PEEK (polyetheretherketone) tube (or slightly smaller). Tubing diameters between sample valve and column, and column to detector should be 0.010" or less (preferably 0.005" diameter).

Using this system and column with optimum flow rate conditions would give an operational back pressure of 50-70% of the system maximum depending upon the mobile phase viscosity. This does not allow much scope for increasing the flow rate or reducing the particle diameter, even though there are benefits to be gained by doing both these things.

While it is clear that there are advantages to be had by performing pumped flow chromatography at higher linear flow rates with smaller diameter particles, this is possible only if we can handle the back pressures generated. Regrettably, the current use of HPLC is confined by the pressure limitations of commercially available

instrumentation. It is also true that HPLC analyses can be made far more 'generic' by the adoption of gradient elution methods [12] . This method of analysis is used to elute a much wider range of solute polarities in the same analysis, by changing the solvent composition during the separation.

2.1.7 The need for miniaturisation

It seems clear for a number of beneficial reasons, that miniaturisation is sensible for liquid chromatography in general. Advantages to be gained by moving to smaller diameter columns include improved mass sensitivity, and the potential for improved performance. It appears that in smaller diameter columns there is a lower degree of flow related dispersion (A-term) of the solute band. This is believed to be because the columns are more homogeneously packed across the smaller diameter, which reduces transcolumn retention variations.

There are also more practical advantages to miniaturisation of the column dimensions, including significant savings in the cost of mobile phases (for the same linear flow rate, a halving of the column diameter means a factor of four drop in the mobile phase consumption). This is even more apparent when we consider that solvent waste can often cost substantially more to dispose of than to buy! A reduction in the cost of filling columns with some of the specialised stationary phases which in some cases, notably chiral phases, can be very highly priced would also be attractive and would make these phases far more accessible than currently.

Coupling of LC to Mass spectrometry is becoming increasingly important as the identification of closely related species is required, for example proteins and peptides. A common way in which LC/MS is practiced involves the use of standard column diameters consuming mobile phase at typical flow rates of 1 ml/min. This however is far above the 'optimum' flow rates associated with MS interfaces, and so the flow is split such that only a controlled proportion of it is entering the MS. This split is normally somewhere between a 20-50th of the original flow and so most of the sample (>95%) is sent to waste.

A further driving force for miniaturisation comes from modern chemistry techniques many of which produce extremely small amounts of sample. Instances of this would be products from combinatorial chemistry experiments and from single-cell analyses.

It seems unlikely that we can continue to maintain our reliance on these 4.6mm formats as it will become increasingly difficult to justify the cost of what is fundamentally a lower performance option, which requires sample amounts inconsistent with future possibilities in sample production and characterisation.

2.1.8 The problems with miniaturisation

There are many problems to overcome with miniaturising the chromatographic separation column without compromising the potential advantages gained by doing so. For good chromatographic performance an important requirement is a well packed,

efficient column giving reproducible and long lasting performance. There is a secondary requirement to maintain the integrity of the chromatography by ensuring that the sample can be introduced, and detected, without losing too much of this performance. As the column dimensions and therefore the column volume are reduced, corresponding reductions in the injector and detector volumes are also required. This becomes increasingly difficult technically as column diameters drop below 1 millimetre. The comparison of column diameter sizes with amounts injected and detector cell volumes illustrates this problem well (Figure 1b).

In recent years much effort, based on predicted advantages, has been put into developing microbore LC [13-25] and yet due to the associated difficulties the technique is still only used by the most accomplished practitioners. Nevertheless, the use of microbore LC in conjunction with MS detection is common, as there is often no need to split the flow and the desire for much smaller sample requirements often outweigh the technical problems. It is likely that as microelectrospray interface development is perfected, then smaller 'optimum' flow rates will be along with still smaller diameter separation systems.

2.2 Capillary electrophoresis

Electroosmosis (EOF) is the bulk fluid flow created at a surface, by the application of an electrical field between two, fluid-connected electrolytes. It originates due to a shear in the layer of solvent close to the surface itself, and this is explained in

more detail in the following section. It was recognised as an alternative way of driving a liquid through a 'bed', in this case a gel, as long ago as 1949 [26-27]. In its early form 'gel electrophoresis' was slow and inefficient and barely gave the same results twice. In more recent times however, this technique has become the technique of choice for biopolymer separations such as proteins and DNA fragments etc. In 1981 the general form of electrophoretic separation was given a massive boost, in work published by Jorgenson and Lukacs [28] which demonstrated the huge improvements in separation efficiency and speed that were possible if electrophoresis was performed in narrow capillary tubes. This spawned a rapid development of instrumentation to support the use of these techniques and capillary electrophoresis became an attractive technique to the chromatographers interested in miniaturisation.

Capillary Electrophoresis (CE) is now a powerful technique widely applied in different areas of research e.g. pharmaceutical, biological, environmental etc. The different separation modes, namely capillary zone electrophoresis (CZE), micellar electrokinetic chromatography (MEKC), isotachophoresis (ITP) and capillary gel electrophoresis (CGE) make CE a very important tool for analysis. All electrophoretic techniques essentially involve the movement of sample ions under the influence of an applied electric field.

CE superficially resembles HPLC but is not chromatography since the separation depends upon differences in electrical properties among analytes rather than differences in the way the solutes distribute themselves between the mobile and stationary phase. The separation is achieved by relative differences in the analytes'

charge to mass which determines their electrophoretic mobility. The higher the ion's mobility, the faster it will move under the applied electrical field, either with or against the background EOF depending on the ion's polarity. The magnitude of this flow is dependent on other factors and is detailed in equation 2.37.

The layout of the instrument necessary to perform CE is very simple and is shown in figure 2. One of the main advantages in using CE is the ability to sample extremely small volumes directly from the sample solution. This is possible because electroosmosis creates an induced flow that will sweep a portion of bulk sample solution onto the capillary. It is also possible to pressure or vacuum inject in exactly the same style. The disadvantage of using electrically-induced sample introduction is the opportunity to introduce discrimination for differently charged species. But the ability to literally 'dip' the separation column into the sample and reproducibly inject is an extremely important one. This eliminates a lot of the problems associated with high-pressure valve injectors that are needed to inject miniscule volumes in small-scale pressure driven systems. Once the sample is loaded, the sample vial is swapped for the running electrolyte vial, the power re-applied and the separation occurs.

2.2.1 The Origin of Electrically-Driven Flow

In a small diameter capillary, consistent with the model being discussed here, there are two ways of driving a liquid flow through the capillary, by the application of hydrostatic pressure, or by the application of an electric field. The two methods can be

used independently or together, but there are distinct differences between the properties associated with them. The factors affecting the optimum use of pressure-driven systems (as in HPLC) have been extensively described previously [30-32]. The factors affecting the equivalent electrodrive systems have been discussed in detail by J.H.Knox [33] and are summarised below. For more detailed discussion of the underlying theory the following references are recommended [34-35].

The flow in an electrically driven system arises as a result of the electrical double-layer which covers all surfaces immersed in liquids , and is termed electroosmosis. In an open capillary tube, this flow originates very near to the inner wall due to the net charge differences between the wall itself (which, when the surface is silica, has a net negative charge due to loss of some positively charged ions to the solution) and the solution phase very near to the wall (which therefore has a net positive charge). This 'charge balance' effect only occurs very close to the wall, typically within 10nm, and is called the "electrical double layer". This means that we may consider the main bulk of the solution (which bears no net charge) to behave like a rod within a tube. The outer surface of the rod is positively charged, while the inner surface of the tube is negatively charged. When a potential is applied across the capillary a shear force is created between the surfaces. This cau*ses* the "rod" or solution to move by virtue of the positively charged edges being attracted to the electrode of opposite polarity, and dragging the main core of the solution along. However, because there is no net charge in the main bulk of solution the flow profile across most of the core is absolutely flat.

Furthermore, as the rod outer surface is negligibly thick the flow as a whole within the capillary is near perfect plug flow.

These differences in flow profiles create limitations in the use of these methods within open tubes. The use of pressure driven systems within open tubes causes significant flow related dispersion across the tube diameter. When the effect of transverse molecular diffusion is taken into account the net dispersion can be calculated from the Taylor equation [36]. If we also account for longtitudinal diffusion we obtain the commonly used equation for calculating the HETP for an **unretained** solute in an open tube;-

$$H = 2D_m/ u + u\, d_c^2 / 96\, D_m \qquad \textbf{(2.31)}$$

After differentiation to give the expression for the minimum value of H we obtain $H = d_c / 7$ at a corresponding eluent velocity of $u = D_m / 14d_c$. It is clear from these expressions and widely accepted that to obtain good performance in a short time frame with conventional equipment the working diameter would need to be about 1μm. Bearing in mind what was said for 180μm capillary LC columns in the previous section and these diameters are quite unrealistic for routine use.

In stark contrast, for electrically driven systems the second term in equation (2.31) does not appear: the plug-like flow profile ensures that there is no flow based solute dispersion. The only dispersive mechanism is axial diffusion, and the expression for H becomes ;-

$$H = 2\,D_m / u \qquad (2.32)$$

With no diameter term now present in the equation for HETP it appears that any capillary diameter may be used without any efficiency loss. The plate number can be calculated from ;-

$$N = L\,u / 2\,D_m \qquad (2.33)$$

Inserting typical values into this expression we obtain figures of N = 500,000 for open tubes irrespective of their diameter. However, as soon as any retention takes place and therefore transcolumn equilibration becomes necessary there is a diameter dependent mass transfer term in the plate height equation and a corresponding massive drop in performance, as discussed below. It is interesting to note that equation (2.33) contains the diffusion coefficient (D_m) in the denominator, and the flow velocity in the numerator. This means that molecules with small diffusion coefficients or bigger molecular weights (eg. peptides, proteins) should give higher efficiencies than smaller molecules. This is the opposite to other existing modes of chromatography. Even more surprisingly the plate count becomes higher the higher the flow velocity.

For **retained** solutes, the relevant equations for pressure and electrodrive systems are given below and are attributable to Golay [8] and Aris [37] respectively.

Pressure Drive $H = 2 D_m / u + (1 + 6k + 11k^2) / \{ 96 (1 + k)^2 \} (d_c^2 u / D_m)$ (2.34)

Electrodrive $H = 2 D_m / u + (k / (1 + k)^2) (d_c^2 u / D_m)$ (2.35)

In the pressure driven system there is a significant contribution to H even when $k' = 0$, and this is the reason why efficient open tubular pressure-driven HPLC cannot be carried out in open tubes wider than a few microns in diameter. There is then a further significant drop in performance (increase in H) when k' is non-zero, as was pointed out by Golay as long ago as 1958. However the situation with electrically driven systems is very different. There is no trans-column equilibration term when $k' = 0$ and this leads to the enormous plate efficiency of CE. But as soon as k' becomes non-zero the second term in equation 2.35 kicks in and H rises dramatically resulting in catastrophic loss of performance. For this reason even the slightest retention has to be avoided in open tubular electrically driven separations.

Further, more detailed discussion of the dispersion theory relating to retained solutes in electrodrive systems has been given by Martin, Guiochon, Walbroehl and Jorgenson [38-39].

2.2.2 More about the double-layer and the Zeta Potential

Electroendosmotic flow , as stated previously, arises in the electrical double-layer which exists at all liquid-solid interfaces. As the surface ionises due to loss of some surface charges , the 'lost' charge is close to the solid surface within the liquid phase. Overall there is a charge balance. Some of this excess charge, termed the Stern Layer, is very close to the solid surface, effectively immobilised to the solid. The rest of the excess charge is more mobile and is free to interchange with the ions in the liquid phase. This region of the liquid phase beyond the Stern layer is known as the 'diffuse' or Gouy layer. Compared to the overall ionic concentration the excess charge is negligibly small. The amount of excess charge falls approximately exponentially with distance from the solid surface. The distance termed the 'double layer thickness ' refers to the distance over which the excess charge falls by the factor e (2.718) and is denoted by the symbol δ. The double-layer is shown diagrammatically in Fig 3. The double layer thickness is calculated using equation (2.36) and some typical values are 10 and 1 nm for 0.001 and 0.01M electrolyte concentrations respectively.

$$\delta = (\varepsilon_\rho \varepsilon_0 \ R\,T / 2\,c\,F^2)^{1/2} \qquad (2.36)$$

where ε_r = dielectric constant or relative permittivity of medium, ε_0 = permittivity of vacuum , R = universal gas constant , T = absolute temperature , c = molar concentration (moles m^{-3}), F = Faraday constant

The potential at the boundary between the Stern layer and diffuse layer is termed the Zeta potential or ζ. This is of the order of between 0-100 mV. When a potential is

applied across the capillary the excess charged ions in the diffuse layer experience a force towards the relevant electrode which creates a shear across the double layers, and results in an electroosmotic flow (EOF). In a packed capillary exactly the same effect is observed and the particles each have their own double layer as discussed below and shown in Figure 4.

The linear velocity of this flow is given by equation (2.37)

$$u = ((\varepsilon_0 \varepsilon_r \zeta)\ (V / L)) / \eta \qquad (2.37)$$

$$= (\varepsilon_0 \varepsilon_r \zeta)\ E / \eta$$

and typically, for a zeta potential of 50mV and E of 50,000 V m^{-1} in water, would be about 1.8 mm s^{-1}. As mentioned earlier in this section the profile of the EOF is 'plug-like' provided that the double layer is small compared to the capillary diameter , However, as the diameter of the capillary approaches that of the double layer δ the flow reduces due to the overlap of the double layers and the flow profile tends to become parabolic. Rice and Whitehead [40] discuss this phenomena in much more detail and some graphical representations of this effect are shown in Fig 5 reproduced from their paper. Knox and Grant [35] also reproduced these graphs and proposed that as a general rule the EOF was acceptable when the ratio $u / u_\infty \geq 0.6$, or when $d / \delta > 10$.

Knox and Grant also extended the argument to packed tubes. In a tube packed with silica particles, a double layer will exist not only at the walls of the containing capillary, but also at the surface of each particle of silica. On application of an electric

field shear at all this extended double layer will occur and the liquid will be drawn along the packed tube at more or less the same velocity as it would be in an open tube. Of course for packed tubes the situation is different in as much as the "channel diameter" no longer refers to the capillary diameter but the mean 'gap' between the particles of stationary phase. This is quite a bit smaller than the particle diameter itself and may be estimated from the ratio of the ϕ values (column pressure resistance factor) for a bed of randomly packed impermeable spheres (where $\phi = 500$) to the value for an open tube ($\phi = 32$) for the equivalent capillary dimensions , this gives ;-

Mean channel diameter / Particle diameter = $(32 / 500)^{1/2} = 0.25$

Therefore for slurry packed capillaries (SPC's , the normal method of production) this suggests that EOF's will start to be reduced when $d_p < 40\delta$. For other methods of packed capillary production such as drawn packed capillaries (DPC's) , where the capillary is packed and then drawn after heating to a smaller diameter , the value of ϕ is 120 and therefore the condition for the EOF maintenance is $d_p < 20\delta$. Table 1. below gives the minimum values of capillary diameter (for open tubular capillaries, OTC's) or particle diameter (for packed tubes) for different electrolyte concentrations that will maintain the condition $u / u_\infty \geq 0.6$ for a 1:1 electrolyte in water. Diameters below those given in the table will cause significant reduction of the EOF and cause the flow profile to become parabolic.

Table 1. Minimum capillary and particle diameters for normal EOF maintenance

c	c	δ	Minm. capillary (d_c) or particle (d_p) diameter / μm		
mol m^{-3}	mol dm^{-3}	nm	OTC $d_c = 10\ \delta$	DPC $d_p = 20\ \delta$	SPC $d_p = 40\ \delta$
10^{-2}	10^{-5}	100	1.0	2.0	4.0
10^{-1}	10^{-4}	31	0.3	0.6	1.2
1	10^{-3}	10	0.1	0.2	0.4
10	10^{-2}	3	0.03	0.06	0.12
100	10^{-1}	1	0.01	0.02	0.04

From the table it can be seen that for the normal expected operating range for the electrolyte concentration of between 0.001M - 0.05M there are likely to be no deleterious effects on either the magnitude of the EOF or indeed the shape of the flow profile. It would appear that particles as low as 0.5μm can safely be used and this should give opportunities to gain enormous performance benefits over current chromatographic systems. The minimum diffusion-limited plate height or $H = 2\ D_m / u$ is now approachable. This means that the efficiency of packed tubes can ultimately equal that of open tubes in the CE mode.

Careful choice of electrolyte concentration is needed to maximise the benefits on all aspects of the chromatographic performance , as the zeta potential ζ is dependent on the concentration and the pH of the electrolyte. In turn the EOF is directly proportional to ζ . Dilute electrolytes which would most benefit ζ would limit the particle size to 1-2 μm and would lead to irreproducible retention times as the 'buffering capacity' would be compromised for ionisable solutes. A more detailed coverage of this subject has been given by Everaerts et al [41].

2.2.3 Flow Rates and the effects of Self-Heating

The linear flow rates for pressure and electrodrive systems are given by the equations below;-

Pressure drive $$u = (d^2 / \phi\, \eta)\, (\Delta p / L) \qquad (2.38)$$

Electrodrive $$u = ((\varepsilon_0\, \varepsilon_r\, \zeta)\, (V / L)) / \eta \qquad (2.37)$$

$$= (\varepsilon_0\, \varepsilon_r\, \zeta)\, E / \eta$$

In these equations $E = V / L$ is the potential gradient along the length of the tube. Under pressure drive, the velocity, u, is proportional to d^2 where d is the tube diameter for open tubes or particle diameter (d_p) for packed tubes. For situations when electrodrive is used the diameter term does not enter the equation for flow calculation

and therefore the eluent velocity does not apparently depend on the tube or particle diameter. As reducing d_p normally leads to increased efficiency, this means, in principle, that no increase in the potential gradient is necessary regardless of the tube or particle diameter in electrodrive systems and, as has already been pointed out, this could lead to massive improvements in performance characteristics for small particles. This of course is not possible for pressure drive systems where the flow rate dependence on the square of the particle diameter means that there is a practical working limit to particle size, before back pressures become unworkable.

So far , for electrodrive systems, it would seem that there are no disadvantages or limitations as to its use and that the improvements over pressure drive should be nothing short of remarkable. However, there is a limit to the maximum performance available using electrodrive which arises from the effects of self-heating. This effect is much greater in electrodrive than in pressure driven systems. The prediction of heating effects in capillary systems has been properly studied by Knox and Grant and is referred to extensively in the following section.

Poppe et al [42-43] have proposed in detail the heating effects from frictional drag as a result of pumping fluids through packed columns. In brief, for an infinitely long cylinder where heat is generated homogeneously and lost through the walls, the temperature difference between the middle and the walls is given by;-

$$\Delta T = Q\, d_c^{\,2} / 16\, \kappa \qquad \textbf{(2.39)}$$

where Q is the rate of heat generation per unit volume within the cylinder and κ is the thermal conductivity of the medium

In pressure drive LC , Q is obtained from the frictional work dissipated in the column, and is given by $\Delta p \, u \, \varepsilon / L$, where ε is the porosity. u is obtained from equation (2.38) and therefore equation (2.40) gives Q.

$$Q = (\varepsilon \, d_p^{\,2} / \phi \, \eta) \, (\Delta p / L)^2 \qquad \textbf{(2.40)}$$

If we combine equations (2.39) and (2.40) we can get an expression for the temperature difference at the centre of the tube, ΔT;-

$$\Delta T = (\varepsilon / (16 \, K \, \phi \, \eta)) \, (d_p \, d_c)^2 \, (\Delta p / L)^2 \qquad \textbf{(2.41)}$$

taking typical values, $\varepsilon = 0.75$, $\Delta p = 100$bar , $d_p = 5\mu$m , $d_c = 5$mm , $L = 100$mm , $K = 0.4$ $Wm^{-1} K^{-1}$, $\phi = 1000$, $\eta = 10^{-3}$ N s m^{-2}, obtained;-

$$\mathbf{Q = 0.2 \ W \ cm^{-3}} \text{ , and } \mathbf{\Delta T = 0.7K}$$

As shown by Knox and Grant, for electrodrive systems, the situation is quite different as here the heat produced is due to the effect of the current flowing through the

electrolyte within the tube and this is given by V^2 / R where V is the voltage across the tube and R its resistance. Introducing the equivalent conductivity λ , and replacing (1/ R) by (λ c A / L) we obtain Q according to equation (2.42) ;-

$$Q = E^2 \lambda c \varepsilon \qquad \textbf{(2.42)}$$

The excess temperature is then given by applying equation (2.39) and we get

$$\Delta T = E^2 \lambda c \varepsilon d_c^2 / 16 K \qquad \textbf{(2.43)}$$

For typical values of E = 50,000 V m^{-1} , λ = 150 $cm^2 mol^{-1} \Omega^{-1}$ = 0.015 $m^2 mol^{-1} \Omega^{-1}$, c = 10^{-2} M = 10 mol m^{-3} , ε = 0.75 , d_c = 100μm , and K = 0.4 W $m^{-1} K^{-1}$ we then obtain **Q = 280 W cm^{-3}** and ΔT = 0.44 K

The heat generated per unit volume is considerably larger (1500 times in the examples chosen) than pressure driven systems and therefore working tube diameters have to be limited in CEC to avoid excessive heating effects. For this reason , miniaturisation is mandatory for electrically driven systems. For pressure systems it is only really necessary to miniaturise when particle diameters becomes very small. This has been understood for some time and has long been recognised in previous work in the fields of isotachophoresis and thin-layer electrophoresis [44].

If the relevant equations are used [33] to assess the contribution of the individual parameters to these dispersion effects in the electrodrive system, as Knox showed, the contribution to the plate height H from self heating should be proportional to $\mathbf{d_c^6 x E^5 x c^2}$ .It is evident from this relationship that small changes in the column diameter , potential gradient and the electrolyte concentration could cause devastating effects to the dispersion arising from self-heating .

For example, if the tube diameter is increased a factor of 2 from 100 to 200μm, then ΔT is increased a factor of 4 to 1.8K and H is increased 64 times to 0.4μm. If the potential gradient were then to be doubled, the value of H would reach 12μm. This would represent an unacceptable change. But, for example, a reduction in c from 0.01M to 0.002M would bring H back down to 0.5μm. Obviously the interplay between the diameter , field strength and electrolyte concentration is critical. For realistic performance expectations it is safe to assume that with fields up to 50,000 V m^{-1} capillaries of up to 200μm can be used with electrolyte concentrations up to 0.01 M (although by careful choice of low-conductivity buffers some leeway is possible).

2.3 Capillary chromatography (CEC), the future of miniaturised systems?

2.3.1 The Use of Packed Capillaries for CEC

In CEC the internal diameter of the packed capillary now contains numerous interconnected channels which vary considerably in terms of size, shape and direction

of orientation. As has already been noted, since the particles of packing are made of silica the surfaces of these channels will carry a zeta potential in the same way as the capillary wall. However, if the zeta potential is the same on the particles as on the tube walls, the EOF will be lower in a packed bed compared to an open tube. because the channels are not axially aligned Therefore if a channel is at an angle ϑ to the axial direction, the effective axial field is E $(\text{Cos } \vartheta)^2$ (where E is the field strength or potential gradient). The overall effect of the reduction in flow when all the individual channels are taken into account is obtained as a weighted average of them all. This situation is the same as for diffusion in a packed bed except that here a concentration gradient is analagous to the potential gradient. The well known 'tortuosity factor' , γ , found in the B-term of the Van Deemter equation [45] makes allowance for this effect. For non-porous spheres the value of γ is about 0.6 , and therefore the EOF of such a packed bed would be about 60% of that in an open tube. γ is somewhat larger when the particles are porous

A second effect arises from the porosity of most HPLC type packing materials. EOF will only occur outside the particles as the pores within the material are so small that they fall well below the diameter at which total double layer overlap occurs. The apparent velocity is then the true velocity multiplied by the value of (extraparticle porosity / total porosity) , which is typically in the range of 0.5 - 0.7 So overall , packed beds are expected to show a slight disadvantage in terms of flow rate. On the other hand, the double layer surface area is massively increased when compared to an open tube and the corresponding increase in double layer capacity should make them

far less susceptible to contamination , and result in much more stable , reproducible separations.

2.3.2 Improvements of CEC over Pressure Driven Systems

In comparison to pressure driven systems CEC gives a more uniform trans-column flow profile since the EOF is independent of channel diameter and should therefore give the same flow in each channel leading to a lower value for the A-term [35,46]. As explained earlier in this thesis we should also be able to use much smaller particles and generate enormous efficiencies from fairly short separation columns. These applications are unlikely to be achieved in the equivalent pressure driven system due to restrictions in either backpressure or time of analysis or complete inability to manage the separation by virtue of lack of efficiency. An extensive modelling study of the individual contributions to dispersion in both types of flow system was carried out by the chromatography group at Hewlett Packard in Waldbronn [46] following on from the work of Horvath [47-48]. Equations are described relating to each aspect of flow and non-flow related dispersion which well illustrate the 'gains' achieved by electrodrive. As was originally pointed out by Knox and Grant, and is evident from graphical representations of the data obtained by the group at HP (Figure 6), the biggest improvements using electrodrive are due predominantly to reductions in eddy diffusion (A term) caused by differences in flow velocities within individual channels, which is increased considerably in pressure driven systems. The reasons for this reduced flow

dispersion in CEC are illustrated diagrammatically in Fig 7. In the pressure driven system the local flow velocity of the solute band is dependent on the channel diameter, leading to an axial spread of solute. This is not the case with electrodrive, leading to inherently less solute dispersion.

2.3.3 Dispersion in Flow versus Electrodrive systems

Pressure driven system

It can be seen from the graph in Figure 8 (pressure) that for even moderate flow rates the system is operating with significant back pressures , and to achieve desirable analysis times pressures above the maximum operating pressure would need to be used.

Electrodrive system

The situation for the equivalent electrically driven system can also be seen in the graph shown in Fig 9. The situation here is quite different as the desired flow rates are achieved at moderate applied voltages and the same efficiency separation is achieved with a shorter packed length. Nevertheless the analysis time is not greatly improved.

However the situation is very different when we consider the predicted advantages of using electrodrive with smaller particles

If we look at the graphs, shown in Fig 10, for the same systems using capillaries packed with 1μm particles, the differences are drastically emphasised. For the pressure driven system it can be seen that although good analysis times, in relatively short times

the pressure required is impracticably large, and in practice would be totally unworkable. The situation for electrodrive shows that very fast analysis can be achieved with quite moderate voltages, illustrating again the enormous advantages which should be possible by using electrodrive and small particles.

Overall then , the limitations for pressure driven systems mean that they cannot feasibly be considered for very high efficiency separations with small , possibly sub-micron particles. By contrast, with electrodrive systems, the lack of dependence of flow rate upon particle size means that very small particles can be used with corresponding improvements in the chromatographic efficiency. The projected performance available from each system based on the likely practical constraints is summarised in table 2 .

	Capillary HPLC		CEC	
Particle size (μm)	Length (cm)	Plates/ column	Length (cm)	Plates/ column
5	50	55,000	50	115,000
3	25	45,000	50	170,000
1.5	10	30,000	50	250,000

Table 2. Achievable efficiencies from Capillary HPLC versus CEC

There are numerous other advantages in sampling and detection systems promised by this emerging technology, that suggest it could represent the 'next generation' in separation science. One thing seems clear: CEC is really the only sensible

way forward which properly exploits truly miniaturised chromatography systems. Further, in conjunction with Mass Spectrometric detection (MS), it will give us some chance to meet the sensitivity requirements of future analytical tasks. The only other aspect that currently stands in the way to the rapid development of this technology is the ability to prepare good quality packed capillaries . To date this has been the 'log jam' [20,35,49]. However, new techniques have been developed to enable this problem to be largely overcome and will be described in the following chapters.

2.4 Review of developments to date.

2.4.1 Instrumentation

CEC in its basic form was first demonstrated by Pretorius in 1974. However, it was not until Jorgenson and Lukacs' work of 1981 [28], that the reduction to capillary dimensions demonstrated the suitability of the technique for true miniaturisation. In 1987 Knox and Grant [33] laid down the theoretical foundations for the development of CEC in its present form. Their extensive predictions of the likely operating limits of the technique, inferred the requirement for miniaturisation of CEC to be mandatory, and gave the first real insight into the huge opportunity for improvements to the chromatographic efficiency available from these type of separations. These predictions hinted that with sub-micron sized particles it should be possible to achieve a previously unobtainable liquid chromatographic performance. Even at this time it was evident that the biggest practical obstacle to further development of the technique was the routine, reproducible production of the columns themselves. Even when a good column was

fabricated, after removal of the polyimide to form a detection window, the column was very fragile and easily broken. Once a good quality column was properly installed in the instrument it was actually very easy to achieve excellent performance. However, it became evident that it was sometimes difficult to maintain this performance over a period of time covering a number of sample injections. A particular problem with injection from a vial of sample is that the column inlet end had to be moved between two vials, and, if this was not performed rapidly, there was opportunity for the column end to 'dry'. This invariably leads to a low-conductivity area in the packed bed which propagates upon application of the electric field, leading to loss of flow. Again, Knox and Grant already anticipated that pressurisation of the electrolyte reservoirs would minimise troublesome effects, be they thermal or operational. Most practitioners of the technique at the time developed modifications to their existing instrumentation to pressurise both electrolyte reservoirs, which greatly improved the robustness of the technique and this lead was followed by most of the commercial vendors. Apart from some custom built instruments for specific purposes, it is still the case that the only commercial instruments to support CEC applications are modified CE instruments with additional electrolyte reservoir pressurisation. Despite this lack of enthusiasm from the manufacturers, many groups have built or modified equipment to enable it to perform specific forms of analysis. Most modifications have been based around the ability to supplement the electrically driven flow with various amounts of pressure assistance, or to deliver variable solvent compositions to the column inlet to perform gradient elution. This has been achieved by the use of conventional pumped flow gradients from

modified HPLC pumps [50] or by the use of electrically generated gradient flows [51]. Due to the 'fixed' position of the electrolyte vials in most commercial kit, these are very inflexible and it is difficult to use columns shorter than a 'minimum' length. Some groups have strived to reduce the overall column length, such that a higher field can be applied, and a faster analysis can therefore be achieved. This approach has been used very effectively by Lane et al to perform CEC separations in a column which is actually inside a modified MS electrospray probe, and so leads straight into the MS, giving both a very rapid analysis and excellent performance [52,53]. They were even able to dispense with the need for a CEC instrument. However, in a fully packed CEC column there is less susceptibility to flow loss and this makes this type of arrangement more robust in routine operation.

2.4.2 Stationary Phases

Most stationary phases used inside CEC columns to date have been typical HPLC stationary phases. These are generally composed of porous, spherical, silica particles of fairly well characterised (narrow) particle size distribution, and consistent pore sizes. These particles are chemically bonded to attach variable length carbon-chain based ligands to impart a hydrophobic surface quality to the outside of each particle. These type of phases are known in HPLC as reverse-phase. This implies that separations are achieved on the basis of differential partition into the hydrophobic layer of the phase, and that to decrease interaction (or retention) within the phase the organic solvent composition of the mobile phase should be increased. Compounds will

generally elute in order of most polar first in these systems. Compounds showing little natural retention are clearly not good candidates for these techniques, as low retention implies that there is a low chance of resolving these compounds from structurally similar compounds, likely to be present as contaminants. One of the attractions of CEC is the opportunity to separate compounds using an electrophoretic mechanism as well as partition. So, for example, even polar compounds which do not appreciably retain in the stationary phase, can often be separated purely by their differential ionic mobilities.

Stationary phases used in CEC have one important requirement. They must have a surface capable of producing an electrical double layer. This is discussed more fully in section 2.3.1. Phases based on silica generally show no problems as the silanol groups at the surface of each particle ionise and produce a good zeta potential. For this specific reason it was common for early work in CEC to utilise the relatively 'old fashioned' non-endcapped stationary phases, such as Spherisorb ODS1. These type of phases are little used in new HPLC methods as these silanols produce unwanted effects for some solutes. However, in CEC these effects are important, as the degree of ionisation of silanols is important to the generation of the zeta potential and therefore the magnitude of the electroosmotic flow (EOF). Anything that affects the ionisation of these silanols, notably pH, will also strongly affect the EOF. This has a very significant bearing on the pH of the mobile phase used in CEC separations. On conventional HPLC reverse-phase materials the pH needs to be relatively high (say above 6) to generate adequate EOF to perform reasonable speed (and performance) analyses. Down at lower pH's the EOF is relatively low. Of course, the inner walls of the capillary columns used are also made

from the same silica material, and behave in exactly the same way. However, not surprisingly, as the total surface area of the stationary phase particles is much greater than that of the wall, the phase dominates the EOF generation [54,55]. Figure 11 demonstrates the pH dependence of EOF for a typical CEC column with ordinary HPLC type material. Different stationary phases show the same type and amount of variation in selectivity that is seen for the equivalent HPLC separations, for neutral compounds (Figs 12 and 13).

Most HPLC type phases that have been used would normally have a relatively small average pore size, in the region of 10nm. With these phases, the pores are too small to support an EOF, as the thickness of the electrical double-layers on each wall (ie the walls of the micro-channel created by the pore), relative to the pore width, means there is substantial overlap. Therefore, there is no electrically induced flow in these pores. If substantially larger pore sizes are used, there is an opportunity to promote through-pore EOF (perfusive EOF) and this has been demonstrated to improve peak efficiencies [56]. This work suggested that with the buffer concentrations used, perfusive EOF was achieved on phase particles with pores >2000nm.

Nevertheless, the most common problem in using regular HPLC stationary phases was still the relatively low EOF's obtained by working with a low mobile phase pH . To support an EOF at lower pH it was necessary to introduce modified phases, containing alternative ionisable groups bonded to the silica, which reduced the dependence of the EOF on the silanol ionisation and supported a good EOF across a broader pH range. The use of these phases was first shown by Smith and Evans [57].

The improved pH versus flow characteristics for two different versions of these phases, compared to a regular phase, are shown in Figure 14. Generally these type of phases are referred to as 'mixed-mode' and each individual stationary phase particle is bonded with a mixture of conventional reverse phase ligands eg C6 or C18/ODS (octadecylsilane) and an ionisable group such as a short alkyl chain sulphonic acid. To promote a negatively charged particle surface, as in the conventional mode of CE and CEC polarity for flow towards the cathode, a sulphonic acid is used. This is described as SCX due to its origin of use being as a strong cation exchanger. Alternatively, SAX (strong anion exchanger), where the ionisable function is a quaternary amine is used, but generally with reversed instrument polarity. Currently, mixed mode phases are being used quite extensively, although some curious phenomena have been observed using these phases to analyse strongly basic compounds [57,58].

Some groups have also experimented with monolithic columns where the 'stationary phase' is created in situ by some polymerisation process, after the column has been filled with the polymer solution. [59].

In principle this avoids any issues surrounding the fabrication of frits within a conventional stationary phase, which have been suggested as being the reason for some problems with sample adsorption etc. However, little work in this area has demonstrated any significant advantages of these monolithics, and doubts have been raised over column to column reproducibility and stability.

Commercially produced columns are now available from a limited number of mainly specialised suppliers and these are proving to perform well in most cases. A

large number of recent publications in the area of CEC describe the use of these commercially supplied columns.

2.4.3 Practice

Since CEC is a hybrid technique of HPLC and CE there are a number of effects which have to be carefully considered when a new application is investigated. As a general consideration it is worth starting with the choice and concentration of buffer. The current generated inside the separation column needs to be limited, to avoid unwanted heat generation. Too little buffer concentration can lead to buffer depletion [60] due to 'consumption' of buffer ions in the relevant buffer reservoirs. Migration of these modified buffers into the separation column can then lead to drifts in concentration and pH leading to EOF variations and corresponding drift in retention times. Figure 15 demonstrates this for three consecutive injections of the same sample. This can be corrected by using higher concentration buffers which are not so susceptible to these effects. However, to avoid adverse heating effects, careful choice of the zwitterionic buffers such as TRIS (Tris(hydroxymethyl)methylamine) or MES (2-(N-morpholinoetanesulphonic acid)) allows high concentrations to be used without incurring too much current rise. The same sample injected five times in succession using a MES based buffer systems demonstrates the improvements seen (Figure 16). Alternatively, regular replenishment of more dilute buffer concentrations has also been shown to minimise depletion effects. Choice of buffers for CEC-MS coupling is

restricted to those buffers that are suitably volatile to be removed during the MS nebulisation process.

In general most separations can be approached with an initially high concentration of organic solvent in the mobile phase. It is usually better to elute the components of a mixture rapidly at low k' in the first test run, and then reduce the eluent strength to promote improved separation, once the analyst is satisfied that nothing further is going to elute from eariler runs. These conditions must also reflect the likely solubilities of the relevant buffers in the overall mobile phase composition. Zwitterionic type buffers are useful here as they are often organic structure based and therefore naturally more soluble in organic solvents than inorganic buffers such as phosphate.

It is important to appreciate that in CEC, the EOF within the column is affected by the composition, concentration and pH of the mobile phase. Most commonly, the development of a CEC method is started by selection of the type of stationary phase, which will have the largest effect on a specific separation, and then adjustment of the mobile phase parameters to give the EOF and separation required. These effects have been evaluated by a number of groups working in this field [54,58,61-66]. The multiple component mobile phases that tend to be used to perform CEC separations can create problems with the reproducibility of the EOF. The EOF is affected by pH and ionic strength, and these variables are themselves influenced by the amount of organic solvent present. For instance it has been shown that adding organic solvent to the electrolyte in CE can alter the pKa of the surface silanol groups to higher values [67].

This effect has also been reported, by a different group, in CEC [63]. It has also been demonstrated that , although higher EOF's are expected and observed at higher pH's, where total silanol ionisation will be expected, there is substantial EOF at lower pH's on some stationary phases [54,58]. All these effects, not least the effect of pH on solute ionisation, must be taken into consideration when method development is contemplated.

Although it appears that CEC is a complicated technique to use for a new separation, the application of this technique to problems is often actually more simple than the application of classical HPLC. As there are sensible practical restrictions to the type of mobile phases likely to be used without running into problems, it is possible to choose a largely generic set of starting conditions. Retention in mixed solute systems (most often the case for real-world separations) is difficult to optimise for all solute polarities, under isocratic conditions. CEC can often be used to separate the less retained (more polar) samples via the parallel electrophoresis mechanism, while the less polar species are separated mainly by partition.

Normally, a mobile phase would be chosen to contain a high concentration of organic solvent (typically 60-80%) and the remaining volume would contain a low overall concentration of electrolyte (buffer). This could be changed to a higher concentration of a zwitterionic buffer if no MS detection is necessary and maximum resistance to buffer depletion is required. If a mixed mode phase is being used then generally a low pH mobile phase will be used. This will maximise ion-suppression of negatively charged species such as carboxylic acids and also protonate strong bases, making them more likely to elute sooner, with an additional ion mobility as well as the

bulk EOF driving them towards the cathode. Care should be taken however, to avoid the deleterious effects sometimes observed, that are thought to be due to ion-attraction between positively charged species, such as protonated bases, and permanently ionised sulphonic acid sites on mixed-mode phases or residual silanols on conventional phases. Euerby et al [68]have shown that, in many applications, the well established theories of HPLC method adjustment can just as easily be applied to CEC.

2.4.4 Applications

To date, the vast majority of applications performed in CEC have been performed for neutral molecules. Or, in the case of most acids as pseudo-neutrals, where ion-suppression is used to suppress the acid group ionising at low pH. Separation of strongly basic compounds is problematic due to the conflicting requirements of wanting good negative charge on the phase to promote good EOF, but not wanting interactions between the solutes and these charges [57]. The most successful solution which has been shown to reduce basic interactions with the stationary phase has been the use competing bases, such as Triethylamine (TEA) in the mobile phase [69]. Compounds which naturally occur as neutrals and require high peak capacity separations, include the environmental pollutants such as polyaromatic hydrocarbons (PAH's), and these have been shown to give excellent CEC separations [66,70-72].

It is the pharmaceutical industry that has mostly encouraged the development of CEC. This is mainly because of its ultimate miniaturisation capabilities, but it also reflects the opportunity to use an orthogonal separation mechanism to that used in

HPLC. To date, most of the applications have not utilised the combined separation mechanisms of mobility and partition. Indeed most users have opted to reduce the complexity of understanding the separation mechanism, by suppressing one or other mode of action. However, notwithstanding these limitations, many very useful applications have been performed including antibiotics [53,73], barbiturates [74], prostaglandins [73], diuretics [57,58,62,75], steroids [53,57,58,68,73,76], macrocyclic lactones [53], peptides [58,77], nucleosides and purine bases [58]. Some of my early work developed applications that were subsequently used to monitor the performance of other separation-based purification techniques such as preparative HPLC (Figures 17 and 18). Also, many separations that were traditionally difficult to achieve using HPLC, have been easily achieved by CEC without barely any adjustment of the CEC column testing conditions (Figures 19 and 20).

For reasons of ultimate miniaturisation, it is in the field of bioanalysis where CEC has the biggest opportunity to improve upon what is possible now. In this area of application, we have seen the analysis of PTH (phenylthiohydantoin)-derivatised amino acids [78] and peptides [79]. The peptide separation utilised polymerically derived stationary phases with large pores (presumably to promote perfusive EOF). There have also been reports demonstrating the analysis of biologically extracted samples by CEC/MS [80,81] either utilising gradient elution [80] or sample stacking injection techniques [81] to exploit higher detection sensitivities. Both these descriptions suggested that good reliability and robustness was observed using these methods. Also, the techniques employed to effect gradient elution are well-suited to the methods used

for sample 'stacking' or preconcentration. By introducing the sample, where possible, in a solvent that does not provide significant elution strength, much larger volumes of sample (sometimes it is possible to consider several column volumes) can be injected than would normally be tolerated without significant loss of performance. As the sample is injected it is effectively immobilised at the top of the column, even though the sample solvent is filling the column volume as it would normally. So, instead of an initial sample 'plug' length so long that it would effectively destroy any chances of efficient peak width and shape, we start with a highly concentrated, narrow band that will give very efficient chromatographic performance when it is eluted. This scenario is particularly likely with samples contained in highly aqueous solvent mixtures, such as urine etc. Coupled with the ability to use gradient elution in mainly 'generic' mode and these two techniques could offer substantial improvements to sampling and detection protocols for bioanalysis.

Other diverse applications of CEC have included the non-aqueous separation of triglycerides of plant origin [82], gradient CEC of equine metabolites [80] and various chiral resolutions [61,62,83]. Recent work on molecular imprinting promises to provide unparalleled specificity by literally encapsulating a molecular 'hole' within a stationary phase which can accommodate one enantiomer, but not the other.

The applications performed to date have NOT demonstrated limitations to future uses of CEC, but rather have emphasised the opportunities that exist for miniaturised systems when we consider the sensible use of electrically driven or even assisted flows. There are many benefits which will accrue from miniaturising chromatography and

particularly its interfacing with concentration dependent detectors. HPLC in its current form, does not easily translate well into miniaturised formats. It is certainly possible, as will be shown later in this thesis, to use column diameters of a dimension suitable for use with pumped or electrically driven flows. What is most intriguing is the best way to use miniaturised columns and the combination of flows to maximum benefit. At this stage of the technique's development, it looks like CEC will find its eventual best uses as a hybrid technique in combination with capillary HPLC, on the same column, on the same instrument platform, arguably the best of both worlds.

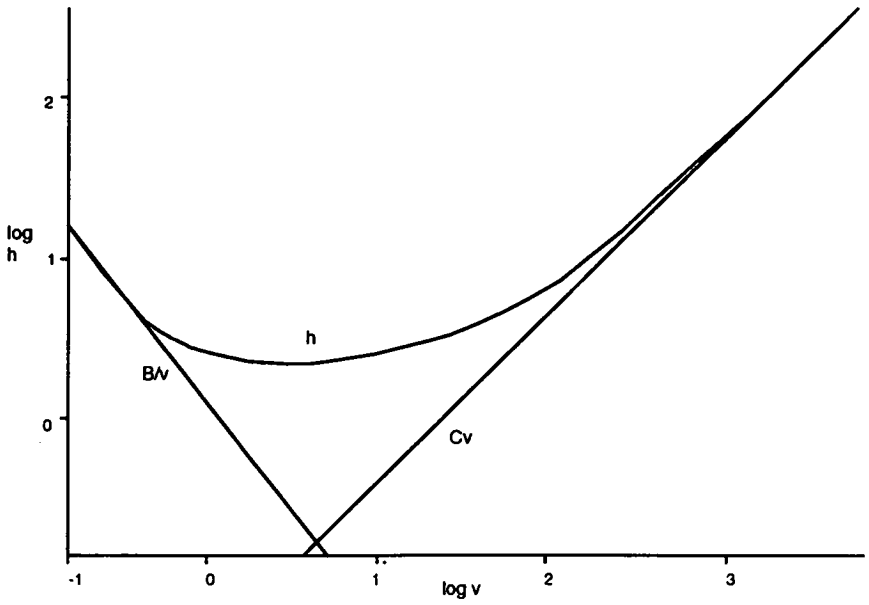

Figure 1. **Logarithmic plot of reduced plate height h, against reduced velocity, v, showing graphically the component contributions from dispersion factors B and C.**

Figure 1a. Schematic diagram of a typical HPLC system layout.

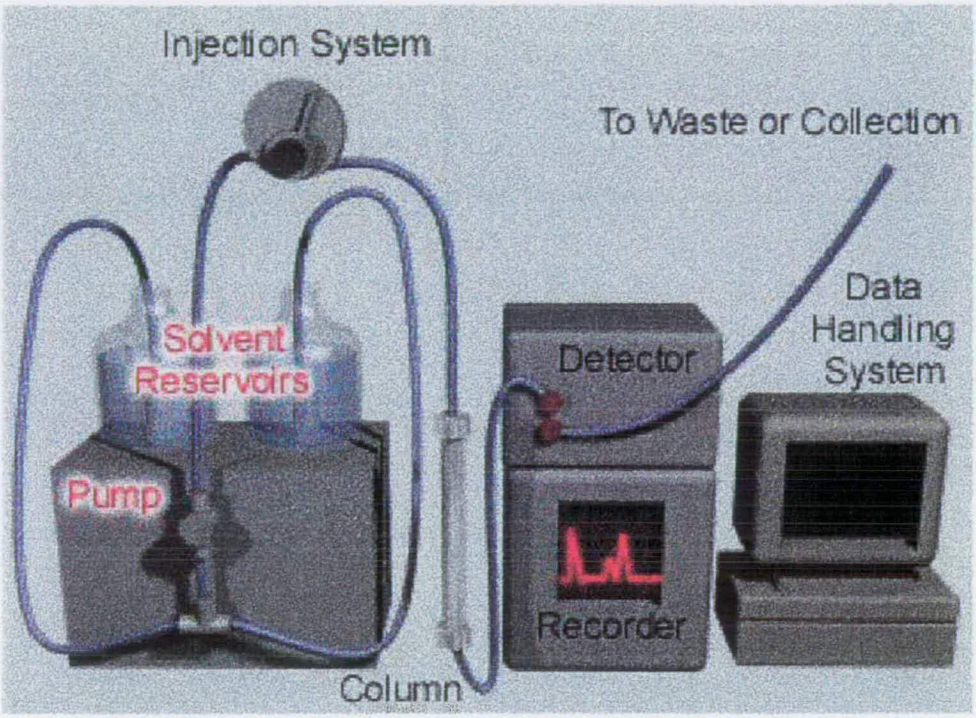

Fig 1b VOLUME CONSIDERATIONS WHEN MINIATURISING CHROMATOGRAPHY

Typical injection volume (µl)	Flow rate (ml)		Typical detector volume (µl)
10-20	1ml/min	4.6mm i.d. 	10 microlitres
4	0.2ml/min	2.0mm i.d. 	2 microlitres
0.1	0.005ml/min	320 micron i.d. 	0.05 microlitres
0.03	0.0015ml/min	180micron i.d. 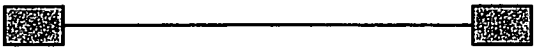	0.015 microlitres

All the above are assumed to be 25cm in length

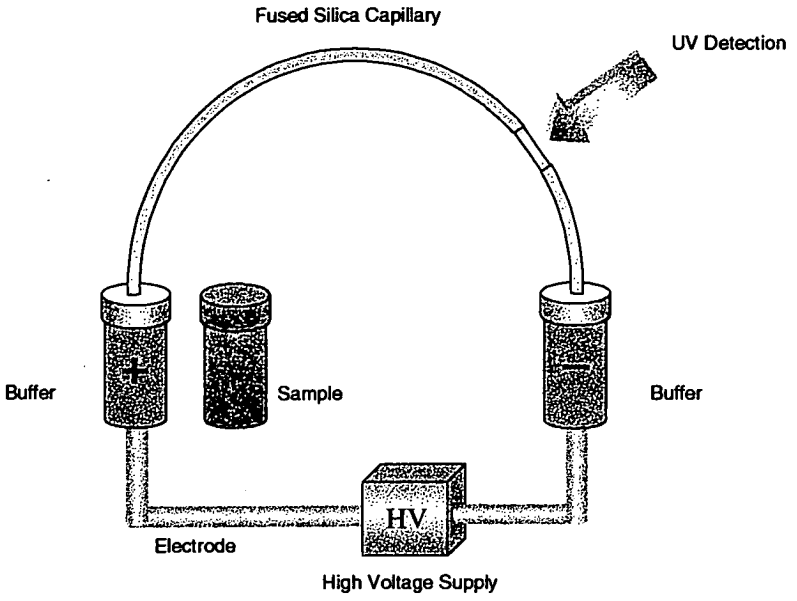

Figure 2. Schematic diagram of CE instrument

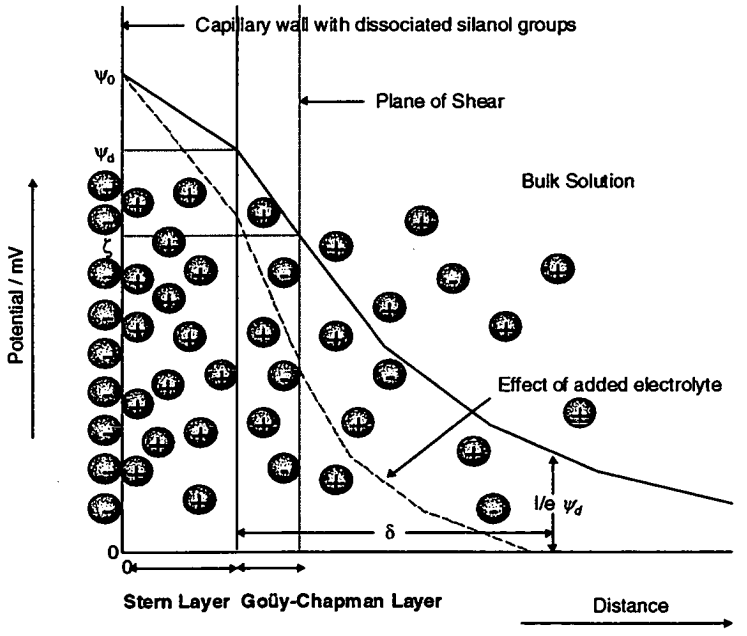

Figure 3. The electrical double layer.

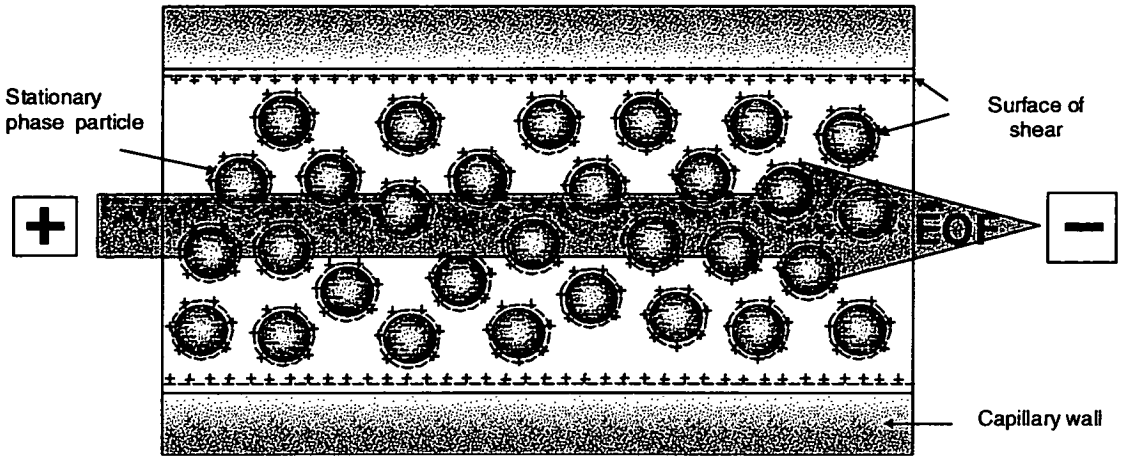

Figure 4. Schematic diagram illustrating double layer around stationary phase particles.

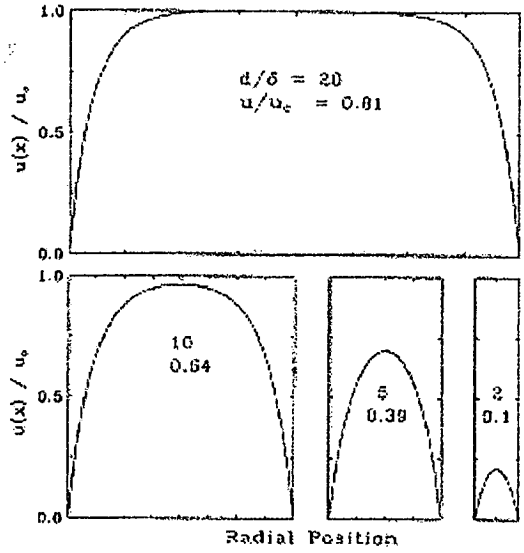

Figure 5. The trans-column velocity profiles for different ratios of tube diameter to double-layer thickness. D/δ is the ratio of tube diameter to double layer. u/u_0 is the ratio of the mean linear velocity to that in a tube with a very large value of D/δ.

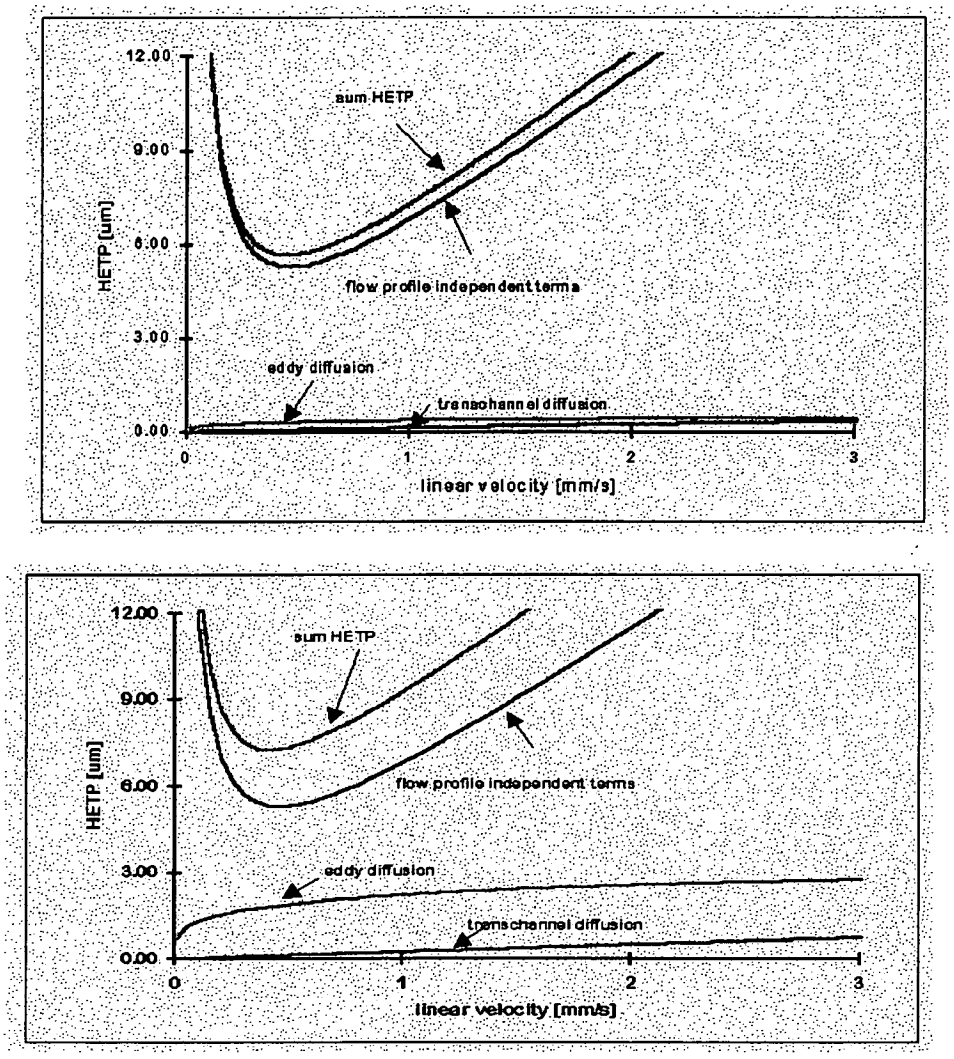

Figure 6. Dispersion contributors in flow (lower) versus electrodrive systems

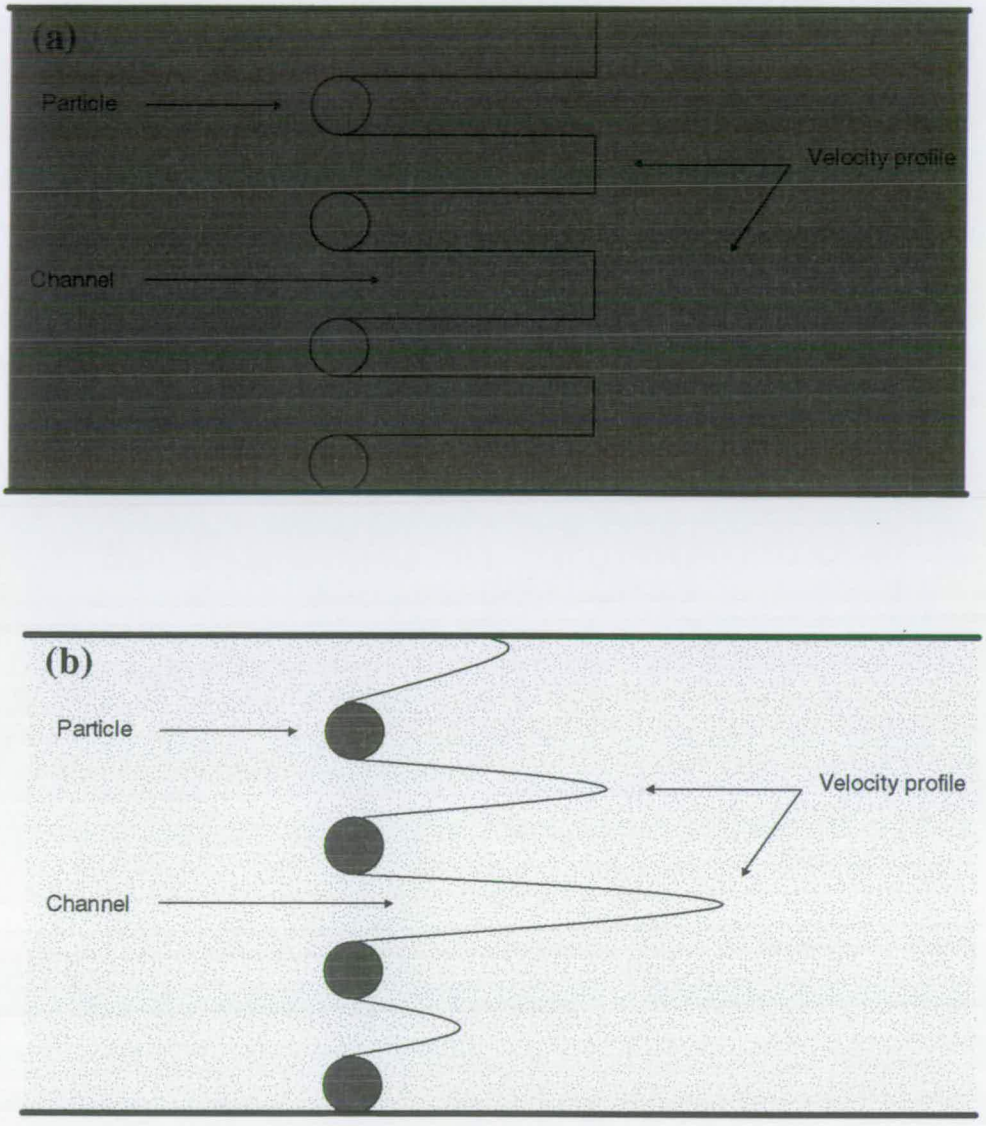

Figure 7. Differences in flow profile for Pressure (lower) versus electrodrive systems.

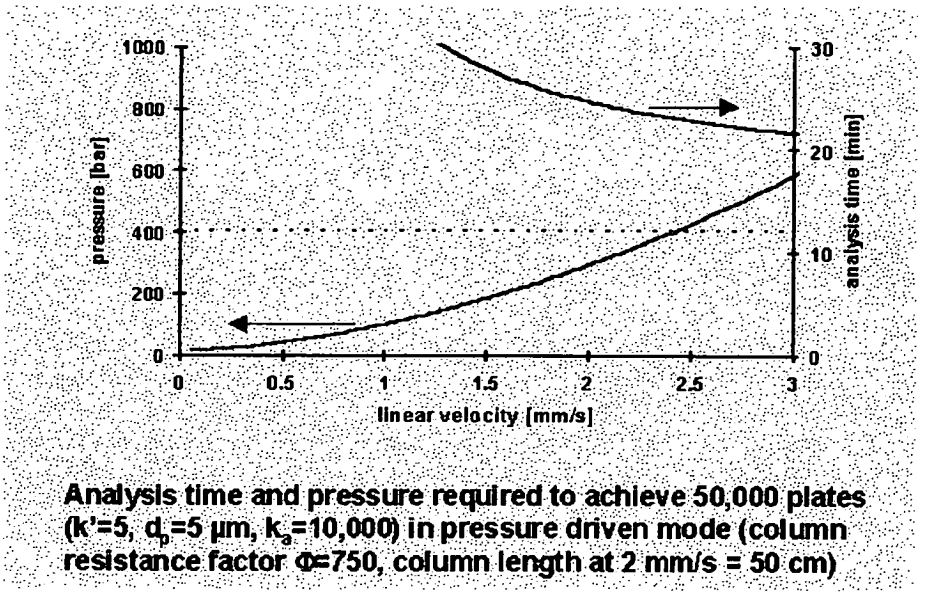

Figure 8. Performance possibilities for electrodrive systems in a packed column containing 5 µm particles.

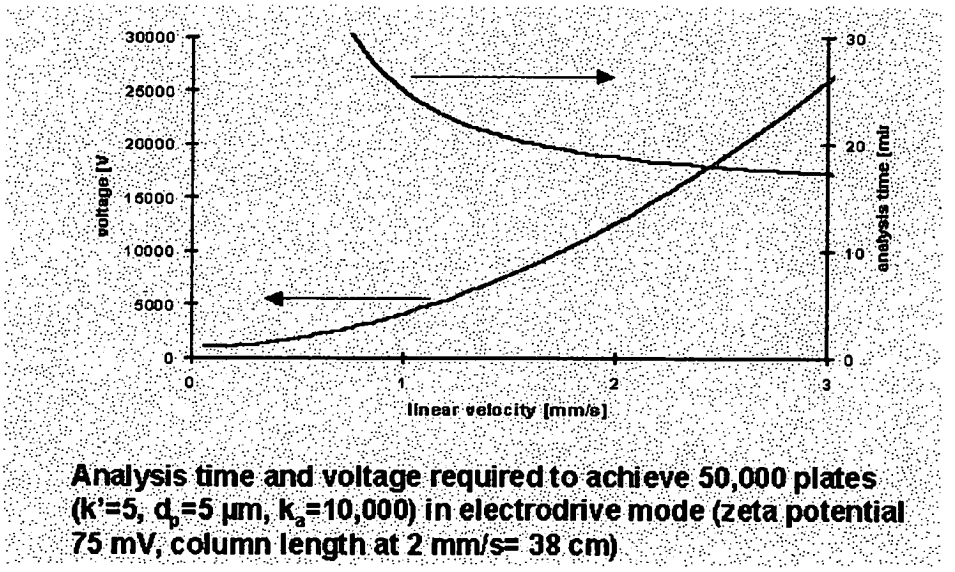

Figure 9. Performance possibilities for electrodrive systems in a packed column containing 5 µm particles.

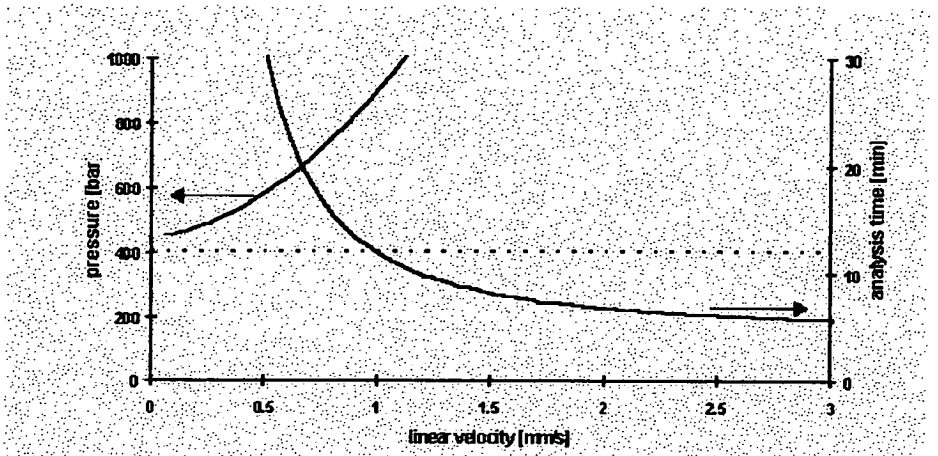

Analysis time and pressure required to achieve 50,000 plates (k'=5, d_p=1 μm, k_a=10,000) in pressure driven mode (column resistance factor Φ=750, column length at 2 mm/s = 14 cm)

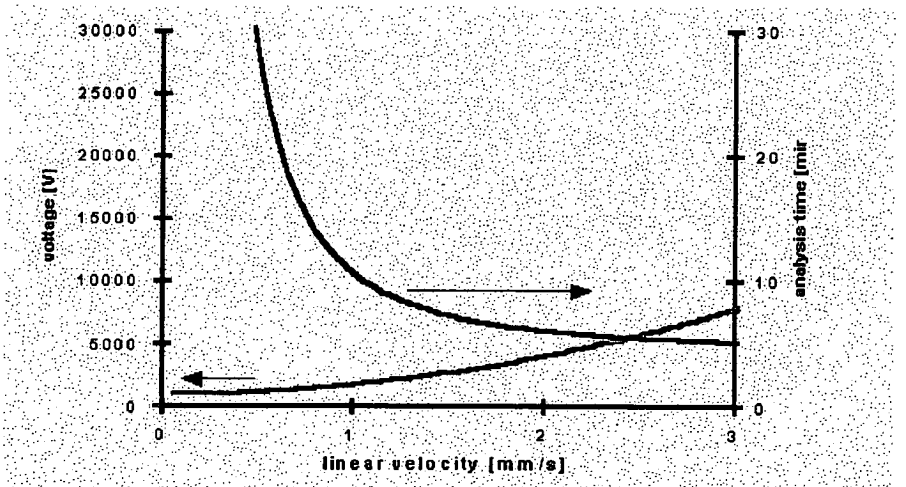

Analysis time and voltage required to achieve 50,000 plates (k'=5, d_p=1 μm, k_a=10,000) in electrodrive mode (zeta potential 75 mV, column length at 2 mm/s= 12 cm)

Figure 10. Comparison of performance possibilities for flow and electrodrive systems in a packed column containing 1 μm particles.

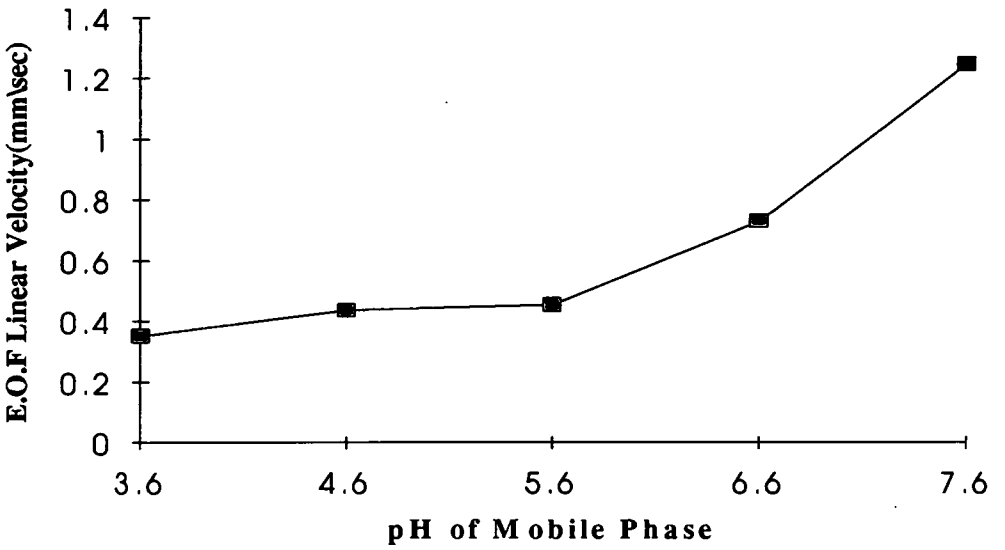

Figure 11. Graph of pH dependence of EOF for a 'typical' HPLC-type material.

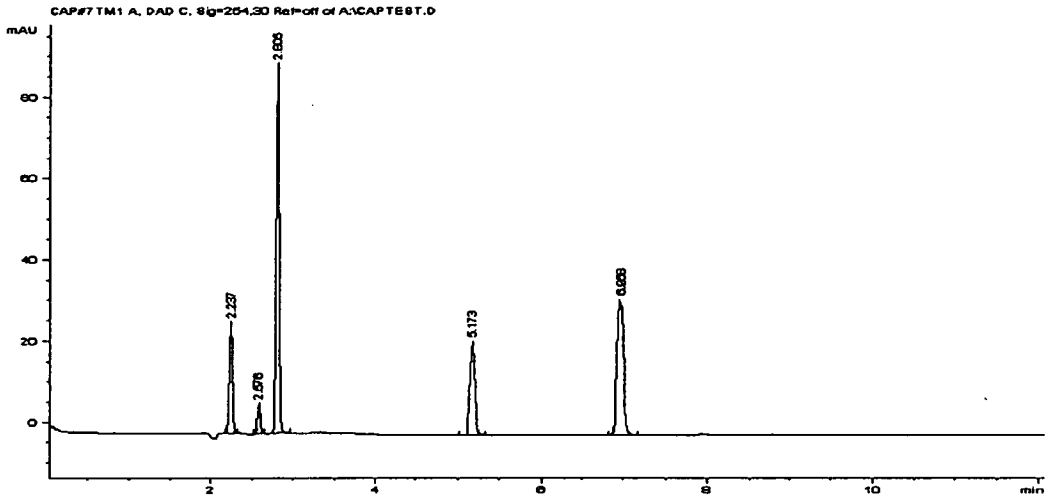

Figure 12. Spherisorb ODS2 (C18) 25cm capillary, Conditions 30kV, Mobile phase 80% CH_3CN / 20% 50mmol/L TRIS buffer, Detection wavelength 254nm, temperature(of capillary cartridge) 15^{o}C . Peaks (in order of elution) ; Thiourea (EOF marker), Benzamide, Biphenyl, Anisole, Benzophenone

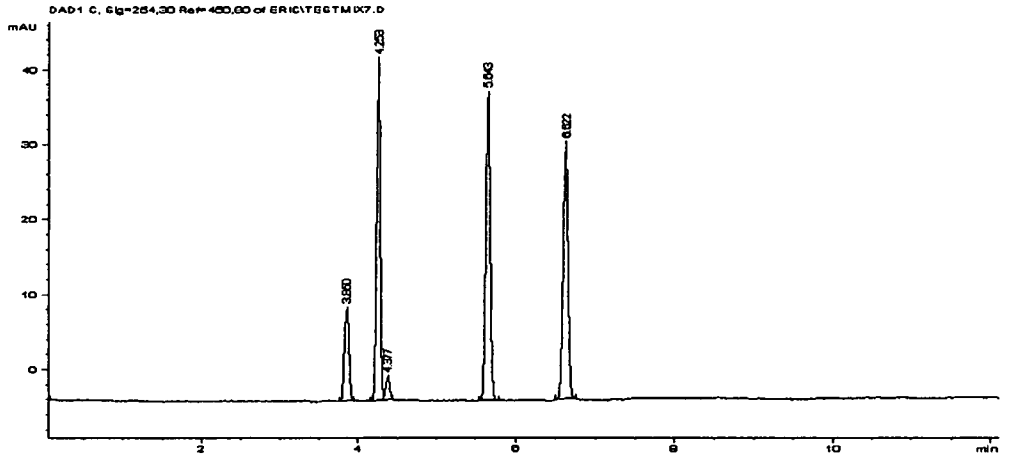

Figure 13. Hypersil ODS (C18) 30cm capillary, Conditions 25kV, Mobile phase 75% CH_3CN/ 25% 50 mmol/L TRIS buffer, Detection wavelength 254nm, All other conditions the same as figure 12.

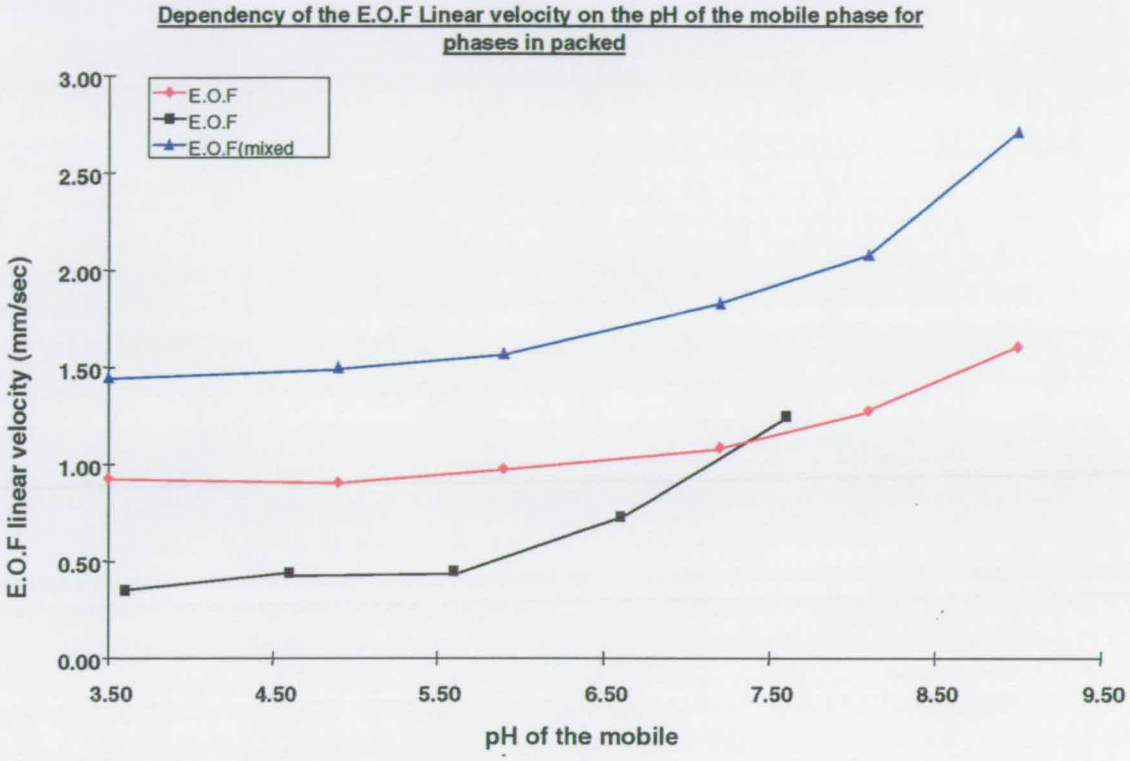

Figure 14. Graph of pH dependence of EOF for different stationary phase types, Ordinary C18 (black), SCX (red) and mixed mode (C18 and SCX, blue).

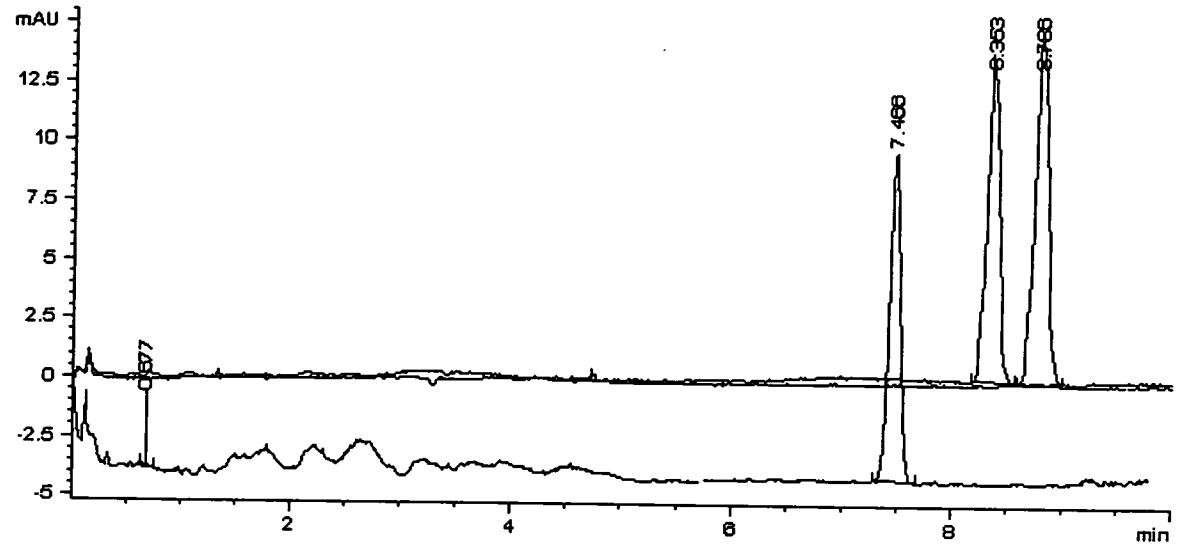

Figure 15. The effect on retention time reproducibility if buffer depletion occurs. 3 consecutive runs of anisole. Mobile phase: 70% MeCN/2mMNa_2HPO_4(pH=7.5). Column: 24cm 5μm Supelcosil ABZ PackedCapillary Voltage:30kV. Temperature of Cartridge:15C

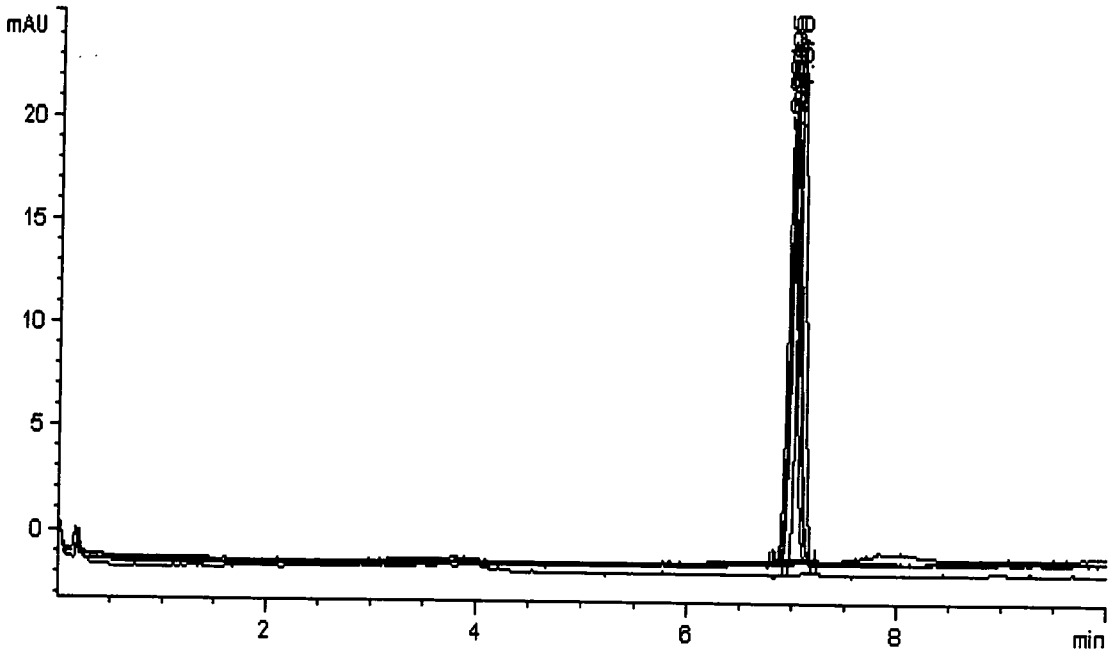

Figure 16 (lower) shows the improvement if correct choice of buffer is made.5 consecutive runs of anisole. Conditions otherwise as for figure 15.

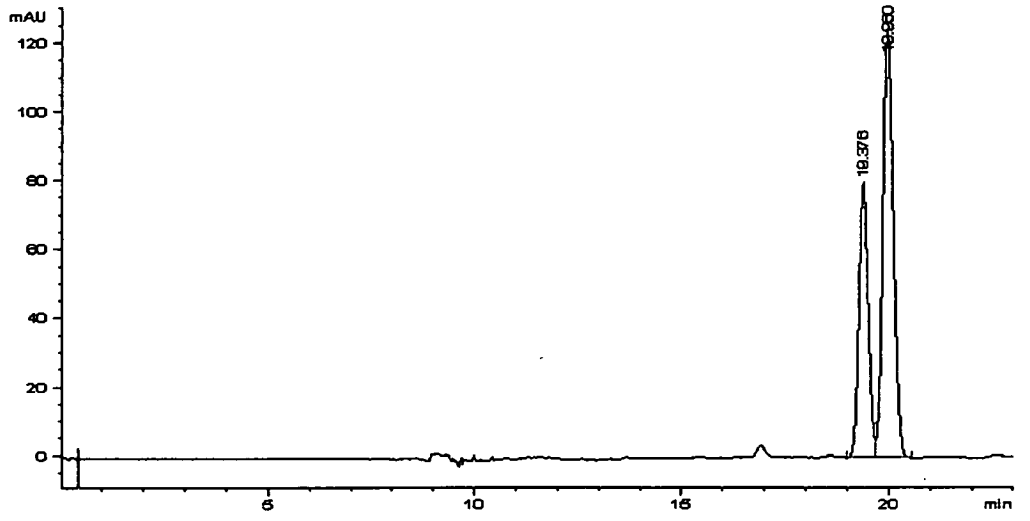

Figure 17. Separation of some synthetically produced intermediate stages in the synthesis of a serine protease inhibitor. Mobile Phase: 60%MeCN/ 20mM MES (pH=6.9). Column: 30cm 3μm Spherisorb ODS2 Packed Capillary. Temperature of cartridge=15C.

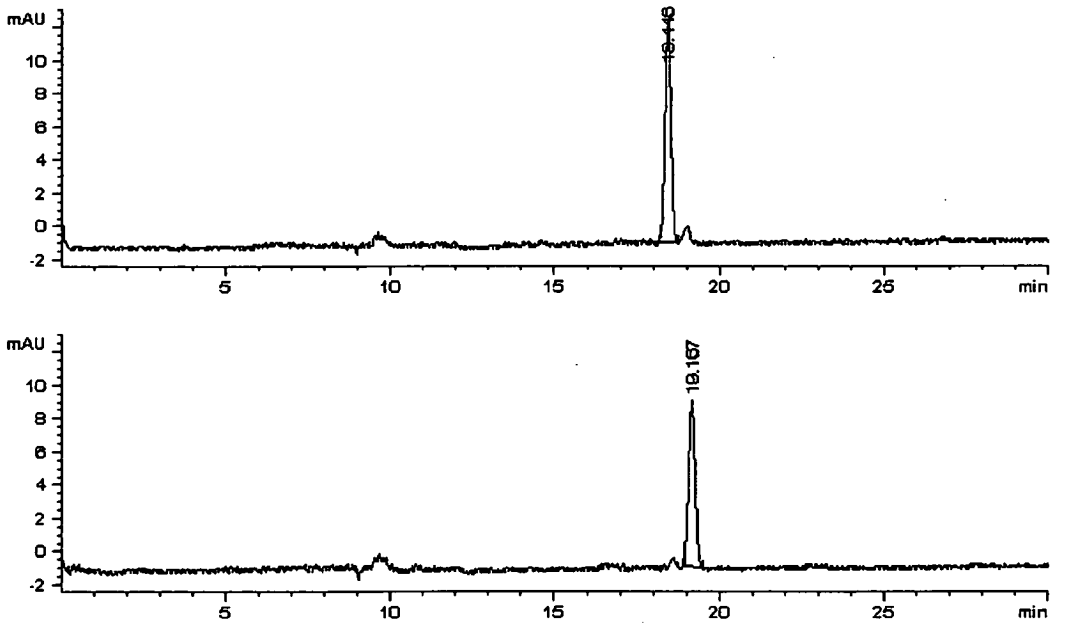

Figure 18. The analysis of the individual isomers after purification using 'closed-loop recycling HPLC'.

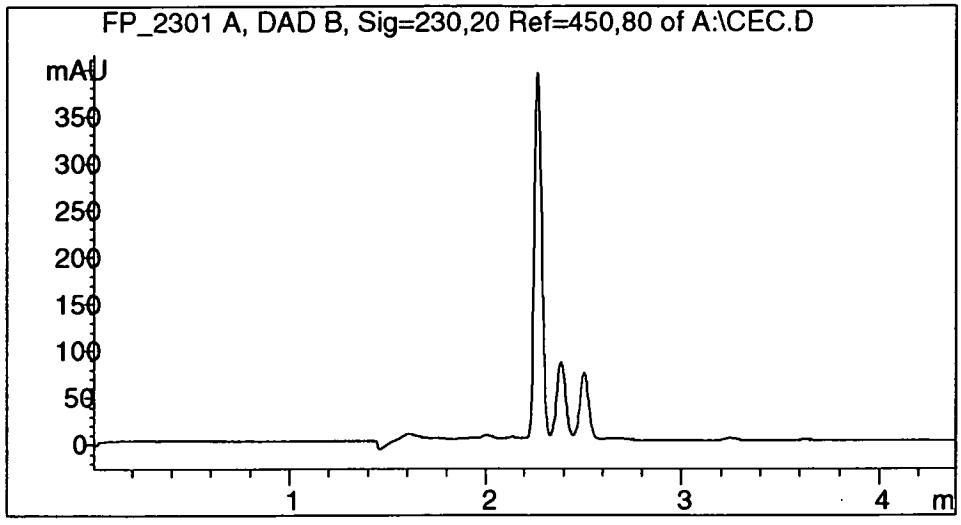

Figure 19. Resolution of Fluticasone Propionate (FP), S-methyl and des-6α fluoro impurities. 25cm Hypersil ODSA column, 30kV (850 V/cm) 80% CH3CN / 5mM Borate, 5 sec sample injection.

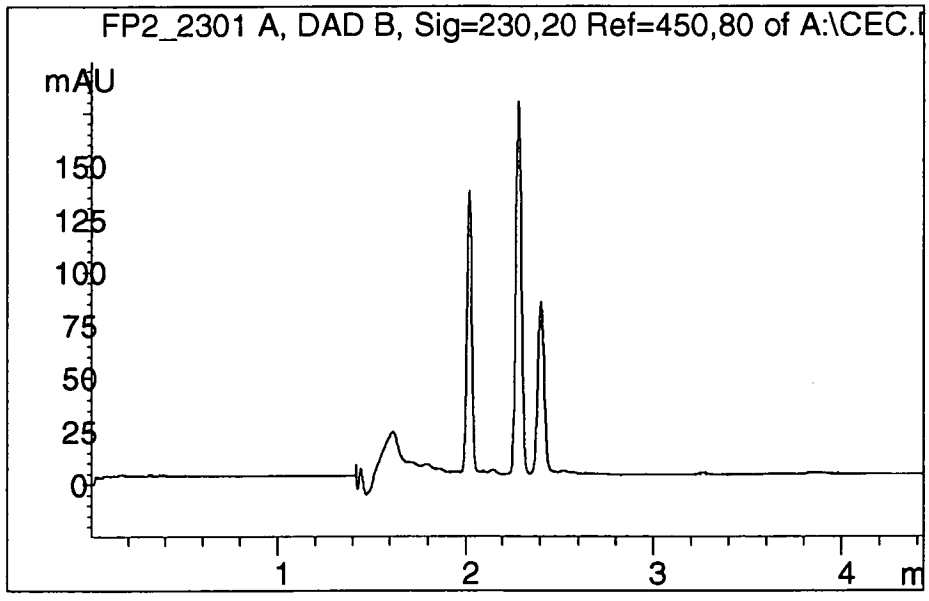

Figure 20. Resolution of FP and des-propionate and chloro-methyl ester impurities...same conditions

References for Chapter 2

[1] A. Martin and R. Synge, J. Biochem., 35, (1941) 1358.

[2] J.J. Kirkland, Gas Chromatogr., Proc. Int. Symp. (Eur.) (1972), 9 39-56

[3] M. Novotny, *Anal. Chem.* 53(12), (1981)

[4] M. Novotny, *Anal. Chem.* 60(8), (1988)

[5] D. Ishii, *J. Pharm. Biomed. Anal.* 2(2), (1984)

[6] J. Knox, J. Chromatogr. Sci., 15, (1977) 352

[7] J. Giddings, Dynamics of Chromatography, Pt 1, Marcel Dekker, New York, USA (1965).

[8] M. Golay, in: E.Desty (Ed), Gas Chromatography 1958, Butterworth, London, 1958 p.35

[9] J.C. Giddings, Anal Chem. 34 (1962), 1186, J.C. Giddings, Anal Chem. 35 (1963), 1338

[10] P.A. Bristow, J.H. Knox, Chromatographia, 10, (1977), 279

[11] J. H. Knox, M. J. Saleem, Chromatogr. Sci. (1969), 7(10), 614-22

[12] I. M. Mutton, *Chromatographia*, 47(5/6) 291-298 (1998)

[13] C. Borra, M.H. Soon, M. Novotny, *J.Chromatogr.* 385, 75 (1987)

[14] M. DeWeerdt, C. Dewaele, M. Verzele, *HRC & CC* 10, 553 (1987)

[15] C.L. Flurer, C. Borra, F.Andreolini, M. Novotny , *J.Chromatogr.* 448, 73 (1988)

[16] C.L. Flurer, C. Borra,S. Beale, M. Novotny , *Anal. Chem.* 60, 1826 (1988)

[17] J.C. Gluckman, A. Hirose, V. L. McGuffin, M. Novotny, *Chromatographia,* 17, 303 (1983)

[18] S. Hoffmann and L. Blomberg, *Chromatographia,* 24, 416 (1987)

[19] K. E. Karlsson, M. Novotny, *Anal. Chem.* 60, 1662 (1988)

[20] R. T. Kennedy, J. W. Jorgenson, *Anal Chem,* 61, 1128 (1989)

[21] T. Takeuchi, D. Ishii, *J. Chromatogr.* 238, 409 (1982)

[22] T. Takeuchi, T. Saito, D. Ishii, *J. Chromatogr.* 351, 295 (1986)

[23] F. J. Yang, *J. Chromatogr.* 236, 265 (1982)

[24] R. T. Kennedy, J. W. Jorgenson, *J. Microcol. Sep.* 2, 120 (1990)

[25] D. C. Shelly, T. J. Edkins, *J. Chromatogr.* 411, 185 (1987)

[26] A. Tiselius, Disc. Faraday Soc., 7 (1949) 164.

[27] R. Synge, Disc. Faraday Soc., 7 (1949) 164.

[28] J. Jorgenson and K. Lukacs, J. Chromatogr. Sci., 218 (1981) 209.

[29] W. G. Kuhr, C. A Monnig, Anal Chem, 1992, 64, 389R

[30] J. H. Knox, M. Saleem, *J. Chromatogr. Sci.* 7, 614 (1969)

[31] J. H. Knox, M. T. Gilbert, *J. Chromatogr.* 186, 405 (1979)

[32] J. H. Knox, *J. Chromatogr. Sci.* 18, 453 (1980)

[33] J. H. Knox, I. H. Grant, *Chromatographia,* 24, 135 (1987)

[34] J. H. Knox, *Chromatographia,* 26, 329 (1988)

[35] J. H. Knox , I. H. Grant, *Chromatographia,* 32, 317 (1991)

[36] Sir G. I. Taylor, *Proc. Roy. Soc.(Lond)* A219, 186 (1953)

[37] R. Aris, *Proc. Roy. Soc. (Lond),* A235, 67 (1953)

[38] M. Martin, G. Guiochon, *Anal. Chem.* 56, 614 (1984)

[39] M. Martin, G. Guiochon, Y. Walbroehl, J. W. Jorgenson, *Anal. Chem.* 57, 559 (1985)

[40] C. L. Rice, R. Whitehead, *J. of Phys. Chem.* , 69, 4017 (1965)

[41] F. E. P. Mikkers, F. M. Everaerts, Th. P. E. M. Verheggen, *J. Chromatogr.,* 169, 1-10 (1979)

[42] H. Poppe, J. C. Kraak, *J. Chromatogr.* 282, 399 (1983)

[43] H. Poppe, J. C. Kraak, J. F. K. Huber, J. H. M. Van den Berg, *Chromatographia,* **9,** 515 (1981)

[44] F. M. Everaerts, J. L. Beckers, Th. P. E. M. Verheggen, *"Isotachophoresis"* J. Chromatogr. Library, Vol. 6, Elsevier Science Publishers, Amsterdam (1976)

[45] J. J. Van Deemter, F. J. Zulderweg, A. Klinkenberg, *Chem. Eng. Sci.,* **5,** 271 (1956)

[46] M. M. Dittman, K. Wienand, F. Bek, G. P. Rozing, *LC-GC,* 13 (10), 800 (1995)

[47] C. Horvath, H. J. Lin, *J. Chromatogr.* 126, 401 (1976)

[48] C. Horvath, H. J. Lin, *J. Chromatogr.* 149, 43 (1978)

[49] S. Hoffmann, L. Blomberg, *Chromatographia*, 24, 416 (1987)

[50] B. Behnke, E. Bayer, *J. Chromatogr.*, 680, 93 (1994)

[51] C. Yan, R. Dadoo, R. Zare, D. Rakestraw, D Anex, *Anal. Chem.*, 68, 2726 (1996)

[52] S.J. Lane, R.J. Boughtflower, C.J. Paterson, T. Underwood, *Rapid Commun. Mass Spectrom.* 9, 1283 (1995)

[53] S.J. Lane, R.J. Boughtflower, C.J. Paterson, M. Morris, *Rapid Commun. Mass Spectrom.* 10, 733 (1996)

[54] M.M. Dittman, G.P. Rozing, *J. Chromatogr.* A, 744, 63 (1996)

[55] M.M. Dittman, G.P. Rozing, *J. Microcol. Sep.*, 9, 399 (1997)

[56] D. Li, V.T. Remcho, *J. Microcol. Sep.*, 9, 389 (1997)

[57] N.W. Smith, M.B. Evans, *Chromatographia*, 41, 197 (1995)

[58] M.R. Euerby, D. Gilligan, C.M. Johnson, S.C.P. Roulin, P. Myers, K.D. Bartle, *J. Microcol. Sep.*, 9, 373 (1997)

[59] E. C. Peters, M. Petro, F. Svec, J. M. J. Frechet, Anal. Chem. (1998), 70(11), 2288-2295

[60] R.J. Boughtflower, C.J. Paterson, T. Underwood, *Chromatographia*, 40, 329-336 (1995)

[61] S. Li, D.K. Lloyd, *J. Chromatogr.* A, 666, 321 (1994)

[62] F. Lelierve, C. Yan, R.N. Zare, P. Gareil, *J. Chromatogr.* A, 723, 145 (1996)

[63] S. Kitagawa, T. Tsuda, *J. Microcol. Sep.*, 6, 91 (1994)

[64] Q.H. Wan, *J. Chromatogr.* A, 782, 181 (1997)

[65] R.M. Seifar, W,Th. Kok, J.C. Kraak, H. Poppe, *Chromatographia*, 46, 131 (1997)

[66] P.B. Wright, A.S. Lister, J.G. Dorsey, *Anal. Chem.*, 69, 3251 (1997)

[67] C. Schwer, E. Kenndler, *Anal. Chem.*, 63, 1801 (1991)

[68] M.R. Euerby, C.M. Johnson, S.C.P. Roulin, P. Myers, K.D. Bartle, *Anal.Commun.*, 33, 403 (1996)

[69] N. C. Gillott, D. A. Barrett, N.s P. Shaw, M. R. Euerby, C. M. Johnson, UK. Anal. Commun. (1998), 35(7), 217-220.

[70] C. Yan, R. Dadoo, H. Zhao, R.N. Zare, D.J. Rakestraw, , *Anal. Chem.*, 67, 2026 (1995)

[71] R. Dadoo, C. Yan, R.N. Zare, D.J. Rakestraw, G.A.Hux, *LC-GC.*, 15, 630 (1997)

[72] S.A. Lister, J.G. Dorsey, D.E. Burton, *J. High Resolut. Chromatogr.*, 20, 523 (1997)

[73] N.W. Smith, M.B. Evans, *Chromatographia*, 38, 649 (1994)

[74] M.R. Euerby, C.M. Johnson, K.D. Bartle, *LC-GC Intl.*, 11, 39(1998)

[75] M.R. Taylor, P.J. Teale, *J. Chromatogr.* A, 768, 89 (1997)

[76] D.B. Gordon, G.A. Lord, D.S. Jones, *Rapid Commun. Mass Spectrom.* 8, 544 (1994)

[77] K. Schmeer, B. Behnke, E. Bayer, *Anal. Chem.*, 67, 3656 (1995)

[78] C. Huber, G. Choudhary, C. Horvath, *Anal. Chem.*, 69, 4429 (1997)

[79] G. Choudhary, C. Horvath, *J. Chromatogr.* A, 781, 161 (1997)

[80] M.R. Taylor, P. Teale, S.A. Westwood, D. Perrett, *Anal. Chem.*, 69, 2554 (1997)

[81] C.J. Paterson, R.J. Boughtflower, D. Higton, E. Palmer, *Chromatographia*, 46, 599 (1997)

[82] P. Sandra, A. Dermaux, V. Ferraz, M. Dittmann, G. Rozing, , *J. Microcol. Sep.*, 9, 409 (1997)

[83] S. Li, D.K. Lloyd, *Anal. Chem.*, 65, 3684 (1993)

Careful choice of electrolyte concentration is needed to maximise the benefits on all aspects of the chromatographic performance , as the zeta potential ζ is dependent on the concentration and the pH of the electrolyte. In turn the EOF is directly proportional to ζ . Dilute electrolytes which would most benefit ζ would limit the particle size to 1-2 μm and would lead to irreproducible retention times as the 'buffering capacity' would be compromised for ionisable solutes. A more detailed coverage of this subject has been given by Everaerts et al [41].

2.2.3 Flow Rates and the effects of Self-Heating

The linear flow rates for pressure and electrodrive systems are given by the equations below;-

Pressure drive $u = (d^2 / \phi\ \eta)\ (\Delta p / L)$ **(2.38)**

Electrodrive $u = ((\varepsilon_0\ \varepsilon_r\ \zeta)\ (V / L)) / \eta$ **(2.37)**

$= (\varepsilon_0\ \varepsilon_r\ \zeta)\ E / \eta$

In these equations $E = V / L$ is the potential gradient along the length of the tube. Under pressure drive, the velocity, u, is proportional to d^2 where d is the tube diameter for open tubes or particle diameter (d_p) for packed tubes. For situations when electrodrive is used the diameter term does not enter the equation for flow calculation

Chapter 3. Introduction to Mass Spectrometry

3.1 Introduction

Mass spectrometry is a powerful analytical tool that provides information about atomic and molecular composition of compounds. A mass spectrometer produces charged particles, which are separated according to their mass/charge ratio (m/z), knowledge of the molecules' charge allows deduction of the molecular weight. Mass spectroscopists normally quote m/z as the molecular weight of an ion divided by the number of electronic charges which it carries. However in fundamental equations m should be taken as the absolute mass of the ion, and z its absolute charge. Various techniques are employed to produce, separate and detect these ions. Some aspects of these different techniques are described in this report, although detailed discussion will focus on electrospray ionisation with a single quadrupole mass analyser, as this was the configuration of the instrumentation used for the work described.

3.2 Development of Mass Spectrometry.

For a technique that is based upon highly sophisticated instruments, with state of the art electronics and computer control, mass spectrometry is actually one of the oldest instrumental methods of analysis. In 1912 J.J.Thompson [1] used electric and magnetic fields to separate and confirm the existence of the two isotopes

of neon. This work was followed by the development of a mass spectrometer by J.W. Aston in 1932 [2] who used an electric field to focus the ions.

The first commercial mass spectrometer was introduced in 1942, by which time research had led to the introduction of the double focussing instrument. This allowed the combination of directional and velocity focusing to produce high resolution mass measurements.

Over the next 20 years, further research lead to the development of alternative mass analysers including the time of flight analyser (TOF) [3], the quadrupole mass filter [4] and the ion trap analyser [5]. These analysers widened the availability of mass spectrometry as they became cheaper to produce.

Ionisation techniques developed rapidly after the initial methods such as electron impact ionisation were developed. The introduction of chemical ionisation [6] and fast atom bombardment (FAB) [7] expanded the range of compounds that could be studied using mass spectrometry. These different ionisation techniques allowed more control of molecular fragmentation and the spectra obtained leading to improvements in the interpretation of mass spectra. They also enabled substances of higher molecular weight to be vapourised and ionised. Further research in the early 1980's lead to further ionisation methods including thermospray [8], electrospray [9,10] and matrix assisted laser desorption ionisation (MALDI) [11].

Mass spectrometry is now routinely capable of providing excellent resolution and sensitivity for a wide range of compounds of molecular weights up to 200,000 using instruments ranging from relatively inexpensive bench-top instruments, to

tandem mass spectrometers [12], and very expensive Fourier transform instruments with superconducting magnets costing up to £1m.

3.3 Basic Instrumentation.

There is no universal mass spectrometer. Indeed there is a bewildering variety. However, certain designs and configurations lend themselves to the solution of specific problems better than others. There are four essential parts to any mass spectrometer:- 1) the inlet system; 2) the ion source; 3) the mass analyser and 4) the ion collection system. To avoid undesired molecular collisions, the instrument operates under a high vacuum. Any collisions would produce deviations in the ion trajectories and ions would lose their charge against the walls of the instrument. In addition, any unwanted ion-molecule collision could produce undesirable fragmentation increasing the complexity of the mass spectrum and biasing its interpretation. Conversely, techniques have been developed, that use **controlled** collisions in specific regions of the spectrometer to enhance fragmentation and help to provide further structural information.

Of particular interest for the work to be described is the technique of Electrospray ionisation, used in conjunction with a quadrupole mass spectrometer. We therefore describe this method of ionisation in detail

3.4 Electrospray mechanism.

Electrospray ionisation takes place in two fundamental stages, the formation of highly charged droplets, followed by solvent evaporation from these droplets to produce charged ions. The overall process is illustrated in Figure 1. Positive or negative ions can be produced. The following discussion will only be concerned with positive ion formation. Any ion-spray source, as illustrated in Figure 2, consists of a central capillary through which the analyte in solution is delivered to the source. Normally this central capillary will have a small diameter of the order of 10-50 μm. Pure electrospray occurs when just an electric field is used to promote emission of charged droplets from a capillary tip towards a counter electrode. This works very well but is limited to eluent flow rates of less than 50 μl min^{-1}. For lots of applications this is not sufficient and other features of pure electrospray, such as the higher tip voltages used for optimum performance, make routine use more troublesome due to electrical discharge problems. For many practical reasons it is desirable to want to use the benefits of electrospray ionisation (EI) under conditions of higher liquid flow rates, surface tensions and electrolyte concentrations. Consequently most EI sources on commercial instruments include a high velocity gas flow, known as sheath or nebulising gas, in the source design. In a simple model, the nebuliser gas takes care of aerosol formation, while the electric field charges the droplets. When compared to pure electrospray, pneumatically assisted electrospray can handle aqueous solutions and higher flow rates without the need for critical adjustment and can be operated at lower field strength so that electrical discharge problems are eliminated. Another advantage to using a

pneumatically assisted spray source is the freedom of positioning the sprayer inside the ion source, since the formation and direction of the spray are controlled by the high velocity gas flow and not by the electric field at the tip of the sprayer. By positioning the spray off-axis (particularly at right angles) stability of operation is improved and penetration of droplets, or more specifically contaminants, is reduced. With the addition of heated nebuliser gas flow rates as high as 2ml min^{-1} are routinely used. These benefits are included in modern instruments to such an extent that when low flow rate ion spray sources are required, the flow rate from the capillary is often inadequate and the flow has to be made up with additional solvent delivered through a sheath. The two main stages in the electrospray ionisation process are as follows.

Stage1. - Formation of highly charged droplets.

This is achieved by establishing a potential difference of 3-6kV between the capillary tip and the counter electrode, which has an orifice through which ions are sampled into the mass spectrometer. As the liquid emerges from the capillary, positive charges are believed to arise as a result of the phenomenon of electrostriction. This is a double layer effect whereby the liquid, which is positively charged at the walls, is ejected so fast from the capillary that the charges are unable to escape back to neutralise the wall charge, and the emerging liquid acquires a positive charge. Electrostriction is just the inverse of electroendosmosis. The axial electrical field then causes the liquid to be drawn into a cone. This is called the

Taylor [13] cone. (Figure 1). The induced field causes some positive ions to be drawn toward the liquid surface, and some negative ions away from it. Any excess charge on a body of liquid will be concentrated at the surface by charge repulsion. At the "Taylor cone" stage the bulk liquid from the capillary is still intact and has not yet broken up into droplets. As shown in Figure 1, the liquid emerging from the capillary is drawn out and narrows as it is stretched by the field, and so drawn down into a narrow tip. It will only stretch in the field if it has positive charge and the counter electrode is negative (or vice versa for negatively charged liquid).

At a sufficiently high capillary tip voltage, the tip of the cone becomes unstable and begins to emit very small positively charged droplets. This is a result of the charge on the droplet producing such a field that it overcomes the surface tension holding the droplet together. Therefore it breaks up into smaller and smaller droplets, each suffering the same fate as more solvent evaporates. The voltage V_o, at which this occurs has been approximated by Smith [14] as equation (3.1)

$$V_o \approx 2x10^{-5}\left(\gamma r_c\right)^{1/2} \ln\left(\frac{4d}{r_c}\right) \qquad \textbf{(3.1)}$$

where γ = surface tension of the liquid, r_c = radius of capillary and d = distance between capillary tip and counter electrode, V_o = the voltage between the tip and the counter electrode.

This suggests that the main factors affecting electrospray are the diameter and position of the capillary and the type of solvent used, or more specifically the influence of the surface tension of the solvents used. Kebarle [15] studied the electrospray performance using different solvents and concluded that methanol and acetonitrile were both suitable solvents to use. Any conditions that lower the voltage required to produce a stable electrospray are generally advantageous.

Stage 2. - Ion formation.

Once the highly charged droplets are formed, evaporation of the solvent causes the droplets to become smaller (shown as a sub-figure in Figure 1). Due to charge repulsion overcoming the surface tension, the droplets undergo a series of ruptures yielding ever smaller droplets. Also, on their flight through gas at atmospheric pressure, the droplets are subjected to shear forces by interactions with the dense gas. As a result of both effects, droplets undergo deformation, which may lead to high local electric fields at protrusions on the droplets' surface. This can also lead to instability and promote droplet break-up. The radius of primary aerosol droplets in electrospray is of the order of 0.5-1μm. The radius of offspring droplets is estimated to be 0.1 μm. While the time needed for complete evaporation of a 1 μm droplet is of the order of milliseconds, the offspring droplets shrink within a submillisecond timeframe. During evaporation of offspring droplets, a second generation of yet smaller droplets may be emitted from the 0.1 μm droplets. Also,

the original 1 μm droplets, having lost part of their mass and charge by release of offspring, will shrink by evaporation and release offspring again. When offspring droplets have shrunk to a radius of approximately 10nm, further disintegration is not supposed to take place in order to remove excess charge at the Rayleigh stability limit. Instead, droplet charge is reduced by the release of ions from the droplet surface. This finally results in the desorption of ions (or ion evaporation) so forming ions of both solvent and analyte in the vapour phase. The point at which this occurs is known as the Rayleigh limit [16] and is governed by the Rayleigh equation (3.2)

$$q = 8\pi^2\varepsilon_0\gamma D^3 \qquad \textbf{(3.2)}$$

(where D is the diameter of the droplet, q is charge)

The exact mechanism of ion evaporation is not known. There are two models that have been suggested.

a. Röllgen Model

This model was first proposed after work by Dole [9] and later discussed in more detail by Röllgen [17,18]. It depends on the formation of extremely small droplets (radius<1nm), which contain one ion. Solvent evaporation from such a droplet will lead to conversion of the droplet to a gas-phase ion.

b. Iribrane and Thompson Model

This model, proposed by Iribrane and Thompson [19,20], assumes ion evaporation (emission) from very small and highly charged droplets as the Rayleigh limit is approached. Typically these droplets have a radius of approximately 8nm and contain seventy charged species. They do not undergo fission but emit gas phase ions. As the number of charges in the droplet decreases emission can still be maintained as a result of a decrease in droplet radius by solvent evaporation. The exact nature of gas-phase ion production is unclear, but it seems unlikely that all of the charges contained within a rapidly reducing droplet size, can be accommodated on the relative small number of analyte molecules remaining in the droplet. It appears more likely that emission of gas phase analyte ions and ionised solvent molecules/clusters also occurs.

There have been criticisms of both models, although the Iribrane model would appear to be more widely accepted. The major fault found in the Röllgen model was reported by Kebarle [15]. He suggested that if the Röllgen model was true, then one would expect that there would be much more abundant small droplets which contain one ion and one or several paired electrolyte ions. The evaporation of solvent from such droplets will lead to gas-phase ion clusters of the type X+(NaCl)n where X is the solute. Kebarle tested this experimentally using NaCl and CsCl and could not find any such clusters. For a more detailed picture of these processes the reader is referred to reviews by Kebarle and Ho [21] or Kebarle and Tang [22].

3.5 Electrospray Instrumentation

Electrospray acts as a combined liquid inlet system and ionisation source. Electrospray is used with flow rates of 1μl - 2ml/min. The source temperature and nebuliser gas flow rate must be adjusted to match the flow rate and aqueous content of the mobile phase, such that a suitable solvent evaporation rate is achieved and this in turn produces adequate ion intensities. For example to consider the source of heat for evaporation of the solvent. If you take something like acetonitrile the heat of vapourisation is around 30 kJ/mole. The heat capacity is about 4 J/g degree or about 160 J/mol degree. Thus the temperature fall for complete evaporation would be 30,000/160 = 190K. For methanol or water the temperature drop would be much greater. This sort of calculation shows that complete evaporation of solvent by self cooling without heat transfer from the outside is not possible, so some source of external heat transfer is required. The only simple source is by gas phase collision. This is one reason for adding 'nebulising gas'.

A make-up flow is used for coupling to very low-flow rate chromatographic techniques, such that optimum flow rates into the MS are preserved. The choice of buffer in the mobile phase is important, as non-volatile buffers such as phosphate are unsuitable. This is because under electrospray conditions they tend to be precipitated out of solution and contaminate the source of the mass spectrometer.

3.5.1 Electrospray Sources

Two different mass spectrometers were used for the work described in this thesis. The source designs are described below.

a) Micromass Platform

Figure 2 shows a schematic diagram of the electrospray source from the Micromass platform mass spectrometer with typical operating voltages shown. Eluent flowing down the central capillary (narrow line) is made up with sheath liquid to a suitable flow rate, and further nebuliser gas is added. This gas may be preheated up to 180^{0}C and this helps the evaporation process. An additional flow of nebuliser gas coaxially around the inlet capillary provides direction to the spray. Overall there is a potential difference of the order of 3-4kV between the capillary tip and the nearest surface and this acts to promote ionisation. This produces a fine 'mist' of charged droplets, as described in the previous sections, and this is sprayed from the capillary onto a counter electrode (or pepperpot HV Lens), which is at a potential of 0.5kV. Ions are transported into the high vacuum system by use of the nozzle-skimmer arrangement, which acts as a momentum separator. The relatively light solvent and drying gas molecules are readily pumped away in the differentially pumped intermediate vacuum stage. The analyte ions are pulled into the mass spectrometer by the potential gradient which exists across the skimmers, or sampling cones.

b) Hewlett Packard MSD.

Figure 3 shows the electrospray source arrangement in the HP MSD. The main difference compared to the Micromass instrument is that the flow is sprayed at right angles to the entrance to the mass analyser. The electrospray nebuliser extends into the spray chamber so that the nozzle is inside the field generated by the mesh electrode. A nebulizing gas also enters the spray chamber in a tube that surrounds the needle. The mesh electrode is held at a voltage that is always 500V less than the entrance to the capillary. The capillary connects the spray chamber to the mass analyser. Electrospray ionisation occurs in the same way as described previously. The combination of strong shear forces in the nebuliser and the electrostatic field generated by the mesh electrode draws the sample solution out and breaks it into droplets. A heated drying gas flows across the entrance to the capillary to aid removal of the solvent and allow the formation of ions.

3.5.2 Mass Analysers

The function of a mass analyser is to separate the ions, produced in the ion source, according to their mass. There are a wide variety of analysers. Scanning analysers, including the quadrupole or magnetic sector detectors, allow only the ions of a given mass to charge ratio (m/z) to go through at a given time. Other analysers use Fourier transformation to allow simultaneous detection of all ions. The time-of

flight (TOF) analyser requires ions to be produced in pulses of very short duration compared to their flight time. This will normally be achieved, for example, by using pulsed laser sources, as are used for MALDI.

Instruments combining several analysers (tandem mass spectrometry) are being developed rapidly. They allow one to obtain a mass spectrum resulting from the fragmentation of an ion selected in the first analyser.

There are three main characteristics of any mass analyser:-

1) The upper mass limit - the highest value of mass/charge ratio that can be measured.

2) The transmission - the ratio between the number of ions reaching the detector and the number of ions produced in the source.

3) The resolving power - the ability to yield distinct signals for two ions with a small mass difference. Two peaks are considered to be resolved if the valley between the two peaks is equal to 10% (magnetic or ion cyclotron resonance instruments) or 50% (quadrupole instruments) of the height of the smaller peak.

Resolution R, can be defined as: -

$$R = m/\Delta m$$

where Δm is the smallest mass difference for which two peaks with masses m and $m+\Delta m$ are resolved.

For the work described in this thesis, a quadrupole mass analyser has been used exclusively. It is therefore appropriate to describe the operation of this type of Mass Spectrometer in some detail.

3.5.3 The Quadrupole Mass Analyser

Paul and Steinwegen [23] first described the quadrupole principle in 1953 and this was later developed further by Shoulders, Finnigan and Story [24] to produce a commercially available instrument.

In a quadrupole instrument, electric fields are used to separate ions according to their m/z ratio, as they pass along the central axis of four parallel, equidistant stainless steel (or molybdenum) rods (poles), which have fixed DC and alternating RF voltages applied to them. (Figure 4)

It is normally arranged, by suitable adjustment of the two field strengths, that only ions of one selected m/z can pass through the rod assembly. In this way the assembly is made to function as a selective mass filter. All other ions are deflected and strike the rods. A mass spectrum is produced by varying the strength and frequencies of electric fields, so as to allow different masses to filter through the system.

The advantage of the quadrupole instrument is that it is relatively simple and cheap to construct. However, the theory governing the ion trajectories is very complicated. A brief description is given in the next section. A more detailed explanation has been described by Dawson [25].

3.5.4 Quadrupole Ion Optics

The four rods of circular cross-section should theoretically have a hyperbolic cross section, but in practice this would be very expensive, and cylindrical rods perform quite satisfactorily if properly spaced. As well as Dawson [25], Gordon et al [26] have reported detailed theoretical studies of ion trajectories in quadrupole systems. The following discussion is limited to cylindrical rods.

Two opposing rods have a potential of $+(U+V\cos(\omega/2\pi)\ t)$ and the other two are at $-(U+V\cos(\omega/2\pi)\ t)$ where U is the fixed DC potential and $V\cos(\omega/2\pi)\ t$ is the RF amplitude at frequency $\omega/2\pi$ and time t. The applied voltages change on the pairs of rods (A,B) as $\cos 2\pi\omega t$ cycles with time.

The resultant electrical potential (Φ) at any position in the (x,y) plane i.e. the plane perpendicular to the axis of the rods, of the quadrupole is given by equation (3.3)

$$\Phi = \frac{x^2 - y^2}{r^2} (U+V\cos(\omega/2\pi)\ t) \qquad (3.3)$$

where r is the distance from the central axis to the rods.

It can be seen that when x=y, $\Phi=0$ and therefore this gives rise to a zero field strength along the central axis of the quadrupole assembly and along the two planes indicated in Figure 4. As a consequence of there being no field along the z axis, ions must first be accelerated in this direction. This is achieved by applying ~5V between the ion source and the quadrupole assembly, through which the ions are accelerated.

At all other positions the oscillating electric field causes ions to be alternately attracted to and repelled by the pairs of rods, as their trajectories oscillate

through the assembly. An ion of a particular m/z can only pass through the assembly at certain values of the parameters U,V and ω. When this occurs the trajectory of the ion is considered to be in stable motion. If the ion strikes the rods, it has a trajectory of unstable motion.

Mathematical solutions of equation (3.3) , first calculated by Mathieu, lead to two factors (a,q) that define the regions of stable ion trajectory. These are given below

$$a = \frac{8zU}{mr^2\omega^2} \qquad q = \frac{4zV}{mr^2\omega^2} \qquad \frac{a}{q} = \frac{2U}{V}$$

(note frequency, $f = \omega/2\pi$). The conditions for stability can be represented on an a, q diagram called a stability diagram (or Mathieu diagram, Figure 5). The shaded area indicates the zone of stable combinations of a and q. The line a/q, drawn on the diagram, is called a mass scan line. Each point on the line is representative of a particular mass. The section of the line (between m_1 and m_2) represents the range of m/z values that would pass through the assembly for those particular values of U,V, and ω. Ideally the line should pass through the stable region as close as possible to the apex (R). This would produce maximum resolution.

For a given assembly, r (the distance from the z- axis to the rods) and f, (i.e. ω. (frequency)) are kept constant. Mass scanning is achieved by varying U and V simultaneously, whilst keeping their ratio constant. The effect of this is to move along a particular a/q line such as that shown in Figure 5, and so scan the mass range. For any specific value of a or q, a specific ion mass is transmitted by the

quadrupole assembly while all other masses are rejected. It would be possible to vary ω and keep U and V constant, but in practice it is easier to change voltages rather than frequencies.

Figure 1: The ion-production process in electrospray including formation of the Taylor Cone.

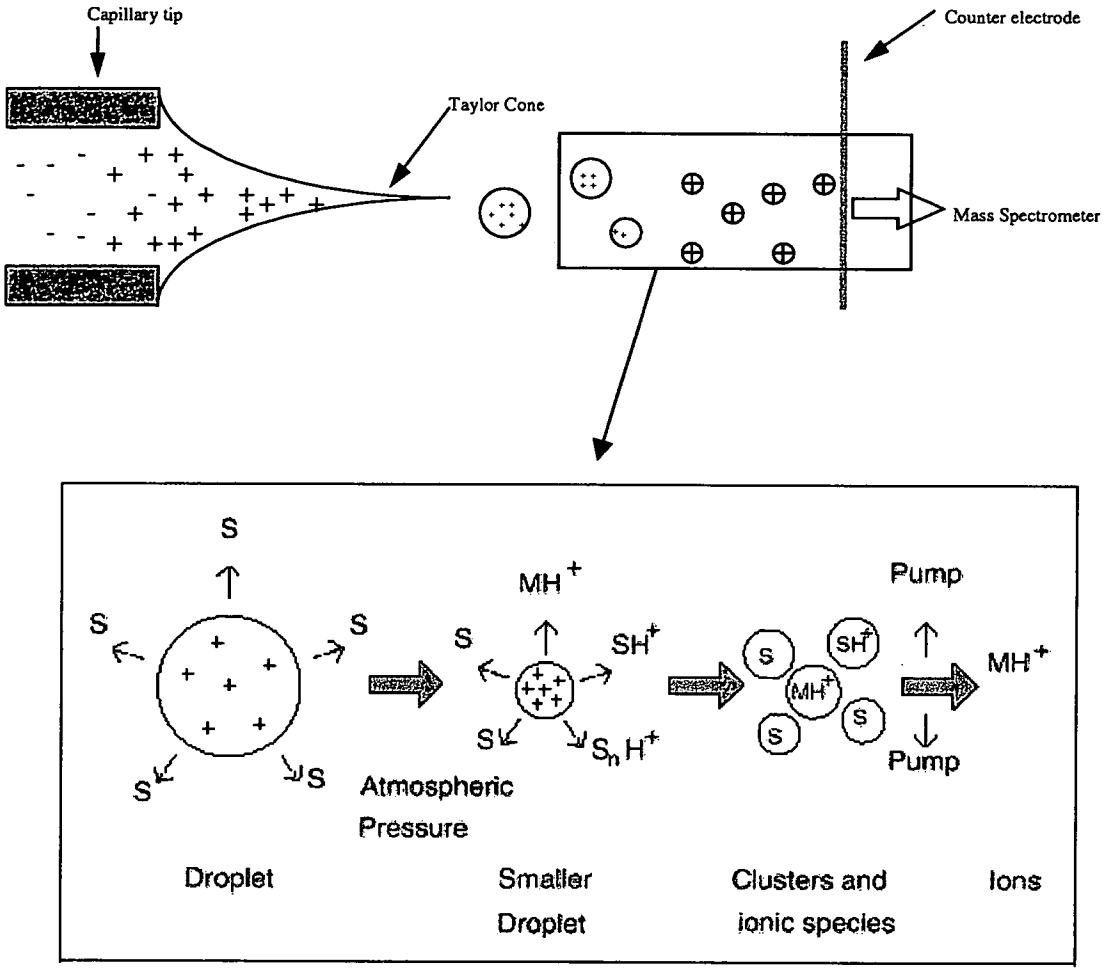

Figure 2: Schematic of Electrospray Source for Micromass Platform

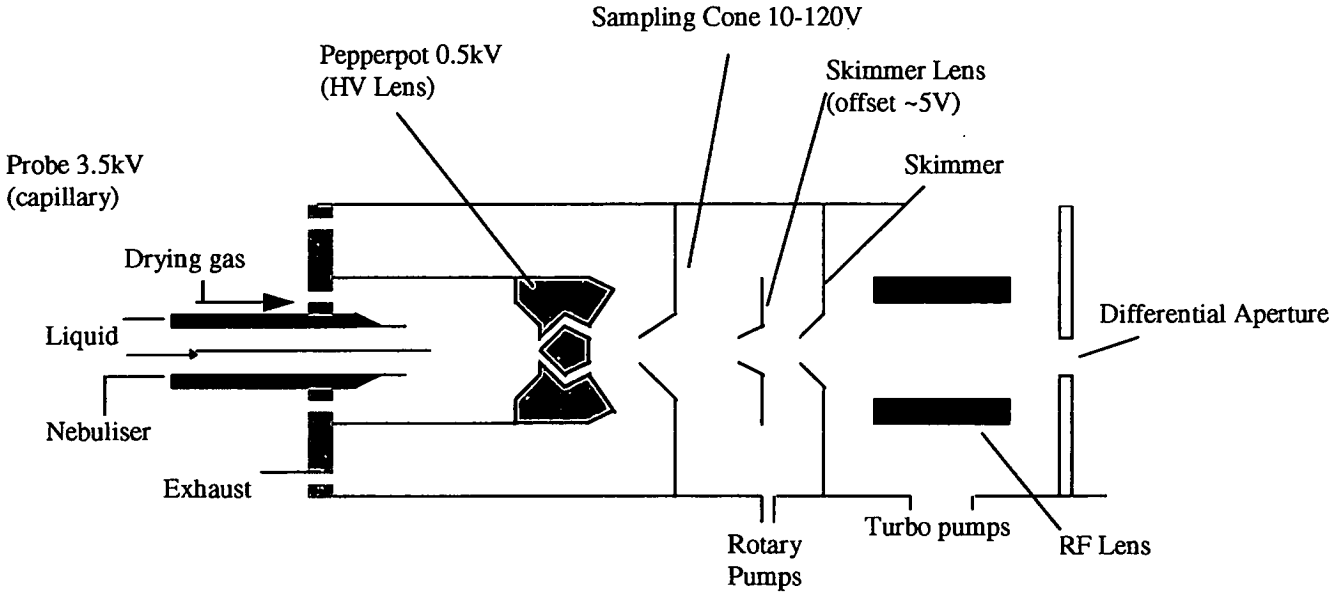

Figure 3: HPMSD Spray Chamber

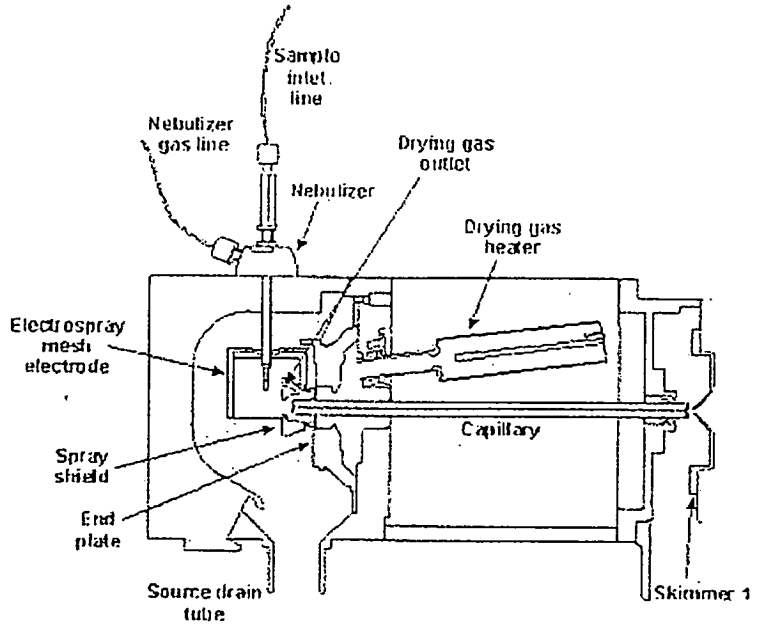

Figure 4 :Layout of quadrupole assembly

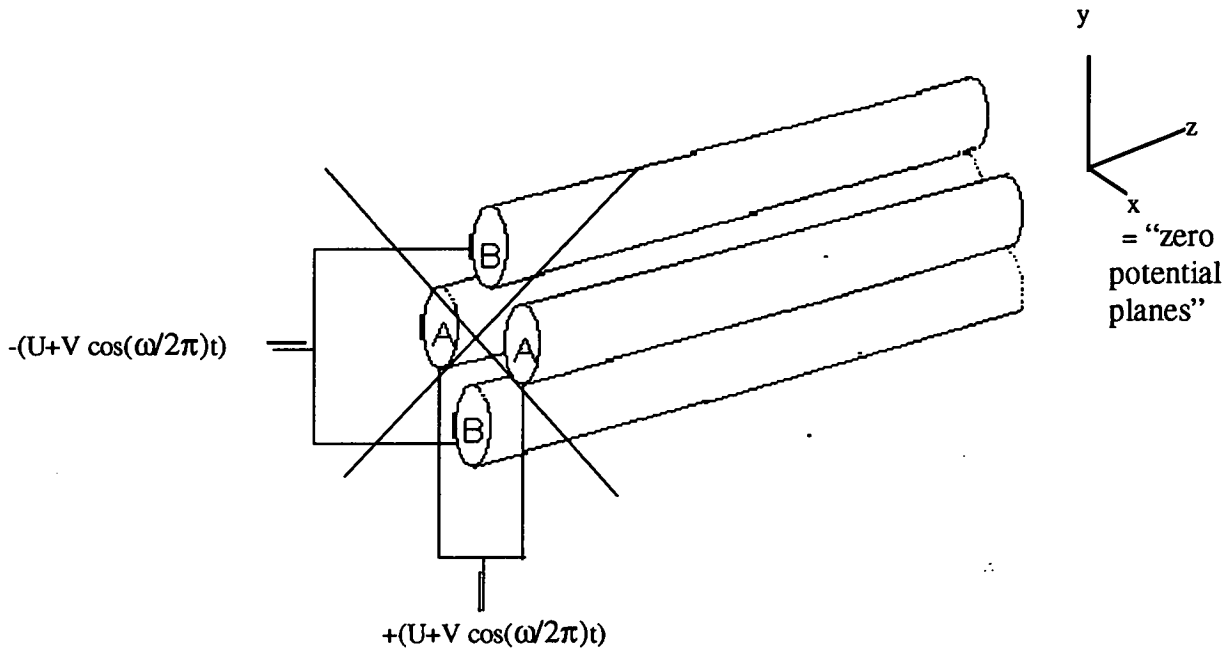

Figure 5: Stability Diagram for Quadrupole Assembly

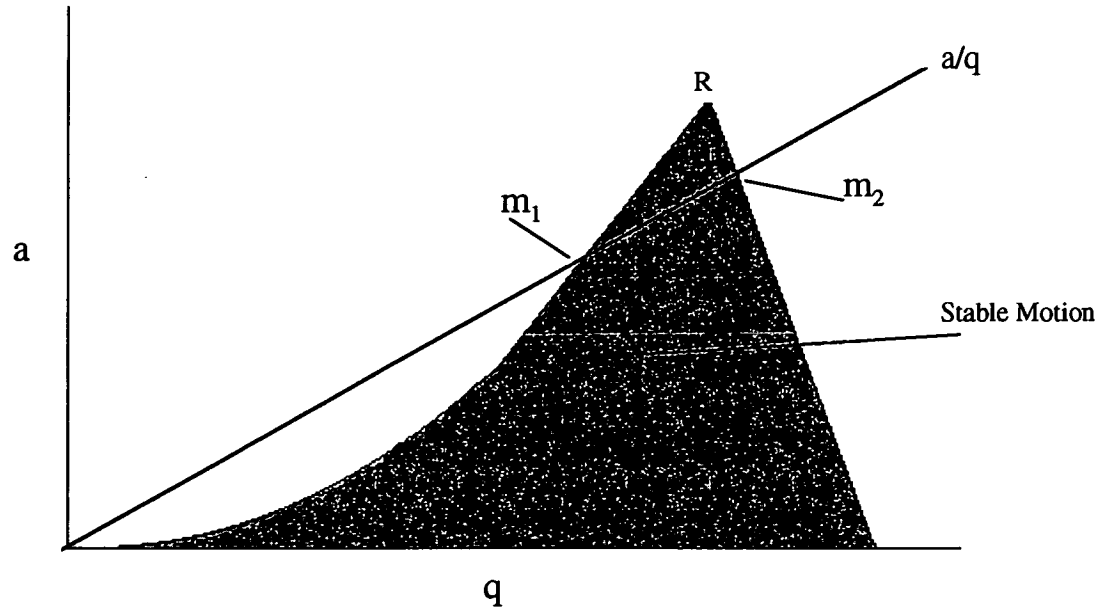

References for Chapter 3

[1] J.J. Thomson 'Rays of Positive Electricity and their Application to Chemical Analysis', Longman Green and Co. London (1913)

[2] F.W Aston 'Mass Spectra and Isotopes' Edward Arnold London (1942)

[3] W.E. Stephens, *Phys Rev.* 69 (1946) 691

[4] W. Paul, H.P. Reinhard, V. Z. von Zahn, *Phys.* 152, 143 (1958)

[5] E. Z. Fischer, *Phys.* 156 1 (1969)

[6] M.S.B Munson, F.H. Field, *J. Am. Soc* 88, 2621 (1966)

[7] M. Barber, R.S. Bordoli, R.D. Sedgwick, A.N. J. Tyler, *Chem. Soc. Chem. Commun.* 325 (1981)

[8] C.R Blakey, M.L. Vestal, *Anal. Chem.* 55, 750 (1983)

[9] M Dole, L.L. Mach, R.L.Hines, R.C. Mobley, L.P Ferguson, M.B Alice, *J. Chem Phys.* 49 2240 (1968)

[10] M. Yamashita, J.B. Fenn, *Phys. Chem.* 88, 4451 and 4671 (1984)

[11] M. Karas, D. Bachmann, F. Hillenkamp, *Anal. Chem.* 57, 2935 (1985)

[12] K.L Busch, G.L. Glish, S.A. McLuckey, *Mass Spectrometry/Mass Spectrometry VCH*; New York (1988)

[13] G.I. Taylor, *Proc. R. Soc. A* A280, 383 (1964)

[14] D.P.H Smith, *Trans. Ind. Appl.* IA-22, 527 1986

[15] M.G. Ikonomou, A.T.Blades, P. Kebarle, *Anal. Chem.* 63, 1989 (1991)

[16] Lord Rayleigh. *Philos.Mag.* 14, 31 (1882)

[17] F.W. Röllgen, E. Bramer-Wegner, L. J. Buttering, *Phys. Colloq*, 45, C9-297 (1984)

[18] G. Schmelzeisen-Redker, .L Buttering, F.W. J. Röllgen, *Phys. Colloq*, 45, C9-297 (1984)

[19] J.V Iribrane, B.A.Thomson, *J. Chem. Phys*. 64, 2287 (1976)

[20] J.V. Iribrane, B.A. Thomson, *J. Chem. Phys*. 71, 4451 (1979)

[21] P.Kebarle, Y. Ho, in R.B.Cole (Editor), Electrospray Ionization Mass Spectrometry, Wiley, New York, 1997

[22] P.Kebarle, L.Tang, Anal. Chem. 65 (1993) 972A

[23] W. Paul, H.S. Steinwedel., *Z. Naturforsch*., 8a, 448 (1953)

[24] R.E. Finnigan., *Anal. Chem*.,66,969A (1994)

[25] P.H Dawson, Quadrupole Mass Spectrometry and Its Application Elsevier; New York (1976)

[26] M. Barber, D.B. Gordon, M.D. Woods, *Rapid Comm. In Mass Spec.*, 4(10)(1990), 422

CHAPTER 4

Instrumentation and Experimental Details

4.1 Instrumentation.

4.1.1 CEC Instrumentation

Hewlett Packard 3D Capillary Electrophoresis Instrument (HP ^{3D}CE) (Hewlett Packard, Waldbronn, Germany) which has modifications to allow the application of up to 12 bar nitrogen gas pressure at each capillary end (via pressurisation of mobile phase reservoirs).

4.1.2 Mass Spectrometry Instrumentation

i) Micromass Platform Single Quadrupole Mass Spectrometer (Micromass, Altrincham, Cheshire, UK) fitted with an electrospray source.

ii) HP1100 MSD (Single Quadrupole instrument) (Hewlett Packard, Palo Alto, USA) fitted with an electrospray source and a capillary electrophoresis interface.

4.2 Chemicals

The following chemicals were obtained from the suppliers shown. All solvents used were HPLC grade, unless otherwise stated.

Acetonitrile - Rathburn Chemicals Ltd, Walkerburn, Scotland

Methanol - Fisons Scientific Equipment, Loughborough, UK

Phosphoric acid, Formic acid, Sodium Borate, Sodium Hydrogen Phosphate, Tris (hydroxymethyl) methyl amine (abbreviated to TRIS throughout thesis), MES (2-(N-morpholinoethanesulphonic acid)) - BDH, Poole, UK

Anisole, Benzamide, Uracil, Benzophenone, Biphenyl, Thiourea, Phenytoin, Prednisolone, Methyl-Prednisolone, Caffeine, Testosterone, Amoxicillin, Cefatrizine. – Sigma Aldrich Chemicals Co. Ltd, Gillingham, UK

4.3 Preparation of Test Mixes

All test mixes were prepared in acetonitrile/water (50:50). The composition and concentration of each mix is stated in the text. The order of elution is also stated in the legend underneath each chromatogram.

4.4 Preparation of Mobile Phases

The exact composition of each mobile phase is given in the text. In all cases the buffer was adjusted to the stated pH, prior to adding the organic modifier. In all cases the mobile phases were prepared by the addition of the respective volumes of each solvent that constituted their percentage contribution in the mixture. The prepared mobile phases were then filtered through a 0.5μm porosity solvent compatible filter, prior to use.

4.5 Injection procedure

All samples analysed on a CEC column were injected electrokinetically onto the packed capillary. This was achieved by placing the sample vial at the anodic end of the capillary and applying the voltage for a short time, normally between 1-10 seconds. This is done automatically on the HP instrument via software control. The injection time and voltage is stated in the legend below each chromatogram. The amount injected is a function of both parameters, such that injecting a sample for twice the duration at a fixed applied voltage (or vice versa), will inject twice the sample amount.

All samples analysed in an open tube by capillary electrophoresis were injected hydrodynamically. This involves applying a small pressure to the anodic end of the capillary, thus allowing the sample to be pumped into the capillary, under the control of a small applied pressure, typically 50mbar. Again, the amount injected is a function of pressure and time applied. The exact injection conditions are stated in the text.

4.6 CEC Columns.

The CEC columns used throughout the experiments described in this thesis were prepared according to the final method, using the ultrasonic probe and slurry chamber, described in chapter 5. Work on later experiments used columns purchased from Innovatech (Stevenage, UK), but prepared using effectively the same methods.

Chapter 5 Capillary Column Production Methods

5.1. Discussion of packing strategy

Packing a very small diameter column (capillary) is much the same in principle as packing a larger one and therefore a very good start can be made by making use of what has been previously reported [1-4]. However, it soon becomes apparent that there are inherent difficulties in trying to 'translate' some of the features of the existing methods to suit smaller systems. Firstly, the effectiveness with which a capillary is prepared depends on the quality of the retaining 'frit' which is inserted into the capillary before filling commences. If this frit is too non-porous it will exhibit too much flow resistance which will lead to slower fill rates and inconsistent packing. If the frit itself has variable trans-frit porosity it will cause significant disturbance to an otherwise well behaved solute band as it migrates through the frit leading to band dispersion effects. Control of these frit manufacturing methods is vitally important to the performance of CEC capillaries and yet can be difficult to maintain due to the extremely small dimensions involved. A full discussion of frit production methods can be found later in the text (section 5.4).

Fundamentally, it seems that in any packing procedure involving spherical particles filling a long, round tube, the packing density has to be maximised. That is that the particles need to fill the smallest occupied space. To be able to stand a reasonable chance of achieving this goal the filling rate has to be maximised such that the particles are literally 'slamming' into one another and therefore imparting as

much settling force as possible to their surrounding particles via kinetic energy dissipation. This is best achieved by using the largest possible packing pressures and the lowest viscosity packing solvent that is consistent with good phase slurrying [4]. When the capillary is filling with stationary phase if there is significant slowing down in the packing rate a streaming effect can be observed under the microscope due to faster solvent velocities down the centre of the capillary compared to the walls. This leads to the centre of the capillary filling ahead of the area near the walls and a subsequent 'column' of phase growing in the centre section with effectively no support from the void areas around it. This column is quite physically unstable therefore and will ultimately collapse, with the result that, as the particles involved have little velocity, they will resettle with little force and pack relatively loosely compared to the surrounding packed bed giving a poorly packed section. Observation of this problem and subsequent testing of the capillaries obtained confirms that these badly packed sections soon resettle under electrophoretic conditions (ie. the particles are able to pack better as they have electrophoretic velocities themselves) and give column voiding leading to a catastrophic loss in chromatographic performance. It is clear that a fast, consistent and preferably easy method of packing is needed.

The factor which most seems to affect the filling rate is the rate of introduction of stationary phase at the capillary inlet. This in turn is highly dependent on the 'local' stationary phase slurry density at the capillary inlet. It is this factor more than any other which controls the effectiveness of capillary packing methods. It has been suggested that slowly packed capillaries give far inferior

performance than is achievable using faster methods [4], although not all of the causes of slower packing are the same in each case. Causes of slow packing include viscous slurry and/or packing solvents, insufficient slurry concentrations , poor frits and low packing pressures (or more correctly low pressures per unit column length). Ironically, using traditional methods adapted from HPLC style packing there is a conflict because slurry solvents tend to be fairly viscous to promote maximum slurry-settling times. When used with small diameter capillaries, where the relative time to fill the capillary is long compared to the equivalent HPLC column, this leads to slow packing rates as the flow rate of packing solvent is severely reduced. By the same reasoning, if a lower viscosity slurry solvent is used , although the packing rate is substantially faster, it becomes slower quite quickly by virtue of slurry settling.

An interesting paradox, clearly a better method of capillary packing is required before routinely prepared capillaries will be capable of giving the necessary performance improvements that are needed to take our analytical techniques into truly miniaturised dimensions.

5.2. Existing packing methods

Most modern microbore HPLC columns and the small number of genuine CEC style columns used to date have been produced via a method of packing that is fundamentally the same as in traditional HPLC columns. The basic concept is to introduce a stationary phase slurry, in a suitable slurry solvent, prior to the column to be packed. After connection of the slurry reservoir (containing the slurry) to the

column, the solvent delivery valve is opened allowing a flow of high pressure packing solvent to 'push' the stationary phase rapidly to the end of the column where it is retained by the frit. The schematic representation of this arrangement is shown in Fig 1a.

Essentially, in an HPLC column the packing of the column is actually achieved very rapidly as there is very little flow resistance caused by the column tubing etc. So the underlying technique in packing is to almost 'immobilize' the dynamic stationary phase slurry by very rapidly filling the column. This way there should be a totally random distribution of particle sizes and very homogeneous packing order. Good columns are produced by a careful 'consolidation' procedure [3,5] involving the conditioning of the column with various solvent mixtures, normally of increasing viscosity, such that the minimum volume is occupied by the maximum amount of stationary phase, effectively the maximum packing density.

This methodology can be used to produce columns for CEC in exactly the same manner. However, in this case things are considerably different as the filling rate is much slower, and the longer it takes, the more the slurry in the reservoir settles out, leading to a situation of diminishing returns. Initially much work was done in trying to optimise the combination of slurry and packing solvents in the equivalent CEC system to enable these methods to produce good capillaries. However there were many problems with being able to pack suitably long capillaries reliably and much skill was needed to have a good chance of doing so. There are some differences in the system used for CEC columns. Firstly because of the longer times taken to pack these capillaries the whole slurry reservoir and capillary rig (or

as much of it as is practically possible) is immersed in an ultrasonic bath to minimise slurry settling and particle aggregation. Although in practice this seems to make hardly any difference as it is unlikely that the ultrasonic waves penetrate the steel reservoir (although they may assist in stopping particle aggregation within the capillary). If the capillary is packed in exactly the same way as an HPLC column the slurry reservoir is generally physically below the column to compensate for the effect that the larger particles would otherwise settle to one end of the slurry reservoir under gravity and consequently the column would have larger average particle diameters as you went along its length. If you do this with the CEC system as shown in Figure 1b, because everything occurs more slowly , the slurry settles such that the filling rate drops to a point where there is a negligible amount of stationary phase entering the capillary and packing effectively terminates. Experience with trying this system shows that for viscous solvents like IPA (which is a very good slurry solvent for most reverse phase materials) the packed lengths obtained are about 30-40cm at best. This in itself would be acceptable, but the last 10cm or so have normally packed much more slowly than the previous length, such that poorly packed sections would almost certainly lead to poor performance or voiding, normally a combination of both in that order. The following table 1 gives a summary of the main approaches tried and the problems encountered.

Table 1 - Packing / slurry solvents for CEC capillary production

Slurry Solvent	Typical Packed Length Achieved	Degree of Success	Reason(s) for failure
IPA	30cm	Reasonable	Packing rate too slow, and later sections poorly packed.
Acetone	20cm	Poor	Too little length achieved, slurry settling too quickly.
Ethanol	30cm	Reasonable	Reasonable compromise, rate of packing slows too quickly for usable lengths.

All experiments performed used a packing solvent the same as the slurry solvent, however due to the extremely small volumes involved only a very small amount of slurry solvent from the slurry reservoir manages to pass through the capillary. Therefore the choice of packing solvent is relatively unimportant and if any of the previous experiments were performed using acetonitrile instead of the solvents listed, no significant change in the outcome was noticed.

If a slightly different approach is taken and the slurry reservoir is connected physically above the capillary as shown in Figure 1c then the system works better, as when the stationary phase settles, as it does to just the same extent, then it falls in the direction of the capillary entrance and the reduction in filling rate is not so severe. This system has been used by Norman Smith [6] and I think he has produced the longest and best capillaries to date using traditionally derived techniques.

However , it would still be highly desirable indeed to have a much improved method of producing these capillaries that relied far less on the speed and skill of the practitioner and was more consistent with the need to commercially produce these separation devices in the longer term.

5.3 The Development of a Novel Method for Producing Packed Capillaries

The biggest problems to overcome to improve the production of packed capillaries are to increase the packed bed filling speed and consistency. Both of these parameters can be improved at once by being able to maintain the slurry density and homogeneity for longer time periods, preferably indefinitely if possible. For this to happen, it seems that the only practical way is to somehow maintain movement of the slurry within the slurry reservoir or chamber. To this end, a slurry chamber was constructed, which allowed stirring within the chamber via construction of a flat bottomed design which sat on a magnetic stirrer plate and was stirred by a small internal stirring flea (see Figure 2).

This allowed the slurry to be stirred vigorously during the packing procedure and it was hoped that this would solve the problem of maintaining the slurry consistency. However, although slightly faster filling rates were observed initially, it was soon evident that aggregation of particles was a major problem, inevitably leading to premature blocking of the capillary, and the stirrer was contributing significantly to the increased incidence of this problem. Another method was needed which did not increase the likelihood of particle aggregation.

Slurries are normally prepared by taking a known mass of stationary phase and adding a known volume of slurry solvent and suspending this mixture in an ultrasonic bath for a convenient period of time, typically at least thirty minutes. It was felt that the only real chance of achieving all the objectives for slurry maintenance was to try and introduce ultrasound within the slurry chamber. Initially an ultrasonic probe was thought likely to be the best way to try and introduce the ultrasound, although it was also clear that a way had to be found to insert this probe and still seal against the required chamber pressure, which would ideally be as high as possible. Early attempts to fix a stainless steel ferrule on the solid titanium probe proved useless, as when inserted in the chamber the ultrasound activity was completely lost, presumably around the chamber itself, a bit like 'the tail wagging the dog'. Care was taken to mount the ferrule, or any subsequent device, at a nodal point (a node in the ultrasound waveform) on the probe such that the ultrasound activity at that point was minimal and therefore no undue stress was experienced by the probe itself. The second design incorporated a flange at this nodal point instead of a ferrule, this gave much more confidence that there would be no problems with the ferrule-style mounting with regards to slipping or giving way completely. Also, it allowed for the design of a 'soft' seal type mounting which would allow the probe to effectively 'float' and not transmit too much ultrasound activity through the chamber. This second design was also built with two joints in the chamber such that the chamber could be loaded with slurry without having to disturb the flange seal, so that once the probe was fitted it could be left in the top half of the chamber permanently.

This design worked beautifully and it was found that capillaries in excess of a metre long could be prepared inside five minutes. To confirm that this device was really having a significant effect on the capillary packing the ultrasound was switched off during packing and a short time later a drastic drop in the packing rate was observed when looking at the capillary under a microscope. On turning the ultrasound back on a corresponding drastic increase in the packing rate was observed. Using acetone as packing/slurry solvent and 3μ particle sizes with 50μ diameter capillary and a packing pressure of 850bar (10,000psi) filling velocities of 2 mm/sec were typically obtained. Using the best of the traditional methods, average filling velocities of 0.2mm/sec were typical, although in these cases it was often fast at the beginning and much more slowly with time. Not much change in the filling rate was noticed when using the ultrasound chamber, whether the procedure was at the beginning or near the end. A full diagram of the ultrasound packing chamber is shown in Fig 3.

Subsequent use of the packing chamber showed clearly that the most inconvenient aspect of its use was actually having to use large tools to tighten and untighten the two halves and each time try and obtain adequate pressure on the seals to ensure good sealing. At this point the top half of the chamber was redesigned to enable a hand-tight unit to be used. This allowed the design of the bottom half to use a 'KAL-RES' seal (a soft chemically resistant rubber) and a defined stop, such that each time it was tightened to the same extent. This design (currently in use) is shown in figure 4.

When using the chamber method of preparing a capillary it could be extremely useful to consider the possibilty of preparing multiple capillaries at once, by manifolding several capillaries from the chamber. This is easily achievable in principle as the packing pump could easily maintain the flow consumption rate of several capillaries, without any significant difficulty in maintaining packing pressure. However, the difficulty lies in producing frits in the capillaries that give a very consistent flow resistance such that the packing procedure does not take the path of least resistance and predominantly pack one capillary in preference to the others.

This problem, and indeed the problem of making reproducible frits in general, can be overcome by using a 'mechanical' frit (see Fig. 5) instead of one prepared in situ. This is achieved by using a stainless steel mesh of sufficiently small porosity which can be held in the equivalent of a miniaturised HPLC type end-fitting. The capillary itself is held in the end-fitting by clamping it within some PEEK tubing with an inner diameter of 0.015'', or approximately 380 μm, which closely matches the outside diameter of the fused silica capillary at 375 μm. By using a stainless steel or a teflon ferrule to hold the PEEK around the capillary ,very good connections are obtained with minimal 'dead' volumes as the capillary end appears flush with the PEEK tubing end. This end can then be very tightly placed against the steel frit giving a very robust frit against which the capillary can be packed very effectively. Of course the packed columns have thermally fused frits prepared before use, as the end-fitting can only be used to prepare packed capillaries, not during use. But once the capillary is packed, putting frits inside the capillary is

very easy using a water flow and a frit filament burner device, and this procedure will be described in detail in the following section.

5.4. Frit requirements and production

There are many difficulties associated with packing very small diameter capillaries as have been discussed previously in this manuscript. One of the crucial aspects of preparing a good packed capillary lies in the production of the frit. The frit will , most importantly, retain the stationary phase within the capillary and allow further slurry liquid to flow through the frit and therefore the packing procedure to continue. The ultimate performance of the frit will depend heavily on the way in which it is prepared and the reproducibilty of the frit making process will influence the column to column reproducibility [7] . There are two main ways of producing frits, either mechanically (as described in the previous section) or by creation in situ using a silica paste. In a capillary of typical CEC dimensions the inner diameter will be 50-100 μm. The most simple method for introducing a porous frit into a capillary like this is to make an *in situ* frit using a method reported previously [8] which uses a mixture of sodium silicate (water glass) and bare silica HPLC type stationary phase.

First a length of capillary is cut using a sapphire or ceramic bladed cutting tool. It is beneficial to cut the end with as flat a face as possible. This end of the capillary is then 'tapped' into a blend of 3-5μm porous silica spheres that have been wetted with a 3:1 mixture of water : sodium silicate solution. The degree of wetting

is not crucial and mixtures from almost dry to a wet paste have been used successfully. This mixture will generally penetrate the capillary to a depth of about 100-200μm. This capillary end (containing the wetted frit mixture) is then inserted into the coiled filament of a filament burning device [8] and at a low temperature (filament just glowing red) is heated for about 10-20 seconds. A diagram of this burner is shown at the end of this section. The filament temperature is then raised to approximately 500-600^{0}C and the frit is heated again to fuse the particles within the mixture together with the silicate solution acting as a sort of 'glue'. The amount of silicate used (ie. how wet the paste is to begin with) will contribute to the robustness and porosity of the frit. The initial heating stage is important to drive off most of the water without too much physical shock to the frit structure. Severe heating will cause local solvent boiling and completely destroy the frit structure. If the procedure is carried out correctly then frits within the capillary will be produced which can withstand very high liquid pressures and which are very porous. The general requirement is for maximum strength and minimum flow resistance. If a good technique is developed frits should be obtained which look like those in Fig 6. It can be seen from the SEM pictures that the particles are very firmly stuck together using the fusing process and the silicate 'glue' can clearly be seen around the particles. When the frit is made it should be tested with a typical liquid pressure that would be used in the packing procedure. This will ensure that it will not fail during the packing, and also the results obtained from pressure testing should give a 'rough' quality control indication as to the porosity of the frit. A good frit will give a nice even spray if pressure tested with a suitable solvent at high pressure (8-10,000 psi),

see Fig 7. When this is done the capillary, now full of test solvent, should be sucked or heated dry before the packing commences.

5.5 Packing procedure

Initially a slurry of the stationary phase was prepared in a suitable solvent to a concentration of between 75-100 mg/ml. This slurry was ultrasonicated for at least 30 minutes prior to introduction into the slurry chamber. The capillary (50μm i.d, Polymicro Technologies, Az ,USA) containing the end frit (either in situ or mechanical) was connected to the outlet fitting of the slurry chamber and the high pressure liquid supply (from the packing pump) was connected to the inlet fitting. The top section , containing the ultrasound probe, was fitted and the ultrasound probe was switched on to maintain a homogeneous slurry. The solvent valve was opened to allow pressurisation of the chamber and consequent liquid flow, and the packing procedure commenced. During the packing procedure the ultrasound probe was left switched on to maintain good slurries and packing rates. Using this method packing rates were adequate to prepare packed lengths of between 70-100cm within 5-10 minutes.

When a sufficiently long length of capillary had been prepared the ultrasound device was switched off. This did not immediately terminate the packing procedure but the rate of packing dropped considerably until, within a short time, it was insignificant. The system pressure was relieved via venting in a controlled manner through a three-way 'bleed' valve restricted by a short length of small bore (throttle)

capillary. Upon depressurisation, the packing solvent was replaced with water and the system repressurised with a water flow to 'consolidate' the packed bed before a 'retaining' frit was fused The retaining frit holds the stationary phase in place, and the fusing of this frit defines the precise packed bed length to be used. This length is generally chosen to fit the particular instrument that is being used. This method of frit production, which is used to create the actual working frits, is performed by setting the temperature of the frit-fusing device to gently heat the capillary. This will enable a small length of capillary packing to be fused whilst not disturbing the packed bed due to flash evaporation of too much water. It is thought that under the high temperature fusing conditions (500-600°C filament temperature) the residual water dissolves enough silica from around the stationary phase to fuse the stationary phase particles together. Frits prepared using this method are highly porous and reproducible (see Figure 8) as there is no contribution from any silicate, as there is in the method for making the original frit. Moreover, the silicate glue is just from particle dissolution. This enables this frit to behave just as if it were an immobilized part of the normal stationary phase, the ideal qualities for a frit, giving effectively a 'fritless column'. It is clear that these particles are fused together in this frit because if the capillary is cut at a point in the packed bed where the phase has not been fused then the particles are free to move and indeed do, as shown in Fig 9. Although the temperatures for fusing are always way above the boiling point of water at atmospheric pressure, of course the frits are created at the 'high pressure' end of the capillary nearest the pump supplying the water flow. The pressures here are in excess of 600 bar and therefore there is no risk of solvent boiling.

It is beneficial however to create the frit at the minimum temperature required to achieve adequate particle fusing and in most cases these temperatures are low enough not to significantly remove the polyimide coating. Removal of the polyimide

coating is highly undesirable as this leads to very fragile regions of the capillary where the coating is removed. Whilst it is unavoidable for the detection part of the capillary or 'window', due to the need for UV transparency, it is beneficial not to remove the coating at the frit positions. Capillaries which have too many fragile areas are very easy to break .

It is difficult to measure the accurate temperature at which the fusing is taking place but a rough guide to the capillary surface temperature can be deduced from the degree of decomposition of the polyimide coating when observed under a microscope after frit formation. The degree of 'charring' can be compared to some reference photographs taken of capillaries which have been subjected to very accurate

temperature scanning in a furnace designed for differential scanning calorimetry (Figure 10.) The first capillary in the photograph shown is untreated and therefore represents the control. The others from left to right are at 500, 550 and 600^0 C. These photographs suggest that thermal decomposition of the polyimide coating occurs from 500 ^{0}C , although quite slowly at this temperature. Towards 600 ^{0} C it becomes rapid and above this temperature it is removed completely, quite rapidly.

It has also been observed on several occasions that different stationary phase materials require slightly different fusing temperatures to obtain stable frits.

Sometimes the filament is very close to the temperature at which it will remove the polyimide, before fusing the frits effectively. In these cases it is sometimes possible to reduce the temperature slightly and increase the duration of fusing to get successful results. However, care must be exercised during this procedure, as if the filament is left on for too long it can cause too much silica dissolution locally, leading to a 'blocked' frit. The data in table 2 gives some summaries for different stationary phase materials used to date. All these frit preparations have been carried while the capillary is under a water flow with a maintained pump pressure of 10,000 psi.

Table 2. Comparison of different frit fusing conditions for different phases.

Stationary Phase	Phase Chemistry (if known)	Minm. Temp for stable frit. (^{0}C)	Fusing duration	Degree of polyimide 'charring'.
ODS*	C18	450	10 secs	Very slight
Phase Sep SCX	Aliphatic sulphonic acid	450	10secs	Very slight
Hypersil mixed mode	Aromatic sulphonic acid and C18	500-550 450-500	10secs 20secs	Significant Slight

* ODS refers to any of the C18 materials used and includes Spherisorb ODS1 and ODS2 and Hypersil ODS and BDS

The retaining frit is prepared a suitable length from the original end frit (normally approximately 35cm which gave a separating length of approximately 30cm when the inlet frit was replaced with a second inlet frit). When this was completed the solvent was changed to approximately 80% CH_3CN / H_2O and the flow was inverted such that the direction of flow was against the retaining frit and away from the original inlet frit. This inversion step was included to allow for any relaxation of the packed bed which may give rise to further settling and subsequent void formation. This system was left for at least 24 hours to allow any settling to take place. Finally, the solvent was again changed to water before preparation of the replacement inlet frit which was created about 5cm in from the original frit to give a working length of approximately 30cm. The detection window was created just downstream of the retaining frit and the completed capillary was detached and mounted in a cartridge holder, ready for use

5.6 Troubleshooting

To check that a capillary is functioning normally , it is advisable to run a test mixture at fairly regular intervals. This is similar to HPLC. The normal procedure would involve running a neutral test mixture such as that shown previously in this manuscript , to ensure adequate quality chromatography is being obtained.

There are many ways in which a CEC separation can be 'interrupted' or affected by a change in the continuity of the separation system. These can be loosely

arranged into three main areas, viz. chromatography problems, baseline problems and current problems. Due to the nature of origin of these different problems there is some overlap in diagnosing and fixing the potential fault. The following sections give guidelines as to spotting the most common problems, and advice on how to correct them.

Chromatography problems.

In CEC , as in HPLC , the main cause of loss of chromatographic separation performance is due to void formation within the column. Fundamentally this is when a gap forms at the top of the separation column, which often prevents proper introduction of the sample band and can cause additional dispersion, sometimes leading to catastrophic losses in performance. In CEC there are added difficulties due to the flow differences between packed / unpacked sections which further destroy the sample introduction, leading to extra problems. In my experience it seems that no matter what packing method is used for producing the packed capillary / column , the stationary phase particles never pack into the minimum available volume. This means that there will be some degree of settling, at some point, leading to a voided column top , however small this void may be. When this occurs, it happens suddenly over a short period of time. This indicates that there is a sudden 'collapse' in a packed bed which until this point was reasonably stable

Under the electric field, the particles, which are negatively charged, will attempt to move against the EOF. Normally though, the EOF is large enough to immobilise the particles against their neighbours, in the direction of flow, to prevent

any movement. However, there are times when the switching on and off of the power in consecutive sample analysis leads to shifts in the bed structure and subsequent void formation. It seems likely that when this occurs the number of 'faults' in the packed bed are reduced and it would appear less likely to happen again. This is encouraging as voided capillaries can be very easily repaired, simply by repeating the frit manufacturing step at the capillary top, when the capillary is reconnected to the high pressure water flow used in the original manufacture. Not only does this regain performance, but it is often improved as we effectively now have a **better** packed column. This voiding phenomena and the performance of the 'repaired' capillary is shown in Figure 11, reproduced from a paper published by the author [9].

These capillaries can easily be recovered by reconditioning in water for a short time and creating a new inlet frit further down the packed bed. The performance of a 'repaired' capillary (after voiding) is shown in Figure 12. This is the same capillary as shown in Figure 11, but shorter due to the new frit creation. It is worth noting that the repaired capillary has since carried out several hundred more analyses. A reasonable argument exists for introducing the electrophoretic voiding step as a means of maximising the capillary performance and lifetime, as it seems far less likely to lose performance again once the original void has been repaired. Apart from this voiding phenomena, the lifetime and robustness of a working capillary largely depends on the way it is handled and the type of samples which need to be analysed.

Baseline (or Detector) problems

When we talk about a 'baseline' in chromatography, we mean the signal obtained from the detector when there is nothing in the detector cell causing an absorbance signal. Ordinarily, if appropriate choices have been made for the mobile phase then a flat, stable signal should be obtained. Under normal flow conditions there should be little, if any disturbances to this signal until such time as something does pass through the detector cell.

When using CEC, the conventional method of detection is to 'look through' the column itself. As the flow is driven electrically and the effective cell path length is small, it is usual to see a very smooth, stable baseline with very low noise characteristics. However, it is not unusual in CEC applications, even those reported in the literature, to see substantial disturbances , indicating that not everything is as it should be. As problems start to develop there is generally an increase in baseline noise. It can be for a number of reasons, but the two most common are irregular 'spikes' due to gas bubbles producing signals almost like 'pseudo-peaks', as they move rapidly through the cell (Figure 13). Or very noisy, random signals that also affect the quality of spectra obtained on instruments equipped with diode-array detection (DAD). The latter interferences are caused by the capillary window shifting in the cell mounting, such that the optical detector beam does not have a clear 'line of sight' across the open section of the capillary window. The detection beam becomes deflected by the last few particles of stationary phase of the retaining frit. This particular problem can be easily rectified by relocating the capillary detection window in the cell-holder.

In the case of the gas bubbles, it is normally necessary to pump the capillary out. If use is continued once regular gas bubbles are being observed, the problem is likely to get worse. The pressurisation of the mobile phase vials is usually required to avoid continual trouble from this particular problem.

If in-line capillary to capillary connections are made, with the electrical earth being made at the connection, then any gaseous products of electrolysis [10] also travel along the connection capillary and can interfere with subsequent optical detection. It is important to configure such systems such that any optical detection is carried out prior to the electrical grounding point [10].

Electrical Current problems

When we refer to current problems we are not actually interested in diagnosing a fault with the electrical parts of the instrument. The measured current on a CEC instrument is effectively an indicator of the amount of power consumed by the column system. Therefore when everything is working well, the value of current displayed should be relatively stable, and consistent for different analyses employing identical conditions. Variability in the current value generally gives an early warning sign that something is starting to fail. Based on practical observation there are two main problems that can be effectively diagnosed by monitoring the current value during an analysis. Most commonly, the current value starts to drop and sometimes 'cycles' between a higher and lower value, but at a lower average value than expected for the conditions. This is usually because there are 'dry spots' forming inside the packed column and local variation in flow rate (EOF) is observed. This

can lead to variable retention times for analyses, that should not be confused with buffer depletion, which gives the same problems but does not produce a variable current reading. If left alone, this will almost certainly get worse and will ultimately lead to a total loss of flow and severe drying of the packed bed. The only certain way of re-establishing constant flow (and current) is to pressure flush the capillary thoroughly before re-use. Again, pressurisation of the mobile phase vials significantly reduces the incidence of this problem occurring. If current loss is quite severe and no chromatographic peaks are detected at all, then it is highly plausible that the capillary has broken, most often at or near the detection window, and should be replaced with a new capillary.

In the relatively rare cases of the current value reading higher than normal, this is nearly always due to there being a 'gap', normally found at the top of the column. This can happen due to a void forming, and is indeed confirmatory evidence along with chromatographic losses. The extreme form of this behaviour is seen when the inlet frit is lost (normally due to it being smashed by collision with a sample vial lid). A gap appears very quickly due to stationary phase being lost from the capillary and the symptoms are almost identical to a voided capillary (indeed it is a voided capillary, without an inlet frit). In these cases the void or missing inlet frit should be repaired by removal of the capillary from the instrument and creation of a new inlet frit (ref).

In all troubleshooting scenarios in CEC, it is very important to stop the application of voltage as soon as a problem is suspected, and remove the capillary from the instrument so it can be inspected. This is best done under a microscope.

Dry areas, which are by far the most common problems, can be observed as 'dark' areas due to refraction differences. Breakages are generally obvious and if it's possible can easily be repaired prior to re-mounting the capillary on the instrument.

Figure 1. Arrangement of different packing layouts for HPLC and CEC

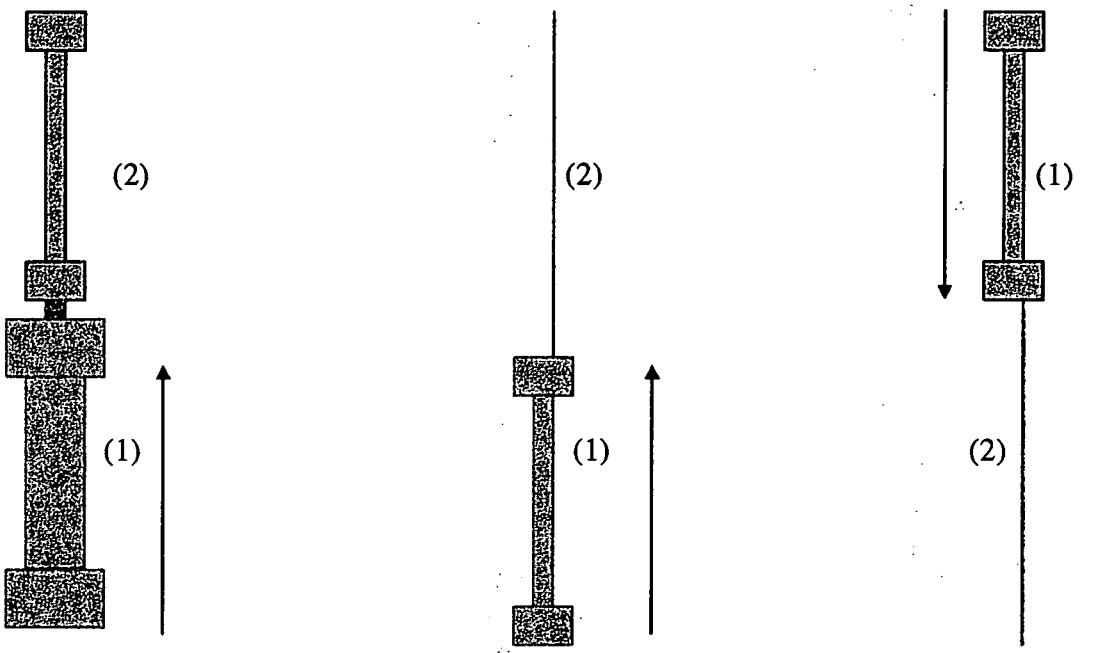

(a) HPLC (b) CEC (c) CEC

(1) indicates the slurry reservoir containing the stationary phase slurry, (2) indicates the column to be packed and the arrow indicates direction of flow of packing solvent.

Fig 2 Schematic views and 3-D view of stirrer chamber

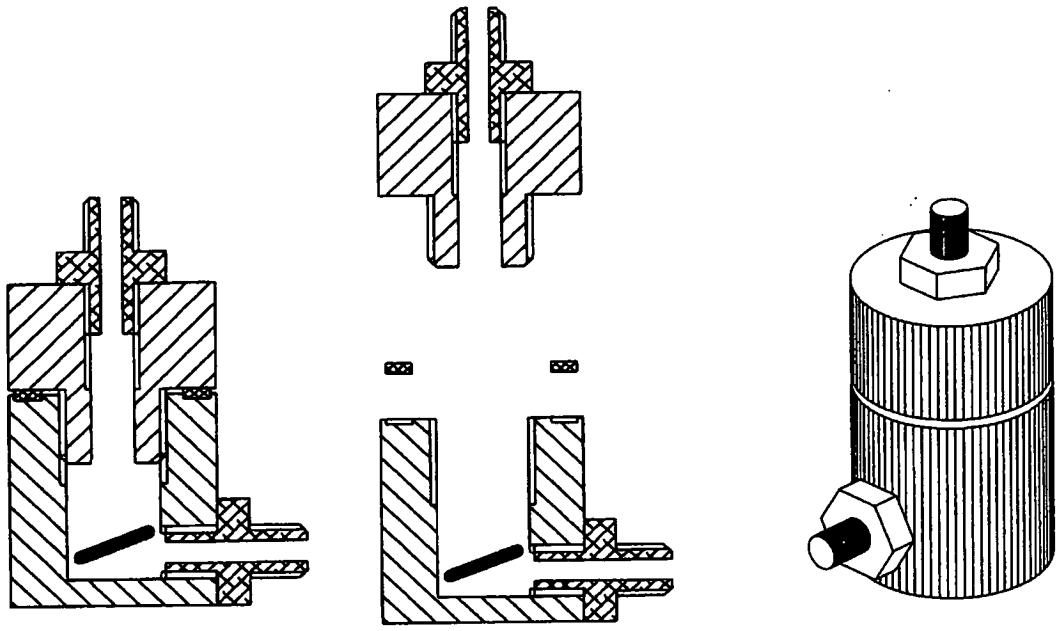

FIGURE 3. SCHEMATIC AND 3D-VIEW OF ULTRASOUND SLURRY CHAMBER

1. Ultrasound probe, 2. Slurry chamber, 3. Solvent inlet (from packing pump), 4. Capillary, 5. Steel support ring, 6. 7. High pressure seals.

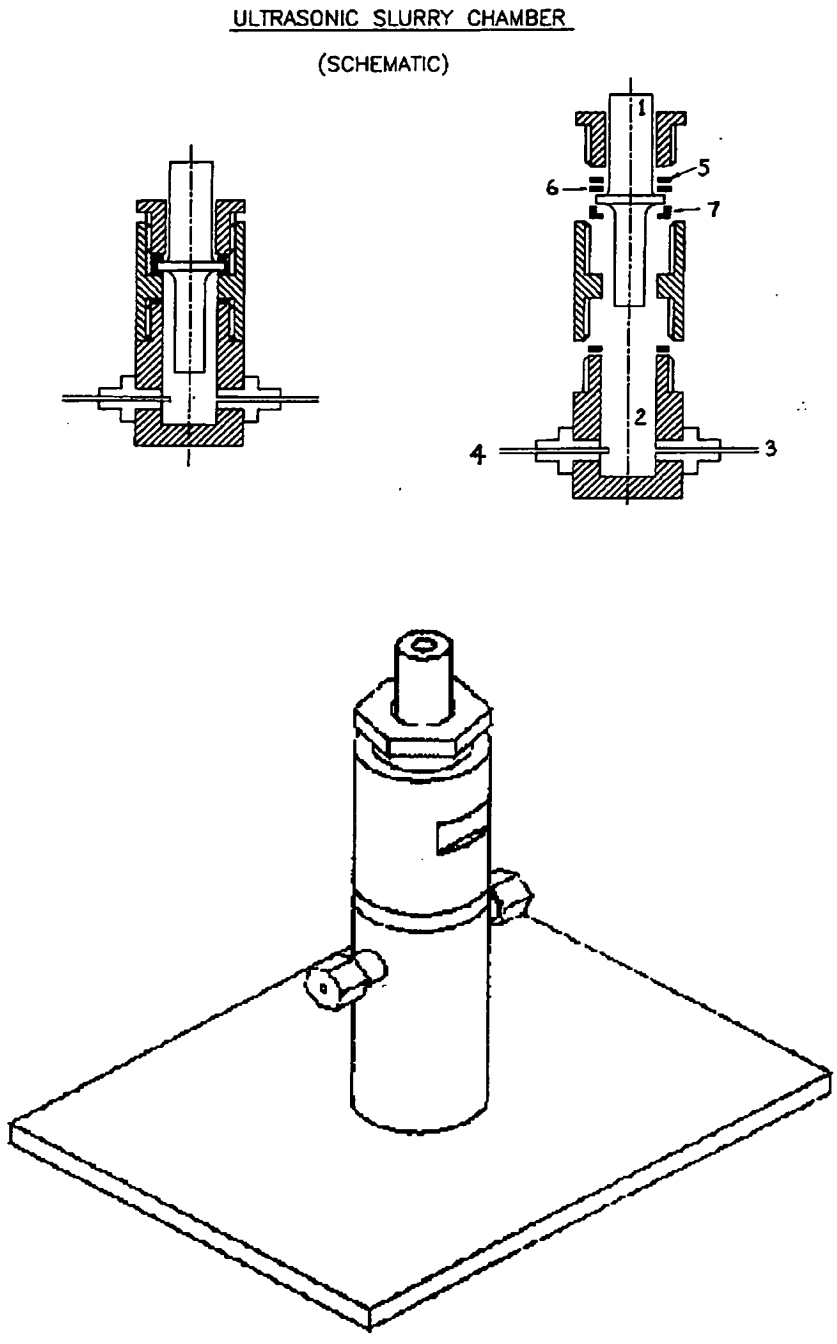

Figure 4 Schematic and 3-D views of latest design chamber. This design facilitated easy removal of the top half to improve slurry loading. Also the use of a defined 'stop' improved the consistency of the sealing mechanism.

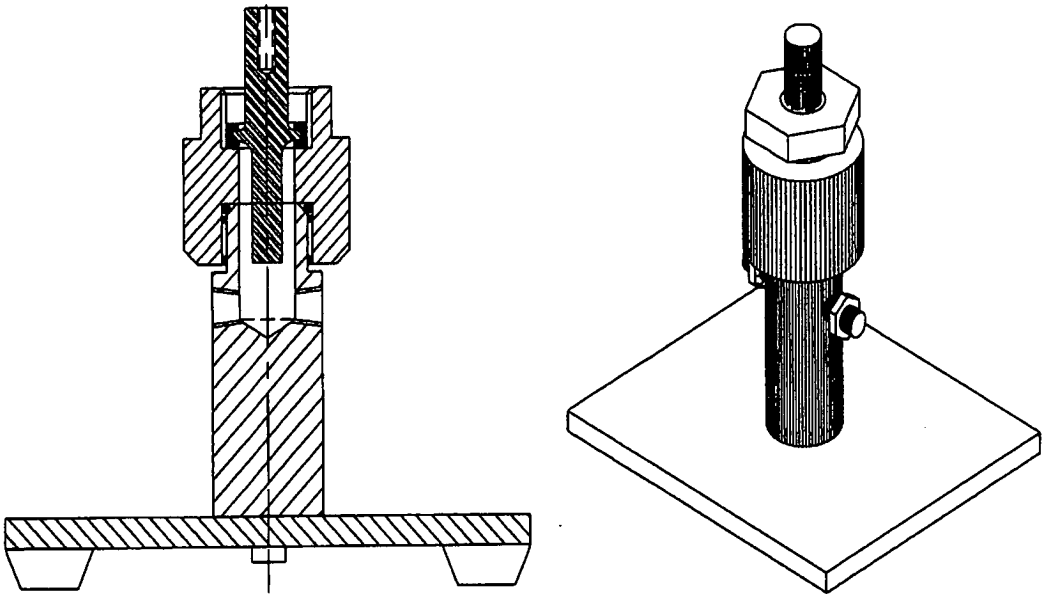

Figure 5. 'Mechanical' frit using a typical HPLC-type end fitting.

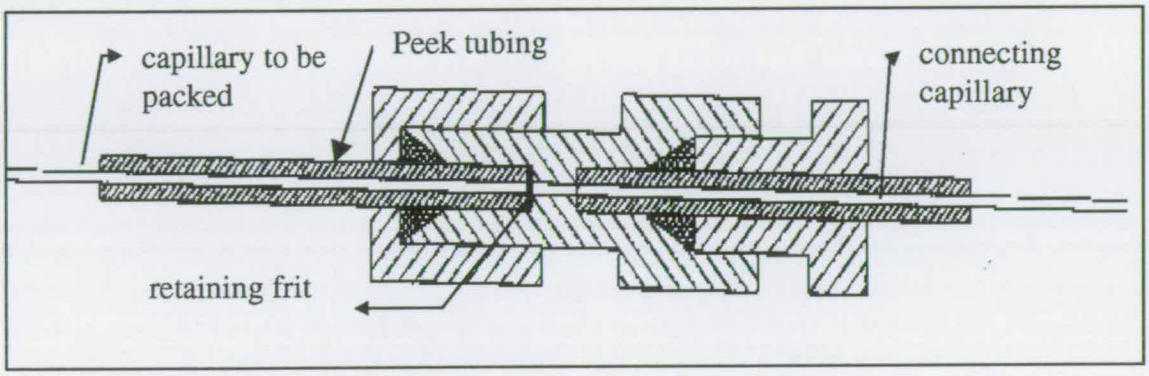

Figure 5a: Photograph of Frit burning device

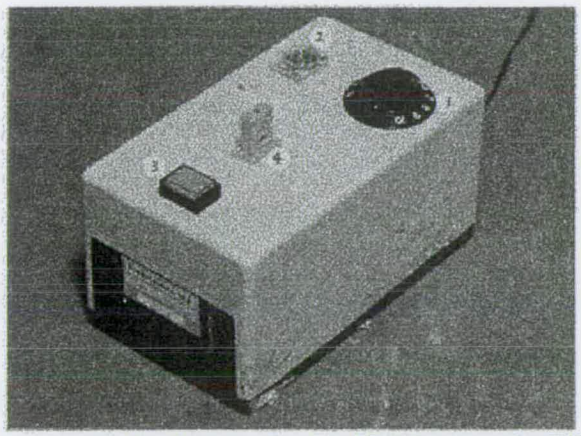

1= Temperature control, 2= Timer, 3= On/Off button 4= Filament

Fig 6 Picture of original end-frit made from aqueous sodium silicate solution. The silica 'glue' can clearly be seen sticking the individual stationary phase particles together

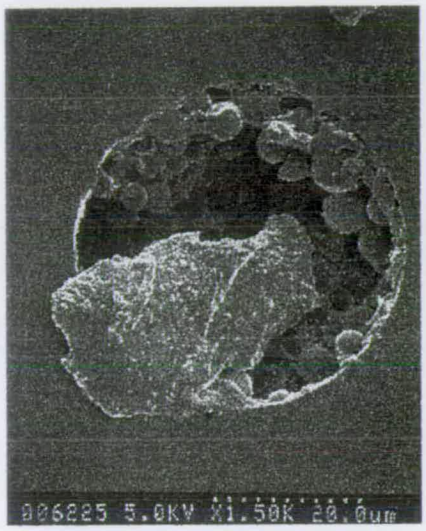

Fig 7 Picture of the solvent 'spray pattern' seen on passing packing solvent through the fabricated end-frit. This gives an indication of the frit porosity and confirms that this fritted column is suitable for packing.

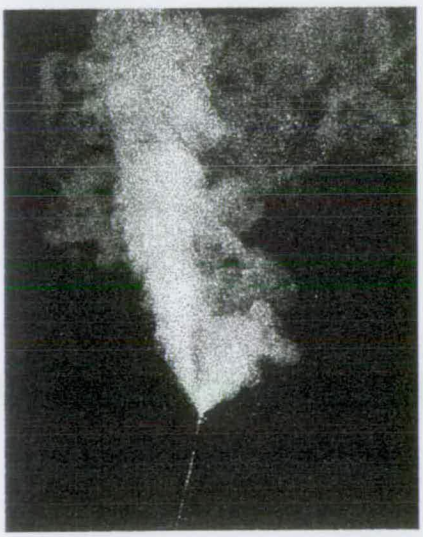

Fig 8 Cross-sectional view of retaining frit, which is fabricated by the thermal fusing of the material while pure water is passing through the column. Unlike the silicate-based frits there is very little silica residue around the particles, just enough to immobilise them and form a robust frit.

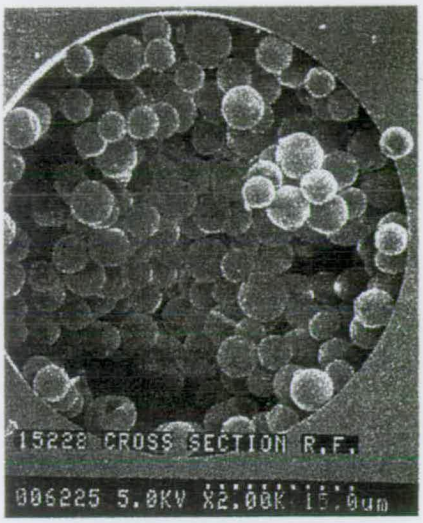

Fig 9 View of cross section of packed bed that hasn't been thermally fused. Evidently if the particles are free to move, they will move.

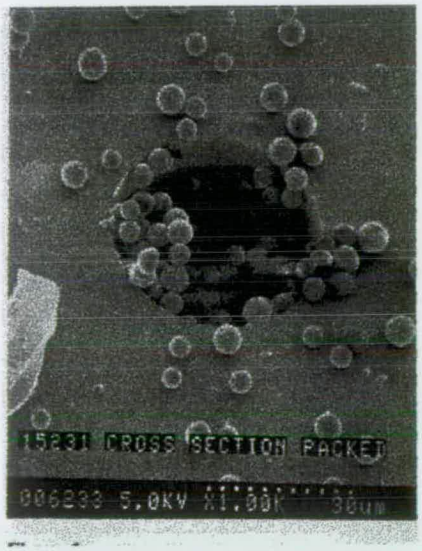

Fig 10 Photograph of fused silica capillaries that have been heated to temperatures of 450,500,550 and 600 C (from left to right). This gives an indication of the colour-change of the polyimide coating with temperature, and allows estimation of the temperature at the capillary surface.

Fig 10a Colour-chart representation of the variation of polyimide colour change with temperature. This can be used as a reference guide to estimate the surface temperature that a capillary was exposed to and is useful to determine optimum frit-fusing conditions.

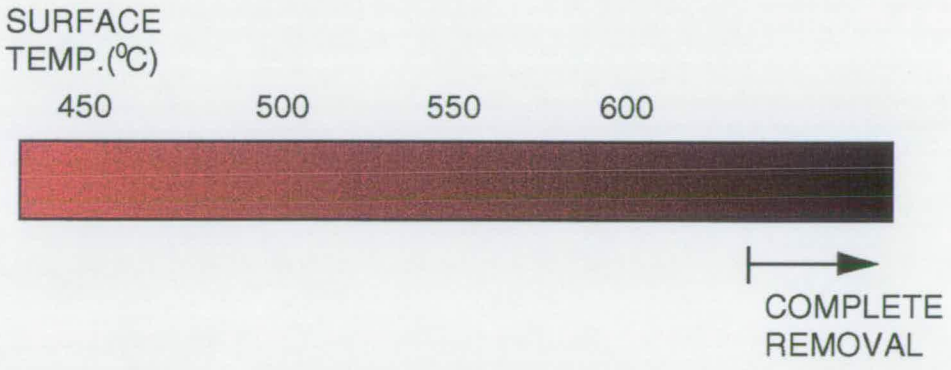

FIGURE 11. DETERIORATION OF CAPILLARY PERFORMANCE DURING USE Capillary 30cm Hypersil ODS, Conditions 25kV, Mobile phase 75% CH_3CN/ 25% 50mmol/L TRIS buffer (pH adjusted to 7.5 with HCl), 254nm, 15°C.Neutral test mixture shown previously

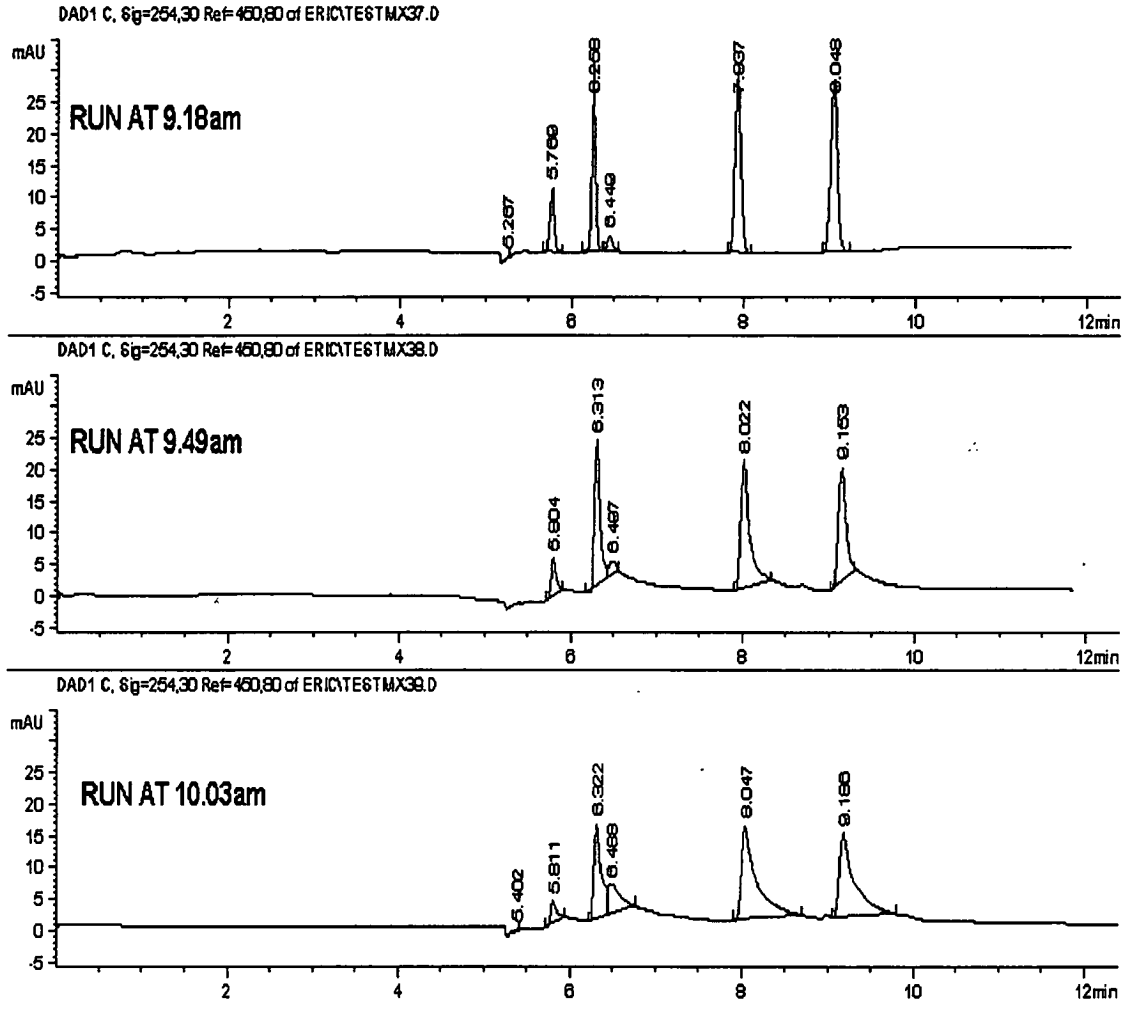

FIGURE 12. BEFORE/ AFTER CAPILLARY PERFORMANCE SHOWING EFFECTS OF CAPILLARY 'REPAIR' A. Performance of capillary before voiding (conditions as for Figure 3.), length 30cm. Identity of compounds is the same as Figure 2B. B. Performance after voiding and subsequent repair, length 25cm
All efficiency figures quoted are rounded to the nearest thousand. Capacity factors are calculated using the relationship $K' = t_r - t_0 / t_0$, and the 'solvent front' as the t_0 marker.

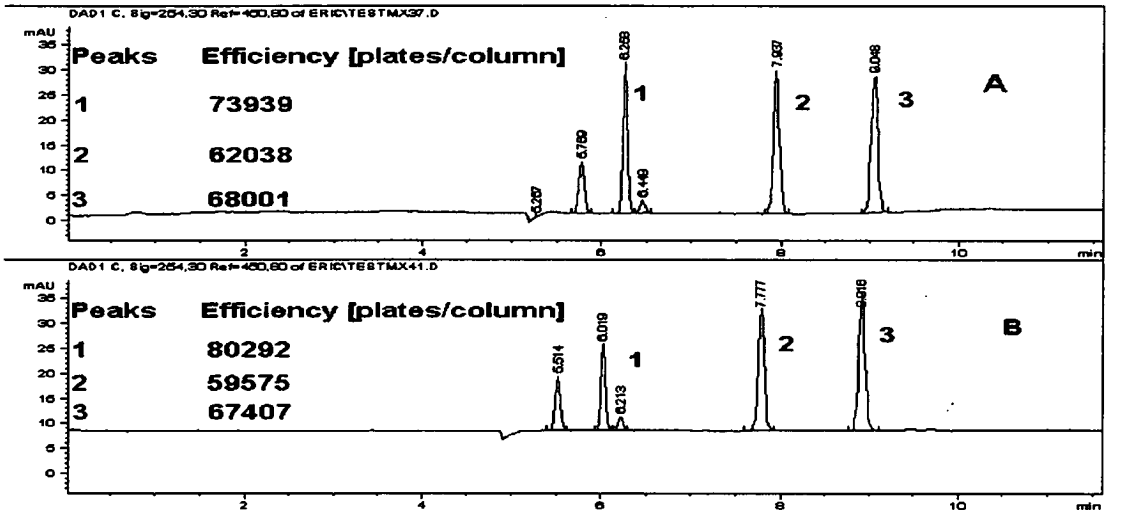

Figure 13. Chromatogram showing effect of gas bubbles interfering with detection signal.

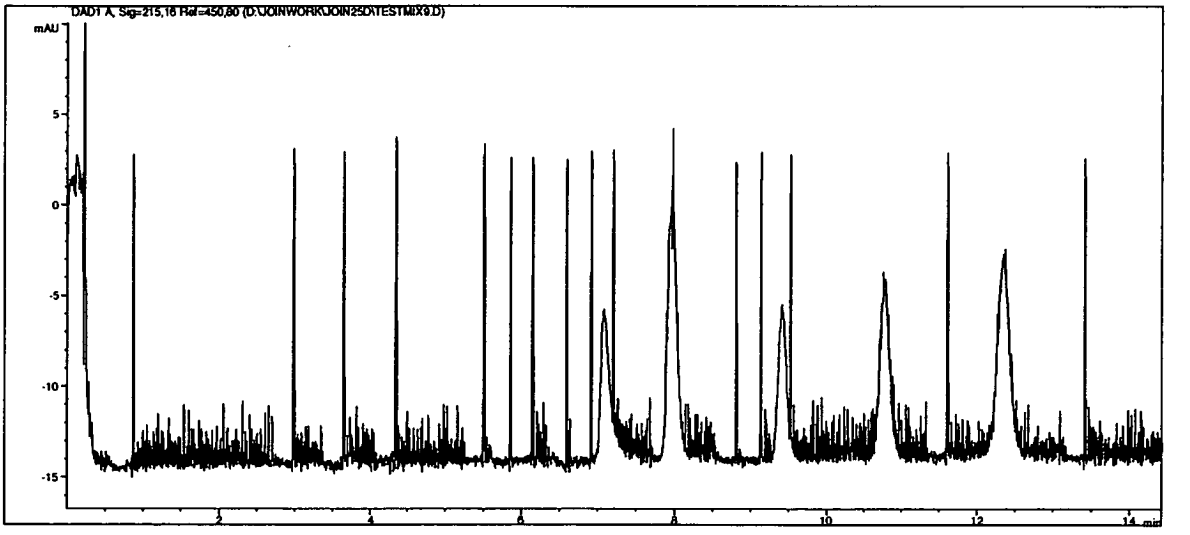

References for Chapter 5

[1]. R. T. Kennedy, J. W. Jorgenson, *Anal Chem,* 61, 1128 (1989)

[2]. R. T. Kennedy, J. W. Jorgenson, *J. Microcol. Sep.* 2, 120 (1990)

[3]. D. C. Shelly, T. J. Edkins, *J. Chromatogr.* 411, 185 (1987)

[4]. M. Verzele, C. Dewaele, D. Duquet, *J. Chromatogr.* 391, 111 (1987)

[5]. S. A. Karapetyan, L. M. Yakushina, G. G. Vasijarov, V. V. Brazhnikov, *HRC & CC,* 8, 148 (1985)

[6]. N. W. Smith, M. B. Evans, *Chromatographia,* 38, 649 (1994)

[7]. H.Rebscher, U.Pyell, *Chromatographia,* 38, 737 (1994)

[8]. R. J. Boughtflower, T. Underwood, C. J. Paterson, *Chromatographia,* 40 (5/6), 329 (1995)

[9]. R. J. Boughtflower, T. Underwood, J. Maddin, *Chromatographia,* 41 (7/8), 398 (1995)

[10]. C.J.Paterson, *PhD Thesis, Manchester Metropolitan University,* (1998)

Chapter 6 . Control of dispersion in coupling CEC columns to various detectors.

6.1 Capillary Electrochromatography - Mass Spectrometry (CEC/MS)

For neutral analytes, chromatographic selectivity should be identical for CEC and conventional RPLC when the same column packing and eluent are used. However, charged solutes will experience a combination of both partition and electrophoretic effects, when analysed using appropriate conditions and the selectivity of CEC will therefore differ from that of HPLC. The main advantage of CEC over HPLC is its capability of high resolution and therefore its greater value for analysing complex mixtures. Such applications are however demanding and require not just the very efficient separation which CEC can provide, but some way to identify the separated components. CEC has distinct advantages in coupling to mass spectrometry since narrower chromatographic peaks produce a higher mass flux and therefore a higher detection sensitivity is obtainable. Also, the flow rates produced by electroosmosis in CEC systems are much more compatible with the optimum rates required by electrospray MS sources. Solute partition based on an immobilised stationary phase also offers a more viable alternative to micellar electrokinetic capillary chromatography (MECC) for the separation of neutrals using electrically driven flows. Electrolytes containing micelles are not compatible with introduction into mass spectrometers, whereas it is, in principle, straightforward to perform CEC separations in the type of mobile phases, containing volatile buffer components, that are compatible with MS requirements. In addition the chromatographic scale of CEC is near ideal for connection to a mass spectrometer to

maximise sensitivity benefits. The issue here is how best to connect CEC with MS, without losing any of the benefits of the individual techniques.

Numerous applications of capillary electrophoresis (CE)-mass spectrometry (MS) have been published and this area has been reviewed by Cai and Henion [1] . Verheij et al [2] and Hugener et al [3] who have both reported the coupling of pressure-assisted-electrochromatography (PEC), a combination of both pressure driven and electroosmotically driven chromatography, with mass spectrometry. In this case, if the pressure contribution to the total flow rate is large, the flow profile and selectivity approach those in a pure pressure driven system . The use of pressure assisted CEC is described later in Chapter 8 of this thesis. Gordon et al have reported purely electrically driven CEC/MS coupling to both continuous flow fast atom bombardment [4] and ESI [5] mass spectrometry. The sensitivity enhancements in detection, and on-line identification that mass spectrometry brings to separation techniques is well established with GLC, HPLC, SFC (supercritical fluid chromatography). It is especially important in miniaturised electrically driven techniques such as CEC, that orthogonal identification methods can be directly coupled since analyte isolation is not a practical option. However, one of the major problems in coupling MS to miniaturised techniques such as CEC is maintenance of peak integrity.

Accordingly the objective of the work described in this chapter was to achieve coupling of CEC and MS with near perfect maintenance of chromatographic quality and good MS detection characteristics. CEC conditions for the separation of fluticasone propionate (Appendix2. Structure) and related impurities have been previously developed and optimised by Smith et al [6]. Confirmation of Smith's

results was considered a useful evaluation target. A schematic for the combined CEC/MS system used is shown in Fig 1.

6.1.1 Preparation of capillary column

The CEC column consisted of uncoated fused silica capillary, 92cm long, 50 μm i.d.,375μm o.d. 25 cm of this column was slurry-packed with 3μm Hypersil ODSA as described earlier in this thesis, leaving 67 cm of open tube. The column was equilibrated with the mobile phase of 80% CH_3CN/5mM sodium tetraborate at pH.9. A second column was prepared with the full length of 92cm packed.

6.1.2 Chromatography

The capillary was mounted in an Isco Model 3850 Electropherograph (Isco Inc. Lincoln, NE, USA) so that the inlet packed section was immersed in the anode buffer and the outlet end linked to the mass spectrometer as described below. Using the first column with 25 cm packed and 67 cm open , the open tube was inserted into the MS source, while uv detection could be used, off line, to monitor the performance of the 25 cm packed section. In this way we were able to determine the additional dispersion produced by the unpacked length of tube. Samples were dissolved in buffer (ca. 1mg/cm^3) and injected electrokinetically (30kV for 5sec or 10sec) by substituting the running buffer with sample solution, making the injection, then replacing the running buffer before reapplying the 30kV voltage, this produced an indicated current of between 2-4μA.

6.1.3 Mass Spectrometry

Mass Spectrometry was carried out on a VG Platform (VG Biotech, Altrincham, Cheshire, UK.) fitted with an electrospray (ESI) source to which the CEC capillary was linked via a triaxial probe (see Fig 1.). The interface consists of two concentric stainless steel capillaries surrounding the inner CEC capillary contained within the probe which is inserted into the mass spectrometer. These stainless steel capillaries are connected to separate tee-pieces as shown in Fig 1. Make-up flow (0.5cm^3/min of 50:50 MeOH/ 0.3% formic acid) from a HP 1050 HPLC pump (HP Ltd, Stockport, UK) was delivered to an Acurate™ micro-flow processor (LC Packings, Amsterdam, The Netherlands) where it was split such that 10μL/min was delivered to the probe tip via the inner capillary. At the probe tip the sheath flow is mixed with the nL/min flow coming from the CEC column before being nebulised using nitrogen delivered via the outer capillary. Care was taken to ensure that the end of the CEC column emerging from the probe tip was immersed in the make-up flow at all times. This maintained stable electrical connection across the column and ensured stable EOF. This was of paramount importance even if the column end was not positionally optimised for maximum MS sensitivity. A voltage of 4kV was applied to both stainless steel tee-pieces to provide high voltage at the probe tip to facilitate the ESI process. This acts as the cathode giving a net potential of 26kV applied across the capillary.

6.2 Results and discussion of initial MS work.

Repeat injections of fluticasone propionate afforded good quality spectra (MH^+ 501; MNa^+ 523) at a reproducible migration time of ca 21mins. However, the electrophoretic peak widths were excessively wide as shown in Figure 2 which gives the chromatogram of a mixture of Fluticasone propionate, and two related impurities of M.Wt 444 and 516, 518 (ca 3:1 for ^{35}Cl, ^{37}Cl). As might have been anticipated, the empty section of the capillary was causing enormous dispersion and to test this hypothesis the unpacked length was shortened so the capillary was able to fit the cartridge in the HP^{3D} CE instrument. The samples were then reanalysed on the HP CEC instrument using the shorter capillary , which allowed UV detection to be performed just after the packed section instead of 65cm away from this point (as in the MS case). The chromatogram obtained is shown in Fig 3. It is clear that the dispersion is much less. The applied voltage for the full length column was 30kV, while for the shortened column it was 9.4 kV. In this way, the field strengths for the two analyses were more or less the same

The chromatograms shown in Figs 3 and 4 show the separation of the same impurities, and some other (different) impurities in the second chromatogram set , with the 'extra' dispersion volume removed. This was achieved by cutting the open tube section down to fit the HP CEC instrument and detecting by uv just after the packed bed. Effectively, the same separation column was used with a much shorter open tube. The first chromatograms in each pair represent the separation achieved at maximum field strength of approximately 850 V/ cm. The second in each pair show the same sample at a field strength of 270 V / cm which is equivalent to the field

strength in the CEC/MS system, as before. This simply allowed comparison of the maximum performance and the performance under equivalent field strength to the MS experiment, but with no additional dispersion.

To enable good performance to be obtained on the CEC/MS system without any unnecessary dispersion, a 92cm capillary was fully packed and mounted into the mass spectrometer as described previously. The separation of Fluticasone propionate and all four related impurities was achieved with excellent efficiency and quality spectra were obtained for each component (Fig 5).

The separation of pairs of diastereoisomers of Cefuroxime Axetil and the E-isomer (ANTI) (Appendix 2, Structures) at ca 2.5% is also shown in Fig 6. with good quality mass spectra obtained for isomeric pairs.

The work just described demonstrates well the principles and potential of coupling CEC/ESI/MS and its possible application in the Pharmaceutical industry. Further enhancements to detection sensitivity may be possible by using larger diameter capillaries where just the capillary flow will be sufficient to maintain stable electrospray. Short columns with high field strengths are desirable for rapid but efficient separations , as has been well illustrated here (Figures 3 and 4). Presently, the VG commercial probe design and its connection to an electropherograph requires column lengths of about 90cms. Chromatographic integrity is maintained into the mass spectrometer if packed columns of this length are used, but diluted field strengths produce long analysis times. Unpacked sections of capillary after a short section of packed bed in a long column produce undesirable dispersion effects, presenting a limitation in using short packed columns within the confinements of the commercial probe design.

6.2.1 Dedicated probe design

The design and construction of a modified probe, where the CEC column and necessary buffer and sample vials were 'self-contained' within the probe itself, was undertaken. This is shown in Figure 6A. The chromatograms obtained [7] confirmed that one-piece, fully packed columns of the shortest practical lengths, with maximum field strength applied, gave excellent performance and short analysis times. CEC/MS also proved to be much more robust and reliable in this format, and pressurisation of the inlet vials was not necessary. This was the result of avoidance of any open tube section between the injection point and the evaporation into the mass spectrometer.

6.3 Conclusions of initial MS work.

Successful CEC/MS has been demonstrated above in which there is no loss of chromatographic performance when the CEC column is coupled directly to the mass spectrometer. There is therefore no doubt that CEC/MS is an important combination of techniques that offers considerable potential for sensitivity and specificity, It combines the chromatographic efficiencies of CEC with the desirable, qualitative identification by MS on a micro scale. However there are currently operational compromises which have to be accepted. The best results are obtained by inserting a fully packed column straight into the MS, but this is best achieved with a bespoke interface designed specifically for the MS instrument. Alternatively a conventional CEC column with optical detection can be coupled via a section of open tube on-line to the MS. But this arrangement does not work very well due to

the unacceptable dispersion caused by the open tube section [7]. The question which now arises is whether it is possible to devise a post column coupling which allows on-line uv detection but does not cause unacceptable band broadening at the MS detection stage.

6.4 Minimising dispersion in CEC-UV-MS coupled systems.

Ideally it would be desirable to detect outside the column itself, following connection of the separation part of the column to an independent detector (cell) [8,9]. However the connection has to be devised to minimise any extra dispersion which would otherwise cause significant loss of peak efficiency. It has been proposed [10] that most of this dispersion arises from discontinuities in field strength and flow velocity resulting from the change in flow profile at the interface between the packed and open parts of the tube. Additional dispersion clearly arises mainly from use of an open tube itself. It also arises from the sudden changes in bore, and from any dead-end appendices at connections.

The goal of the work in the remainder of this chapter is to investigate the possibilities of making CEC column connections to open tubes and yet enable performance losses to be minimised, so that the use of CEC-UV-MS can become a workable reality.

6.5 Band spreading in the open tube following CEC.

As shown above, open tube sections of the same diameter, following the packed part of the tube, cause unacceptable dispersion in CEC. This mainly due to a

change from essentially plug flow in the packed section of the tube to partially parabolic flow in the open section. In a typical configuration the column is a one piece arrangement with the electric field across the whole column, i.e. from the inlet of the packed column to the outlet of the open tube section. The exact nature of the flow profile as a solute band exits from the packed to the open section is not well understood, but Rathore and Horvath [10] have recently proposed models which strongly support recent imaging of these processes. However, this describes only the immediate section of a few column diameters after the frit. Further on, a partially parabolic flow is established. This is because the volume flow rate along the tube is fixed by the EOF from the packed section, while the wall velocity in the open part of the tube is likely to be different, and will not match the overall linear velocity from the packed part of the column. A partial parabolic flow profile has to exist to compensate for this. The magnitude of this partial parabolic flow depends upon the exact EOFs in the two parts of the tube, and cannot easily be estimated. However even a small amount of parabolic flow will have a disastrous effect as calculations using the Taylor equation will show. Coming back to the situation of the packed tube followed by an open tube, one might proceed on the basis that the EOF (linear) was the same in the packed and open parts of the tube. In this case the mismatch in the open part of the tube is due to the change in porosity from 60% in the packed tube to 100% in the open tube. Thus the linear wall velocity in the open section will be 100/60 times as great as is sustainable by the volume flow from the packed section. A parabolic flow component is thus required to maintain the overall flow rate and will be in the reverse direction.. We can compare this 'model' to the one developed by Knox [11] for the treatment of thermally induced dispersion effects by

using equation 7.7, Chapter 7. This would suggest an effective flow value of 40/60 (analogous to $\frac{\delta\bar{u}}{u_{mig}}$) times the volume flow rate from the packed column. If we substitute this value in equation 7.7 we can see that the total 'extra' dispersion will be about 4/9ths that expected for totally pressure derived dispersion. This approximation is in good agreement with the experimentally measured values of dispersion.

Other factors that affect the operational arrangement of the CEC system are also important. To realistically couple rapid CEC separations to sensitive MS based detection systems, it would be preferable not to dilute the field strength across the packed section of the column by an additional length of open tube, but simply to apply the field across the packed section of the column. It is certainly possible to ground the column at the connection interface to the open tube, but this would mean that the flow profile after the connection would revert to that of pure hydraulic flow. Dispersion would then be appreciably worse than when there was a background electroosmotic flow.

To calculate the effect on efficiency of adding a length of open tube of varying diameter to the CEC column, we need to add the volume variances of each component of the system, and thus calculate the total variance of the system. The total variance of the system is then compared with the variance from the packed column alone. Tables 1 and 2 show the symbols and typical values used throughout the calculations.

Table 1 - symbols and typical values for CEC parameters used throughout the calculations.

CEC PARAMETERS	SYMBOL/EQUATION	TYPICAL VALUE
Packed tube diameter	D	100 μm
Packed tube length	L	200mm
Bed porosity	ε	0.6
Elution time (unretained solute)	t_m	200s
Linear flow rate	$u = \frac{L}{t_m} = \frac{4F_v}{\pi D^2}$	1mm/s
Number of plates	$N = \frac{L}{H}$	100,000
Plate height	H	2 μm (calculated)
Volume flow rate	$F_v = \frac{\pi D^2 \varepsilon u}{4} = \frac{\pi D^2 \varepsilon L}{4t_m}$	0.4μl/min (calculated)
Length standard deviation	$\sigma_{z,col} = (HL)^{1/2} = \frac{L}{N^{1/2}}$	0.6mm (calculated)
Volume standard deviation	$\sigma_{v,col} = (\frac{\pi D^2 \varepsilon}{4}) \frac{L}{N^{1/2}}$	3nl (calculated)
Volume variance from column	$\sigma^2_{v,col} = (\frac{\pi D^2 \varepsilon}{4})^2 \frac{L^2}{N}$	

Table 2 - symbols and typical values for open tube parameters used throughout the calculations.

OPEN TUBE PARAMETERS	SYMBOL/EQUATION	TYPICAL VALUE
Open tube diameter	d	25 μm
Open tube length	L_t	100 mm
Diffusion coefficient	D_m	10^{-9} m^2/s
Peak width (at half height)	$P_{w1/2}$	2s (measured)
Linear velocity	$u_t = \frac{4F_v}{\pi d^2}$	14 mm/s (calculated)

Volume standard deviation	$\sigma_{v,tube} = (H_t L_t)^{1/2} (\frac{\pi d^2}{4})$	10 nl (calculated)

Plate height for the open tube is calculated from the Taylor equation (or Golay equation with $k' = 0$)

$$H_t = \frac{d^2 u_t}{(96 D_m)}$$

$$= \frac{F_v}{24\pi 4_m}$$

$$= \frac{D^2 \varepsilon u}{(96 D_m)} \quad = \frac{(\sigma_{z,tube})^2}{L_t} \qquad \textbf{(6.1)}$$

Length standard deviation, $\sigma_{z,tube} = (H_t L_t)^{1/2}$ **(6.2)**

$$= \frac{P_{w1/2} u_t}{2.355} \quad \text{(calculated from data)}$$

Volume standard deviation, $\sigma_{v,tube} = (H_t L_t)^{1/2} (\frac{\pi d^2}{4})$ **(6.3)**

$$= \frac{\sigma_{z,tube} d^2 \pi}{4}$$

(calculated from data)

Volume variance from column, $\sigma_{v,col}{}^2 = (\frac{\pi D^2 \varepsilon}{4})^2 \frac{L^2}{N}$ **(6.4)**

Volume variance from tube, $\sigma_{v,tube}{}^2 = H_t L_t (\frac{\pi d^2}{4})^2$ **(6.5)**

$$= \frac{\pi^2 D^2 \varepsilon u L_t d^4}{(96)(16 D_m)}$$

$$= \frac{\pi^2 D^2 \varepsilon L L_t d^4}{(96)(16 D_m t_m)}$$

The combined variance from the combined column and tube (equations 6.4 & 6.5) is then given by;

$$\sigma_{v,tot}^2 = \sigma_{v,col}^2 + \sigma_{v,tube}^2$$

$$= \sigma_{v,col}^2 \left(1 + \frac{\sigma_{v,tube}^2}{\sigma_{v,col}^2}\right)$$

$$= \sigma_{v,col}^2 \left(1 + \left(\frac{L_t}{L}\right)\left(\frac{d}{D}\right)^2 \left(\frac{d^2}{D_m t_m}\right)\left(\frac{N}{96\varepsilon}\right)\right) \qquad \textbf{(6.6)}$$

If we substitute in some typical values into equation 6.6, and for this calculation choose a smaller column diameter such as 25 μm then we have;-

$\frac{L_t}{L} = \frac{1}{2}$; $\frac{d}{D} = \frac{1}{4}$; $d = 25 \times 10^{-6}$ m ; $D_m = 10^{-9}$ m^2/s ; $t_m = 200$s ; $N = 10^5$; $\varepsilon = 0.6$

Then for these values; $\sigma_{v,total}^2 = (1 + 0.17) \times \sigma_{v,col}^2 = 1.17 \sigma_{v,col}^2$

That is, the 'extra column' dispersion adds 17% to column dispersion itself, so efficiency is reduced by 17% and resolution (proportional to $\sqrt{N}$) by about 8%. In what follows we call the factor 1.17 the 'dispersion factor'. The effect of choosing different diameters of open tube when L_t / L = ½, with a main CEC column of 100μm diameter is shown in Table 3. To get less than 20% additional dispersion, the tube diameter must be less than about 25μm. Equation 6.6 shows that the dispersive effect of additional tubing is extremely sensitive to its diameter (factor d^4) but

relatively insensitive to its length (factor $(L_t / L)^1$, so it is the tube diameter which must be carefully considered in making any connection of CEC to a distant piece of equipment. These calculations , of course, make no allowance for any dispersion which will arise from joins between tubes whether of the same or of different diameters.

Table 3. Calculated dispersion factor when open tubes of different diameter are connected to 100μm bore CEC columns for $\frac{L_t}{L} = \frac{1}{2}$.

Diameter (μm)	50	40	30	25	20	15	12	10
Dispersion factor (column dispersion is 1)	3.71	2.11	1.35	1.17	1.069	1.022	1.009	1.004

6.6 Experimental

6.6.1 Instrumentation.

A Hewlett Packard (Waldbronn, Germnay) HP^{3D} CE (with CEC vial pressurisation) was used throughout. All one-piece CEC columns used were 100μm internal diameter (i.d.) and approx. 375μm outer diameter (o.d.) containing Waters Spherisorb C6/SCX mixed-mode stationary phase (Innovatech, Stevenage, UK.). Unless otherwise stated the columns were 30 cm in length. Due to the nature of this work, which involved multiple runs on each column system, occasional breakage of the inlet frit was inevitable. If this occurred a new frit was fabricated [12] as close as

possible to the original. Any adjustments to field strength were made accordingly. No particular attempt to correct the data for packed length was made, as any resulting effects were insignificant. When column connections were used, they were fabricated where possible from the original one-piece column, which was cut at the retaining frit and this end was polished using a simple home-made polishing unit. This consisted of a thick-walled aluminium tube with a flat PTFE face at one end. A small hole of approximately 0.4mm was drilled through the teflon face so that the capillary end to be polished could protrude through a short distance, the rest of the capillary running inside, through the aluminium tube. To hold the capillary in place a locking ferrule and nut was fixed onto the far end of the tube and this allowed the 'locking' of the capillary with a defined length of the capillary tip protruding from the teflon face. This whole assembly was then mounted in a guide block, which could be moved only perpendicularly with respect to the cutting face of a cutting stone. This enabled the capillary end to be polished until it was completely flat with respect to the teflon face and completely perpendicular to the capillary walls. This column was connected to the open tube section, which was also polished at the connection end. The connections were made by a small piece of PTFE tubing of slightly smaller i.d. than the capillary o.d. This gave a 'tight' fit but care was taken to ensure no swarf from inside the PTFE tubing blocked the connection of the capillary ends. In cases where the electrical connection was made at the connection point, the open tube part of the capillary was painted with a graphite paste ('Leit C', Protana, Denmark). This covered the end face of the capillary and a suitable length of the outside tube, to a point where a convenient electrical earth could be connected via a brass connector as shown in Figure 7. Open tube lengths varied according to

the necessary distance required between the column end frit and the detection position. The overall length of the whole column for these experiments was equal to the packed column length + extra open tube length to detection point + 8.5 cm (open tube from detector to cathode). The configuration of the open connecting tube was varied: in length from 3 to 25cm, and in diameter from 25 to 100μm.

All runs were performed with the mobile phase vials pressurised to 12 bar and columns were initially conditioned at an applied voltage of 15kV under these conditions. The mobile phase vials were replaced regularly to avoid buffer depletion. All samples were injected electroendosmotically. Due to the variable overall column length, the injection conditions were 260v/cm for 10s (for a 30cm one-piece packed column this was typically 10kV for 10s).

The Mass Spectrometer used was a Hewlett Packard 1100 series MSD fitted with the CE electrospray interface.

6.6.2 Chemicals and materials.

Suppliers of the chemicals used for this work are given in Chapter 4 (experimental). The mobile phase employed throughout these experiments was acetonitrile (ACN) / 50mM NaH_2PO_4 (pH=3.5), 50:50. The buffer pH was adjusted with phosphoric acid, prior to mixing with the ACN. The chromatography test mixture used for the separations and subsequent data measurement was composed of 1. Thiourea (flow marker), 2. Benzamide, 3. Anisole, 4. Benzophenone and 5. Biphenyl (in order of elution) all dissolved at 0.5mg/ ml in the mobile phase. The pharmaceutical mixture used for the CEC-UV-MS separation was composed of thiourea, phenytoin, prednisolone, methyl-prednisolone, caffeine, testosterone,

amoxillicin, cefatrizine at a concentration of 125μg/ml of each compound, also in order of elution.

6.7 Experimental Design.

The primary objective of the experimental work was to measure the additional dispersion factor resulting from various configurations of the open tube leading to the detection system, which necessarily follows the frit terminating the CEC column. The different configurations which have been examined are shown in Figure 8.

Experiment 1 (column configuration shown in Figure 8A) investigated the dispersion with a simple extension of the packed column by open tubing of the same bore and no break in the capillary (this effectively represents a 'conventional' CEC column). Three positions of the detector window were examined ranging from very close to the frit (normal position denoted by N), 10 and 25 cm from the frit (denoted by R and S).

Experiment 2. The first detection measurements were carried out using the one-piece column from experiment 1. Detection was performed at 3cm from the retaining frit at a point P illustrated in Figure 8A. These measurements were used as 'unbroken column' reference values to compare the effects of column joining carried out in experiment 2.

In a second set of measurements, the CEC column was coupled to an open tube of the same diameter by means of a join and sleeve. The earth connection could then be made either conventionally at the column end (Figure 8B) or at the join

(Figure 8C). Throughout Experiment 2, detection measurements were performed at distances of 3cm from the frit for each of these two column configurations, at points labelled U and V respectively.

Experiment 3 (Figure 8D) The bore of the open tube was reduced to 25μm. Joining was always required and the electrical earth was always made at the join. Detection was at 3 and 10 cm from the frit.

Dispersion values for detection at N in Experiment 1, were used in all subsequent experiments as reference values for the peak variance produced by the packed column alone. For measurements of dispersion in experiments 2 and 3, this original column from experiment 1 was cut at the frit and joined to the 100μm and 25μm open tubes respectively.

6.8 Observations of joining columns.

When the earth connection is made at the join of the column and the open tube, electroosmotic flow before the join is replaced by hydraulic flow after the join, the volume flow rate remaining the same. The hydraulic flow then causes a pressure drop across the open part of the tube. This is readily calculated from the Poiseuille equation;

$$\Delta p = 32\,\eta\, L\, u_{tube} / d_c^2 \qquad (6.7)$$

for typical values, $\Delta p \cong 1 \times 10^5\ N/m^2$ or about 1 atmosphere. This means that fairly simple push-fit tubing type connections may be used even if we decide in practice to use significantly longer lengths of connecting tube.

Additionally, when a CEC column is connected 'on-line' via a push-fit connection, into a connecting tube with the electrical earth made at this join, we have an 'on-flow' electrode system. This means that any gaseous products of electrolysis will travel down the tube. Hydrogen gas may be produced at the cathode connection and interfere with any downstream optical detection [13]. This means careful consideration needs to be given to the precise layout of the earth connection with respect to any optical detection. The stability of the experiments carried out in this chapter suggest that the slight Δp generated by the small diameter connection tubing would be enough to prevent this being a significant problem. It is interesting to consider whether this bubble generation could be used advantageously to measure volumetric flow rates with acceptable accuracy in these systems.

6.9 Results and discussion.

6.9.1 Dispersion factors for different CEC column/ open tube configurations.

The following results are given as volume variances and 'dispersion factors' representing the ratio of (the total volume variance) to (the volume variance measured at N). The total variance therefore includes any extra dispersion measured at the detection point. The total variance will also reflect any dispersion arising from physical connections. The capital letters in the title bar of the result tables refer to the relevant detection points in each experiment as shown in Figure 8.

Experiment 1.

This experiment was performed to measure the amount of dispersion in normal CEC operation in a one-piece column. Test mixture separations were carried out and detection at different distances from the frit were compared. This work was performed at a field strength of 450V/ cm.

It can be seen from table 4 that there is extensive dispersion associated with the solute bands travelling through the open tube section of the column. Also, that this dispersion appears to increase quite soon after the frit. This would be too much loss in performance to tolerate, as the distances shown are likely to be smaller than the 'real' distances needed to connect to a mass spectrometer.

Table 4. Dispersion Factors for a 100μm one-piece column with detection at different distances from the frit (Experiment 1).

Peak	Volume Variances (nl^2)					Dispersion Factor = variance at (R) or (S) / variance at (N)	
	(N)	(R)	(R-N)	(S)	(S-N)	(R)	(S)
1	36	136	100	247	211	3.77	6.86
2	42	150	108	287	245	3.54	6.77
3	72	158	86	265	197	2.20	3.67
4	92	199	107	360	268	2.17	3.94
5	150	243	93	363	213	1.62	2.42
Mean			99		226		

(From the earlier estimate of expected dispersion, based on the 'backwards parabolic disturbance' being about 4/9ths of the total expected from the Taylor equation,

variances of 110 and 290 nl^2 would be expected from detection at points R and S respectively.)

Experiment 2.

This experiment was performed to assess the contribution to dispersion made by connections of the packed column to a different open tube, such that a physical 'break' (join) in the capillary was required. The effect of making the earth connection at this joining point, instead of at the end of the open tube section, was also investigated. The data in table 4 suggests the profile of the solute band appears to degrade rapidly as it emerges from the packed section into the open tube, for a conventional one-piece column arrangement. Therefore in Experiment 2 detection was attempted as close to the frit as practically possible, limited only by the physical distance between the frit, the connection tubing and detection interface (minimum 3 cm, see Figure 8B). When the earth is made at the connection point (as it is for data shown in Table5, column V), there is no electrical field across the open tube section of the capillary and therefore there will be only pressure-derived flow in the open section. This should degrade the performance further still. The data in this experiment (2) was obtained by operating a similar column at a different field strength of 740 V/ cm using column arrangements described in Figures 8B and 8C, results are shown in table 5.

As expected, the results from Experiment 2 show that the dispersion increases as physical connections are made between capillaries and also if the electrical earth is made at the connection point. There is a tendency for the later eluting peaks to show higher variance values than the earlier ones, this is particularly

evident when the electrical earth is made at the join and hydraulic flow exists in the open tube. These experiments are for packed and open tube sections of the same diameter. As predicted from Experiment 1 the dispersion in these systems was too great and would only be significantly worse under these experimental conditions.

Table 5. Dispersion Factors for a 100μm column (Fig 8b) with detection at 3cm and different electrical earth points (Experiment 2).

Peak	Volume variances (nl^2)							Dispersion Factor		
		Continuous		*Added tube Earth at end*		*Added tube Earth at join*				
	N	P	P-N	U	U-N	V	V-N	P	U	V
1	44	71	27	98	54	144	100	1.62	2.25	3.30
2	52	82	30	107	55	148	96	1.57	2.05	2.83
3	70	89	19	119	49	184	114	1.26	1.69	2.61
4	86	116	30	152	66	238	152	1.36	1.77	2.78
5	121	161	40	191	70	285	164	1.32	1.57	2.35
Mean			29		59		125			

Experiment 3.

This experiment was again performed at 740 V/cm field strength using a 100μm diameter packed column but connected to a 25μm diameter open tube. The same measurements of dispersion, as in previous experiments, were made at detection distances of 3 and 10 cm from the retaining frit, denoted by W and X respectively. Results are shown in Table 6. The results obtained from Experiment 3

suggest that the extra dispersion observed within the 25μm open tube is considerably less than with a tube of equal diameter to the packed column. The values for extra variance obtained between the 3 and 10 cm detection points in the 25μm open tube are very variable, especially for later retained peaks, and the reason for this is not clearly understood. From calculated values for the 25μm tube we should expect about 12 (nl^2). The values of dispersion factors less than unity shown in column W are probably a result of there being less dispersion associated with detection in 25μm, at only 3 cm away from the join, than inherently occurs in normal detection at a 'finite' distance (N) from the frit. It is clear from both experiments 1 and 2 that the solute band profile in conventional CEC is deteriorating rapidly, so it seems highly plausible that even 'normal' detection includes significant inherent dispersion.

6.9.2 Discussion of Additional Variance

In this section the observed additional variances produced by the various configurations of tubing added to the packed bed are compared with those calculated using the Taylor equation.

$$\sigma_{v,tube}^{2} = L_t \pi d^{4} \frac{F_v}{384 D_m}$$

If the measured values of tube induced variance (measured from Experiment 1), represented as average peak volume variances (for all peaks except the flow marker) are compared to the values expected from the Taylor equation for laminar flow, the results are shown in Figure 9.

For detection distances between N (~0) and 3, 10 and 25cm away from the packed column end frit, variance values of 76, 254 and 636 (nl^2) are expected from the Taylor equation with laminar flow. Measured values (from experimental set up 2a) are 30, 100 and 230 (nl^2), calculated as averages from the values given in Table 4. This suggests that the flow profile in the open tube when the field is across the whole column (Figure 8A), is somewhere in between 'EOF derived plug-flow' and laminar flow. For comparison purposes, data was also obtained for the same 3cm detection distance but with the electrical earth made at the column join. This produces pure laminar flow in the connecting tube. Here the peak volume variance was measured as 86 (nl^2), calculated from average values given in Table 5, corrected for the effects of the join. This compares well with the calculated value of 76 (nl^2). This data, and the earlier 'dispersion factors' data, support the Taylor model of laminar dispersion occurring in the open tube.

Table 6. Dispersion Factors for a 100μm column joined to 25μm open tube with electrical earth at the join (Experiment 3).

Peak	Volume Variance (nl^2)				Dispersion Factor	
	(N)	(W)	(X)	(X-W)	(W)	(X)
1	44	62	76	14	1.41	1.74
2	52	56	63	7	1.07	1.21
3	70	57	78	21	0.80	1.11
4	86	64	101	37	0.75	1.18
5	121	89	150	61	0.73	1.24
Mean				37		

6.9.3 Dispersion associated with CEC-MS coupling.

The data shown previously supports the principles of using smaller diameter connecting tubes when coupling CEC columns to remote detectors. However, to make on-line comparisons of UV and MS peak widths, it was impractical to use the UV data obtained through the 25μm tube due to lack of detection sensitivity. For the purpose of this experiment detection was carried out in the 100μm open tube just after the frit in a standard CEC column. This column was then joined to a 25μm diameter tube of approximately 75 cm in length, as shown in Figure 10. This allowed measurements of the peak widths by UV and MS detection, to be carried out on-line from the same chromatographic run of three test components (1. caffeine, 2. prednisolone and 3. dexamethasone, in order of elution), shown in Figure 11. The dispersion data is shown in Table 7.

Table 7. Comparison of peak volume variances obtained at the UV and MS detectors for 100μm CEC column coupled to the MS with 75cm of 25μm tube.

Peak	Volume variance (nl^2)		Dispersion Factor
	UV	MS	
1	114	366	3.21
2	135	283	2.10
3	137	298	2.17

The dispersion factor shown is calculated from the ratio of the volume variances at the MS and UV detectors. From a theoretical standpoint the expected minimal dispersion factor for the coupled system shown would be 1.255. This would

be based on the assumption that a 'perfect join' existed between the CEC column and the 25μm diameter joining tube, and that only Taylor dispersion in the joining tube contributed to extra band broadening. This type of join is not possible in this experimental set up. In the case here, extra dispersion is introduced by the short length of 100μm tube between the connection and detection points (detection volume) and by the joint connection itself. It is possible to make reasonable corrections for this extra dispersion. These corrections, have either been measured in experiments earlier in this manuscript, or calculated. Volume variances of at least 30, 30 and 50 (nl^2) are introduced by the detection volume, capillary join and Taylor dispersion through the connecting tube respectively. The first peak is also unexpectedly broad at the MS, which is probably due to sample overload. When corrections for these extra column effects are made by subtracting these additional volume variances from the MS values, we have dispersion factors for peaks two and three of 1.37 and 1.35 respectively. These values are in good agreement with those expected from the theoretical predictions, considering the difficulty in fabricating a consistent electrically earthed join between the capillaries.

This data supports the use of the column with smaller diameter connection tubing (not more than a quarter of the diameter of the separation column) and the minimum length that is practical, to connect to a mass spectrometer. Ideally, for on-line UV detection to be performed, it should be carried out immediately after the retaining frit. Due to the lack of sensitivity in detecting optically through such small diameter capillaries, it is desirable to utilise a higher sensitivity cell as has been reported previously [8,9].

Chapter 6 Figures

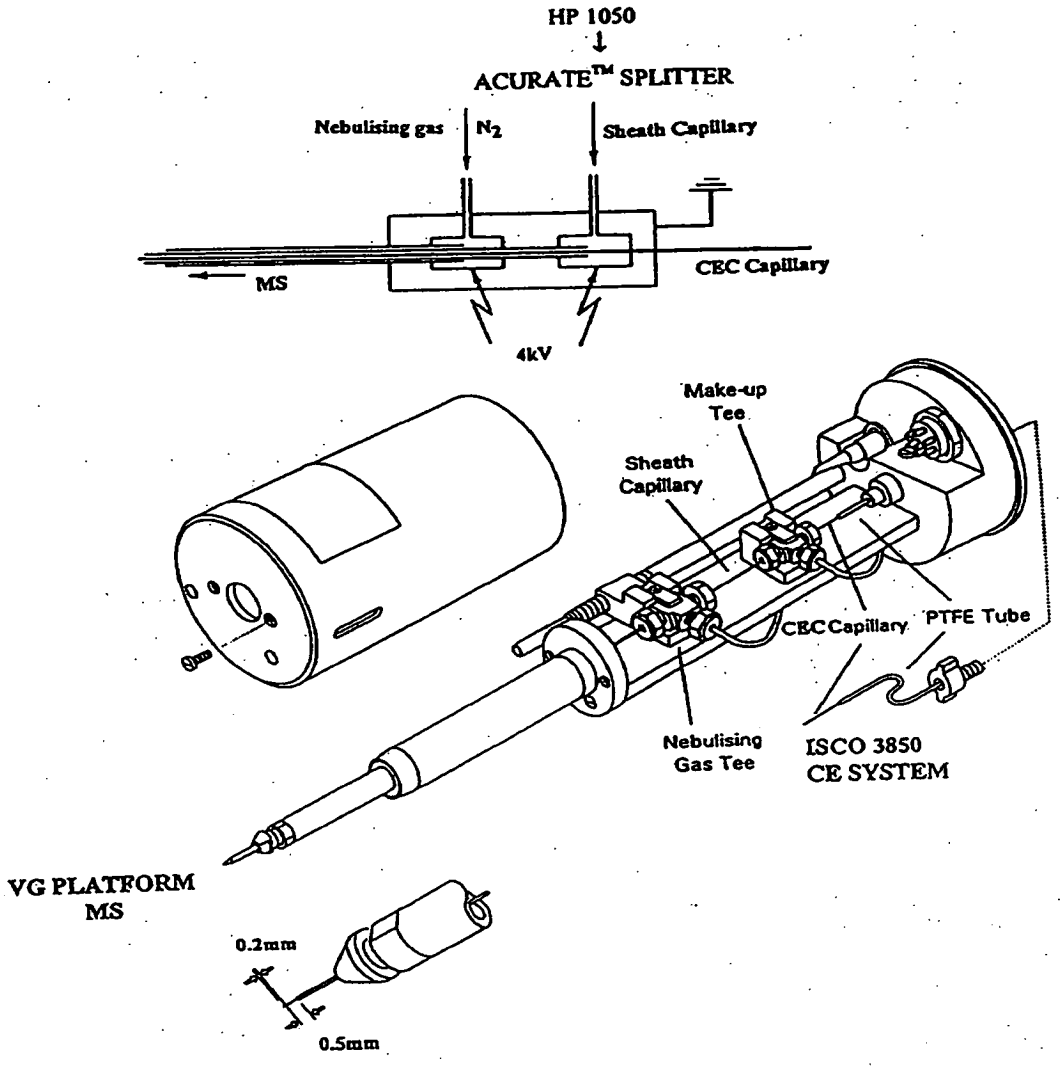

Fig 1. Schematic diagram of the standard layout CEC/MS probe

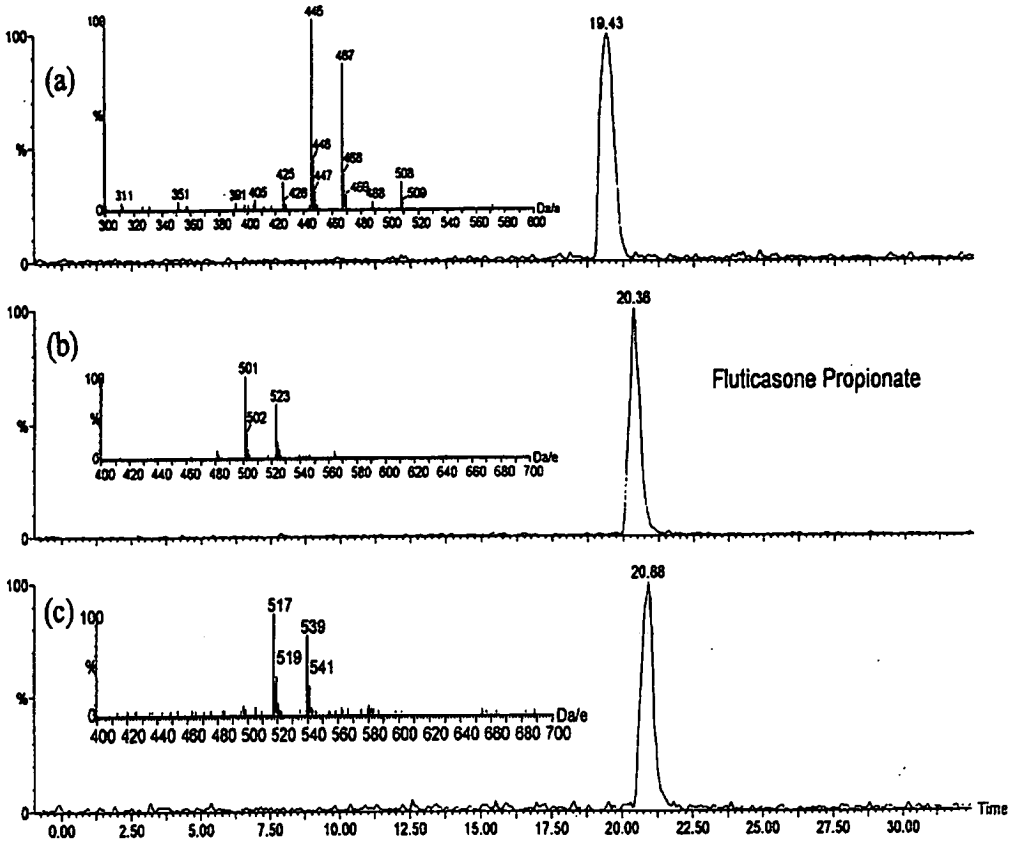

Fig 2. CEC/MS of Fluticasone Propionate and related impurities (a) MW 444, (b) MW 500, (c) MW 516

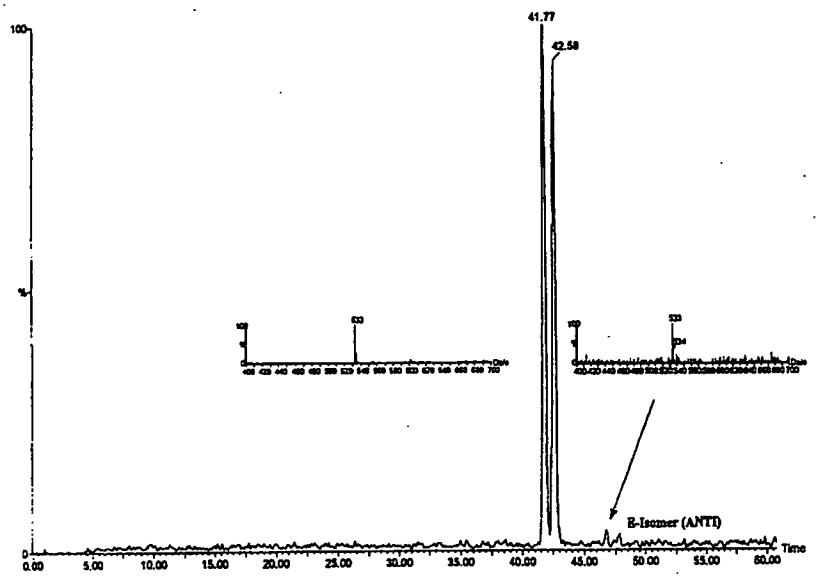

Fig 6. CEC/MS of diastereoisomeric pairs of Cefuroxime Axetil Syn and Anti isomers

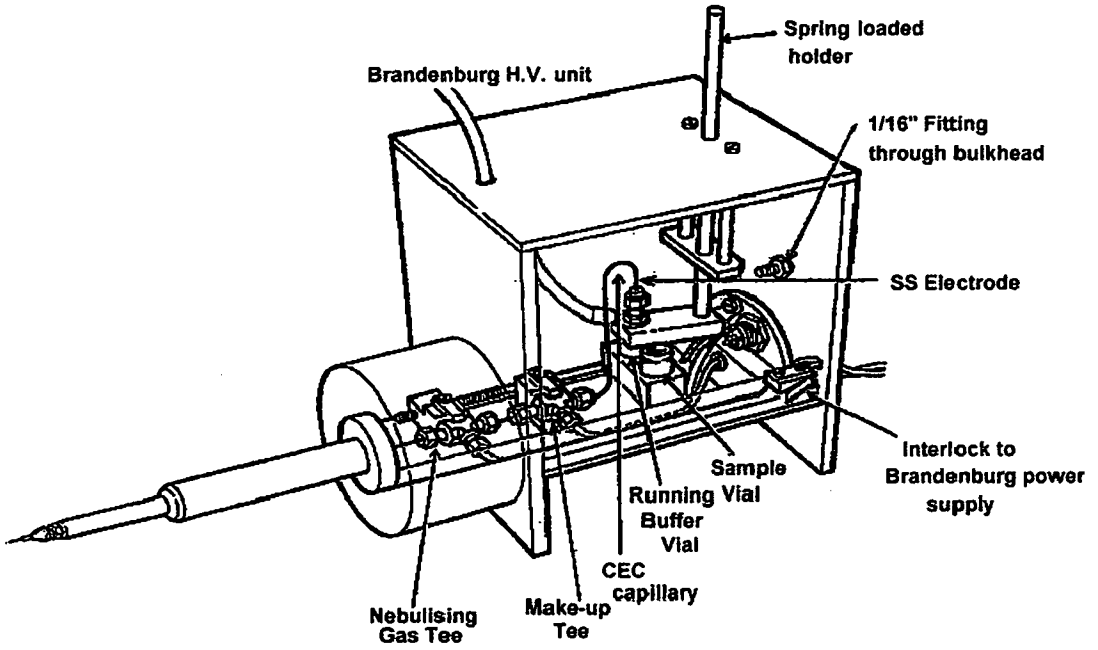

Figure 6A. Design of 'dedicated' probe with self-contained CEC sampler to enable use of shorter CEC columns with higher field strengths.

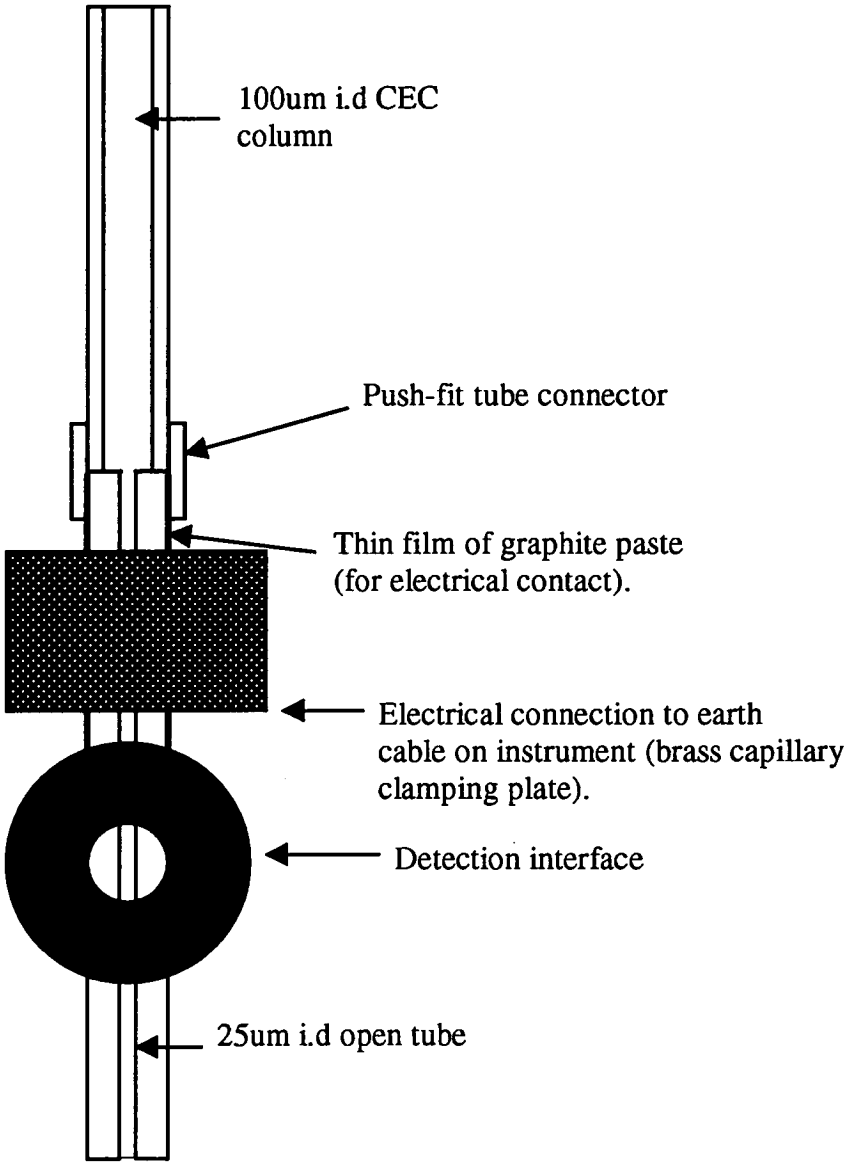

Figure 7. Schematic diagram of column to capillary joining utilising electrical earth connection at join

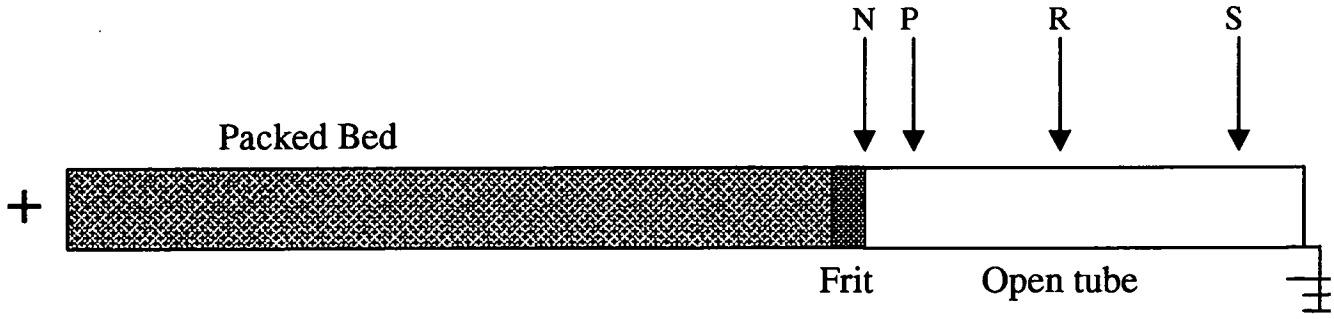

Figure 8a

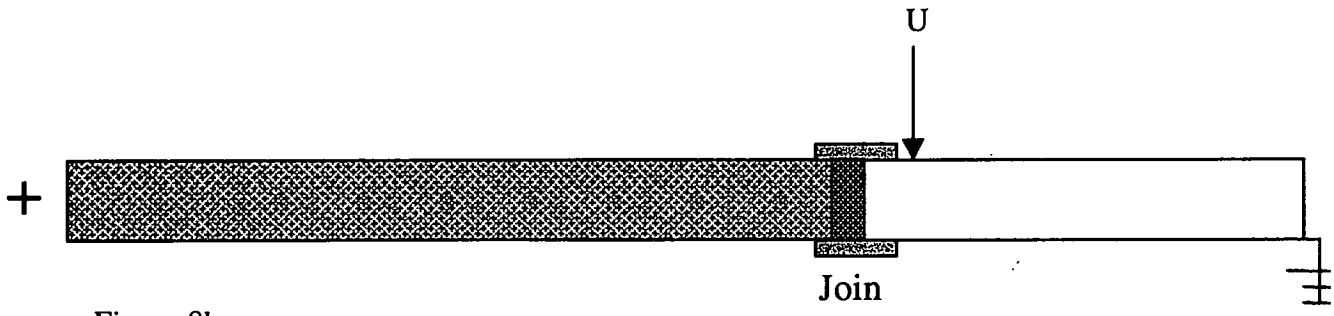

Figure 8b

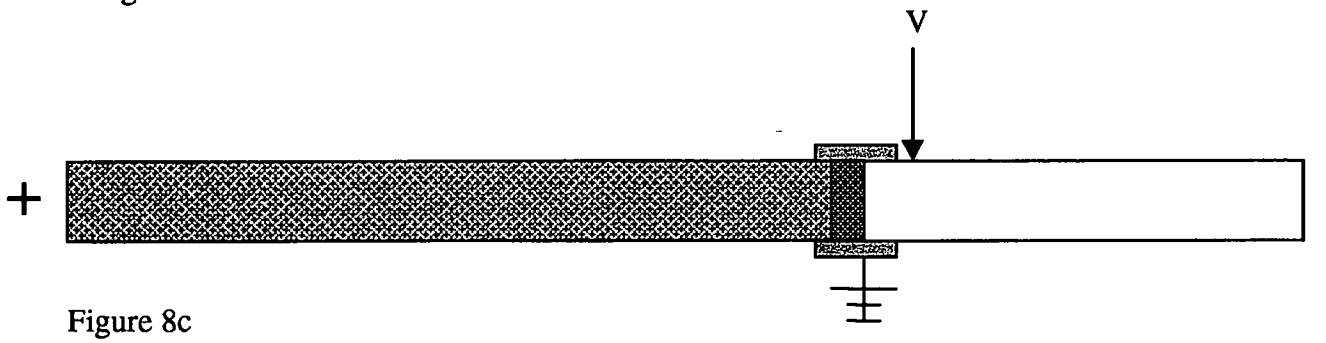

Figure 8c

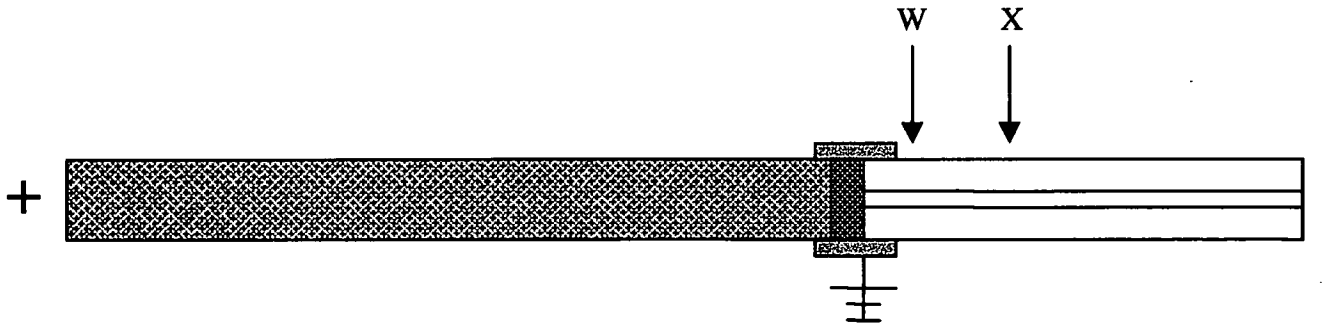

Figure 8d

Figure 8 (a,b,c,d) Various column / tube layouts for different dispersion experiments

Figure 9. Graph to compare extra peak volume variance obtained when detecting at variable distances from end frit in a conventional CEC system (ie electrical field across the whole column), with that predicted from the Taylor equation (for only laminar flow) for a 100μm one-piece column.

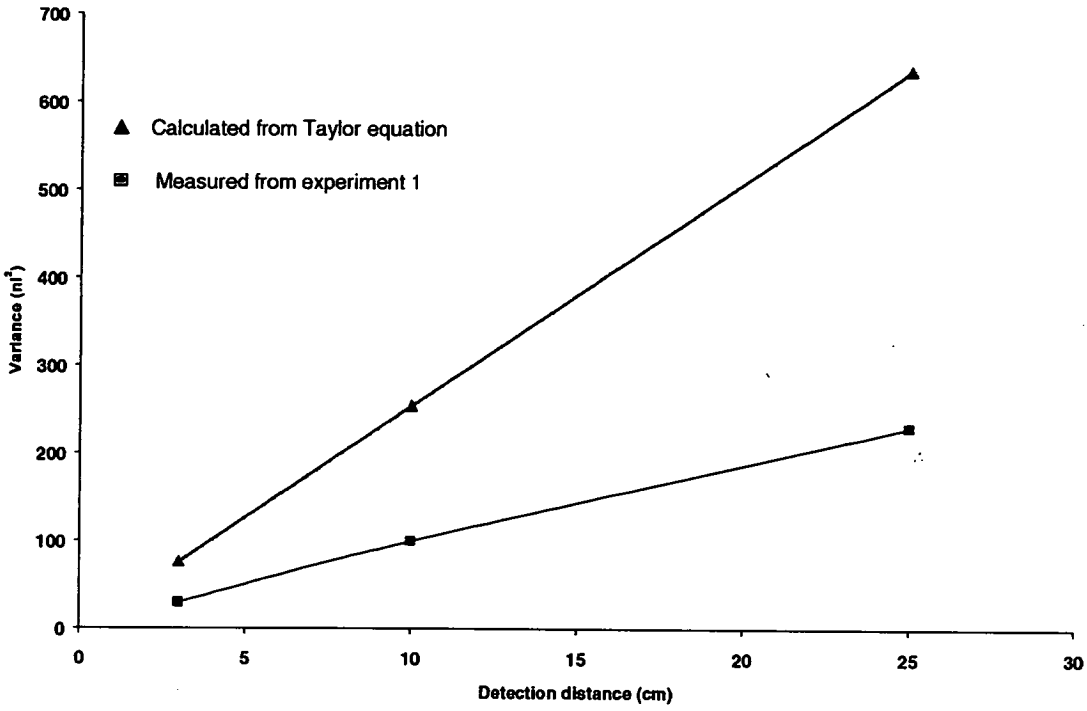

Figure 10. Schematic arrangement of column , detector and connecting tube arrangements for
comparing peak variances between UV and MS detectors

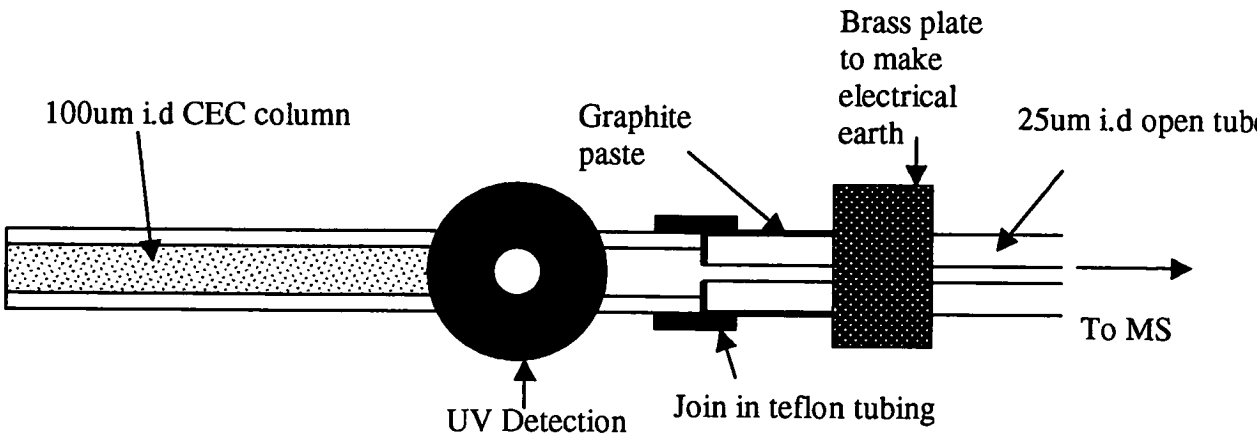

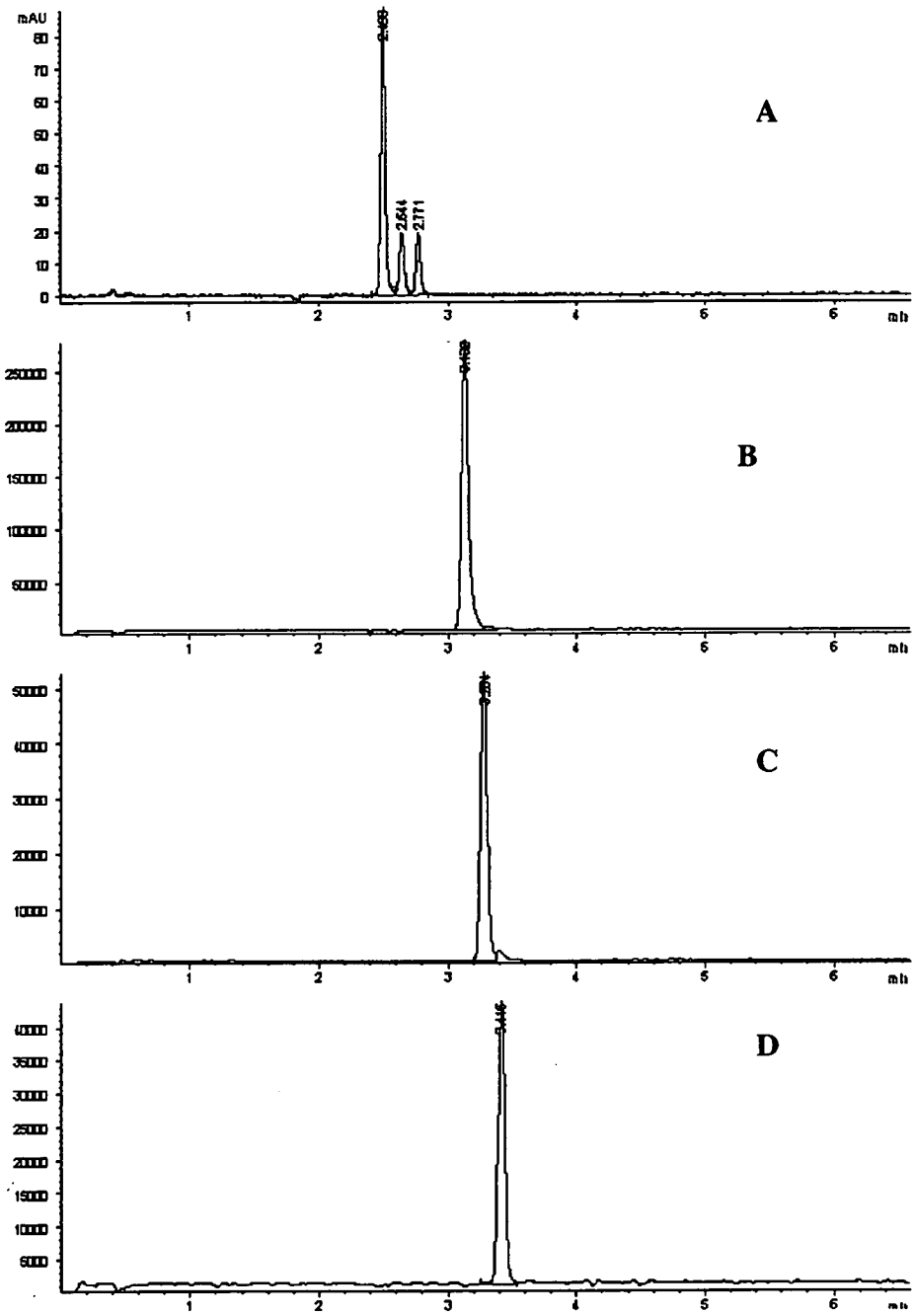

Figure 11. Chromatograms obtained from coupled CEC-UV-MS system. Chromatogram A is on-line UV signal (215nm). B, C and D are the SIM MS signals for caffeine (MH+ 195), prednisolone (MH+ 361) and dexamethasone (MH+ 393) respectively. Mobile phase 60% MeCN / 40% 20mM NH_4OAC (pH 4). Applied field 25kV. Injection 10kV for 5s.

References for chapter 6

[1] J. Cai., J. Henion, *J. Chromatogr.*, **A703,** 667 (1995)

[2] E. R. Verheij, U.R. Tjaden, W. M. A. Niessen, J.van de Greef, *J. Chromatogr.*, **554,** 339 (1991)

[3] M Hugener, A. P. Tinke, W. M. A. Niessen, U. R. Tjaden, J. van de Greef, *J. Chromatogr.*, **647,** 375 (1993)

[4] D. B. Gordon, G. A. Lord, D. S. Jones, *Rapid Commun. Mass Srectom.* **8,** 544 (1994)

[5] D. B. Gordon, G. A. Lord, L. W. Tetler, C. M. Carr, *J. Chromatogr,* **700 (1/2),** 27 (1995)

[6] N. W. Smith, M. B. Evans, *Chromatographia,* **38,** 649 (1994)

[7] S.J. Lane, R.J. Boughtflower, C.J. Paterson, M. Morris, *Rapid communications in mass spectrometry,* 10 (1996) 733-736

[8] I.S. Lurie , R.P. Meyers, T.S. Conver, *Anal Chem,* 70(15), (1998) 3255-60

[9] M.M. Dittmann, G.P. Rozing, G. Ross, T. Adam, K.K. Unger, *J. Cap. Electrophoresis*, 4(5), (1997), 201-12.

[10] A.S. Rathore, Cs. Horvath, *Anal. Chem.* 70, (1998) 3069-77.

[11] J.H.Knox, *Chromatographia,* 26, (1988)329-37.

[12] R.J. Boughtflower, C.J. Paterson, T. Underwood, *Chromatographia*, 40 (1995) 329-336.

[13] C.J.Paterson, *PhD Thesis, Manchester Metropolitan University* (1998).

Chapter 7. Thermal Effects in CEC

7.1 Introduction

Capillary separation techniques have much to offer the future of miniaturised chromatographic analysis. Improvements in speed, performance and selectivity are all possibilities to be properly explored, but it is important to understand their limitations. CEC, as CE, uses an electrical field across the column to generate a liquid flow inside the column. Both require an electrolyte to maintain stable electrical conduction. The ohmic resistance generates heat and this limits the ranges of parameters such as column diameter, electrolyte concentration and field strength which may be used before performance deteriorates.

The thermal limitations of CE have been discussed by Knox [1] and studied experimentally by Knox and McCormack [2,3]. In capillary electrophoresis (CE) the plate efficiency, according to theory, should be proportional to the applied voltage. This applies up to the point at which electrically derived heat, generated within the capillary, starts to contribute to peak dispersion. There are two thermal factors which cause additional peak dispersion: the first is the difference in temperature (T) between the capillary and its surroundings, and here the additional dispersion is largely due to the change in solute diffusion coefficient (Dm); the second is the parabolic temperature profile within the core of the capillary, which causes a corresponding migration rate profile across the column. This in its turn causes additional dispersion because transverse diffusion is necessary to iron out the differences in migration rate profile. A schematic representation of the likely thermal profiles in a typical capillary layout is shown in Figure 1 [1]. It is also

apparent that there is a concurrent deviation from linearity of the dependence of the electroendosmotic velocity (EOF) upon field strength (E) [2].

The temperature of the contents of the capillary is increasing, relative to outside the capillary, but there is still very little temperature difference between the inner wall and the core of the capillary. So the apparent 'speeding up' of the EOF in relation to E is due solely to a reduction in the viscosity of the eluent [2]. This can occur without necessarily having much effect on the flow profile across the column bore. The biggest temperature difference is between the capillary and the outside air. This will remain the case while the cooling ability of the external environment is unchanged. For natural convection systems (where no extra cooling mechanism is used) Knox proposed [1] that capillary diameters of 100μm could be used with power consumption of up to $300Wcm^{-3}$, which would give a temperature difference of about 50K between the capillary wall and outside air. The temperature difference inside the capillary within the core region would be about 1K. For forced convective air cooling, the temperature differences in equivalent systems can be reduced by approximately a factor of five. Ideally Knox suggests that the forced air cooling rate should be $>10\ ms^{-1}$. Increasing the heat loss from the capillary is the key factor to minimising performance loss. It is when heat builds up within the capillary, that the temperature gradients formed across the capillary bore, will seriously reduce the performance of the system, due to the development of parabolic band migration profiles across the column.

In the case of CEC there are more contributory factors to dispersion in a packed column than in CE. These come about due to the presence of the stationary phase inside a CEC column. Extra dispersion will be caused by the flow around and

through the stationary phase particles and by solute partition into the particles. When we consider the optimal use of CEC as proposed by Knox [1] , it appears that for ultimate performance we need to move towards sub-micron particles. If we substitute a typical value for this particle size (say 0.5μm or less) into the A and C terms of the Van Deemter equation and calculate the individual contributions to the plate height caused by these terms [1] they become small compared to the diffusional contribution (B term). Under these ultimate conditions where the only dispersive contribution comes from axial diffusion, the plate height in electrically driven systems is given by; -

$$H=2\,D_m/\,u \qquad (7.1)$$

we then obtain the following simplified relationships; -

Ultimate plate height $H = 2\,D_m\,\eta\,/\,\varepsilon_0\,\varepsilon_r\,\zeta\,E$ ie. $H \alpha\ 1\,/\,E$ **(7.2)**

Ultimate Plate Number $N = L\,/\,H = \varepsilon_0\,\varepsilon_r\,\zeta\,V\,/\,2\,D_m\,\eta$ ie. $N \alpha\ V$ **(7.3)**

Ultimate void time $t_0 = L\,/\,u = L^2\,\eta/\,\varepsilon_0\,\varepsilon_r\,\zeta\,V$ ie. $t_0 \alpha\ L^2$ (7.4)

(To sweep one column volume) and $t_0 \alpha\ 1\,/\,V$

The implications of these relationships are obvious. To perform the most efficient CEC separations in the shortest analysis times we need to use short columns filled with small particles and use high voltages. However the use of such

high fields, other things being equal, will increase the amount of heat generated within the column. The achievement of "ultimate performance" in CEC requires that such thermal effects be minimised.

In his paper of 1988 [1] Knox discussed the theoretically expected boundaries of operation for capillary electroseparation methods. He proposed that an acceptable limit for the band broadening arising from thermal effects was 10% of that arising from the normal chromatographic dispersion. Thus, considering the ultimate performance of CEC, $H_{thermal}$ should not be greater than 10% of H_{diff} (as given by equation 7.2).

In electroseparation systems where heating effects occur, a parabolic temperature variation will exist across the capillary bore, giving rise to an additional parabolic flow disturbance, superimposed on the uniform migration velocity of solute moving along the tube. Additionally there will be a parabolic variation in the capacity ratio over the column cross section due to the variation of k′ with temperature.

We can compare the parabolic flow variation in CEC to that seen in normal pressure driven flow. This variance, in units of length is given by Taylor's equation [4] ;-

$$\sigma_z^2 = \frac{L d_c^2 \bar{u}}{96 D_m} \qquad (7.5)$$

By analogy, to get the additional dispersion arising from a parabolic velocity profile superimposed on the normal migration velocity in CEC, the mean velocity $\bar{u}$ of the Taylor equation can be replaced by the mean excess velocity $\delta\bar{u} = \frac{1}{2}\delta u_{mig}$ in the electrically driven case, where δu_{mig} is the difference between the velocity at the axis of the tube and the wall and given by;-

$$\frac{\delta u_{mig}}{u_{mig}} = \theta_{core} \sum \alpha_i = \alpha\theta_{core} \qquad (7.6)$$

where θ_{core} is the difference between the temperature at the capillary axis and the inner wall. α is the fractional change in any given property per Kelvin. In this case we are concerned with the change in flow rate and the summation of α is over all relevant effects which contribute to the parabolic profile and for calculation is given a value of 0.03. This value is estimated and is composed of a contribution of 0.02 from the likely variation in flow rate and 0.01 due to the variation in partition coefficient across the tube bore. Both these variations are caused by any superimposed effect of the temperature profile. The likely range of values of α for these systems is 0.01-0.04 [1].

The effective distance of migration of the extra disturbance becomes $\frac{\delta\bar{u}}{u_{mig}} L$,

Making these substitutions in equation 7.5 gives;-

$$\sigma_z^2 = \frac{\delta\bar{u}/u \, L d_c^2 \delta\bar{u}}{96 D_m} = \frac{(\delta\bar{u}/u)^2 L d_c^2}{96 D_m} u \qquad (7.7)$$

We then substitute for $\frac{\delta\bar{u}}{u} = \frac{1}{2}(\frac{\delta u_{mig}}{u}) = \frac{1}{2}\alpha\theta_{core}$ **(7.8)**

And that extra contribution to plate height from thermal effects are given by;

$$H_{th} = \sigma_z^2 / L = (\frac{\delta\bar{u}}{u})^2 d_c^2 u_{mig} / 96 D_m \qquad (7.9)$$

Or,

$$H_{th} = (1/2\alpha\theta_{core})^2 d_c^2 u_{mig} / 96 D_m \qquad (7.10)$$

Where the σ_z represents the extra axial distance travelled by the solute in the core region of the tube due to thermal effects. If we substitute the expression for θ_{core} [1] ;-

$$\theta_{core} = Q d_c^2 / 16 \kappa = (E^2 \lambda c \varepsilon)(d_c^2 / 16 \kappa) \qquad (7.11)$$

and use the electroendosmotic velocity as u_{mig} then the total expression for H_{th} becomes; -

$$H_{th} = 10^{-8} (\varepsilon_0 \varepsilon_r \zeta / D_m \eta \kappa^2) E^5 d_c^6 \lambda^2 c^2 \qquad (7.12)$$

It can be seen from this relationship that the dependence of H on the capillary diameter and field strength in particular is severe, and it seems clear that if conditions of operation are not sensibly controlled a rapid, probably catastrophic decline in performance will be observed when E and/or d_c are increased beyond critical limits. As an example if we consider a system with E = 50,000 V m^{-1} and c = 10 mol m^{-3}, H_{th} = 0.006μm for d_c = 100 μm and 0.4 μm for d_c = 200 μm, a very substantial rise in H for a doubling of the capillary diameter. Of course we are really most interested in the contribution that H_{th} makes to total dispersion. As mentioned earlier if we impose the condition that $H_{total} > 10H_{th}$, then the limitations for this condition to apply are given by equating $H_{thermal}$ (equation 7.12) with 10 x H_{diff} (equation 7.2) to ultimately give:-

$$d_c^3\,(\mu m)\; E^3\,(kV\ m^{-1})\; c\ (mol\ dm^{-3}) < 3 \times 10^9 \quad \textbf{(7.13)}$$

Assuming an approximate value of α (from equation 7.6) of 0.03.

If these limitations are arranged as boundary conditions table 1 is obtained [1].

TABLE 1

Operational limits under which thermal contribution to plate height is < 10% that from axial diffusion according to eqn 7.14.

	E (kV m^{-1})	10	20	50	100	
C/mol dm^{-3}		1500	750	300	150	d
	0.001	1	5	30	120	Q
		2	3	4	6	θ
		700	350	140	70	d
	0.01	12	50	300	1200	Q
		6	8	15	19	θ
		320	160	60	30	d
	0.1	120	500	3000	12000	Q
		20	26	40	50	θ

d = Maximum allowed tube diameters Q = Heat production rate in W cm^{-3}

θ = Temperature difference in K between tube wall and surrounding air, with air flow of 10 m s^{-1}.

The values in the table are obtained by fixing the value of c and E then calculating d_c, Q and θ are consequential.

The arguments so far have dealt with scenarios for ohmic heating based upon heat loss from typical open tube systems, which have been considered to contain a typical mobile phase of 50/50 v/v organic solvent and aqueous. The thermal conductivities (κ) of the tube contents have a direct effect on heat loss, as can be seen from the dependence of thermal contribution to plate height (H_{TH}) in equation

7.12, on the inverse square of κ. In terms of the limiting conditions for restricting thermal contributions in equation 7.13 there is a direct relationship to κ.

Therefore the higher the thermal conductivity of the column contents, the better the heat loss, and the farther the operational conditions can be pushed before we hit the performance wall. For the packed CEC column case, we can approximate the value of κ to a weighted average of 1.0 W m^{-1} K^{-1} (from a 40% contribution from the mobile phase at 0.4 and 60% stationary phase at 1.4). This value compares with the value for an open tube, containing just mobile phase of 0.4 W m^{-1} K^{-1}. This would give us an operational limit for packed column CEC of, for an estimated value of α of 0.03 as;

$$d_c^3\,(\mu m)\; E^3\,(kV\ m^{-1})\; c\ (mol\ dm^{-3}) < 8 \times 10^9 \qquad \textbf{(7.14)}$$

This 'rise' in the limiting condition is attributable to the increase in the value of κ for a packed column arrangement. Notwithstanding the above theoretical analysis, a practical determination of the thermal limits of CEC by direct measurement of performance under varying conditions is highly desirable. The remainder of this chapter describes such direct experiments. A range of operating conditions has been chosen, to determine the borderline for failure of CEC due to thermal problems.

7.2 Experimental design to test thermal contributions in CEC

All experiments carried out during this work were performed on a Hewlett Packard HP ^{3D} CE with forced air-cooling of the capillary at a rate of approximately 10 m s^{-1} (HP instrument specification figures). The cartridge temperature was set at 15°C unless otherwise stated. All electrolyte (buffer) concentrations are quoted as overall solution concentrations.

When changing operating conditions the following procedure was adopted.

1. The applied voltage was switched off prior to removal of the existing eluent vials.
2. The new eluent vials were automatically moved into position by the movement of the autosampler and vial-lifting arms.
3. When a new eluent was being introduced the voltage was initially applied at 10kV. This enabled conditioning of the column with the new eluent without running into problems with premature heating. Typically this would be left to condition for 30-45mins or until a stable current reading had been obtained. When this was achieved the experimental voltage was applied.
4. All experiments in the new eluent system were carried out in order of the least 'thermal load' first. This allowed for the maximum amount of data collection prior to thermal problems being met.
5. If 'thermal collapse' was encountered, the experiment was stopped, the column 'recovered' with a low conductivity eluent such as 50:50 v/v ACN: H_2O to re-solvate the phase, and the experiment

repeated. In extreme cases duplicate measurements were made either side of column recovery if it was possible to do so.

As shown earlier, the thermal contributions to the plate height in CEC are expected to be proportional to E^5, d_c^6 and c^2. On a conventional instrument such as the Hewlett Packard CE there is a practical limitation as to the minimum length of capillary used (and therefore the maximum field, E), and also the maximum inner diameter (as this defines the maximum outer diameter that will fit in the optical interface). This allows some flexibility but also means that buffer concentration (c) is the most easily variable quantity. Given these instrumental constraints it was possible to vary the field up to 80kV/m, tube bore from 50 to 150 μm, and buffer concentration up to 100 mM.

Initial experiments (designated E1) were 'sighted' by substituting the limiting parameters imposed by the instrument design into equation 7.13. With a maximum operating field strength of 80kV m^{-1} and a practical capillary diameter maximum of 150μm, the working buffer concentration under these 'maximum' conditions (ie $H_{th} < 10\%$ of H_{total}) or

$$d_c^3\,(\mu m)\; E^3\,(kV\ m^{-1})\; c\ (mol\ dm^{-3}) > 3.3 \times 10^9$$

is calculated for a sodium phosphate buffer to be about 2mM. For columns of diameter 50μm, the limiting buffer concentration would be 50mM. The columns were tested under otherwise identical testing conditions using a multiple component neutral test mixture. Electrical fields up to 80 kV m^{-1} were used with buffer

concentrations of 2.5, 6.25, 12.5 and 25 mM in columns of, 50, 100 and 150μm diameter.

Subsequently, a second set of experiments (E2) was performed to enable comparison of the performance characteristics for the same set of capillary diameters, with higher buffer concentrations up to100mM. This set of experiments, as seen in the results section, pushed the performance limits much harder and, as anticipated, not all combinations could be used for every capillary diameter.

7.3 Results and Discussion

7.3.1 Experiments E1

Experiments E1 were set up to vary operational parameters such as Field Strength (E), capillary diameter (d) and buffer concentration (c) and see the effect on CEC performance. Parameters such as plate height (H), current (I) and EOF were evaluated to determine the operational 'goalposts' before CEC performance deteriorated beyond useful benefit, if at all. The data were plotted as follows:

1. Figure 2: Plate height (H) vs. Field strength (E).
2. Figure 3: Current (I) vs. Field Strength (E)
3. Figure 4: Current (I) vs. Buffer Concentration (c)
4. Figure 5: EOF (u) vs. Field strength (E)
5. Figure 6: Current vs. EOF (u)

A typical set of data, for the 100μm diameter column, is shown in Figures 2-6. The traditional plate curves (H vs. Field Strength) measured using the moderately

retained Benzamide (peak 2) as the solute, are relatively flat, indicating that once the diffusion limitation is overcome (at low flow rates), there is little loss in performance at higher flow rates. This is largely expected for conditions of low thermal contribution (ie. when diameters are small and overall buffer concentrations are low). It is not known why the plate curves for different buffer strengths do not effectively overlay, as they do for higher buffer concentration series described in the next section under Experiments E2. Although this is a common observation in CE when using very low buffer concentrations and may be due to depletion effects, it is clear from the plots of current (I) versus field strength (E) for different buffer concentrations (Figure 3), where a proportional relationship is expected between the current and buffer concentration at fixed field strength, that this is not what is being observed. The values of current vs. concentration at various applied fields are plotted for comparison in Figure 4. This shows near linear relationships but the lines do not go through the origin as expected. However, the proportionality of the different fields at the intercept suggest a 'consistent' residual current probably due to the electroosmotic contribution to the current. This deviation from expected behaviour is also seen for the other experiments in this series. If u is plotted against E (figure 5), a slight curvature in the plot is expected at conditions where thermal effects start to reduce the viscosity of the electrolyte, leading to an 'apparent' increase in u relative to E. When u is plotted against I, straight lines should be observed. Figure 6 demonstrates that this is reasonably well observed. Although there is significant scatter in the points there is no underlying trend.

These rather poor results suggested that something was wrong with the execution or design of these experiments. It was felt that too high an acetonitrile

composition might have been used (75% used in E1 experiments). With such a high organic content, ion-pair formation may be occurring, especially at the higher buffer concentrations, and this could lead to inconsistent readings in the current. We would expect to see reduced values for the current reading at higher buffer concentrations as $A^+ + B^- = AB$ would not give a current linear with concentration if there was a significant proportion of AB. However, if ion-pairing is occurring this will have negligible effect on u as this depends on the zeta potential.

To check on the performance of electrolytes containing lower percentages of organic solvent, experiments were performed to test the principle in open tubes.

7.3.2 Measurement of Current (I) versus Buffer concentration (c) for open tubes of 50μm diameter at various solvent/buffer compositions.

Experiments comparing EOF (u) and current (I) to buffer concentrations (c) were repeated for organic solvent compositions of 0%, 25%, 50% and 75% acetonitrile with the remainder being composed of NaH_2PO_4, at overall volume concentrations of between 2 and 100mM. The u vs. c plots are shown in Figures 7-10 and the I vs. c plots are shown in Figures 11-14. It can be seen from the I-c plots in Figures 11-14 that non-proportional behaviour is seen most predominantly for the plot of 75% acetonitrile content. Approximately linear behaviour is seen up until higher concentrations of buffer are used and then a suppression of current values is seen. Plots using lower quantities of solvent show more closely linear relationships between the current and buffer concentration, although the 5mM point in Figure 12 is consistently low for all field strengths. This was deemed to be an error in the buffer preparation. Of course, at the higher buffer concentrations (this is particularly

the case when the organic solvent composition is low), the current obtained is substantial at high field strengths. This leads to exactly the curvature in the I-E plots that is expected due to the viscosity of the electrolyte falling. It appeared that much better I-c proportional behaviour was observed, using electrolytes with total organic solvent compositions below 50%.

Overall, it is clear from the sighting experiments that using the relatively limited range of buffer concentrations in experiment E1, significant thermal effects are not encountered. The results show that it would be beneficial to perform any further experiments in reduced organic solvent composition electrolytes, and when using higher organic composition, over a wider range of buffer concentrations. In this latter respect it is worth noting that when using CEC as opposed to CE, relatively high concentrations of organic solvent are often used, in which the solubility of buffer salts may be low. It may then be that the thermal limits are not often reached under practical CEC conditions. It is, of course the purpose of the experiments described in this chapter to determine whether this is the case or not. Accordingly, the second set of experiments, E2, were devised to expose the system to a higher thermal 'load' by utilising lower overall organic concentrations (50%) which enabled higher buffer solubilities and therefore concentrations to be used. It was hoped that this would allow the system to be tested under conditions, which could lead to significant loss of performance, or even failure of the system.

Plots of the standard parameters are shown in Figures 15-27 for the experiments E2 on each column diameter. The buffer concentrations tested were 25, 50, 75 and 100mM. The use of 50/50 v/v acetonitrile/ buffer allowed overall buffer concentrations of four times the previous maximum and allowed testing of the

system under conditions of higher power consumption, where thermal effects should be far more pronounced.

7.3.3 Thermal Data for 50μm diameter columns in experiment E2

The data for experiments E2 for the 50μm column are shown in Figures 15-19, with each of the following plots being shown in order;

Figure 15: Plate height (H) vs. Field strength (E).

Figure 16: Current (I) vs. Field Strength (E)

Figure 17: Current (I) vs Buffer Concentration (c)

Figure 18: EOF (u) vs Field strength (E)

Figure 19: Current (I) vs. EOF (u)

It can be seen from the plot of HETP versus E (Figure 15) that the plate curve is very flat for most of the buffer concentrations with no apparent loss of efficiency at higher field strengths. Likewise there is no significant trend in H as the buffer concentration is increased in contrast to the data of series E1. There is now good proportionality between I and c as shown in Figure 17. This is also supported by the other plots where little deviation from expected behaviour is seen. At the highest buffer concentration of 100mM however, there is evidence of an increase in both HETP and the expected current value (Figures 15 and 16 respectively). There is also a significant upward curvature in the u versus E plot (Figure 18) indicating a slight drop in viscosity of the electrolyte due to temperature rises inside the capillary

bore. These indications are consistent with the predicted limits suggested by equation 7.13.

Overall, the experiments for 50μm diameter columns in E2 show the expected behaviour. Only at the most demanding conditions of operation is there evidence that thermal contributions are starting to affect performance. By contrast, the same experiments in E1 show significant variability between buffer concentrations, the low buffer concentrations giving significantly lower efficiency figures. The high (75%) acetonitrile concentration also affects the predicted behaviour, particularly at higher buffer concentrations, where deviations from expected current values are observed.

7.3.4 Thermal Data for 100 μm diameter columns in experiment E2.

For 100μm diameter capillary it is reasonable to expect that at least four times as much power will be consumed than with 50 μm bore tubes. This is likely to cause more serious deterioration of performance and even complete breakdown at the higher field and buffer strengths. This data is presented in Figures 20-23.

It is obvious from looking at the plots for the 100μm diameter column that significant heat is being generated inside the capillary at the most demanding operating conditions. In fact it was not possible to use the 75 and 100mM buffer strengths at field strengths higher than 50 kV/m without losing either the flow or exceeding the maximum power capability of the instrument. Even at 50kV the 100mM buffer system is very unstable and is not giving a true reading of the current (Figure 21). There is an increasing upward curvature in both the u versus E and I

versus E plots (Figures 22, 21). The plots of I versus u give excellent straight lines (Figure 23), except for the 100mM buffer system which gives spurious readings of current due to breakdown at E > 40 kV/m.

Calculation using expression 7.13,

$$d_c^3\,(\mu m)\; E^3\,(kV\; m^{-1})\; c\;(mol\; dm^{-3}) > 3.3 \times 10^9$$

for this system gives;-

$$d_c^3\,(\mu m)\; E^3\,(kV\; m^{-1})\; c\;(mol\; dm^{-3}) = (100)^3\,(40)^3\; 0.1 = 6.4 \times 10^9$$

This value is approximately two-fold higher than the proposed limit. Our results are therefore consistent with expression (7.14) Under more extreme conditions than this (i.e. higher field, larger bore, higher buffer concentration), heating inside the capillary will lead to rapid deterioration in chromatographic performance and eventually catastrophic failure.

7.3.5 Thermal data for 150 μm diameter columns in experiment E2.

Due to the difficulty in acquiring data at high field strengths with 100μm diameter columns, the field strength for 150μm diameter experiments was increased in smaller steps (for higher concentration buffers). This enabled more data points to be collected before system breakdown. A common observation when performing these experiments was inability to reach the next set of operational conditions due to

system instability during the column conditioning step This was most often preceded by a surge in the current value when a new concentration buffer was first used, followed by an unstable and gradually rising current. It was generally difficult to obtain consistent chromatography when these effects appeared and consequently, at the limits of operation, occasionally only one measurement was possible before performance was lost. It was apparent that this was exactly what had been expected. We were approaching conditions of operation corresponding to the predicted 'wall'. Even when these borderline conditions were reached there was still an element of escalation, where there was a 'build-up' to failure of the system. Generally if the column was flushed out and reconditioned at a lower buffer concentration, normal performance was regained. For the 150μm diameter column the maximum stable conditions for operation were with 75mM buffer concentrations at field strengths not greater than 40 kV/m. Beyond this field strength, and system instability made it impossible to record consistent data. Under these conditions,

$$d_c^3\,(\mu m)\; E^3\,(kV\ m^{-1})\; c\ (mol\ dm^{-3}) = (150)^3\,(40)^3\ 0.075 = 16 \times 10^9$$

so it is hardly surprising that thermal breakdown of the system occurred. The data plots are shown in figures 24-27.

It can be seen from these plots that minimum plate height is achieved at fairly low field strengths, even for the 25mM buffer concentration. There is a very slight rise in HETP for both the 25mM and 50mM plots at higher fields, and H-values are a bit higher overall than for the 100 μm columns. It was not possible to operate the 50mM system at field strengths higher than about 50 kV/m. The 75mM

system was limited to operation at less than 40 kV/m, although at these modest field strengths the HETP was still dropping. It is not known why the HETP obtained for the 75mM buffer system at these low fields is discernibly lower than for the lower buffer concentrations. Attempts to operate the 75mM system at significantly higher fields resulted in instability.

7.3.6 Summary of Thermal Effects data for all column diameters.

1. Plots of H vs. E – The plots of this type for 50μm diameter columns are shown in Figures 2 and 15 for experiments E1 and E2 respectively. When using low concentrations of buffer (2-20mM, Figure 2) there are noticeable differences in the plate height for different buffer concentrations. It would appear that a minimum of 20mM buffer overall is required to obtain the maximum performance. At higher concentrations of buffer than this (20-100mM, Figure 15) there is negligible difference in the plate height obtained and performance is not compromised until the highest buffer concentrations are used. There is the first indication at 100mM buffer in Figure 15 that H is rising, due to thermal contributions. When compared to the same plot for 100μm column diameter (Figure 20) it is clearly seen that rises in H are seen for some of the different buffer concentrations, which approximately correlate for conditions of the same thermal load. That is because these operating conditions are getting close to the 'wall' and attempts to raise operating conditions any further would cause collapse of the system. For 150μm diameter columns the plate heights are slightly higher

than in the equivalent 50-100μm systems and the plot is relatively flat until the higher operating conditions are reached. It is only possible to consider using high field strengths with buffer concentrations <25mM overall.

2. Plots of I vs. E – Generally a linear relationship is expected for this type of plot, until such time as conditions are reached that cause temperature rises that affect (lower) the viscosity and show a corresponding increase in current. There should be proportional increases in current with applied field. This was not seen for the E1 experiments and was retested at different organic solvent composition to check experimental design. These open tube experiments confirmed that this non-linearity in E1 was exacerbated by too high a solvent composition. Experiments in E2 showed expected behaviour for all column diameters with increasing curvature of the plot corresponding to higher operating conditions.

3. Plots of I vs. c – These plots should show similar behaviour to the plots in the previous section. At high buffer concentrations and fields, ohmic heating affects the viscosity and current as explained previously. Therefore increasing upward curvature of the plots away from linearity is expected at higher operating conditions. Experiments E1 showed poor adherence to linearity, but all other experiments showed the expected behaviour. The only exception is shown in Figure 11, which is an open tube experiment at 75% acetonitrile composition. Here, there is downward curvature away from linearity. This was deemed to be due to ion-pairing and this was reinforced by the I-u plot for the same experiment which showed compatible behaviour.

4. Plots of u vs. E – These plots are expected to be linear until ohmic heating prevails and reduces the viscosity of the eluent leading to an apparent increase in u relative to E. At low thermal loads the expected behaviour is seen with near linearity observed. Flows are slightly higher in lower buffer concentrations, as expected. This applies until the effect of viscosity reduction 'kicks-in'. At conditions of higher thermal load the plots show increasingly large 'upswing' particularly in the bigger column diameters.

5. Plots of I vs. u – These plots are expected to be linear. This is true even when conditions are used that produce significant heating effects. This is because the current and flow velocity are affected in the same way by changes in the eluent viscosity and the plot should therefore remain proportional. This behaviour is observed for E2 experiments until instability is reached and reliable data is difficult to obtain. Even here, the plots are relatively linear. In cases of excessive thermal load such as that shown in Figure 21 for the 100mM buffer at the highest field strength, it is clear that an unreliable measurement is being obtained. Here, there is a corresponding loss in the linearity of the I-u plot as expected. Experiments E1 showed poor adherence to linearity for these plots as the high solvent composition used appeared to promote ion-pairing effects. This affects the current and not u, so this is to be expected. Evidence for ion-pairing is also supported from the plot in Figure 11.

7.4 Calculation of the Capillary Temperature from Data Obtained in E2.

Thermal effects are clearly discernable in the various plots presented above and they occur predominantly at the more extreme operating conditions (high field, high buffer concentration, large capillary bore). It is therefore relevant to obtain some independent experimental measurement of the column temperature. It is difficult to measure the temperature directly within the capillary, but it can be estimated most readily by using the relationship between viscosity and temperature for the desired mobile phase composition. From published data for acetonitrile/water mixtures [5], relating the viscosity to composition, a graph can be plotted which effectively relates these two variables (see Figure 28). For the purposes of this work we will assume that this data holds for acetonitrile/ buffer mixtures.

The equation obtained by fitting a cubic equation to the curve of Figure 28 for 50/50 v/v acetonitrile/water is:

$$T = (-156.56\eta^3) + (421.65\eta^2) - 439.11\eta + 460.752 \qquad \textbf{(7.15)}$$

This equation may be used to derive the average internal capillary temperature from knowledge of the viscosity of the mobile phase under any particular operating conditions. The temperature calculated is an average of the temperature at the wall and in the centre of the capillary. Knox [1] showed that the temperature variation here is negligible compared to the temperature difference between the outside capillary wall and the environment.

This temperature dependence of viscosity and its pronounced effect on both the EOF and the current allows us to utilise two alternative methods for calculating

the temperature. As the temperature increase leads to corresponding increases in both variables, calculation of the relative increase in either of them will allow calculation of the temperature. For a typical set of conditions the calculations are performed thus;

$$\text{As} \quad u_{e0} = \varepsilon_0 \varepsilon_r \zeta E / \eta \tag{7.16}$$

$$\text{Then,} \quad u_{e0} / E = \varepsilon_0 \varepsilon_r \zeta / \eta \tag{7.17}$$

Plotting u_{e0} / E versus E for a range of E values with everything else constant will give a curve for which the value of $\varepsilon_0 \varepsilon_r \zeta / \eta$ can be obtained at ambient temperature. Although there is a slight dependence of ε_r on temperature, it is not very significant so it is reasonable that the value of $\varepsilon_0 \varepsilon_r \zeta$ can be assumed temperature independent. Therefore the change in u_{e0} / E reflects the change in eluent viscosity, and hence eluent temperature using equation 7.15. Alternatively, the current can be obtained from the equation;

$$I = \pi r^2 \lambda c E \tag{7.18}$$

(It is then assumed that the conductivity is inversely proportional to viscosity. This in its turn assumes that the sizes of the ions with their hydration shells are independent of temperature.)

$$\text{And} \quad \lambda c = C_1 / \eta$$

$$I / E = \pi r^2 C_1 / \eta \tag{7.19}$$

to give curves for I / E vs. E where the intercept at ambient temperature provides us with $\pi r^2 C_1$ and this also allows calculation of the viscosity and corresponding

temperature. Curves of u_{eo} vs E and I/E vs E were plotted using a commercial software package (Curve Expert version 1.3) to obtain intercept values which could then be correlated with the viscosity values. The corresponding temperatures were then calculated from equation 7.17. Calculated values for the viscosities and temperatures for the complete range of operating conditions are shown in the Tables 2-4 (pages 217-220). In all the tables shown in this section T_A and T_B refer to the temperatures calculated using the u variation and I variation with viscosity respectively. Figures in bold represent data readings taken from experiments where the system showed instability, prior to collapse. These values have not been included in contributions to average values.

7.5 Conclusions of Thermal limits for CEC operation.

The experiments carried out in this chapter give very clear guidelines as to the operational limits of CEC before thermally induced effects spoil the performance. It can be considered that there are two limits for practical operation. The first is the point at which thermally induced gradients across the bore of the tube, superimpose an additional axial dispersion on the solute band, leading to an increase in the plate height. Knox [1] suggested that this thermal effect should be limited to no more 10% of total plate height. This effect starts to exceed these conditions when the power consumption of the capillary system exceeds about 6 W m^{-1}. These conditions correspond to a value of d_c^3 (μm) E^3 (kV m^{-1}) c (mol dm^{-3}), of about 8 x 10^9 (average value across all diameters and conditions). This is very consistent with that predicted earlier in the text. This prediction is itself based on a correction of Knox's earlier prediction [1].

The second limit is reached if operation is continued beyond this point, until a power consumption of about 10-11 W m^{-1} is obtained. At this point the operational wall is hit and the system is on the verge of collapse, most likely due to substantial temperature rises within the capillary and loss of conductivity/ flow. At this point the use of the system is compromised and remedial action will almost certainly be required. No performance benefit is achieved beyond the first limit of operation.

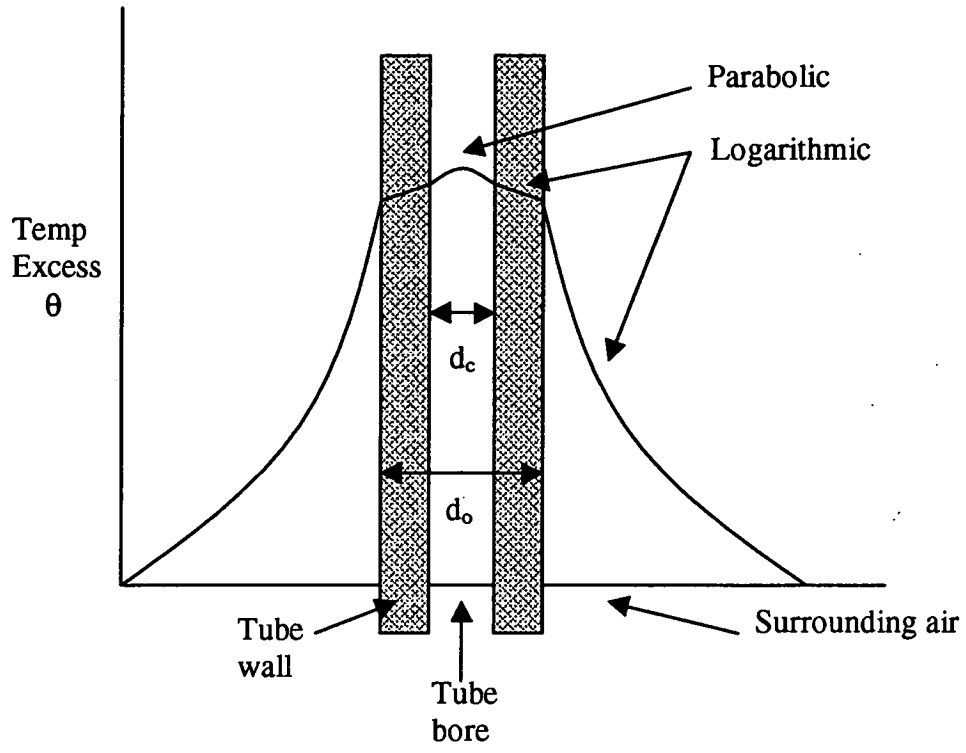

Figure 1. The semi-quantitative representation of the temperature profile across a capillary containing electrolyte heated by the passage of an electric current.

Figure 2. Plot of H vs E for 100μm at different buffer strengths.

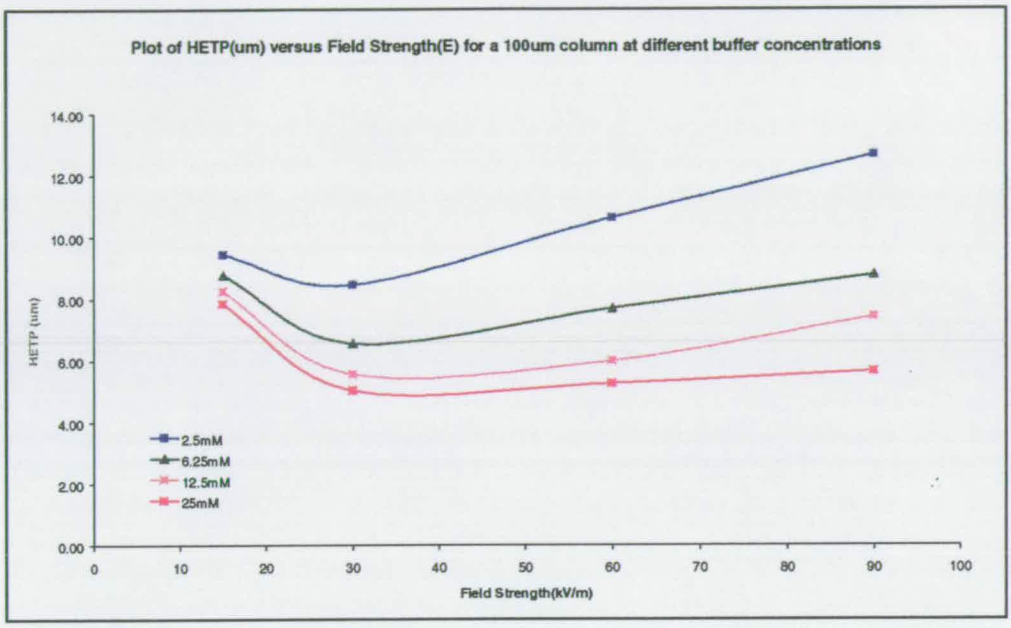

Figure 3. Plots of I vs E for a range of different buffer strengths in 100μm column.

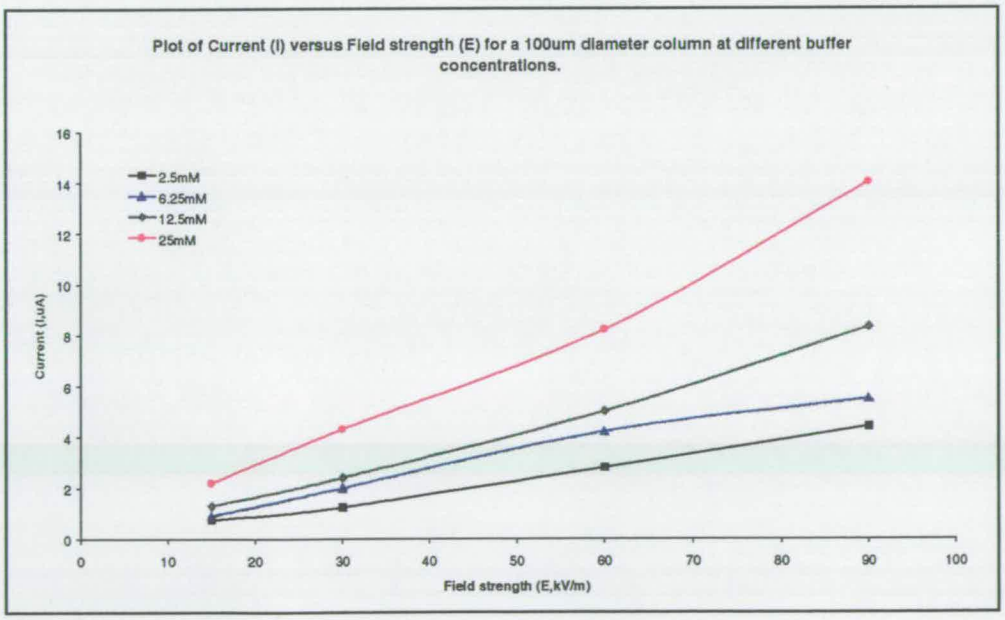

Figure 4. Plot of the current (I) vs. buffer strength (c) for same system at various applied field strengths.

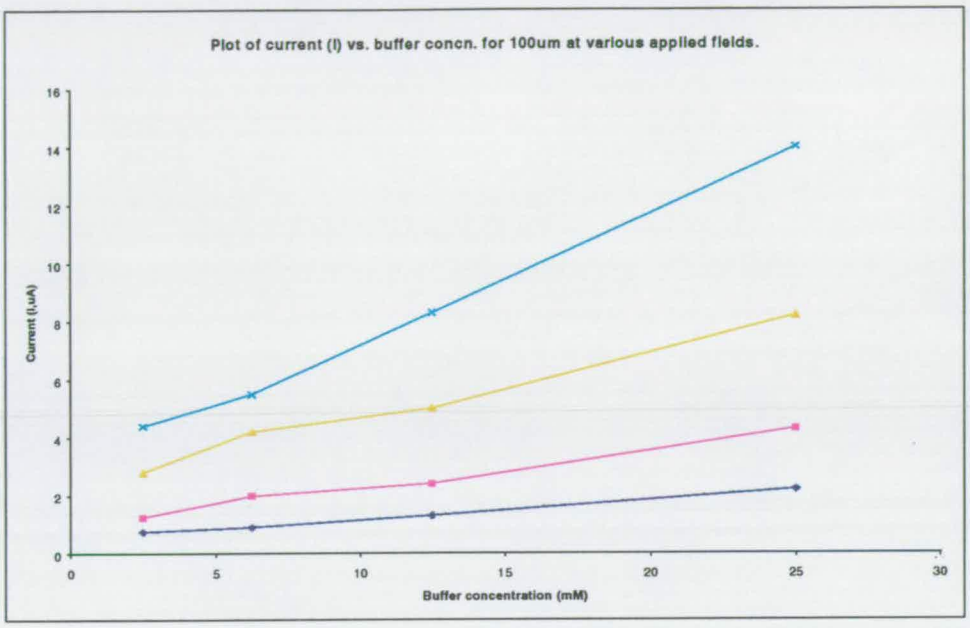

Figure 5. Plot of EOF (u) vs field strength (E) for same system.

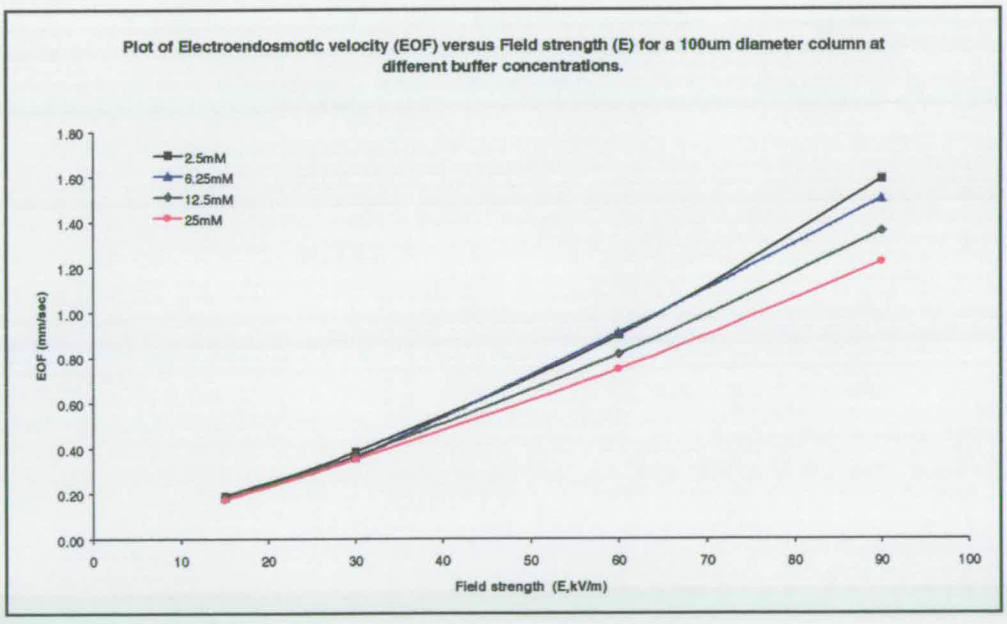

Figure 6. Plot of current (I) vs. EOF (u) for same system.

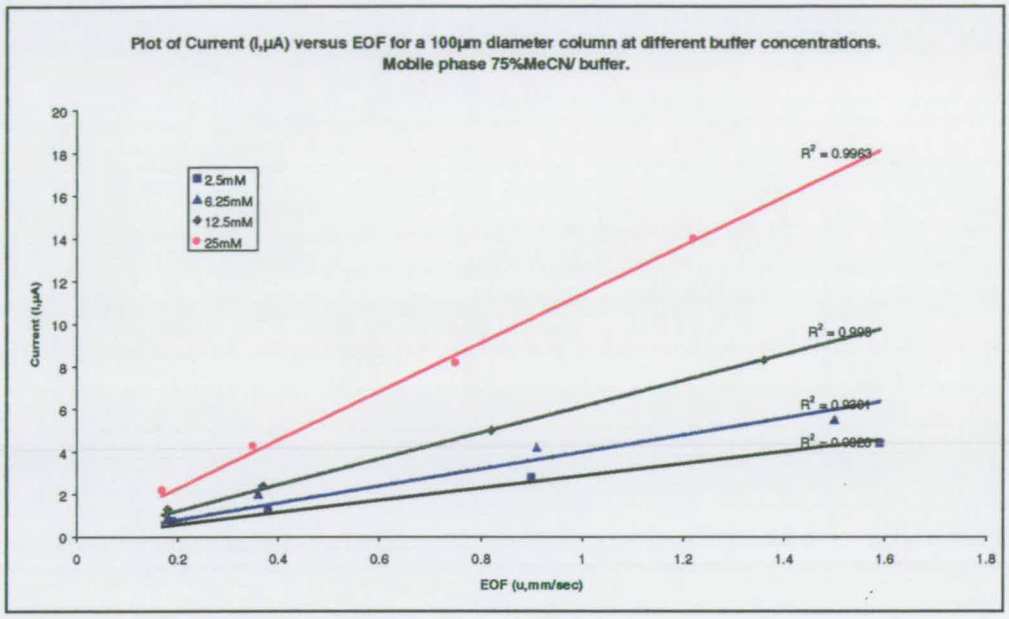

Figure 7. Plot of I vs. E for 50μm open tube with 75% ACN/buffer mobile phases.

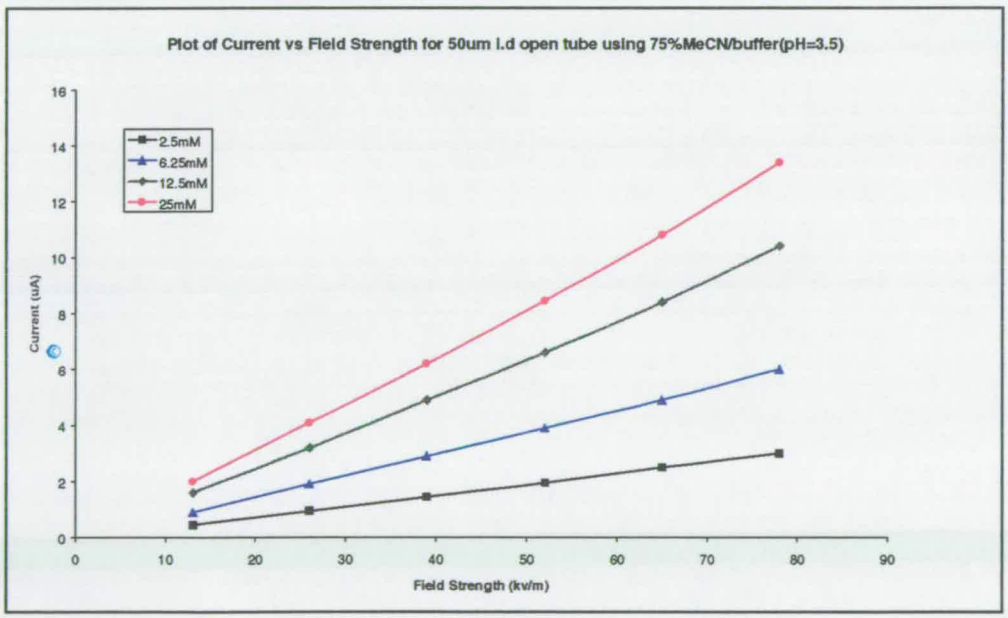

Figure 8. Same plot as Figure 7 for 50% ACN/ buffer mobile phases.

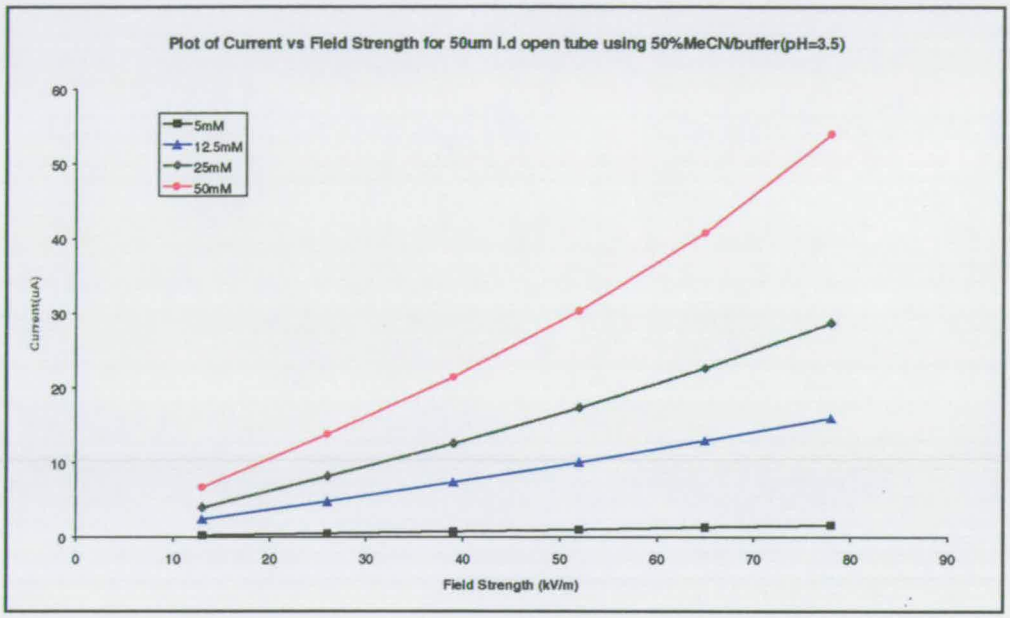

Figure 9. Same plot as Figure 7 for 25% ACN/ buffer mobile phases

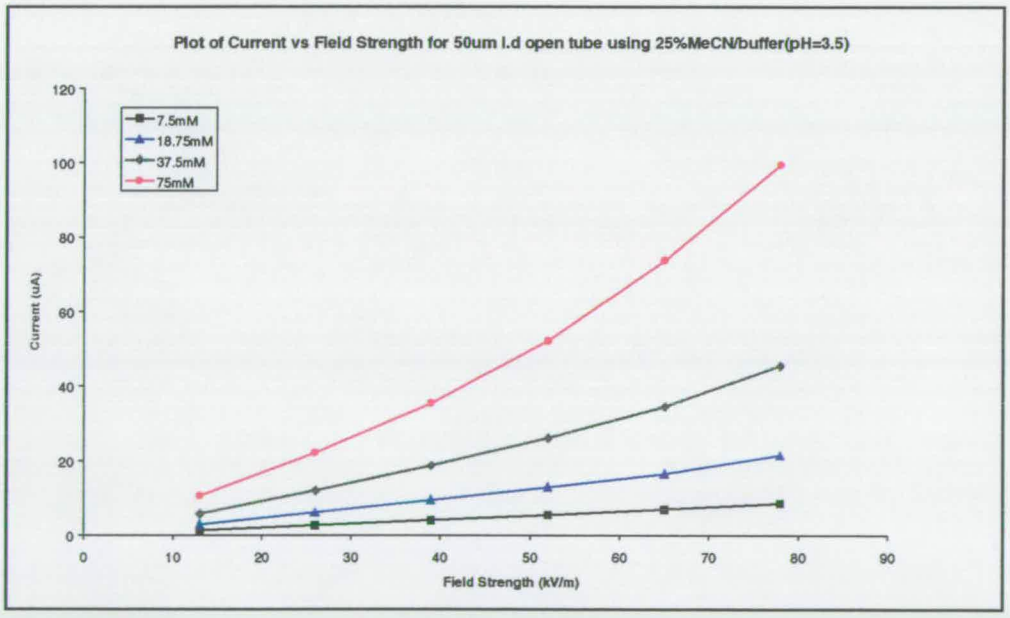

Figure 10. Same plot as Figure 7 for 0% ACN/ buffer mobile phases

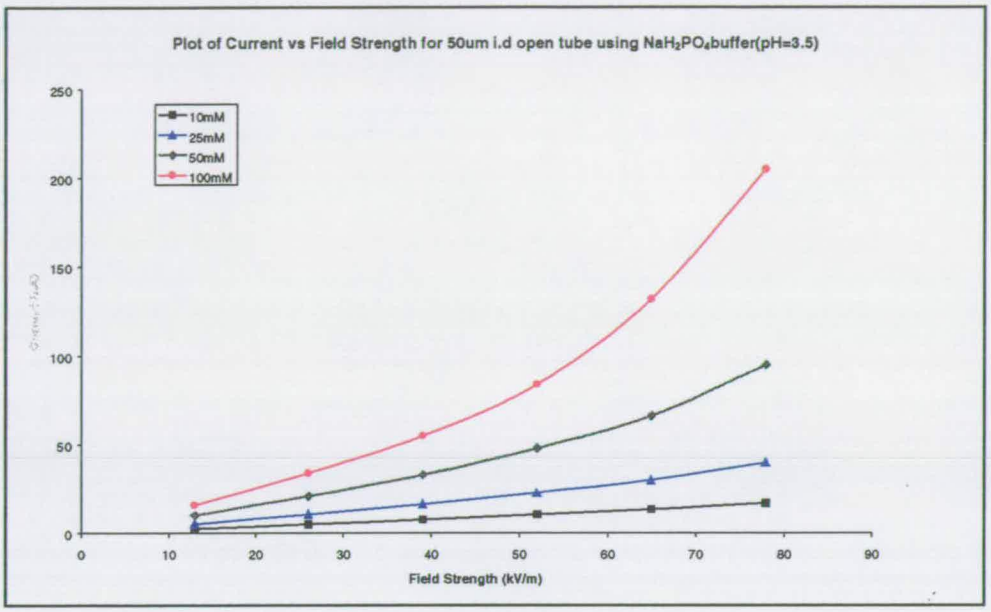

Figure 11. Plot of Current (I) vs. Buffer strength (c) for 50μm open tube with 75% ACN/ buffer mobile phases.

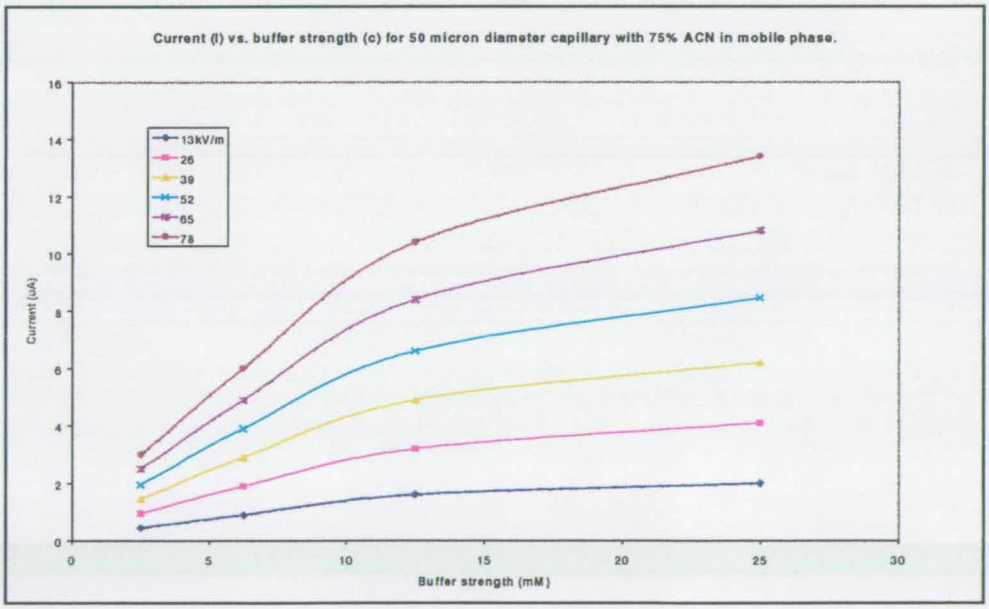

Figure 12. Same plot for 50% ACN/ buffer mobile phases.

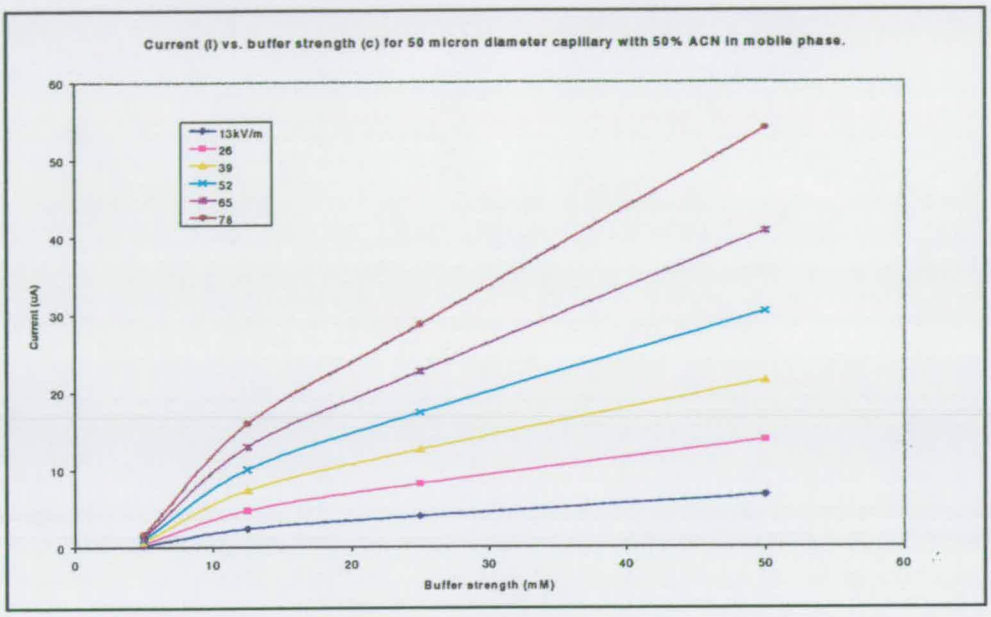

Figure 13. Same plot for 25% ACN/ buffer mobile phases.

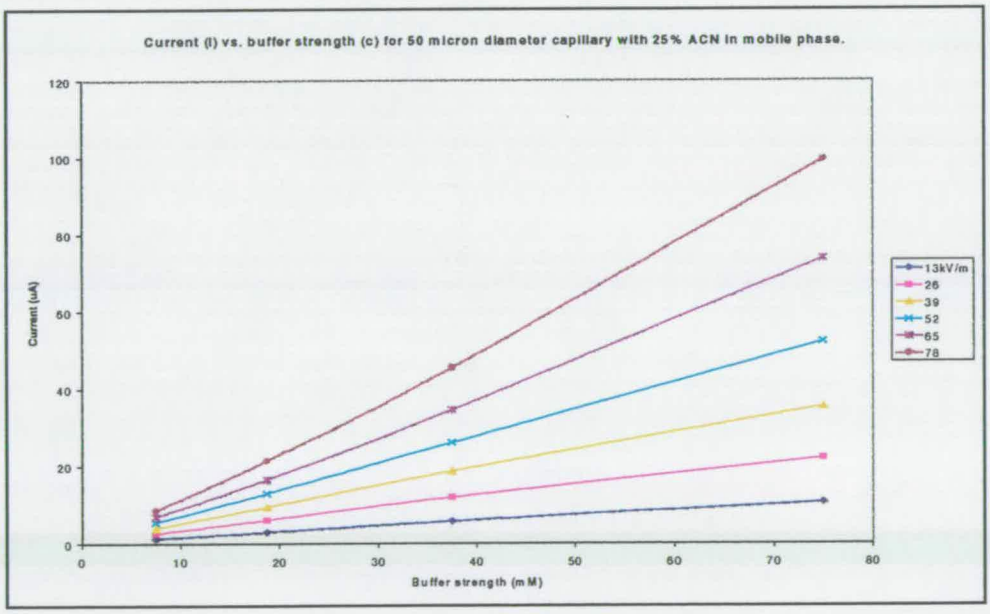

Figure 14. Same plot for 0% ACN/ buffer mobile phases.

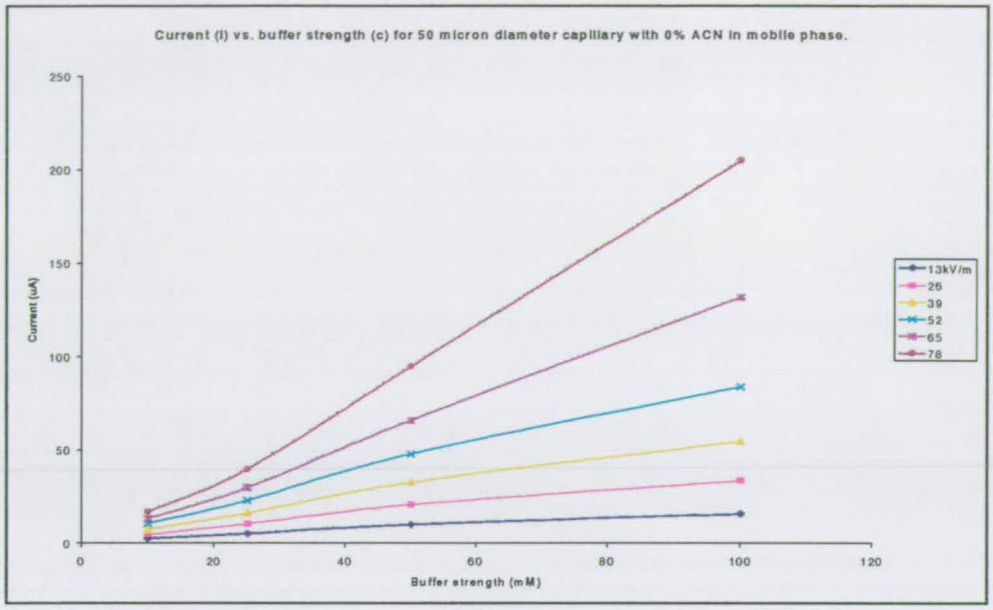

Figure 15. Plot of HETP (H) vs. E for a 50μm diameter column at different buffer strengths.

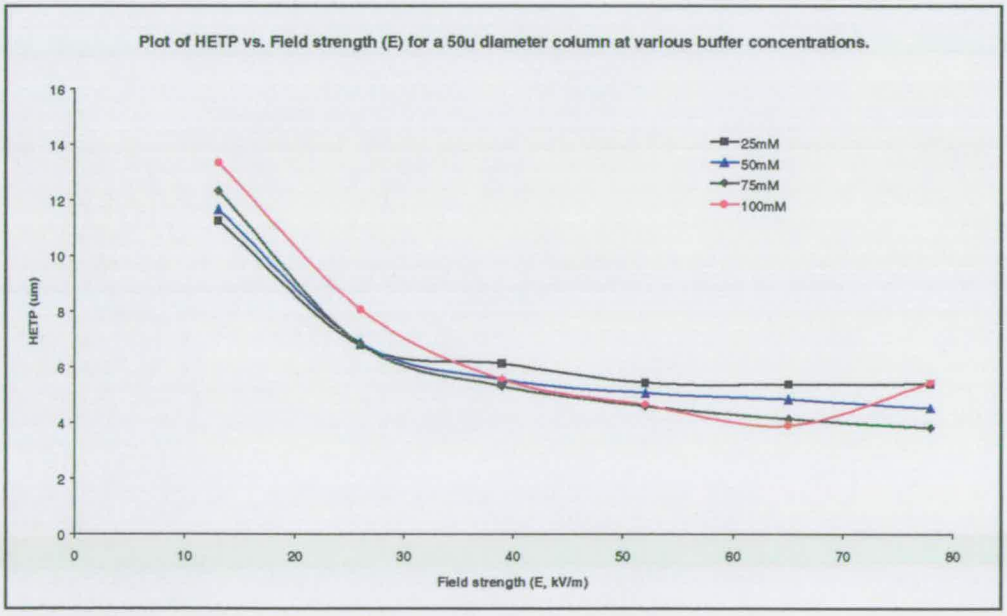

Figure 16. Plot of Current (I) vs. E for a 50μm diameter column at different buffer strengths

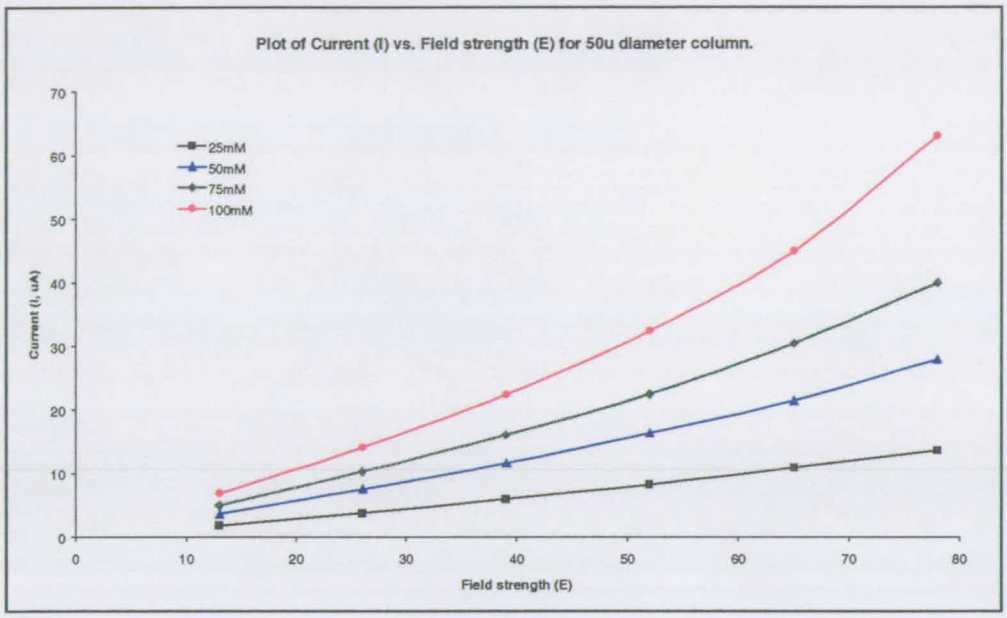

Figure 17. Plot of I vs. c for 50μm column at various field strengths.

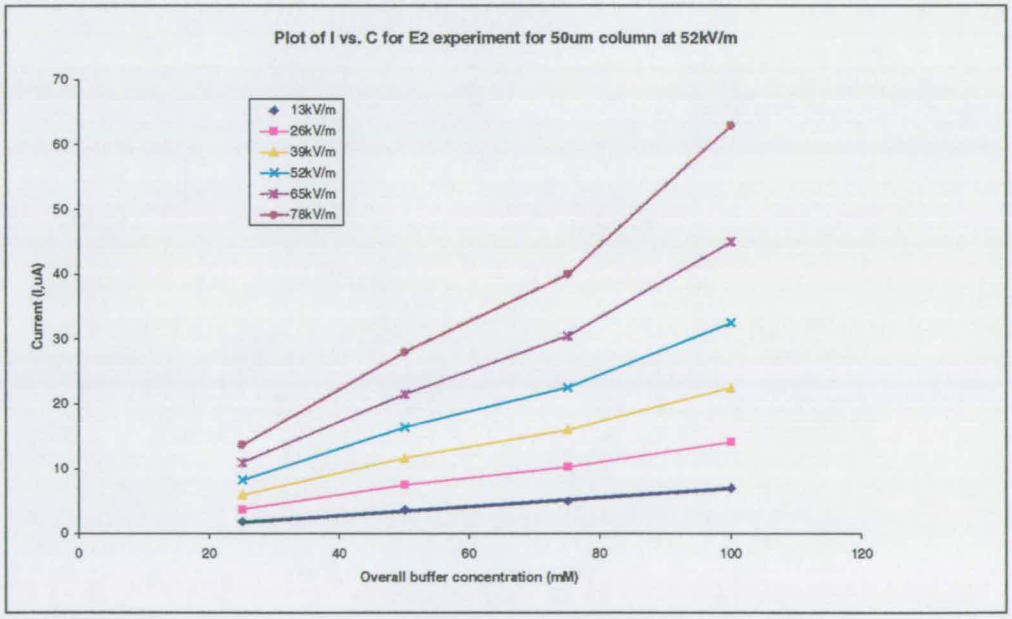

Figure 18. Plot of EOF (u) vs. E for a 50μm diameter column at different buffer strengths

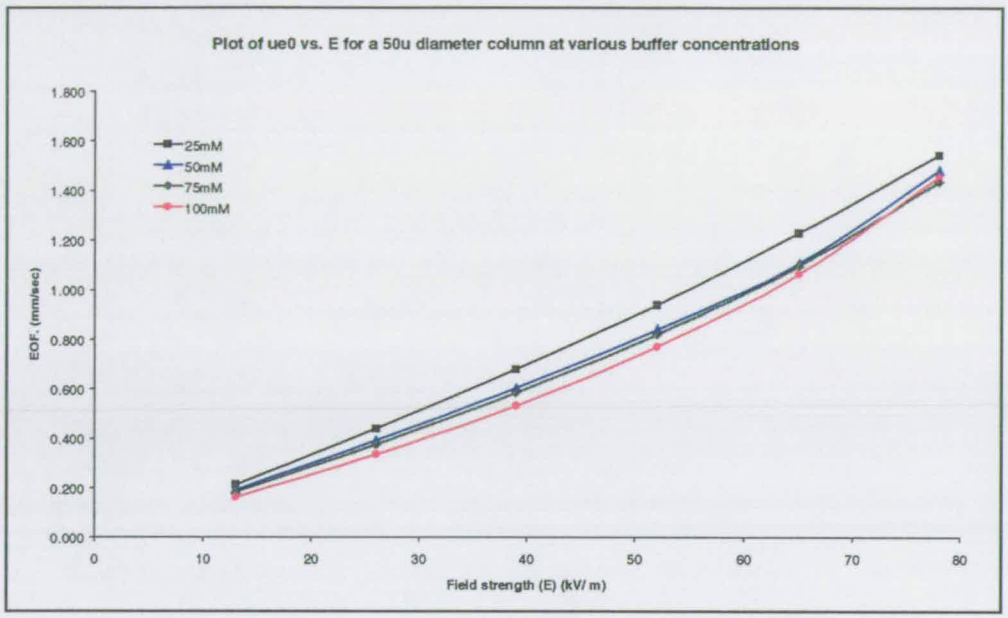

Figure 19. Plot of Current (I) vs. u for a 50μm diameter column at different buffer strengths

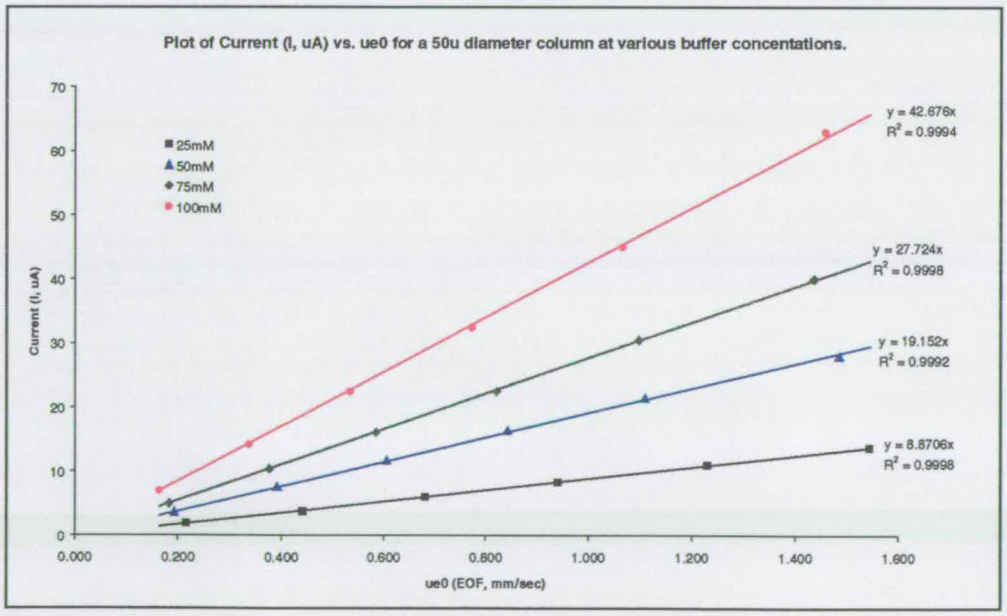

Figure 20. Plot of HETP (H) vs. E for a 100μm diameter column at different buffer strengths.

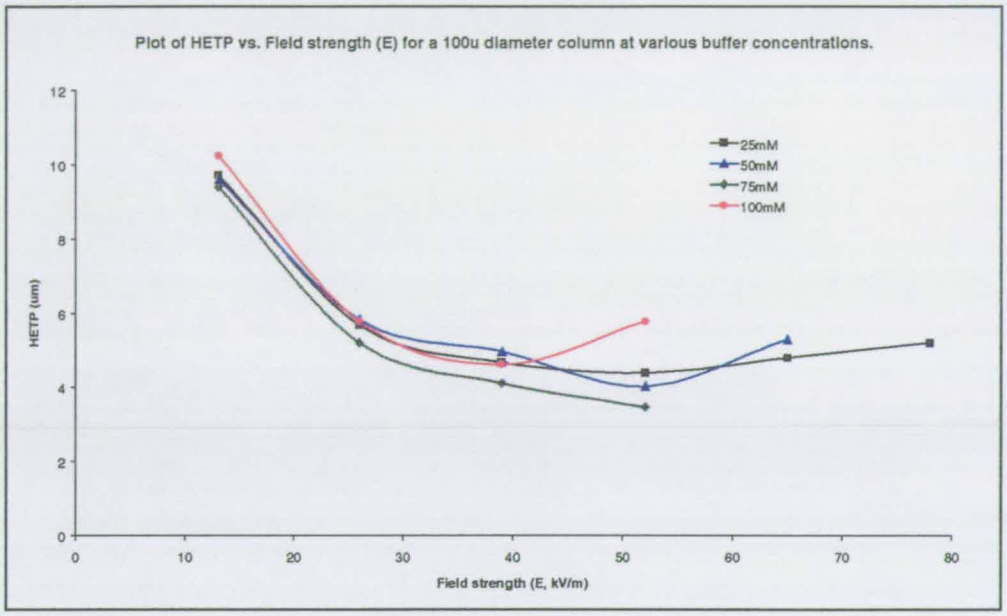

Figure 21. Plot of Current (I) vs. E for a 100μm diameter column at different buffer strengths

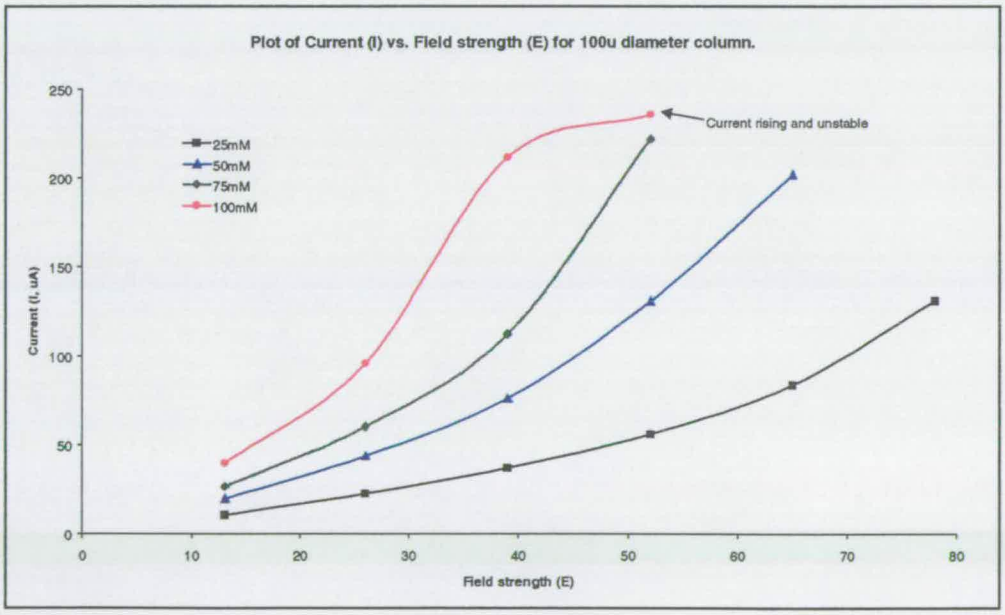

Figure 22. Plot of EOF (u) vs. E for a 100μm diameter column at different buffer strengths

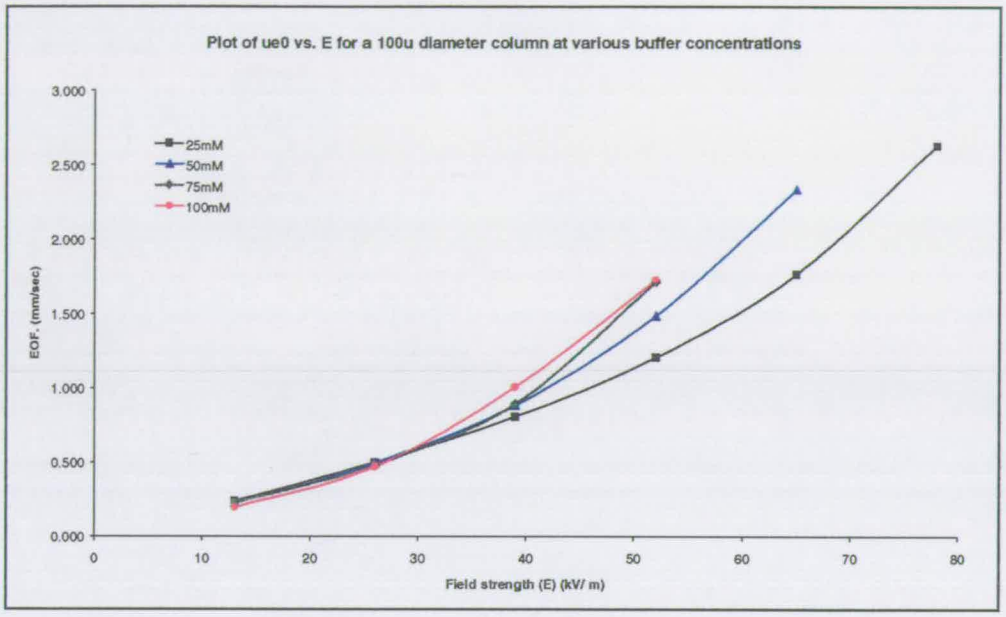

Figure 23. Plot of Current (I) vs. u for a 100μm diameter column at different buffer strengths

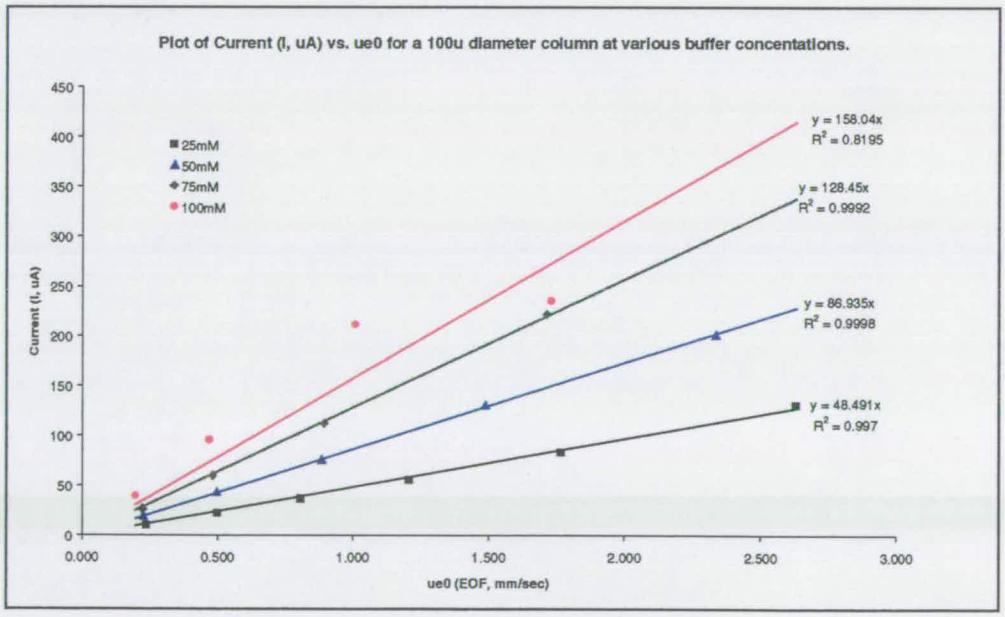

Figure 24. Plot of HETP (H) vs. E for a 150μm diameter column at different buffer strengths.

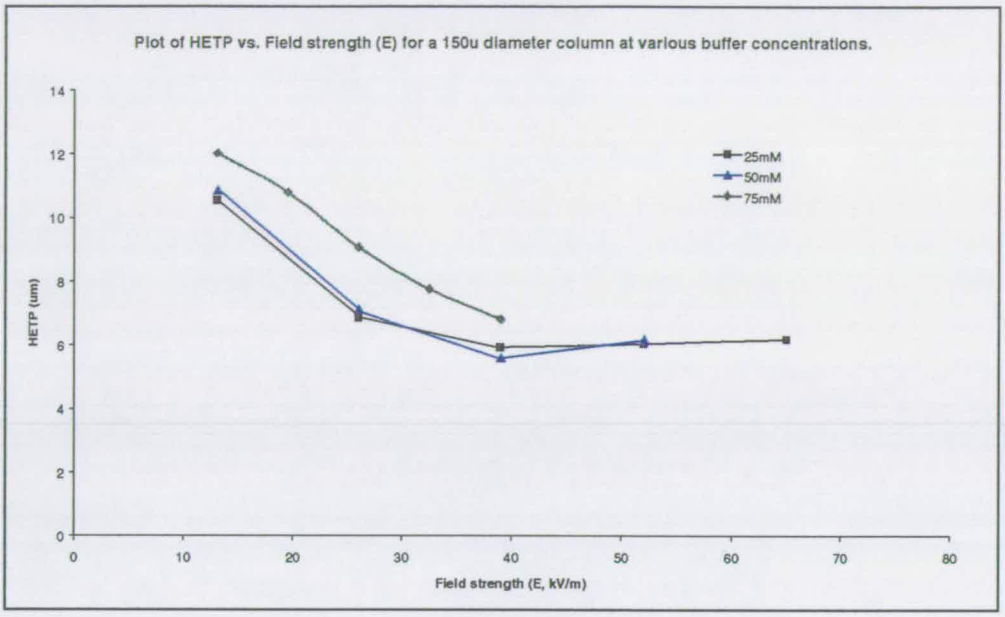

Figure 25. Plot of Current (I) vs. E for a 150μm diameter column at different buffer strengths

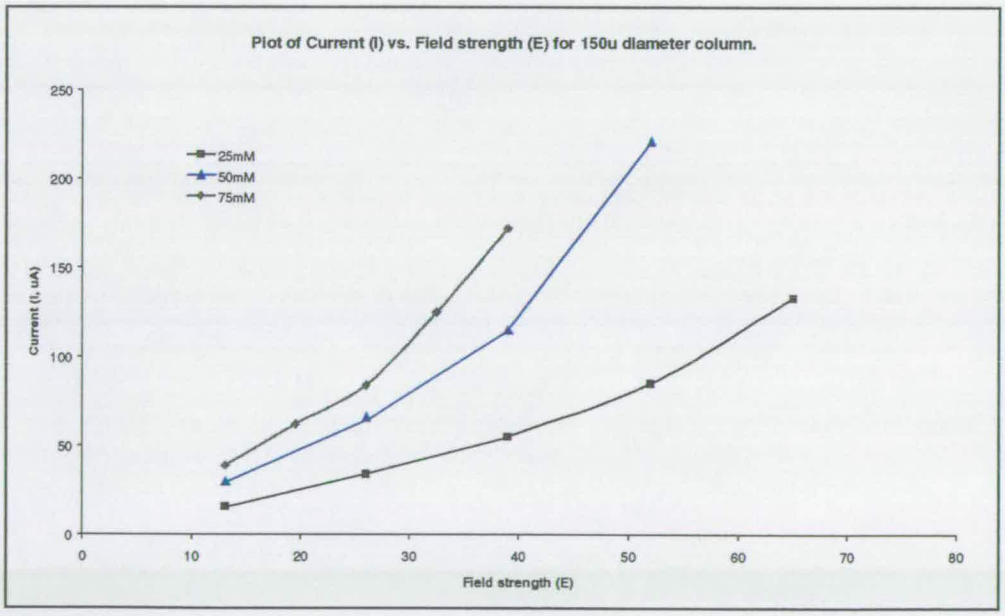

Figure 26. Plot of EOF (u) vs. E for a 150μm diameter column at different buffer strengths

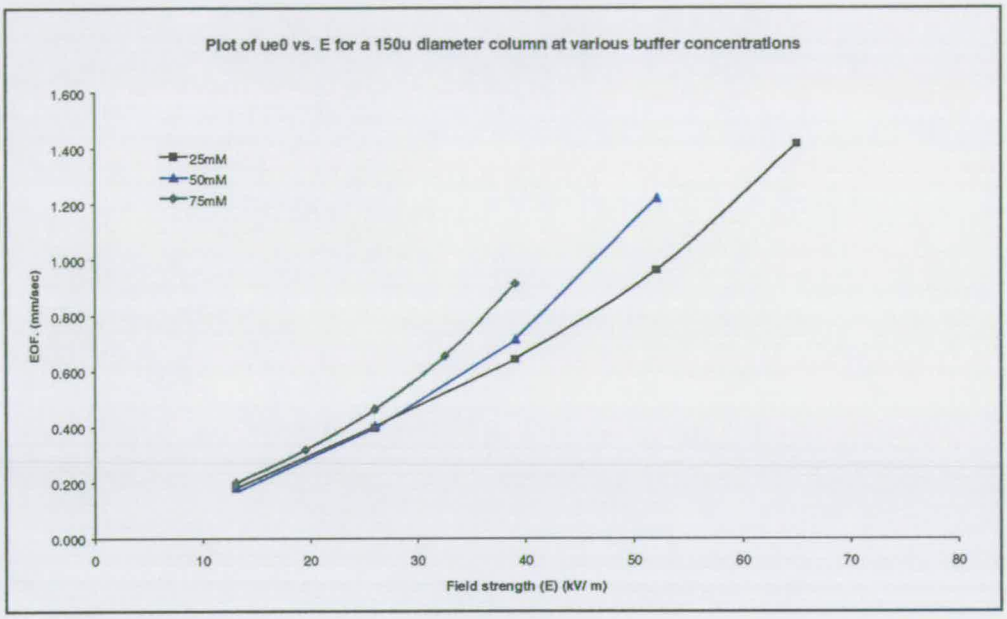

Figure 27. Plot of Current (I) vs. u for a 150μm diameter column at different buffer strengths

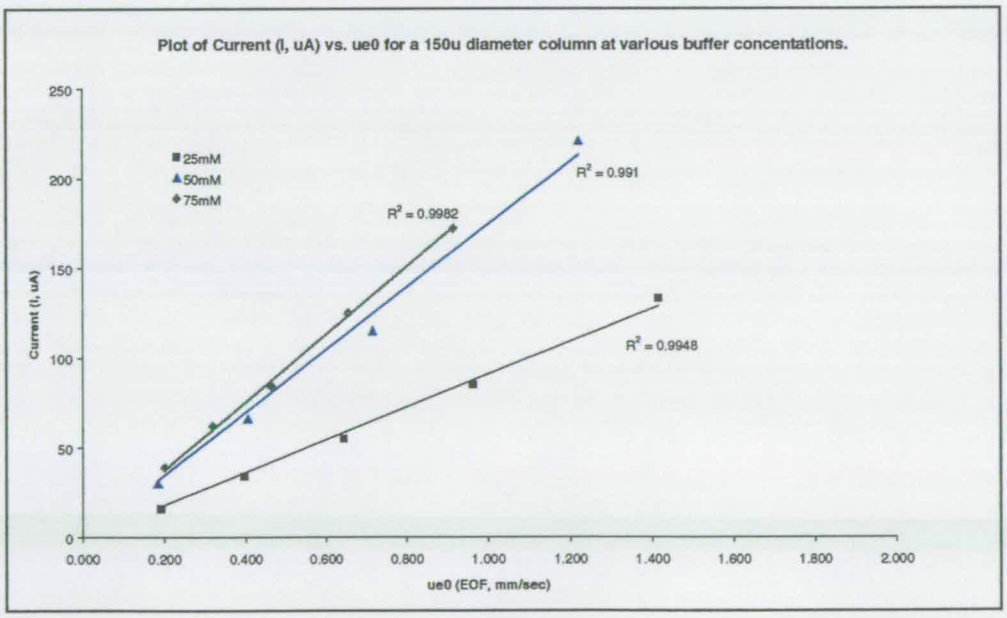

Figure 28. Plot of the viscosity of the mobile phase (at 50% ACN/H2O) with temperature.

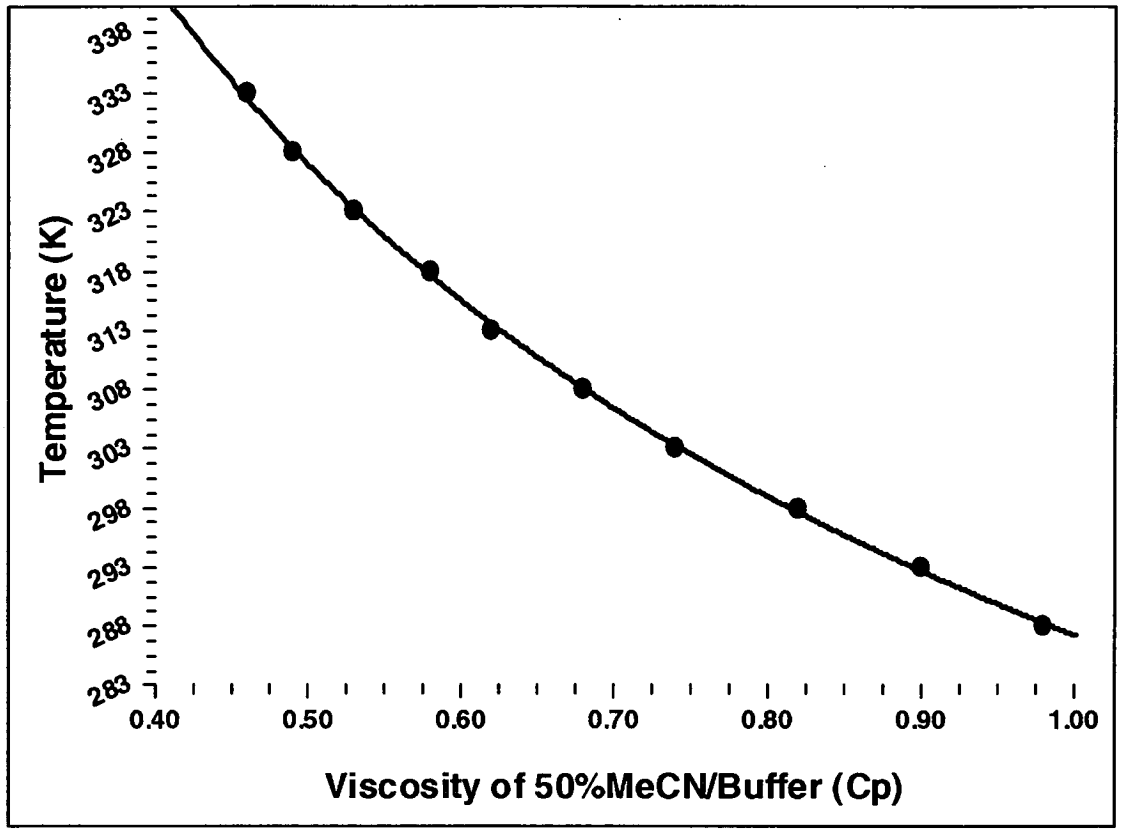

TABLE 2. Viscosity and temperature as a function of power consumed for a 50μm diameter column using 50% CH3CN / buffer.

	Experimentally Measured				*Calculated – see text*					
Buffer Strength	E (kV/m)	I (μA)	EI Wm^{-1}	EOF (mm/s)	η_A (Cp)	η_B (Cp)	T_A (^{0}C)	T_B (^{0}C)	T_{av} (^{0}C)	'Knox condition' $(d_c^3 E^3 c) \times 10^9$
	13	1.85	0.024	0.213	0.962	0.963	16.1	16.1	16.1	0.007
	26	3.8	0.098	0.440	0.933	0.937	18	17.7	17.8	0.055
25mM	39	6	0.234	0.681	0.905	0.891	19.6	20.5	20.0	0.185
	52	8.3	0.432	0.941	0.873	0.858	21.6	22.5	22.0	0.439
	65	11	0.715	1.230	0.835	0.810	23.9	25.5	24.7	0.858
	78	13.7	1.069	1.544	0.798	0.780	26.3	27.5	26.9	1.48
	13	3.7	0.048	0.193	0.985	0.973	14.7	15.5	15.1	0.013
	26	7.6	0.198	0.392	0.967	0.948	15.8	17.1	16.5	0.109
50mM	39	11.7	0.456	0.605	0.941	0.923	17.5	18.5	18.0	0.370
	52	16.4	0.853	0.842	0.902	0.878	19.8	21.3	20.1	0.878
	65	21.5	1.397	1.109	0.856	0.837	22.6	23.8	23.2	1.72
	78	28	2.184	1.484	0.768	0.772	28.3	28	28.2	2.97

	Experimentally Measured				*Calculated – see text*					
Buffer Strength	E (kV/m)	I (μA)	EI Wm^{-1}	EOF (mm/s)	η_A (Cp)	η_B (Cp)	T_A (^{0}C)	T_B (^{0}C)	T_{av} (^{0}C)	'Knox condition' $(d_c^3 E^3 c) \times 10^9$
	13	5	0.065	0.183	0.959	0.967	16.3	15.8	16.1	0.021
	26	10.4	0.270	0.377	0.932	0.934	18	17.9	18.0	0.168
75mM	39	16.1	0.628	0.585	0.900	0.901	19.9	19.9	19.9	0.556
	52	22.5	1.170	0.821	0.855	0.860	22.7	22.4	22.6	1.32
	65	30.5	1.982	1.098	0.799	0.793	26.2	26.6	26.4	2.57
	78	40	3.120	1.436	0.733	0.725	30.8	31.3	31.1	4.45
	13	7	0.091	0.164	0.970	0.973	15.7	15.5	15.6	0.027
	26	14.2	0.369	0.338	0.939	0.959	17.6	16.3	16.9	0.219
100mM	39	22.5	0.877	0.534	0.890	0.908	20.5	19.5	20.0	0.741
	52	32.5	1.690	0.773	0.821	0.838	24.8	23.7	24.2	1.75
	65	45	2.925	1.066	0.744	0.757	30	29.1	29.5	3.43
	78	63	4.914	1.458	0.653	0.649	37.3	37.6	37.4	5.93

TABLE 3. Same data for a 100μm diameter column using 50% CH3CN / buffer.

	E (kV/m)	I (μA)	EI Wm^{-1}	EOF (mm/s)	η_A (Cp)	η_B (Cp)	T_A (^{0}C)	T_B (^{0}C)	T_{av} (^{0}C)	'Knox condition' ($d_c^3 E^3 c$) x 10^9
	13	10.6	0.138	0.238	0.949	0.943	17.0	17.3	17.2	0.055
	26	22.6	0.588	0.498	0.908	0.885	19.5	20.9	20.2	0.439
25mM	39	37.1	1.447	0.806	0.841	0.808	23.5	25.6	24.5	1.48
	52	56.1	2.917	1.207	0.750	0.713	29.6	32.3	31.0	3.51
	65	83.6	5.434	1.766	0.641	0.598	38.3	42.5	40.5	6.86
	78	131	10.22	2.630	0.516	0.458	51.9	60.1	56.0	11.86
	13	19.9	0.259	0.226	0.985	0.986	14.7	14.6	14.6	0.109
	26	43.8	1.139	0.495	0.898	0.896	20.1	20.2	20.1	0.878
50mM	39	76.3	2.976	0.884	0.755	0.772	29.2	28.0	28.6	2.96
	52	131	6.812	1.487	0.598	0.599	42.5	42.3	42.4	7.03
	65	202	13.13	2.336	0.476	0.486	57.4	56.0	56.7	13.73
	13	26.7	0.347	0.224	0.996	0.920	14.0	18.7	16.3	0.164
	26	60.2	1.565	0.481	0.930	0.816	18.1	25.1	21.6	1.32
75mM	39	112.3	4.380	0.893	0.751	0.656	29.5	36.9	33.2	4.45
	52	222	11.54	1.713	0.522	0.443	51.1	62.4	56.7	10.54
	13	40	0.520	0.197	0.856	0.923	22.6	18.6	20.6	0.219
	26	96	2.496	0.469	0.720	0.769	31.7	28.2	29.9	1.76
100mM	39	212	8.269	1.009	0.502	0.522	53.7	51.1	52.4	5.93
	52	236	**12.27**	1.731	0.390	**0.626**	71.3	**39.7**	**71.3**	**14.06**

TABLE 4. Viscosity drop and temperature rise as a function of power consumed for a 150μm diameter column using 50% CH3CN / buffer. Buffer strength shown in table.

	E (kV/m)	I (μA)	EI Wm^{-1}	EOF (mm/s)	η_A (Cp)	η_B (Cp)	T_A (^{0}C)	T_B (^{0}C)	T_{av} (^{0}C)	'Knox condition' $(d_c^3 E^3 c) \times 10^9$
	13	16	0.208	0.191	0.982	0.983	14.9	14.8	14.8	0.185
	26	34	0.884	0.397	0.942	0.925	17.4	18.4	17.9	1.48
25mM	39	55	2.145	0.643	0.873	0.858	21.6	22.5	22.0	5.00
	52	85	4.420	0.962	0.779	0.740	27.6	30.2	28.9	11.9
	65	133	8.645	1.414	0.662	0.591	36.4	43.2	40.8	23.2
	13	30	0.390	0.183	0.918	0.988	18.9	14.5	16.7	0.370
	26	66	1.716	0.405	0.829	0.898	24.3	20.1	22.2	2.96
50mM	39	115	4.485	0.715	0.703	0.773	33.0	27.9	30.4	10.0
	52	221	11.49	1.220	0.550	0.536	47.8	49.4	48.6	23.7
	13	39	0.507	0.200	0.917	1.000	18.9	13.7	16.3	0.556
	19.5	62	1.209	0.318	0.864	0.944	22.1	17.3	19.7	1.87
75mM	26	84	2.184	0.464	0.790	0.929	26.8	18.2	22.5	4.44
	32.5	125	4.062	0.655	0.700	0.780	33.3	27.5	30.4	8.68
	39	172	6.708	0.914	0.601	0.680	42.1	34.9	38.5	15.0

References for chapter 7

[1] J.H.Knox, *Chromatographia,* 26, (1988) 329-37.

[2] J.H.Knox, K.A.McCormack, *Chromatographia,* , 38(3-4), (1994) 207-14.

[3] J.H.Knox, K.A.McCormack, *Chromatographia,* , 38(3-4), (1994) 215-21

[4] Sir G. I. Taylor, *Proc. Roy. Soc.(Lond)* A219, (1953) 186

[5] H.Colin, J. C. Diez-Masa, G.Guiochon, T.Czajkowska, I.Miedziak, *J.Chromatogr.* 167 (1978) 41-65.

Chapter 8 The use of pressure assisted flow systems for CEC operation (pCEC)

8.1 Introduction

CEC undoubtedly offers very substantial improvements to some aspects of the way in which we currently perform miniaturised chromatography. Work shown in the two previous chapters in particular, highlights clearly some of the restrictions in the use of the technique. It is important to maximise the 'gains' available by using CEC to the best practice whenever possible. However, it is also the case that some of the beneficial aspects of CEC are achieved at the expense of practical robustness, at least at the present time. As we are using electrically driven flows it is always a requirement to maintain electrical conductivity across the column. Practically this means maintaining a well-solvated packed bed, and ensuring that the open tube section is full of mobile phase. If this is not the case at any time, it is likely that flow will be lost. If this is not recognised immediately, remedial action will almost certainly involve removal of the column for reconditioning with fresh mobile phase, via connection to a high pressure pump. This is an unacceptable interruption if it is other than a rare occurrence. Additionally, it is more than likely to result in a broken column. Causes of flow loss can be as trivial as solvent evaporation from the column end, while it is being moved from elution reservoir to sample reservoir and back. I suspect that this is the most common reason for first-timers not achieving any results from CEC and probably dismissing it as 'too difficult' to use.

8.2 Pressure-assisted or pure EOF?

So, in principle, just being able to pressurise the column whilst it is mounted in the instrument would be a significant improvement. This would allow recovery of flow loss without removal of the column. Going one stage further and using the option of an alternative pressure flow or a variable amount of pressure assisted flow would seem, at first glance, like a backward step. This would certainly produce an inferior flow profile and reduce chromatographic efficiencies. However, if the total contribution of pressure flow, compared to the overall EOF, was small, then the effect on performance would be tolerable. More importantly perhaps, the small, constant flow contribution from the pressure would keep the column 'wet' and maintain flow consistency. This would substantially improve reliability and raise confidence that once a column was installed it would continue to perform. At higher pressure contributions to the total flow, accepting some extra performance drop, it would still be very useful to study the often more predictable outcome of a separation using predominantly pressure driven flows. Pressure and EOF could also be used together to promote higher, combined linear flow rates. The application of the electric field would of course affect charged solutes during the separation. If necessary, it would also be possible to apply a negative field to affect the relative migration rate of certain charged species, while an overall pressure flow kept everything moving towards the detector. The possibilities exist to combine the operation of the column with either flow type and even a combination of both. This effectively realises the opportunity to perform capillary LC, CEC or both on a single instrument platform. If the design of the pressure flow option is carefully considered, it

should also be possible to change the composition of mobile phase during a separation, making gradient elution in either mode possible. Having used CEC a considerable amount during the work shown in this thesis, and being aware of the wider practice of liquid based separations and their limitations, I believe this to be the most practical current use of electrically driven flows.

As an illustration of the state of the art for CEC, this chapter will contain data and chromatograms obtained from the use of a prototype design instrument in collaboration with Agilent (ex Hewlett Packard). This instrument is a clever modification of an existing CE instrument. The modified parts are shown in Figure 1. It uses different length concentric electrodes (Fig 1(1)) to allow delivery and removal of a variable composition solvent to the electrolyte vial during application of the electric field. By appropriate choice of outlet capillary (2) dimensions and bulk flow rates, a significant pressure can be generated in the electrolyte vial. This allows the mode of flow delivery to be chosen as pumped flow only (no field applied), EOF only (no significant flow rate into the vial, but field applied) or a combination of both. As the pumped flow is delivered on a bulk scale from a binary channel HPLC pump, and reduced down to capillary requirements via inbuilt flow-splitting, gradient elution can be performed in any mode. In pumped flow mode we are effectively using constant pressure flow, due to the pressure generated in the 'seal vial' as a result of a fixed resistance 'restrictor' capillary placed at the solvent outlet (this acting as an inbuilt flow–splitter). In this way, the higher the bulk flow entering the vial, the higher the constant pressure generated for flow delivery. Normally, sample is introduced

electrokinetically as in conventional CEC, but an LC sample valve was added to this instrument to enable pressure injections as well.

8.3 Experiments in pure and combined flow modes.

8.3.1 Experimental

A 21cm x 100um i.d CEC column packed with 3μm C18 bonded silica gel was used for all the work described. An isocratic mobile phase of 70% MeCN/ 30% 20mM TRIS buffer was delivered from an HP1100 pump to the inlet seal vial. The test mix used consisted of 1.Thiourea (EOF marker), 2. Benzamide, 3. Anisole, 4. Benzophenone and 5. Biphenyl, all at a concentration of 1mg/ml each.

Four separate experiments were performed:-

Pure Pressure drive

The HP1100 pump bulk flow rate was set from 0.5 – 4ml/min to deliver a driving pressure of 33-326 bar.

Pure Electrodrive

Voltages of 5 –30kV were applied across the column. The pump flow rate was set to 0.15ml/min to give a nominal10 bar pressure assistance. This was considered to produce a negligible effect on the flow compared to the electroosmotic flow.

Constant Pressure with Electrodrive assistance

The HP110 flow rate was set to 3.5ml/min to deliver a constant seal vial pressure of 285 bar. A range of voltages (5-30kV) were additionally applied across the column

Constant Voltage with Pressure Assistance

A constant voltage of 25kV was applied across the column. A range of flow rates were delivered from the HP1100 pump to give additional pressure assistance of between 10 and 326 bar

The test mix was injected electrokinetically (10kV for 5s) and analysed three times under each set of conditions.

8.4 Results

For each experiment the following parameters were calculated: -

- Mobile phase Linear Velocity (mm/sec) based on the retention time of Thiourea
- Volumetric flow rate (nl/min)
- Number of Theoretical plates on column for peak 3
- Reduced velocity (v)
- Reduced plate height (h) for peak 3

Tables 1-4 show all the results obtained. The conclusions from each individual experiment are discussed below.

Table 8.1. Pressure drive flow only

Pressure across column -(bar)	Flow from Pump ml/min	Retention time of Thiourea (t_o) (min)	Linear Velocity (mm/sec)	Volumetric Flow rate nl/min	Plates on column of Peak 3	Reduced Velocity ν	Reduced plate Height (h) Peak 3
326	4	3.32	1.05	253.32	27364	3.24	2.62
285	3.5	3.45	1.01	243.58	26756	3.12	2.68
236	3	4.56	0.767	184.21	26275	2.36	2.73
190	2.5	5.46	0.641	153.93	24607	1.97	2.91
145	2	7.16	0.489	117.25	21516	1.50	3.33
103	1.5	9.95	0.352	84.42	17218	1.08	4.16
66	1	15.31	0.229	54.86	12270	0.70	5.84
33	0.5	31.06	0.113	27.05	6572	0.35	10.90

Table 8.2. Electrodrive only

Voltage across column (kV)	Retention time of Thiourea (t_o)	Linear Velocity (mm/sec)	Volumetric Flow rate(nl/min)	Plates on column of Peak 3	Reduced Velocity ν	Reduced plate Height (h) Peak 3
30	1.183	2.96	710.06	31007	9.09	2.31
25	1.511	2.32	555.92	33867	7.11	2.12
20	2.03	1.72	413.39	35526	5.29	2.02
15	2.89	1.21	290.46	35441	3.72	2.02
10	4.78	0.732	175.77	30293	2.25	2.17
5	10.67	0.328	78.75	17116	1.01	4.19

Table 8.3. Constant 25kV with variable pressure assistance.

Voltage across column (kV)	Flow from Pump (ml/min)	Pressure Across column (bar)	Retention time of Thiourea (t_o)	Linear Velocity (mm/sec)	Volumetric Flow rate(nl/min)	Plates on column of Peak 3	Reduced Velocity ν	Reduced plate Height (h) Peak 3
25	0.15	10	1.9235	1.82	436.70	28526	5.59	2.51
25	0.5	33	1.64	2.13	512.20	27520	6.55	2.60
25	1	66	1.53	2.29	549.02	27689	7.03	2.59
25	1.5	103	1.45	2.41	580.91	27335	7.43	2.62
25	2	145	1.37	2.55	612.69	27031	7.84	2.65
25	2.5	190	1.30	2.69	646.15	26793	8.27	2.67
25	3	236	1.24	2.82	679.61	26065	8.70	2.75
25	3.5	285	1.175	2.98	714.89	25000	9.15	2.87
25	4	326	1.125	3.11	746.67	24134	9.56	2.97

Table 8.4. Constant pressure flow (285bar) with variable voltage assistance.

Voltage across column (kV)	Flow from Pump (ml/min)	Pressure Across column (bar)	Retention time of Thiourea (t_o)	Linear Velocity (mm/sec)	Volumetric Flow rate(nl/min)	Plates on column of Peak 3	Reduced Velocity	Reduced plate Height (h) Peak 3
0	3.5	285	3.45	1.01	243.48	26756	3.12	2.68
5	3.5	285	2.98	1.17	281.93	27629	3.61	2.59
10	3.5	285	2.34	1.50	358.82	28732	4.59	2.49
15	3.5	285	1.82	1.92	460.65	27603	5.90	2.60
20	3.5	285	1.46	2.40	577.32	26703	7.39	2.68

8.4.1 Pressure drive only (Table 8.1)

The maximum linear velocity obtained was 1.1mm/sec. A bulk flow rate of 4ml/min from the HP1100 pump gave a vial pressure of 326 bar. It was thought prudent that a maximum pressure of 285bar (@3.5ml/min) was a sensible working limit. Use of higher pressures caused problems due to leaking of the seal vial.

Good performance was obtained using the column in effectively a micro-LC mode. The average efficiency of peaks 3,4 and 5 was 128,00 plates per metre, or a reduced plate height of 2.84. Figure 2 shows a plot of reduced plate height vs. reduced velocity. It is possible that the minimum plate height value has not quite been reached. The ability to produce higher linear flow velocities could enhance the performance of the system in pressure drive, and significantly reduce analysis times, leading to higher sample throughputs.

The dependence of linear velocity upon pressure is given by the flow equation:

$$u = \Delta p \, d_p^2/(\phi \eta L)$$

The pressure resistance factor, ϕ, is normally around 1000 for a bed packed with porous silica spheres. ϕ is readily calculated from the data of Table 8.1.

Assuming L = 0.21 m, $d_p = 3\ 10^{-6}$m, $\eta = 10^{-3}$ SI units, 1 bar = $1.013\ 10^5$ n/m^2, and taking $u = L/t_o$ it is readily shown that

$$\phi = 1.23 \times \Delta p\ (\text{bar}) \times t_o\ (\text{min})$$

The values so obtained run from 1209 to 1331 with a mean of 1273. This is slightly higher than expected, but the value of Δp will include any system derived pressure contributions.

8.4.2 Electrodrive only (CEC mode)

In CEC mode reduced plate heights of 2-2.2 were obtained when applying a voltage of 20kV or 25kV. This gave an average peak efficiency of 165,000 plates per metre, which is not a particularly high value for CEC, although this is by no means optimised. Figure 3 shows a plot of reduced plate height vs. reduced velocity for electrodrive only. It can be seen that the lowest reduced plate heights are achieved at a reduced velocity of between 3 and 7. This corresponds to a linear flow velocity of 1.8-2.4mm/sec when applying between 20-25kV. At 30kV the linear velocity increases to 3mm/sec and this would appear to be too high leading to an increase in the reduced plate height. As expected, overall the column gave a better performance using electrodrive than pressure drive. Figure 4 shows a comparison plot of reduced plate

height vs. reduced velocity for Peak 3 for both modes of operation. Figure 5 shows the chromatogram of the test mix using electrodrive and pressure drive, this illustrates well the improvement in speed of analysis using EOF.

8.4.3 Constant Pressure with Electrodrive assistance

Figure 6 shows a plot of reduced plate height vs. reduced velocity for 5-30kV voltage assistance for the column under constant system pressure of 285bar (3.5ml/min from pump). The optimum performance is achieved with a voltage assistance of 10kV, giving average peak efficiencies of 130,556 plates per metre and a reduced plate height of 2.8. The use of voltage assistance has increased the linear velocity to 1.5mm/sec. This is composed of 1mm/sec from the pressure drive and approximately 0.5mm/sec from the voltage assistance. At higher voltages the reduced velocity increases above 7 and a corresponding loss in performance is observed. Overall the voltage assistance slightly improves the performance, but more importantly, offers the possibility to manipulate both the separation of charged species during an analysis, and substantially increase the linear flow rate.

8.4.4 Constant Voltage with Pressure Assistance

Figure 7 shows a Plot of Reduced plate Height (h) vs. Reduced velocity (v) for Constant voltage @ 25kV (1.9mm/sec) and varying Pressure assistance (33 - 326 bar). The

reduced plate height remains fairly constant up to a pressure assistance of 145bar (2ml/min from pump). Under these conditions the mobile phase linear velocity through the column is still dominated by the electrodrive. The contribution from the pressure drive at 145bar is only 0.5mm/sec. As the pressure assistance increases to 1.1mm/sec at 4ml/min the performance decreases. This also corresponds to a reduced velocity of higher than 7. It would appear that pressure assistance can be used, without significant loss in performance, as long as the EOF forms the main contribution to the total linear velocity.

8.4.5 Electrokinetic vs. Pressure injection

Figure 8 shows the analysis of the test mix after making a) a pressure injection via the Valco HPLC-type valve and b) an electrokinetic injection. The column was run in pressure drive mode at a system pressure of 285 bar. There is no significant difference between the chromatographic performance obtained. It should be noted with pressure injection, due to the flow being split after injection, less sample is injected onto the column than when using electro-injection and hence the peak areas are smaller. However the relative peak areas are the same. Overall this illustrates that it is straightforward to configure this system to perform pressure injection. This may prove useful if samples cannot easily be electrokinetically injected, for example neutral solutes at conditions of very low EOF. It is especially important where it is possible that some components of the sample are experiencing bias due to different electrophoretic

mobilities during electrokinetic injection (ie. more highly charged components will apparently be 'enriched' in the solute mixture.)

8.4.6 Gradient elution mode.

Until now we have considered only isocratic CEC (ie. CEC with constant mobile phase composition throughout run). In HPLC Isocratic elution methods are generally used for simplicity, and when the components requiring separation are similar in polarity. This is generally true only when a compound is well characterised and no unexpected components are likely to be present. In the real world, where new products are being developed, this is rarely true. It is much more likely that, aside from the target compound, there are numerous other components in the sample. In these situations we need to maximise our chances that we elute everything that went onto the separation column. Otherwise we are not confident that we are seeing a representative 'snapshot' of our sample quality. The accepted best way to do this is to change the composition of the mobile phase during analysis, from low to high elution strength, and elute components in order of increasing hydrophobicity (for reverse phase mode). This allows a wide range of compound polarities to be eluted in the same analysis. However, it also adds to the sophistication of the instrumental set-up and creates extra problems. Nevertheless, it is such a powerful and successful mode of analysis that the extra complications are relatively unimportant. For CEC to offer tangible benefits to the broad base of chromatographers in different industries, it must at least demonstrate the same capabilities as they already take for granted when using HPLC.

Using gradient elution, injected solutes generally enter the column under low elution strength conditions, ie. low organic solvent and high aqueous composition. This encourages adsorption into the stationary phase. The principle of separation is based on selective desorption of each solute component, during the progression of the organic solvent gradient. Therefore the more polar compounds elute early in the gradient, followed by increasingly hydrophobic components. Each individual component is probably only undergoing conventional partitioning into the stationary phase over a narrow range of organic solvent change. The objective is actually to desorb and elute the prior component before the following one starts to desorb. While this will never be as selective a separation for components of similar polarity as isocratic operation, it is more applicable to a much wider range of samples. So much so that it is common in modern industrial companies to use mainly 'generic' gradient methods as a first try for analysing literally everything. Consequently, CEC again must compete with the existing best practice in HPLC and offer at least the same benefits.

8.4.6.1 Pressure driven gradients.

The prototype instrument has a capability to perform gradient elution CEC. This can be performed in pure CEC mode , with no pressure assistance, or with chosen levels of pressure assistance. With no pressure assistance it is known that we could run into significant stability and robustness issues. So for the work shown in this chapter there is always at least 1ml/ min bulk flow rate going into the split, giving a constant seal vial pressure of about 65-90 bar, depending on solvent viscosity throughout the gradient.

Under comparable conditions to these, this would represent no greater than a 10% contribution from the pressure derived flow. It was felt that this would not cause significant performance losses.

It is important to confirm that any gradient mode of analysis has a reproducibly delivered gradient. However, it is not easy, or practical to measure the actual composition of eluent leaving the column. In a split-type system like the seal vial principle used here, the pressure change seen throughout the gradient is a result of the resistance experienced by the waste flow leaving the vial through the outlet or restrictor capillary. There is obviously some pressure due to the small amount of flow going through the column, but it is not possible to resolve it into individual contributions. Therefore we have to rely on spiking the organic solvent with a UV absorbing compound (acetone @ 280nm) and monitoring the progression of the gradient through the column using the uv detector to monitor the outlet composition. This is critical to appreciating the most relevant and useful way to induce the flow, such that reproducible and preferably rapid gradients are made. A number of tactics were attempted to generate the required flow rates inside the separation column so not too steep a gradient was achieved. If this happens then all components tend to elute together. What is needed is a continuous, smooth change in solvent composition giving a steadily increasing 'elution wave' of solvent moving through the column. Mixing effects due to excessive dead volumes, or delays in gradient onset due to excessive dwell volumes, all contribute to lowering the reproducibility of the gradient delivery. Figure 9 shows the gradient profile obtained when purely pressure drive was attempted at a bulk flow of 3ml/min. The flow

rate through the column is too slow and so the entire solvent gradient, being delivered as a bulk flow past the column end with a small amount going up the column, changes over a small length of column and is delivered as almost a step change The only option to smooth this effect out is to make the compositional changes over much longer time periods. This only prolongs the analysis time. Changing the gradient in step changes, with bigger delays between changes as shown in Figure 10, emphasises the improvements in profile, but also the unacceptably long wait to reach a stable state. Also, it can be seen that at the change thresholds strange 'mixing' effects often occur that are surprisingly reproducible but not desirable.

8.4.6.2 CEC-driven gradients

With electrically driven flows, as we have already seen earlier in this chapter, much higher induced flows are possible without the restriction of back pressure. This is a very important point in delivering gradient profiles reproducibly. The linear gradient (the most widely used and useful method) shown in Figure 11 is generated using an applied voltage of 25kV with a bulk flow pressure assistance of 1 ml/ min (@ 80 bar). The profile is excellent, indeed better than any pressure created profile. It is also reproducible as the following Figure 12 of four overlaid gradients demonstrates. This is possible because the EOF sweeps the gradient through the column much more rapidly and with little mixing losses. The analysis of a gradient test mixture widely used for quality checking HPLC gradient methods is shown in Figure 13. The peaks are very well resolved and average peak widths at the base are about 7 seconds for the first few

peaks and about 4 seconds for all peaks after peak 4. This offers the potential for huge peak capacity separations for complex mixtures, where in favourable cases typically 10-12 peaks per minute of chromatogram are obtainable. These applications are only just starting to be properly explored and dedicated instrumentation is still not properly available, but the separation of peptides shown in Figure 14 gives a glimpse of what is going to be possible.

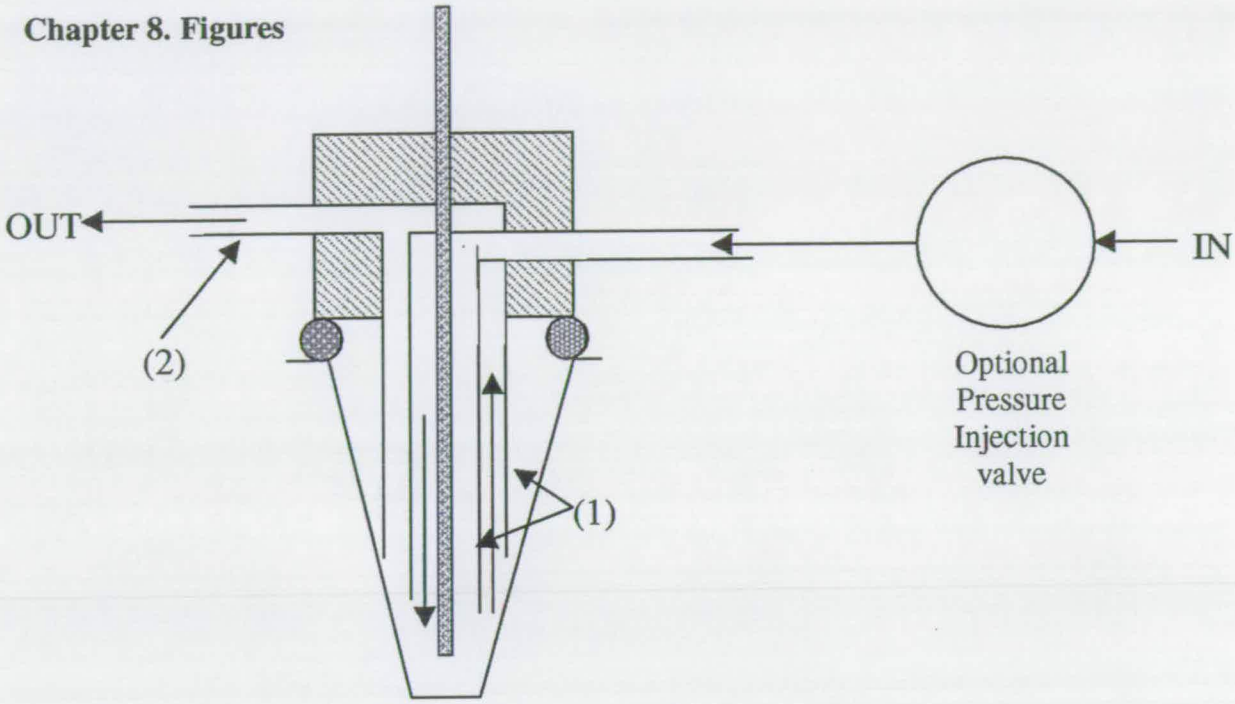

Figure 1. Schematic diagram of the inlet vial modifications to the CEChrom instrument.

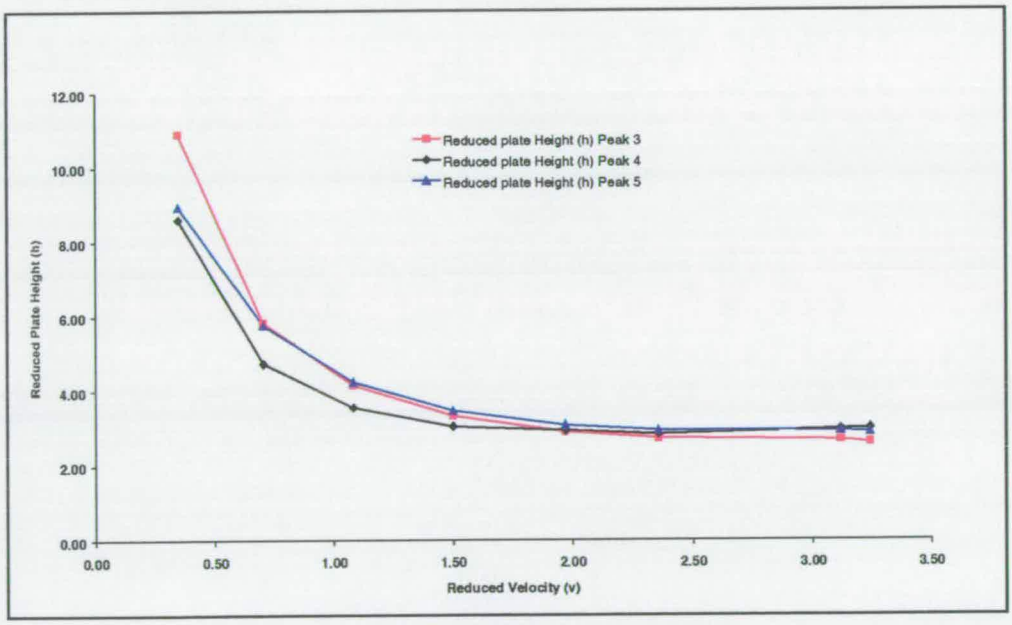

Figure 2. Plot Reduced plate Height (h) vs. Reduced velocity (v) for Pressure drive

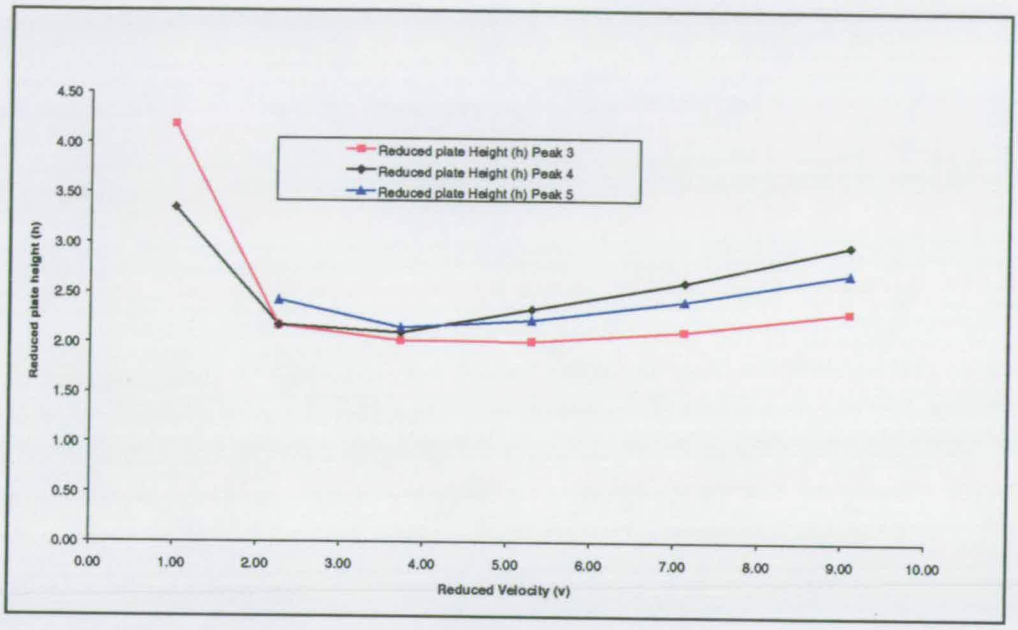

Figure 3. Plot of Reduced plate Height (h) vs. Reduced velocity (v) for EOF

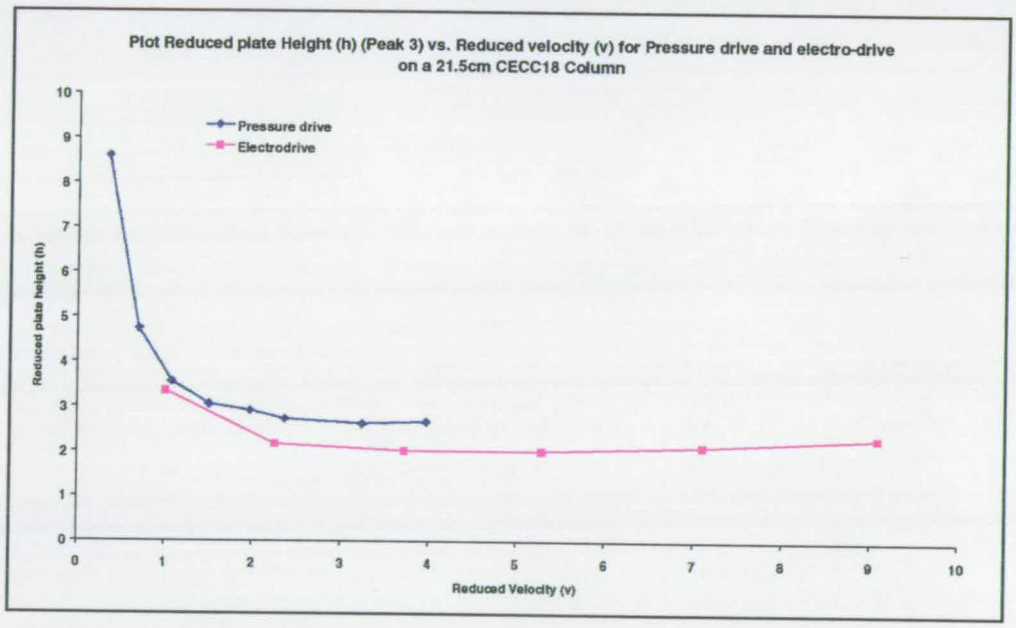

Figure 4. Comparison plot of plate curves for EOF versus pressure drive.

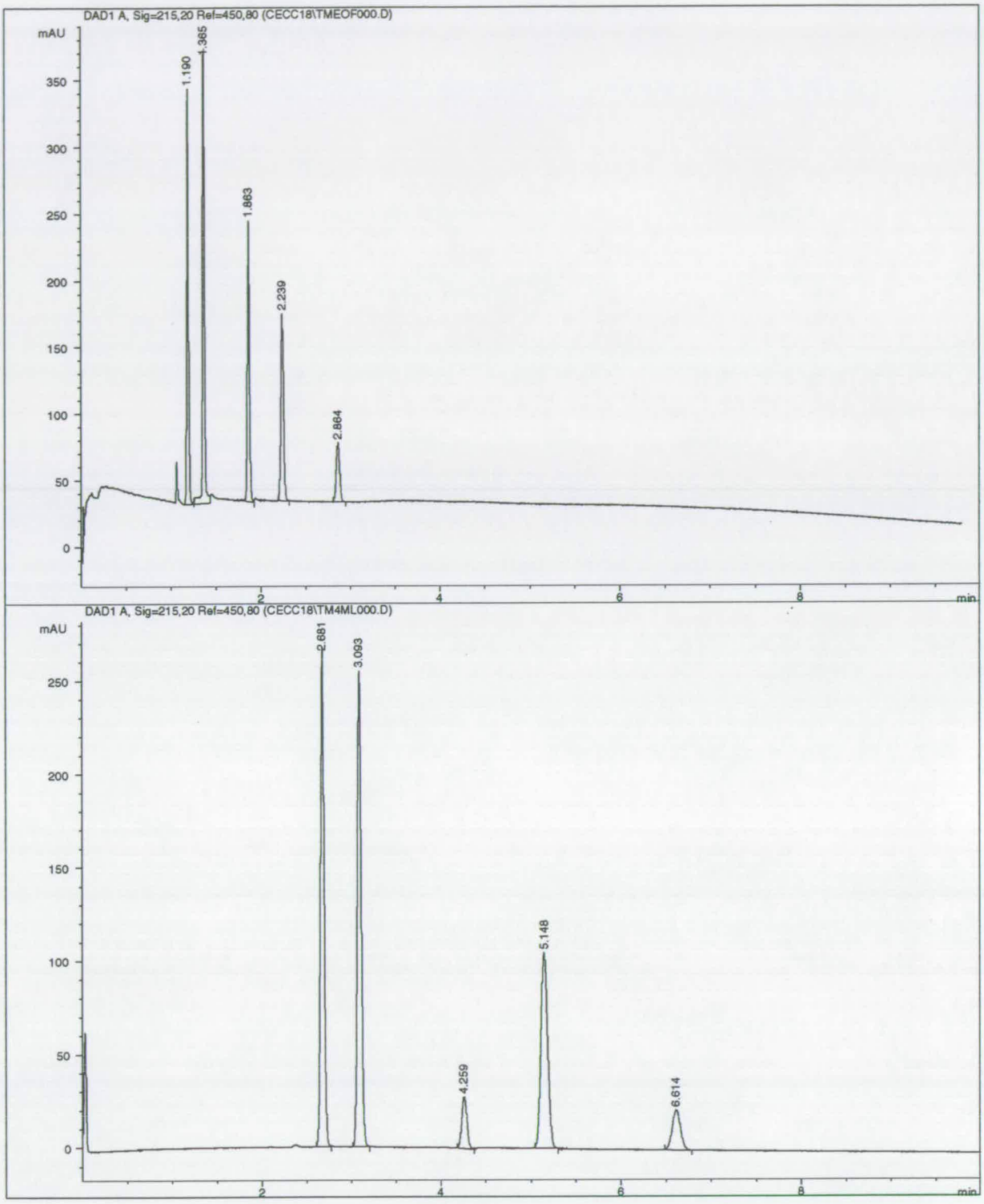

Figure 5. Comparison of chromatograms obtained by EOF(top) and pressure.

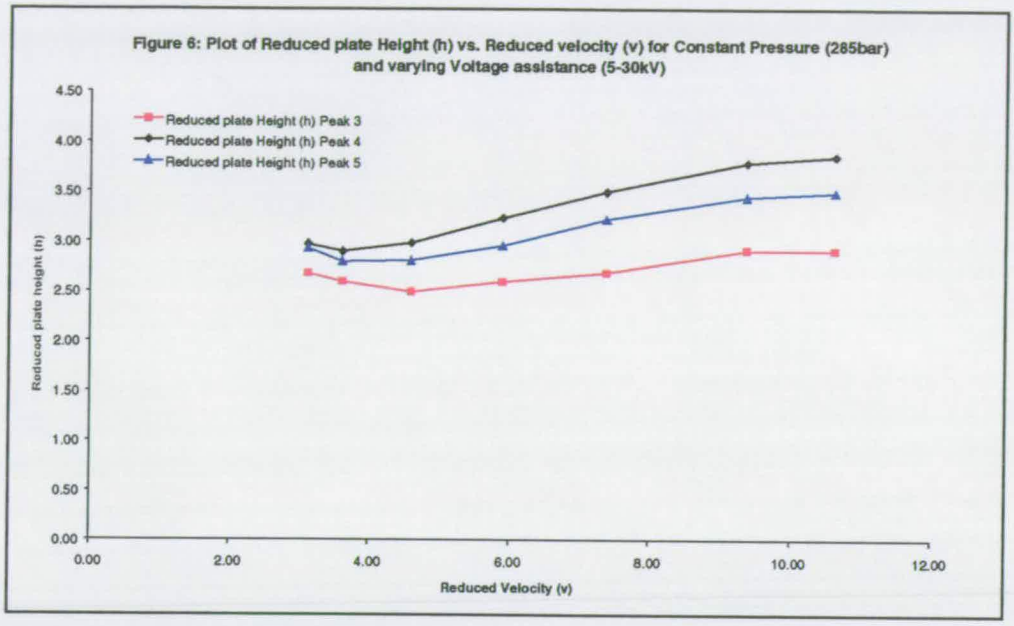

Figure 6. Plate curve for constant pressure (285bar) flow with varying EOF assistance.

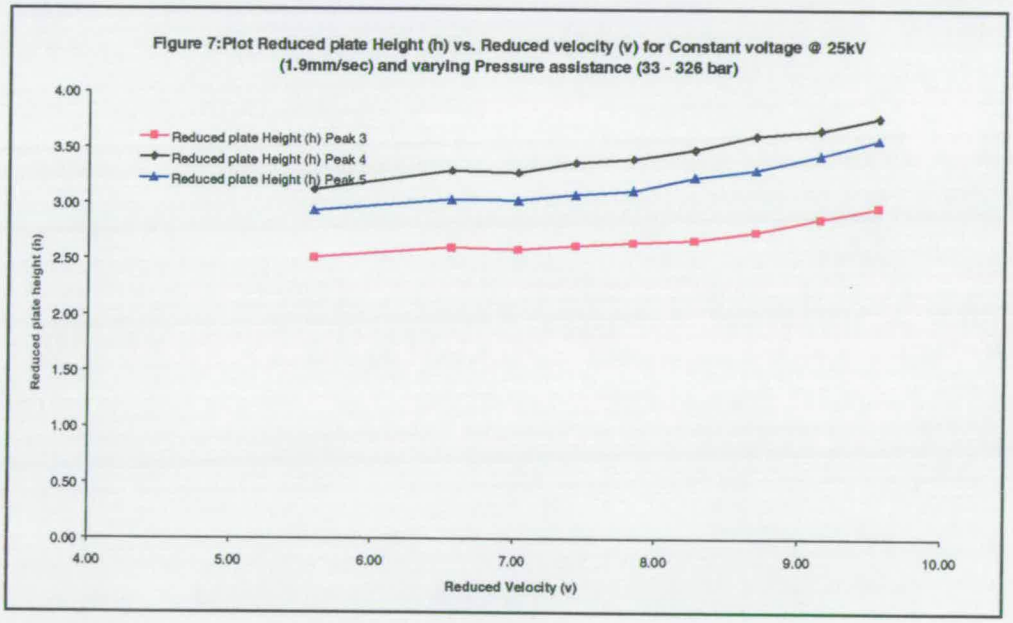

Figure 7. Plate curve for constant EOF (25kV) with varying pressure assistance.

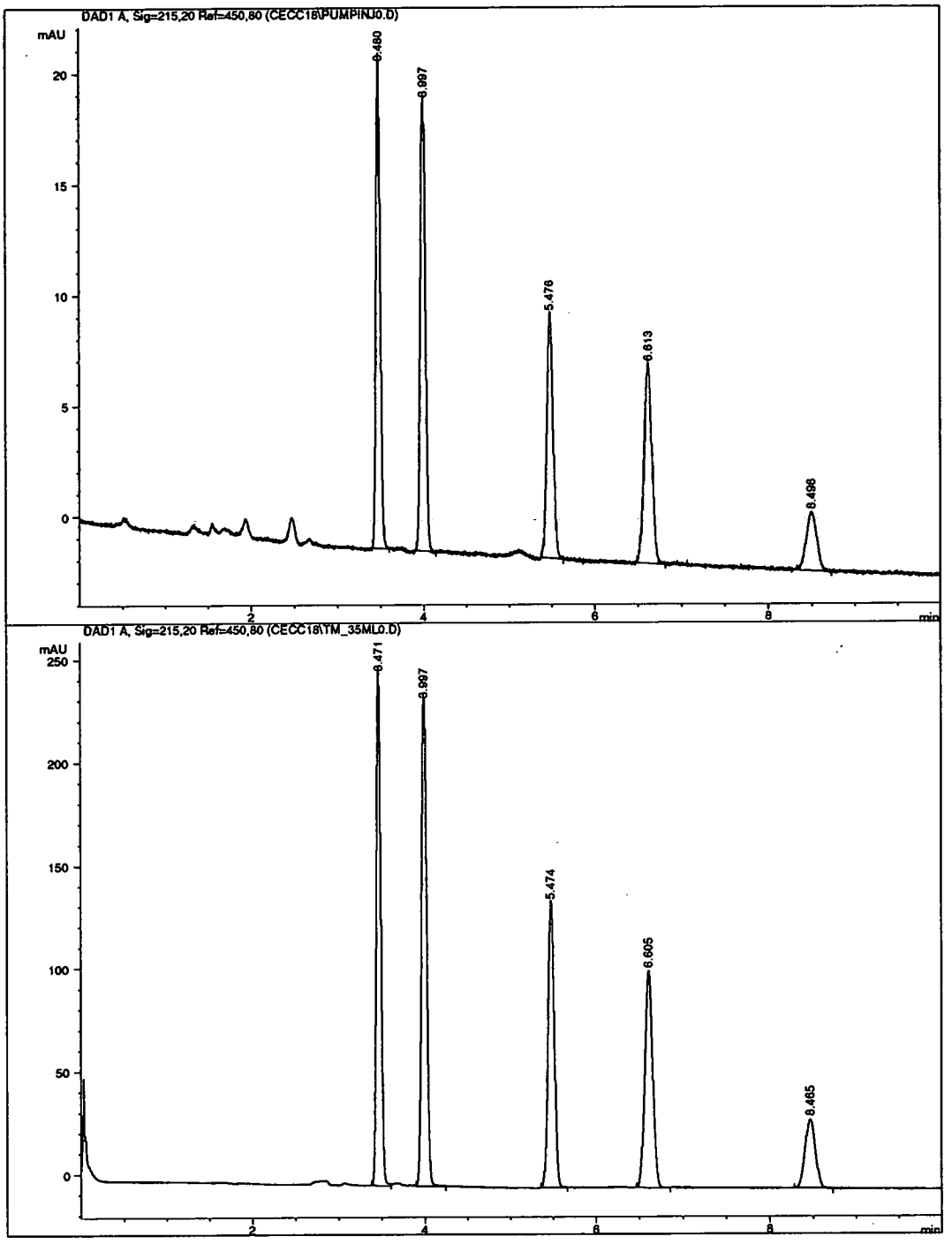

Figure 8. Comparison of Pressure (top) versus Electrokinetic injection for same sample with pressure driven flow.

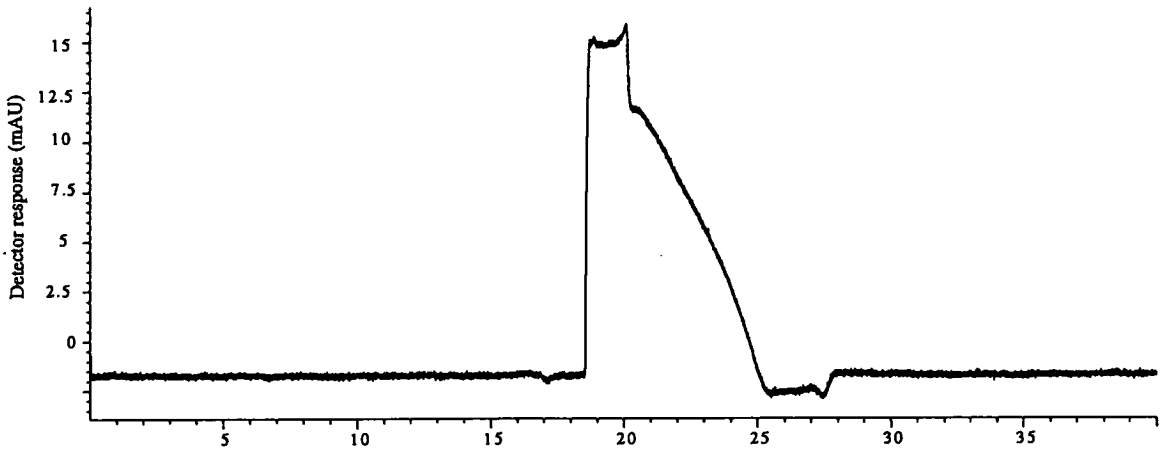

Figure 9. The gradient profile obtained from acetone-spiked acetonitrile when attempted using pressure drive only. Linear gradient change as below.
Chromatographic parameters : Capillary : 100μm X 25 cm - Hypersil CEC C18 Mobile phase - pump A : 20 mM TRIS, pH 7.8 pump B : MeCN (2% acetone) Detection : 280 nm Gradient Profile :20% B held for 5mins, then to 80%B in 5mins, hold at 80% for 10 mins, then reset to 20% in 5 mins. Pressure flow rate 3ml/min (bulk)

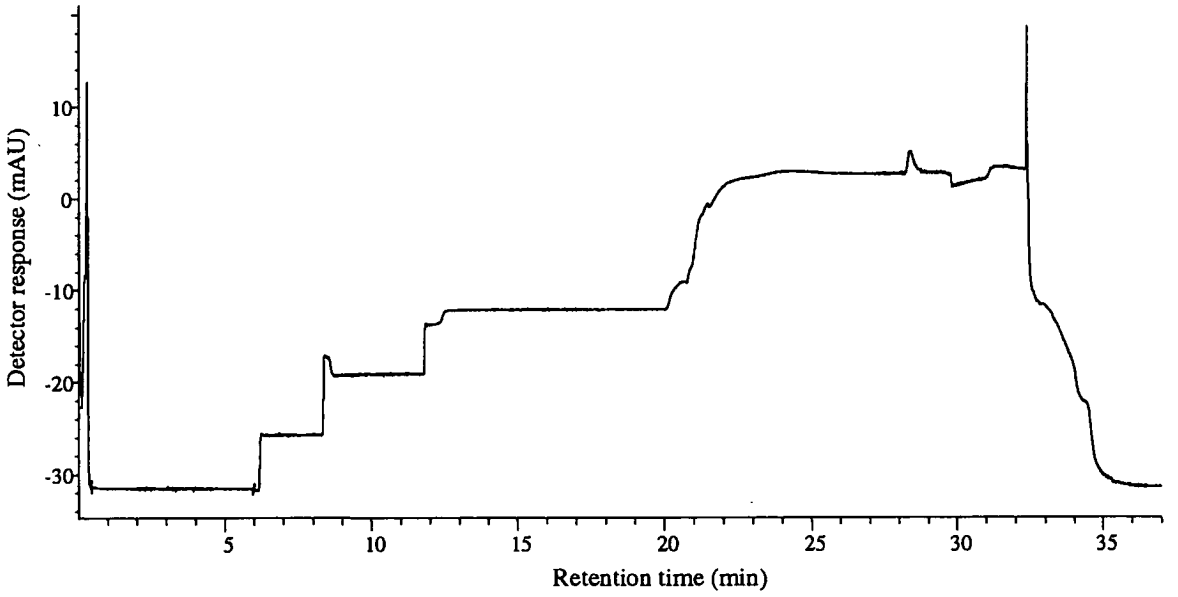

Figure 10. The step gradient profile obtained for the same pressure driven flow.
Conditions as for figure 8 except gradient profile as follows : 0-1 min 0% B, 1-5 min 20% B, 5-9 min 40% B, 9-17 min 60% B,17-45 min 100% B

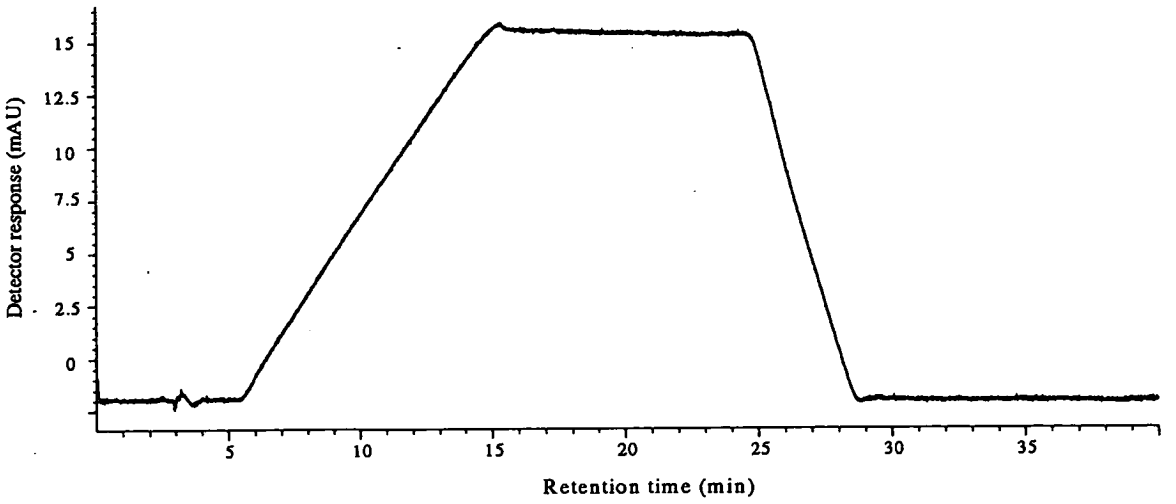

Figure 11. The gradient profile obtained with electrically driven flow at 25kV, pressure assistance at 2ml/min (bulk flow).
Chromatographic parameters : Capillary : 100µm X 25 cm - Innovaphase C6/SCX Mobile phase - pump A : 20 mM TRIS, pH 7.8, pump B : MeCN (2% acetone) Detection : 280 nm Gradient Profile :0-2 min hold at 20% B, to 80% B linear gradient between 2-12 min, 12-20 min hold at 80% B, reset to 20% B between 20-25 min.

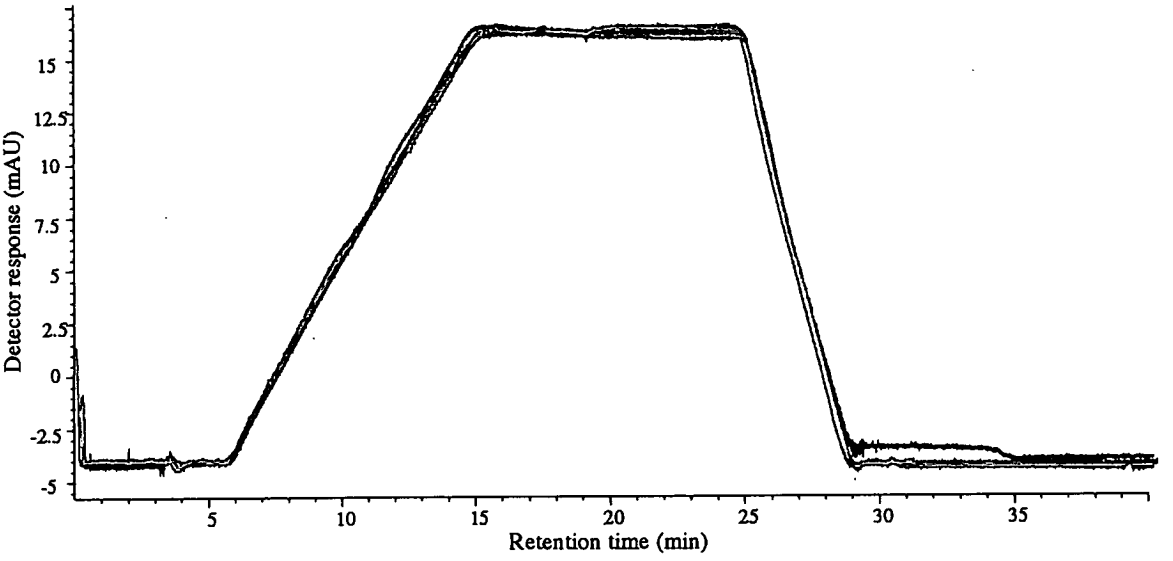

Figure 12. Four consecutive gradients as detailed in Figure 11.

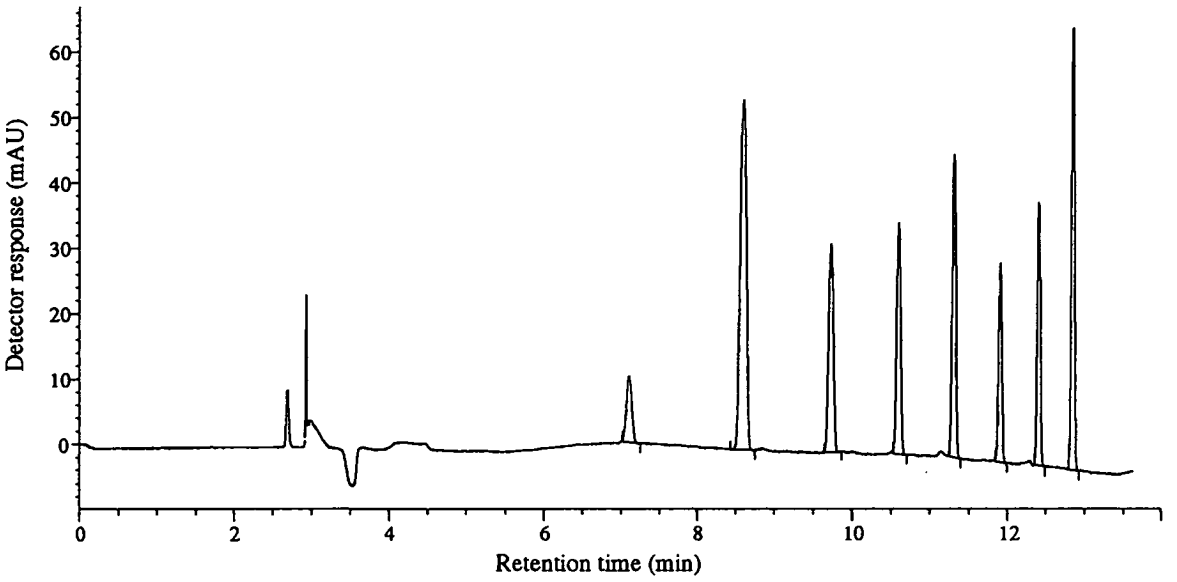

Figure 13. Gradient analysis of Valko test mixture.
Conditions as for Figure 11, Test mix contains : Quinine, Benzyl alcohol, Phenol, Acetophenone, 3-Methyl-4-nitrobenzoic acid, 4-Chlorocinnamic acid, Octanophenone

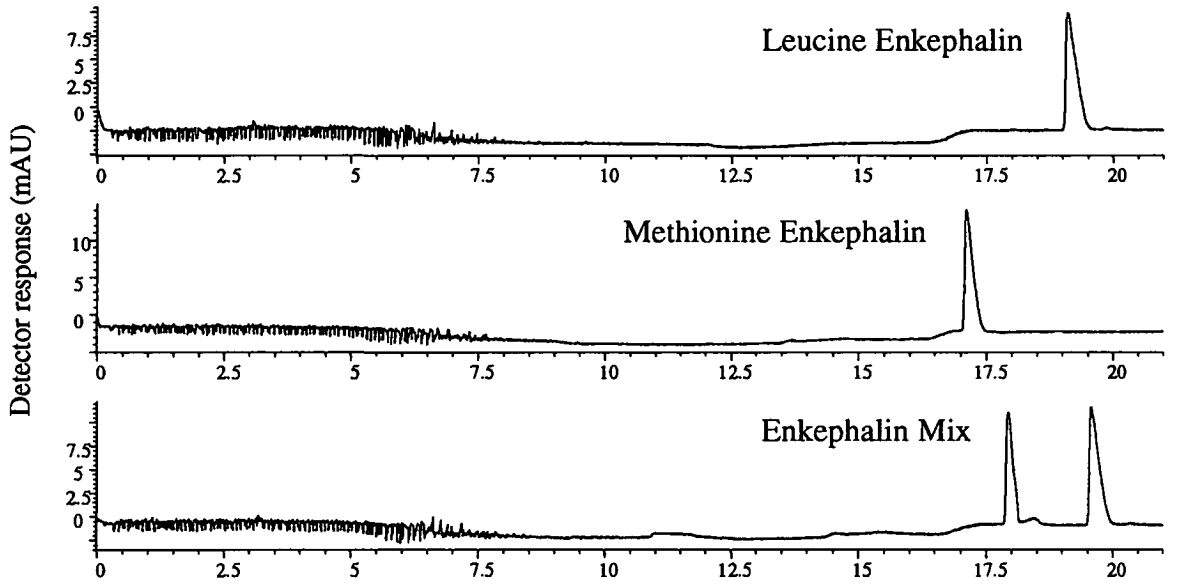

Figure 14. Separation of some peptide samples using gradient CEC.
Conditions as for Figure 11, except detection wavelength 214nm.

Chapter 9. Conclusions and future directions

CEC offers performance improvements over HPLC. Due to the inherently lower dispersion produced by the electrically induced flow profile, it gives typically 2-3 times better efficiency than the same system used with pressure flow. It is also by design a miniaturised process. This offers further benefits of reduced eluent consumption, smaller sample requirements and better compatibility with mass spectrometric detectors. These advantages are particularly useful when we consider the extra difficulty of miniaturising HPLC. Miniaturisation of chromatographic systems is becoming increasingly desirable. Future developments will demand the analysis of smaller samples, at faster rates, with increasingly complex separations required. These demands are already starting to exceed the capabilities of conventional HPLC systems. Systems will require more column efficiency, operation at higher flow rates and detection of the undiluted eluent in the most sensitive detectors available. CEC offers the opportunity to achieve these goals.

The main obstacles to using CEC reliably are the relatively unstable nature of purely electrically driven flows in packed beds, the lack of good quality CEC columns and the lack of dedicated instruments to perform CEC analysis. Also, CEC shares some of the same problems with HPLC of miniaturising the separation system without incurring dispersion related losses.

The work detailed in this thesis contributes considerable advancements in most of these areas. The section on column production introduces the designs and procedures

which have subsequently been used as the basis of the most successful commercial production of CEC columns. The work on coupling CEC to MS has allowed sufficient optimum use of these systems to demonstrate that future analysis requirements are possible, and guided subsequent effort towards the routine coupling of these techniques along these lines. The later chapters showing pressure-assisted CEC demonstrate the practicality of performing CEC based analysis that is as reliable as current HPLC systems. Proper optimisation of these type of uses will ultimately deliver CEC in a reliable format which will encourage a whole new audience of users to reap the benefits available.

9.1 Dispersion

The work detailed and reported in Chapter 6 was performed to assess the amount of dispersion introduced by various column and tube coupling arrangements. Until now, work done in CEC has mostly been performed in one-piece columns, comprising a contiguous tube of uniform diameter, with an open section necessarily following the packed bed. These arrangements are unsuitable for connection to remote detection, as the open tube section causes unacceptable deterioration in the peak quality due to broadening of the peak. It was found that to maintain peak integrity across practically useful distances, the coupling of the separation (packed) column should be made with an open tube of no more than one quarter of its diameter. To achieve this, and maintain the ability to apply adequate field strengths, the electrical ground connection should be made at the point of the join. With this arrangement, the

dispersion in the open tube can be predicted by the Taylor equation. It is also possible to introduce a small volume UV cell at this point, although the electrical connection should be made 'downstream' of this. Adopting these recommendations it is possible to obtain a two-piece 'joined' column giving excellent chromatographic performance, which can be transported rapidly, without significant losses, to remote detectors such as MS.

9.2 Thermal limits of operation.

Previous work in open tubes has suggested the existence of an operational 'wall' for electrically driven systems. Described in detail in Chapter 7, this comes about because of the critical dependence of the plate height on field strength, column diameter and to a lesser extent buffer concentration. Upon extending these principles to packed tubes, with appropriate correction for factors influenced by the change in tube design, it was found that problems arose whenever the operational settings were close to those predicted. This operational 'wall' was met consistently, irrespective of the particular combination of operational parameters used. The point at which performance loss was deemed excessive was noted for the different experiments performed. The practical and theoretical values matched very closely indeed, and this allowed limits to be set, restricting the maximum operational parameters chosen for different column diameters. As a guide it was found that maximum power consumption levels of about 7-8 W m^{-1} were tolerable before the wall was hit. When the conditions were pushed too hard, a significant drop in performance was observed. If conditions were pushed even further a

complete collapse in the flow system was normally seen. Recovery of the column via off-line conditioning was always required if this occurred. It generally proved to be disastrous to allow this to happen.

Whilst it is possible to use CEC above the thermal limits suggested in this work, nothing significant is gained from doing so. If faster analysis is needed by the use of short columns and higher fields, it is sensible to choose a lower conductivity buffer and/or a narrower column. Alternatively if a volatile (MS compatible) buffer is required, use a moderate concentration (<20mM overall). Bigger diameter columns, such as 150μm and above have to be used with care, as it is easy to lose performance altogether due to thermal escalation and subsequent flow loss. However, in the author's view these diameters also represent the most versatile solution as they are amenable to pumped flow systems. The dispersion associated with joining to other capillaries is also reduced when larger diameter columns are used. This can often compensate for slightly lower performance.

9.3 Practical robustness of electrically driven separations and coupling to MS.

In principle and in practice, CEC delivers the predicted improvements in most aspects of its use. However, CEC is physically limited for practical purposes to columns of <200 μm diameter. At this scale of column dimensions it is extremely difficult to acquire off-column optical detection, in a separate UV cell, in a conventional HPLC-type way. There is always a compromise in a flow cell based system between maximising path length (increases sensitivity) and minimising volume (to minimise

dispersion). Work in this thesis has demonstrated that whilst the achievement of this 'ideal' set-up of CEC-UV-MS is practically achievable, it is not routine and requires a high level of skill to do well. Consequently, most users still opt for on-column detection in a one piece column. Unfortunately this gives only minimal UV detection sensitivity and presents quite a challenge to maintaining stable flows. It is mainly the problem of unstable flow that reduces users' confidence in using these systems. If CEC is performed straight into the MS, with no UV detection or open tube section, the stability of operation is significantly improved. However, work in Chapter 8 has highlighted the early promise shown by pressure assisted CEC. Moderate amounts of pressure driven flow during CEC separations add much improved stability to the flow. Unattended operation becomes a reality and qualitative evaluation is enhanced by the ability to compare selectivity effects between electrically and pressure driven separations. This mode of operation also offers the chance to use gradient elution and this allows more 'generic' style analysis to be performed.

9.4 The future for miniaturised separations

It is my opinion that these combined systems also represent a very good way forward to using electrokinetic sampling from minuscule volumes and yet pressure driven flows at very high driving pressures. The current limitation to using very high pressure capillary LC is that the sample valves used are the 'weak-link' and will leak at modest pressures. It is comparatively easy to pump small volumetric flow rates directly through small diameter columns, even very long ones, if the sample can be introduced

directly into the column beforehand. This would present an immediate opportunity to perform high peak capacity separations, with high resolving power, and flow rates compatible with the most sensitive MS detection.

In parallel, as recent literature has already demonstrated, we will see the development of microfabricated, planar, 'chip' type separation columns [1]. It should be possible to fabricate 'dispersion-minimised' porous structures within the flow channels of such chips, and specific surface chemistry to be attached as required. The detection channel will be etched such that the detection path length is maximised and useful optical detection will again be possible. It is likely that eluent exiting the chip structure will be sampled into the nanospray source of a time-of-flight MS (TOF-MS). This will enable maximum sensitivity and accurate mass to be obtained on even the very narrowest peaks. Overall, this should enable routine use of high quality separation and detection methods that can chemically and structurally characterise complex mixtures in total volumes of less than single microlitres.

References

[1] Jacobson, Stephen C.; Ramsey, J. Michael. Chem. Anal. (N. Y.) (1998), 146(High-Performance Capillary Electrophoresis), 613-633.

Appendix 1. Molecular structures of cefuroxime axetil (upper) and fluticasone propionate (lower).